The Isl1/Ldb1 complex orchestrates heart-specific chromatin organization and transcriptional regulation

Luca Caputo

The Isl1/Ldb1 Complex orchestrates heart-specific chromatin organization and transcriptional regulation

Dissertation
Zur Erlangung des Doktorgrades
Der Naturwissenschaften

Vorgelegt beim Fachbereich Biochemie, Chemie und Pharmazie
Der Goethe-Universität
In Frankfurt am Main

von
Luca Caputo
aus Trieste (Italien)

Frankfurt am Main, 2015

Table of Contents

Table of Contents 3
Table of Figures 7
1. Zusammenfassung 11
2. Summary 16
3. Introduction 18
3.1. Murine Heart Development 19
3.1.1. Cardiac neural crest cells 22
3.1.2. Proepicardium 22
3.1.3. Transcription Factors in the First Heart Field 23
3.1.4. Transcription factors in the Second Heart Field 24
3.1.5. Pancardiac Transcription factors 25
3.1.6. Transcription Networks in Second Heart Field 27
3.1.7. Signalling Pathways in the Second Heart Field 29
3.2. Islet-1 35
3.2.1. Isl1: Gene and Protein structure 35
3.2.2. Isl1 in development 36
3.2.3. Isl1 involvement in Congenital Heart Diseases 38
3.3. Ldb1 39
3.3.1. Ldb1: Gene and Protein structure 39
3.3.2. Ldb1 in development 41
3.4. Three-dimensional genome organization 43
3.5. Long-range enhancer-promoter interactions 45
4. Aim of the Thesis 48
5. Results 50
5.1. Ldb1 Knockout prevents cardiac differentiation 50
5.1.1. Ldb1$^{-/-}$ derived embryoid bodies do not beat 50
5.1.2. Mesoderm is formed in Ldb1 KO embryoid bodies 51
5.1.3. Ldb1 knock out affects the expression of Second Heart Field transcription factors 52
5.2. Specific Deletion of Ldb1 in Second Heart Field is embryonic lethal 53
5.3. Ldb1 depletion causes Isl1 ablation 55
5.4. Isl1 is poli-ubiquitilated and degraded 56
5.5. Ldb1 protects Isl1 at protein level 58
5.6. Interaction of Isl1 and Ldb1 59
5.7. Isl1-Ldb1 interaction stabilize Isl1 at protein levels 60
5.8. Ldb1 and Isl1 interact in cardiac progenitors 60
5.9. Generation of Ldb1, Isl1 or Isl1/Ldb1 stable ES cell lines 61

5.9.1. Overexpression of Isl1 and Ldb1 affects the differentiation of all cardiovascular lineages 62
5.9.2. Overexpression of Isl1 or Ldb1 affects the expression of cardiac progenitor markers 63
5.10. Isl1 and Ldb1 interact genetically 64
5.10.1. Double heterozygous embryos have heart abnormalities 64
5.10.2. Decrease number of cardiomyocyte at E14.5 66
5.10.3. Expression of cardiomyocyte and SHF markers is decreased at E9.5 67
5.11. The dimerization domain of Ldb1 is required for SHF development 68
5.11.1. Isl1 progenitor population is present in DN-Ldb1 injected embryos 68
5.11.2. Loss of function of Ldb1 causes defects of the zebrafish heart 69
5.11.3. Reduced expression of cardiac markers in DN-Ldb1 injected embryos 71
5.11.4. Establishment of stable cells lines in the $Ldb1^{-/-}$ ESCs 73
5.11.5. Overexpression of full length Ldb1 but not DN-Ldb1 rescues the cardiomyocyte differentiation defect of $Ldb1^{-/-}$ cells 74
5.11.6. DN-Ldb1 inhibits early mesoderm progenitor 75
5.11.7. Ldb1 but not DN-Ldb1 restores expression of cardiac progenitor markers ... 77
5.11.8. Ldb1 but not DN-Ldb1 rescues the expression of endothelial cells markers .. 77
5.12. Ldb1 and Isl1 form a complex to regulate downstream targets 79
5.12.1. Isl1 binding sites are found in the Mef2c promoter 79
5.12.2. Isl1/Ldb1 transcriptional complex binds to several regulatory regions in the Mef2c locus during development 81
5.12.3. Isl1 binding sites are found in the Hand2 regulatory regions 82
5.12.4. Isl1/Ldb1 transcriptional complex binds to several regulatory regions in the Hand2 locus during development 84
5.13. Ldb1/Isl1 transcriptional complex promotes long range interactions 85
5.13.1. Ldb1/Isl1 transcriptional complex facilitates long range interactions at the Hand2 Locus 85
5.13.2. Ldb1, but not DN-Ldb1 rescues the chromosomal looping at the Hand2 locus 87
5.13.3. Ldb1/Isl1 transcriptional complex facilitates long range interactions at the Mef2c Locus 88
5.13.4. Identification of a novel putative Mef2c enhancer 93
5.13.5. Dynamic interaction to the Mef2c promoter correlates with different Mef2c isoforms expression 94
5.13.6. DN-Ldb1 overexpression prevents chromatin looping formation 95
5.13.7. DN-Ldb1 binds Mef2c and Hand2 loci similar to Ldb1 95
5.13.8. Mef2c promoter and AHF cooperate during transcription 96
5.14. Ldb1 orchestrate a network for transcriptional regulation and coordination in three-dimensional space during heart development 97

5.15. Cardiac transcription binding sites are enriched in AHF-interacting sequences... 101
5.16. Ldb1 control Second Heart Field differentiation 102
6. Discussion 104
6.1. Ldb1 and Isl1 co-operate to promote cardiac differentiation 105
6.2. Ldb1 regulates Isl1 at protein level 107
6.3. The ability of Ldb1 to promote long range interaction is needed for proper cardiac differentiation 108
6.4. Isl1/Ldb1 complex facilitates enhancer-promoter interaction in Mef2c and Hand2 loci 109
6.5. A dynamic promoter-enhancer interaction controls Mef2c isoform switch during cardiogenesis 112
6.6. The Isl1/Ldb1 transcriptional complex coordinates a three dimensional network during heart development 113
7. Future Perspective 116
8. Materials and Methods 118
8.1. Materials 118
8.1.1. Chemicals 118
8.1.2. Kits 120
8.1.3. Enzymes 120
8.1.4. Buffers and media 120
8.1.5. Plasmids 123
8.1.6. Primary Antibodies used for Western Blot analysis 125
8.1.7. Secondary Antibodies used for Western Blot analysis 125
8.1.8. Primary Antibodies used for Immunofluorescence analysis 126
8.1.9. Secondary Antibodies used for Immunofluorescence analysis 126
8.1.10. Antibodies used for ChIP 126
8.1.11. Primary Antibodies used for FACS analysis 126
8.1.12. Secondary Antibodies used for FACS analysis 127
8.1.13. Bacterial Strains 127
8.1.14. Cell Lines 127
8.1.15. Zebrafish strains 127
8.1.16. Mouse lines 128
8.1.17. Primers used for genotyping mouse embryos 128
8.1.18. Primers used for RT-PCR analysis Mus Musculus 128
8.1.19. Primers used for Mef2c isoforms absolute quantification 130
8.1.20. Primers used for ChIP analysis Mus Musculus 130
8.1.21. Primers used for 3C-seq Analysis 131
8.1.22. Primers used for 3C-qPCR Analysis 131
8.2. Methods 132
8.2.1. Cell Culture and Transfection 132

8.2.2. Luciferase Assay 133
8.2.3. Immunoprecipitation 133
8.2.4. Chromatin Immunoprecipitation 133
8.2.5. RNA Isolation, RT-PCR, and Real-Time PCR 134
8.2.6. Chromosome Conformation Capture Assays- 3C-Seq and 3C-PCR 134
8.2.7. DNA extraction from tail pieces 135
8.2.8. DNA extraction from embryos 135
8.2.9. Genotyping 135
8.2.10. Whole mount in situ hybridization analysis of mouse embryos 135
8.2.11. Histological analysis 136
8.2.12. Flow Cytometer Analysis 136
8.2.13. Immunofluorescence of Embryoid Bodies (EBs) 137
8.2.14. GO Analysis 137
8.2.15. mRNA synthesis 137
8.2.16. mRNA injection 137
8.2.17. Whole mount in situ hybridization analysis of Zebrafish embryos 137
8.2.18. Live imaging of Zebrafish embryos 138
8.2.19. Zebrafish emryos whole mount immufluorescence 138
9. References 139
10. Appendix 161
10.1. Affirmation 161
10.2. Ethical Statement 161
10.3. Publications 161
10.4. Conferences and Retreats 161
10.5. Awards 162
10.6. Curriculum Vitae 163
10.7. PhD Portfolio – MGK 164

Table of Figures

Figure 2.1 Schematic representation of murine heart development 20
Figure 2.2 Two distinct progenitor populations contribute to the heart. 21
Figure 2.3 Schematic representation of the transcriptional networks in the SHF 28
Figure 2.4 Scheme of the different signaling pathway acting on the SHF 29
Figure 2.5 Regulatory network in the SHF 30
Figure 2.6 Scheme of Isl1α protein 35
Figure 2.7 Screenshot of the murine Ldb1 transcripts 39
Figure 2.8 Alignment of murine Ldb1 isoforms. 40
Figure 2.9 Scheme of Ldb1 protein showing the different protein domains 40
Figure 2.10 Alignment of murine Ldb1 and zebrafish Ldb1 41
Figure 2.11 Chromosome Territories in human cell nucleus 43
Figure 2.12 Hox genes clusters are organized in three dimensional domains 45
Figure 2.13 Ldb1 and CTCF control long-range interaction in the *ß-globin* locus 47
Figure 3.1 Are Ldb1-mediated long range promoter-enhancer interactions important for cardiac development? 48
Figure 4.1: Schematic representation of the differentiation process of the embryoid bodies 50
Figure 4.2 Beating analysis 51
Figure 4.3 Ldb1 depletion blocks cardiomyocyte differentiation 51
Figure 4.4 Scheme of the differentiation process of mesodermal cells 52
Figure 4.5 Mesodermal formation is not affected in Ldb1 depleted EBs 52
Figure 4.6 SHF markers are downregulated in $Ldb1^{-/-}$ EBs 53
Figure 4.7 Ldb1 depletion in the SHF 54
Figure 4.8 Ldb1 deletion in SHF causes growth arrest at E9.5 and cardiac defects 54
Figure 4.9 Phenotype analysis of $Isl1^{Cre/+}Ldb1^{flox/flox}$ embryos 55
Figure 4.10 Depletion of Ldb1 causes depletion of Isl1 in EBs. 56
Figure 4.11 Depletion of Ldb1 causes depletion of Isl1 in E8.5 embryos 56
Figure 4.12 Isl1 is poli-ubiquitinated. 57
Figure 4.13 The LIM2 domain of Isl1 is critical of Isl ubiquitinilation 57
Figure 4.14 Ldb1 stabilizes Isl1 58
Figure 4.15 Ldb1 interaction stabilizes Isl1. 59
Figure 4.16 LIM1 domain of Isl1 mediates the interaction with Ldb1 59
Figure 4.17 Ldb1 binds to Isl1 and protects it from proteasomal degradation 60
Figure 4.18 Isl1 and Ldb1 physically interacts during cardiogenesis 60
Figure 4.19 Beating analysis of EBs overexpressing Isl1, Ldb1 and their combination 61
Figure 4.20 Generation of stable ES cell lines 62
Figure 4.21 Isl1 and Ldb1 increase the differentiation of all cardiovascular lineages 63
Figure 4.22 Ldb1 expression affects SHF marker genes expression 64
Figure 4.23 $Isl1^{+/-}$ $Ldb1^{+/-}$ displayed cardiac defects 65
Figure 4.24 $Isl1^{+/-}Ldb1^{+/-}$ embryos displayed thinner RV 65
Figure 4.25 Cardiomyocyte number is reduced in $Isl1^{+/-}$ $Ldb1^{+/-}$ embryos 66
Figure 4.26 Expression of cardiac genes is compromised in haplodeficient embryos 67

Figure 4.27 Scheme of the experimental approaches to study the role of long-range interactions during cardiac development 68
Figure 4.28 DN-Ldb1 is ubiquitously expressed in *D.rerio* embryos 69
Figure 4.29 DN-Ldb1 overexpression causes brain and eye defects 69
Figure 4.30 DN-Ldb1 overexpression causes bradycardia and arrhythmia 69
Figure 4.31 Isl1+ cells do not differentiate 70
Figure 4.32 DN-Ldb1 injected embryos have shorter atria 71
Figure 4.33 Reduced expression of *bmp4* and *mef2cb* in the atria of DN-Ldb1 embryos. 71
Figure 4.34 Isl1 positive population is not affected by DN-Ldb1 overexpression. 72
Figure 4.35 SHF marker genes expression is downregulated in DN-Ldb1 embryos 73
Figure 4.36 Generation of stable ESCs line in *Ldb1*$^{-/-}$ background 74
Figure 4.37 Ldb1 overexpression restores cardiac differentiation 75
Figure 4.38 Ldb1 overexpression restores cardiac marker genes expression 75
Figure 4.39 FACS analysis of early Flk1^{+}PdgfR-a^{+} cardiovascular progenitors 76
Figure 4.40 Ldb1 and DN-Ldb1 rescue Isl1 protein levels in d5 EBs 77
Figure 4.41 SHF marker genes *Mef2c* and *Hand2* are upregulated upon Ldb1 overexpression 77
Figure 4.42 Ldb1 restores the expression of endothelial marker genes 78
Figure 4.43 Ldb1 expression represses smooth muscle genes 78
Figure 4.44 Alignment of mouse and human *Mef2c* promoter 80
Figure 4.45 Isl1/Ldb1 transcriptional complex bind to *Mef2c* regulatory elements in EBs 81
Figure 4.46 Isl1/Ldb1 transcriptional complex bind to *Mef2c* regulatory elements *in vivo* 82
Figure 4.47 Alignment of conserved mouse and human *Hand2* OFTRV enhancer 83
Figure 4.48 Alignment of conserved mouse and human *Hand2* proximal promoter 84
Figure 4.49 Isl1/Ldb1 transcriptional complex bind to *Hand2* regulatory elements in EBs 85
Figure 4.50 Isl1/Ldb1 transcriptional complex bind to *Hand2* regulatory elements *in vivo* 85
Figure 4.51 Scheme of the experimental procedure 86
Figure 4.52 Schematic representation of the *Hand2* genomic locus 86
Figure 4.53 Ldb1 mediates *Hand2* promoter-enhancer interaction in d5 EBs 87
Figure 4.54 DN-Ldb1 can not rescue the interaction between OFT enhancer and promoter 88
Figure 4.55 3C-seq analysis of the *Mef2c* locus 90
Figure 4.56 Dynamic conformation of the Mef2c locus during EBs differentiation 90
Figure 4.57 Dynamic conformation of the Mef2c locus during embryoninc development 90
Figure 4.58 Alignment of mouse and human *Mef2c* interacting regions with AHF in the promoter area. 91
Figure 4.59 Alignment of mouse and human *Mef2c* interacting regions with AHF in the 3' region of *Mef2c* locus 92
Figure 4.60 Isl1/Ldb1 transcriptional complex binds to 3C-seq identified regions 93
Figure 4.61 Region interacting with the Mef2c-AHF are enriched for enhancer chromatin marks 94

Figure 4.62 *Mef2c* isoform switch during cardiac differentiation 95
Figure 4.63 Full length Ldb1 restores the 3D conformation of the *Mef2c* locus 95
Figure 4.64 DN-Ldb1 is recruited to the regulatory elements of *Mef2c* and *Hand2* .. 96
Figure 4.65 Synergistic effect of Isl1 and Ldb1 97
Figure 4.66 Ratio of over representation of GO pathways in WT cells over KO using the *Mef2c*-AHF as viewpoint 98
Figure 4.67 Ratio of over representation of GO pathways in WT cells over KO using the *Mef2c*-promoter as viewpoint..... 98
Figure 4.68 Intra- and interchromosomal interactions detected in the 3C-seq approach..... 100
Figure 4.69 Ldb1 mediates tissue specific interaction of cardiac genes with the *Mef2c-AHF* enhancer 100
Figure 4.70 Cardiac transcription factors binding motifs are enriched in the genomic regions interacting with the *Mef2c-AHF*..... 101
Figure 4.71 Interacting genes expression is sensitive to Ldb1 levels..... 102
Figure 4.72 Sinergistic effect of Isl1 and Ldb1 on the expression of interacting genes 102
Figure 4.73 Genes identified in the 3C-seq approach are downregulated in *Isl1*$^{+/-}$ *Ldb1*$^{+/-}$ embryos. 102
Figure 4.74 Proposed model of the role of Ldb1 during SHF differentiation 103

Table 2.1 Transcription factors and epigenetic regulators mutations linked to CHD in humans.....18
Table 2.2 Mutant phenotypes of transcription factors involved in myocardial development.....27
Table 4.1 *Isl1*$^{+/-}$ *Ldb1*$^{+/-}$ animals die at birth.....64
Table 4.2 Genes involved in cardiac development or cardiomyocyte function interacting with *Mef2c-AHF*..... 99

1. Zusammenfassung

Herzahnenzellen halten großes Potenzial für verbessernde Therapien in Herzunordnungen. Jedoch bleiben die molekularen Mechanismen, die Herzahnenzellvergrößerung und Unterscheidung regeln, schlecht definiert. Angeborene Herzkrankheiten (CHD) sind eine bedeutende Ursache der Sterblichkeit in Menschen. Mehrere Herzphänotypen im Menschen sind mit Veränderungen in Abschriftenfaktoren und epigenetic Modifikatoren verbunden worden.

Das Herz ist das erste Organ, um sich, wegen seiner entscheidenden Rolle im Verteilen der Nährstoffe im sich entwickelnden Embryo zu formen. Während embryogenesis wird das Herz von einem allgemeinen Ahnen an gastrulation erzeugt, der sich in zwei verschiedene Bevölkerungen absondert, hat die ersten und zweiten Herzfelder genannt. Das erste Herzfeld (FHF), die erste Bevölkerung, um am embryonischen Tag 6.5 (E6.5) zu erscheinen, brennt am midline durch und differenziert in den myocardium der funktionellen Herztube. Studien in verschiedenen Tiermustersystemen haben demonstriert, dass nach diesem anfänglichen Schritt Isl1-positive Ahnenzellen des zweiten Herzfeldes (SHF) dazu abwandern und zu vorderen und venösen Polen des Herzens beitragen. In der Maus Isl1-positive Ahnenzellen trägt zur Ausflussfläche (OFT) und der rechten Herzkammer (RV) des sich entwickelnden Herzens, sowie dem Teil der Atrien bei. Isl1-positive Zellen sind mehrstark und differenzieren in die ganze Hauptabstammungsgegenwart im kardiovaskulären System. Die molekularen Mechanismen, die diesem Prozess unterliegen, werden schlecht verstanden.

Während der embryonischen Entwicklung müssen Zellen eine neue Identität erwerben. Dieser Schalter der Identität schließt dreidimensionale Genomreorganisation und eine koordinierte Reihe von groß angelegten Transcriptional-Änderungen ein. Das Verwenden 3C basierte Annäherungen mehrere Studien haben vorgeschlagen, dass, während CTCF zusammen mit Cohesin stabile, bestimmende Langstrecken-DNA-Wechselwirkungen vermittelt, um die allgemeine Angleichung von chromatin, Zelltyp aufrechtzuerhalten, spezifische

Abschriftenfaktoren, in Verbindung mit ihrem cofactors, Vermittlerkomplex, Cohesin und CTCF an der Abstammung - und mit dem geometrischem Ort spezifische DNA-Wechselwirkung beteiligt werden können.
Die Regulierung von Transcriptional des Genausdrucks spielt eine wichtige Rolle im Herstellen der Ungleichheit von Geweben und Zelltypen. Langstrecken-DNA-Wechselwirkungen sind auch der kritischen Wichtigkeit für Erweitererbefürworterwechselwirkungen. Aktive Erweiterer, die durch die histone Modifizierung H3K4me1 und H3K27Ac gekennzeichnet sind, wirken mit ihrem verwandten Promoter aufeinander, um das transcriptional Ergebnis abzustimmen. Ein f die am besten studierten Beispiele dieses Mechanismus der Handlung ist der ß-globin geometrische Ort. Während erythropoiesis wirkt das Kontroll "Supererweiterer"-Gebiet des geometrischen Orts (LCR) physisch auf eine folgende Weise mit dem Befürworter der verschiedenen globin Isoform aufeinander. Diese Wechselwirkungsereignisse werden durch einen Abschriftenkomplex vermittelt, der GATA-1, LMO2 und Ldb1 enthält.

Diese Hintergrundinformationen zusammen mit den Kenntnissen habend, dass Isl1 und Ldb1 fähig sind, um am Proteinniveau aufeinander zu wirken, und dass Ldb1-/-Mausembryos an ungefähr E9-E9. 5 wegen des Musterns von Defekten und Abwesenheit des Herzens sterben, haben wir Hypothese aufgestellt, dass die Wechselwirkung zwischen Isl1 und Ldb1 eine kritische Rolle in der Unterscheidung von SHF Ahnen durch das Herstellen einer permissiven 3D-Angleichung im Kern spielen kann.

Um diese Hypothese zu prüfen, forsche ich erstens nach, wenn Ldb1 eine Rolle in der SHF Unterscheidung haben, habe ich Ldb1-/-in embryoid Körpern unterschieden und habe die dramatische Verminderung des Ausdrucks von wichtigen Herzgenen sowohl am Ahnen beobachtet (Hand2, Fgf10, Tbx1 als auch Mef2c), und cardiomycyte hat Bühne (Tnnt2, Mlc2-a, Mlc2-v), aber nicht früher mesodermal Bühne (Mesp1, Bry, EoMes) unterschieden. Außerdem mit einem Isl1-cre [3] ich ablated Ldb1 spezifisch in der SHF Ahnenbevölkerung und beobachtet ein Phänotyp, der Isl1-/-, mit der

Abwesenheit/Verminderung OFT und RV und embryonischer Tod an E10. 5 ähnlich ist.

Wie man zeigte, hat Ldb1, der dazu bindet, Proteine wie Isl1 Zu LIM-enthalten, sie vor der proteosomal Degradierung geschützt. Während Isl1 mRNA Niveaus eigentlich unchaged in abgeleitetem EBs von Ldb1-/-waren, wurde Isl1 an Proteinniveaus völlig abgeschafft. Wir konnten zeigen, dass die Schwergängigkeit von Ldb1 zu Isl1 auf eine dosisabhängige Weise gekonnt hat, Isl1 in HEK293T stabilisieren und vor der proteasome-vermittelten Degradierung auf eine ähnliche Mode des proteasomal Hemmstoff-MG 123 schützen.

Zu prüfen, ob Isl1 und Ldb1 physisch während cardiogenesis aufeinander wirken, den ich co-immunoprecitation des endogenen Proteins in einer für Herzahnenzellen bereicherten Bühne mit einem a-Ldb1 Antikörper durchführe, der Wechselwirkung bestätigend. Diese Ergebnisse weisen darauf hin, dass Ldb1 und Isl1 mit einander während cardiogenesis funktionell aufeinander wirken könnten. Der Überausdruck von Isl1, Ldb1 und der zwei zusammen, hat Herzunterscheidung in EBs, mit den Kombinationen von Isl1 und Ldb1 erhöht, die höchsten Effekten zeigend. Als nächstes haben wir bewertet, ob Isl1 und Ldb1 genetisch während der Herzentwicklung aufeinander wirken. Isl1/Ldb1 verdoppeln sich haplodeficient Embryos sterben perinatal, und die phenotypical Analyse in der späten-gestion Bühne hat strenge Herzabnormitäten (d. h. malrotation der großen Behälter, dünneren und kleineren RV) als vermeintliche Todesursache offenbart. Die QRT-PCR-Analyse der früheren Embryos hat die dramatische Verminderung des wichtigen SHF Anschreibers wie Hand2, Mef2c und Fgf10 offenbart.

Um zu bestätigen, dass Langstreckenwechselwirkungen durch den Isl1/Ldb1 Komplex vermittelt haben, sind von kritischer Bedeutung für die Unterscheidung des SHF Ahnen, ich drücke ectopictally eine gestutzte Form von Ldb1 aus, der am dimerization Gebiet (DN-Ldb1) in fruchtbar gemachten Zebrafish-Eiern Mangel hat. Wie man zeigte, ist DN-Ldb1, während noch fähig, um Isl1 zu binden und zu schützen, nicht im Stande gewesen, Langstrecken zu vermitteln. DN-Ldb1 zebrafish Embryos haben Herzabnormitäten gezeigt und haben Ausdruck von Herzanschreibern (d. h. hand2, mef2cb) ähnlich den isl1 Mutationsfischen reduziert.

Die Verstärkung der kritischen Rolle, dass die genomic 3D-Angleichung durch den Isl1/Ldb1 Komplex vermittelt hat, hat während der Herzunterscheidung nur volle Länge die Ldb1 Wiederherstellung im Ldb1-/-ESCs konnte Herzunterscheidung, das spontane Schlagen, den Ausdruck des Ahnen (d. h. Hand2, Mef2c, Fgf10) und cardiomyocyte (d. h. Mlc2-a und Mlc2-v) Anschreibergene retten, während der Überausdruck von GFP (Kontrolllinie), Isl1 oder DN-Ldb1 keine Effekten hatte.

Schließlich forschen wir nach, wenn Hand2 und Mef2c, Gene, deren Ausdruck durch den Verlust - oder Gewinn der Funktion von Ldb1 in allen geprüften Modellen betroffen wurde, direkte Ziele des Komplexes sind. Die Initiale in der silico Analyse von Hand2 und Mef2c geometrischen Orten hat mehrere Isl1 verbindliche Seiten offenbart, die zwischen Maus und menschlichen Genomen erhalten sind. Die Analyse von ChIP vom cardiogenic Gebiet von E8. 5-E9. 0 Mausembryos und von in vitro hat differenziert EBs hat Schwergängigkeit des Isl1/Ldb1 Komplexes auf einigen dieser genomic Gebiete gezeigt.

Ldb1 kontrolliert ß-globin Genausdruck durch die Erleichterung von Langstreckenwechselwirkungen zwischen LCR und Befürworter. Zu Eseln, wenn ein ähnlicher Mechanismuskontrollausdruck der Zielgene von Isl1/Ldb1 wir 3C gestützte Feinprobe leisten. Ich habe ein Vierschneidenden Enzym (NlaIII) verwendet, um den relativ kleinen Hand2 geometrischen Ort zu analysieren. Wechselwirkungen zwischen dem Befürworter und dem Erweiterer, Hand2 Ausdruck in OFT und RV steuernd, konnten im wilden Typ EBs und im Ldb1-/-EBs beobachtet werden, der Ldb1, aber nicht in undifferenziertem ESCs oder in EBs das Überausdrücken von GFP, Isl1 oder DN-Ldb1 überausdrückt. Diese Ergebnisse wurden nachgeprüft, die Analyse mit einem verschiedenen Vierschneidenden Enzym (DpnII) wiederholend.

Folgender 3C-Seq vom Mef2c geometrischen Ort wurde durchgeführt. Wir haben den Mef2c Vorderen Herzfelderweiterer (Mef2c-AHF) und der proximale Befürworter als zwei unabhängige Gesichtspunkte verwendet. Vielfache Wechselwirkungen innerhalb des Genkörpers wurden im Mef2c geometrischen Ort mit dem Befürworter als Gesichtspunkt entdeckt, dessen einige ein niedrigeres Signal im Ldb1-/-EBs gezeigt haben. Der Mef2c-AHF wirkt andererseits spezifisch mit dem Befürworterbereich und mit dem 3' Ende des Mef2c Gens, in wildtype EBs, aber

nicht im Ldb1-/-EBs aufeinander. Die Wechselwirkungen vom Mef2c-AHF wurden in EBs und von in verschiedenen Stufen der embryonischen Entwicklung isolierten Zellen unabhängig gültig gemacht. Von Interesse, während die Wechselwirkungen zwischen Mef2c-AHF und 3'UTR Gebiet in der verschiedenen untersuchten Zeit unveränderlich waren, haben wir gekonnt hat einen Schalter zu einem Gebrauch eines inneren Befürworters in späteren Stufen der Unterscheidung in vitro und in vivo beobachtet.

Als wir die Kontakte der zwei Gesichtspunkte auf eine Weitgenomweise analysiert haben, haben wir eine spezifische Bereicherung für mit der Herzentwicklung verbundene GO mit Genen beobachtet, die mit dem Mef2c-AHF in wildtype Zellen aufeinander wirken. Diese spezifischen Wechselwirkungen wurden in KO EBs verloren, oder als die Wechselwirkungen des Befürworters analysiert wurden. Wir konnten auch einige dieser Wechselwirkungen in unabhängig unterschiedenem EBS und im cardiogenic Gebiet von E9.0 Embryos, aber nicht im Schwanzgebiet bestätigen, wo der Mef2-AHF nicht aktiv ist. Außerdem ist der Ausdruck von Genen, die in der nächsten Nähe zum Mef2c-AHF gefunden sind, von den Niveaus des Isl1/Ldb1 Komplexes stark abhängig.

Im Beschluss während meiner Doktorstudien konnte ich zeigen, dass die Voraussetzung von Ldb1 für die Herzahnenzellunterscheidung und SHF Entwicklung zweifach ist: (i) bindet Ldb1 zu Isl1 und schützt ihn vor der proteasomal Degradierung; (ii) orchestriert Der Isl1/Ldb1 Komplex ein Netz für die transcriptional Regulierung und Koordination im dreidimensionalen Raum in Herzahnen, Herzahnenzellunterscheidung und Herzentwicklung steuernd.

2. Summary

Cardiac progenitor cells hold great potential for regenerative therapies in heart disorders. However, the molecular mechanisms regulating cardiac progenitor cell expansion and differentiation remain poorly defined. Here we show that the multi-adaptor protein Ldb1, which mediates interactions between different classes of LIM domain transcription factors, is a multifunctional regulator of cardiac progenitor cell differentiation. Ldb1-deficient embryonic stem cells (ESCs) show a markedly decreased expression of second heart field (SHF) marker genes and subsequently impaired cardiomyocyte differentiation. Conditional ablation of Ldb1 in the early SHF using an Isl1-Cre driver led to embryonic lethality at Embryonic day (E)10.5 with cardiac abnormalities including a significantly smaller right ventricle and a shortened outflow tract, supporting a crucial role of Ldb1 in the SHF. Mechanistically we show that the importance of Ldb1 for SHF development is two-fold: On the one hand, Ldb1 binds to Isl1 and protects it from proteasomal degradation, as a consequence of which Ldb1-deficiency leads to an almost complete loss of Isl1+ cardiovascular progenitor cells. On the other hand the Isl1/Ldb1 complex promotes long-range promoter-enhancer interactions at the loci of the core cardiac transcription factors *Mef2c* and *Hand2*. Chromosome conformation capture followed by sequencing (3C-seq) identified specific Ldb1-mediated interactions of the Isl1/Ldb1 responsive *Mef2c* anterior heart field enhancer with genes which play key roles in cardiac progenitor cell function and cardiovascular development. These interactions are of critical importance to regulate the expression of the downstream target genes since their expression levels are strongly dependent on the Ldb1/Isl1 levels. Overexpression of an Ldb1 mutant, which contains the LIM interaction domain and thereby can protect Isl1 protein from degradation, but lacks the dimerization domain and thus cannot promote long-range interactions, does not collaborate with Isl1 to regulate the expression of their common targets and results in defects in Isl1+ cardiac progenitor differentiation. In this thesis we show one of the first examples of genome-wide chromatin reorganization mediated by a developmental regulated, cell type specific, transcription complex. Ldb1 in concert with Isl1 promotes long range promoter-enhancer and enhancer-enhancer interactions in order to create active chromatin

hub where gene important for heart development can be co-regulated. Moreover, Isl1 and Ldb1 genetically interact during heart development, as *Isl1/Ldb1* haplodeficient embryos show various cardiac anomalies. The dosage-sensitive interdependence between Isl1 and Ldb1 in the expression of these key factors in cardiogenesis, further supports a key role of the Isl1/Ldb1 complex in coordinating a three dimensional genome organization, upstream of a regulatory network driving cardiac differentiation and heart development.

In conclusion, the Isl1/Ldb1 complex orchestrate a genome-wide three dimensional chromatin reorganization resulting in a transcriptional program responsible for the differentiation of multipotent cardiac progenitor cells into cardiomyocytes.

3. Introduction

Congenital heart diseases (CHD) is a significant cause of mortality in humans. Several cardiac phenotypes in human have been linked to mutations in transcription factors and epigenetic modifiers (Table 2.1) (Andersen et al., 2014; Buckingham et al., 2005), such as for the Holt-Oram Syndrome resulting from *TBX5* haploinsuficiency (Bruneau et al., 2001) and the DiGeorge Syndrome from *TBX1* (Andersen et al., 2014; Buckingham et al., 2005; Jerome and Papaioannou, 2001; Merscher et al., 2001). Table 2.1 summarizes single-gene mutations which cause CHD.

Gene Symbol	Protein Function	Type of CHD
CITED2	Transcriptional co-activator	I
FOXH1	Forkhead box TF	I
FOXP1	Forkhead box TF	I
GATA4	GATA-binding TF	I, S (8p23.1 Syndrome)
GATA6	GATA-binding TF	I
IRX4	Iroquois Homeobox TF	I
NKX2-5	Homeobox TF	I
NKX2-6	Homeobox TF	I
TBX1	T-box TF	S (DiGeorge Syndrome)
TBX5	T-box TF	S (Holt-Oram Syndrome)
TBX20	T-box TF	I
SALL4	Zinc finger TF	I, S (Duane-radial ray Syndrome)
TFAP2B	AP-2 TF	I, S (Char Syndrome)
CHD7	Bind to H3K4me3	S (CHARGE Syndrome)
KMT2D	H3K4 methyltransferase	S (Kabuki Syndrome)
EP300	Histone Acetyltransferase	S (Rubistein-Taybi Syndrome)
CRENNP	Histone Acetyltransferase	S (Rubistein-Taybi Syndrome)
EHMT1	H3K9 methyltransferase	S (Kleefstra Syndrome)

Table 3.1 Transcription factors and epigenetic regulators mutations linked to CHD in humans: I Isolated CHD; S syndromic CHD; TF, transcription factor (adapted from Andersen et al., 2014; Bruneau et al., 2001).

3.1. Murine Heart Development

The heart is the first organ to form, due to its crucial role in distributing the nutrients in the developing embryo. Myocardial cells, which are mesoderm derivatives, arise from the anterior region of the primitive streak at E6.5 during gastrulation, from cells expressing the earliest cardiac markers *Mesp1* and *Mesp2* (Jerome and Papaioannou, 2001; Kitajima et al., 2000; Merscher et al., 2001; Saga et al., 1999). These cells migrate in the anterior-lateral direction to form the cardiac crescent-shaped structure, which fuse at the midline to form the early heart tube that rapidly begins to pump blood (Andersen et al., 2014; Buckingham et al., 2005).

The region of the crescent that gives rise to the linear heart tube is referred to as the first heart field (FHF), shown in red in Figure 2.1 and 2.2 (Vincent and Buckingham, 2010). This early cardiac tube derived from FHF provides a scaffold for subsequent growth. This early structure will give rise to the left ventricular myocardium (Vincent and Buckingham, 2010). Early studies in chick (Kitajima et al., 2000; la Cruz et al., 1977; Saga et al., 1999; Stalsberg and DeHaan, 1969) and mouse (Buckingham et al., 2005; Virágh and Challice, 1973) show a requirement of a distinct cardiac progenitor cell population at the arterial and venous poles of the heart. A second population of progenitor cells lies medially and posteriorly to the crescent and due to morphogenic movement. It is then located behind the heart tube, extending posteriorly and also anteriorly into pharyngeal mesoderm. This progenitor population is referred to as second heart field (SHF), shown in green in Figure 2.1 and 2.2 (Buckingham et al., 2005; Kelly et al., 2001; Vincent and Buckingham, 2010).

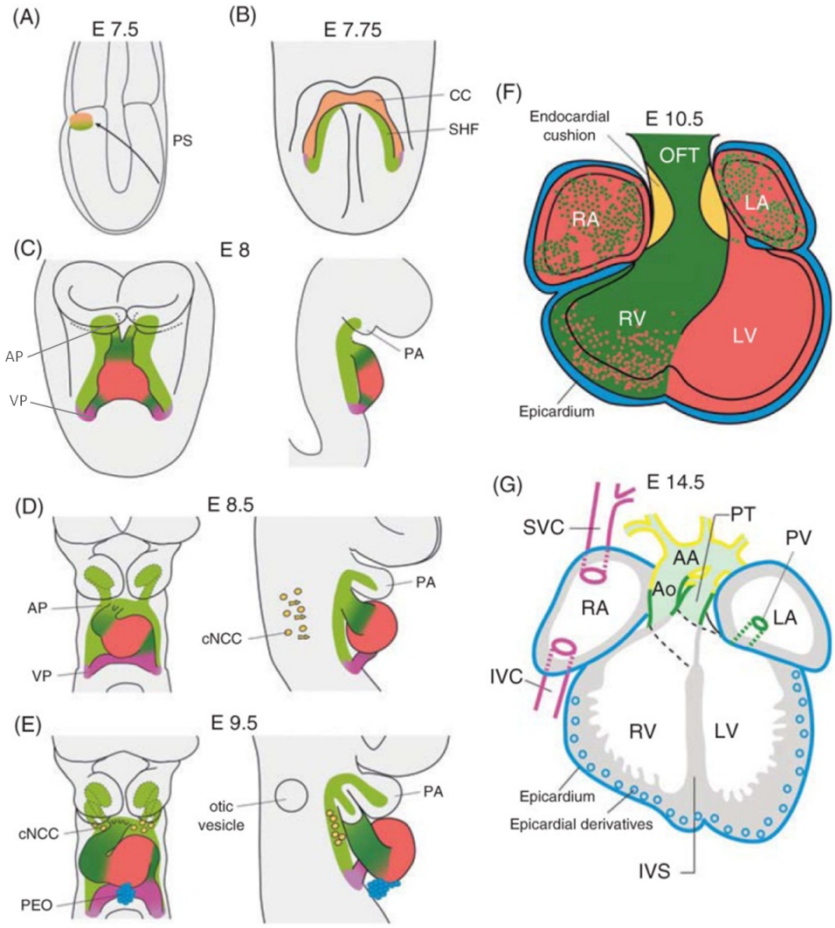

Figure 3.1 Schematic representation of murine heart development: First heart field (FHF) progenitors population is marked in red, second heart field (SHF) progenitors in green. **(A)** Origin of cardiac progenitors from the primitive streak (PS). **(B)** Formation of the cardiac crescent (CC), the SHF lies medial to it. **(C)** At the linear heart tube stage SHF progenitors migrate to the atrial pole (AP) and on the venous pole (VP) of the developing heart (dark green). **(D and E)** The heart tube undergoes looping and cardiac neural crest cells (cNCC) migrate towards the AP. The proepicardial organ (PEO) contributes to the VP. **(F)** The spatial contribution of FHF and SHF progenitors in the looped heart at E10.5 is shown. Outflow tract (OFT), right atrium (RA), left atrium (LA), right ventricle (RV), and left ventricle (LV). **(G)** The mature heart that underwent septation. Interventricular septum (IVS), aortic arch (AA), aorta (AO), pulmonary trunk (PT), pulmonary vein (PV), superior caval vein (SVC), inferior caval vein (IVC), and pharyngeal arches (PA) (adapted from Meilhac et al., 2004; Vincent and Buckingham, 2010).

One key step in the refinement of distinct regions of cardiac progenitors was the identification of *Isl1* as a heart field marker first in chick and mouse (Cai et al., 2003; Mjaatvedt et al., 2001; Waldo et al., 2001; Yuan and Schoenwolf, 2000). Isl1 derived cells contribute to the outflow tract (OFT), the right ventricle (RV), part of the atria and part of the left ventricle (LV) (Cai et al., 2003; Kelly et al., 2001). The finding of two different cardiac progenitor populations was further reinforced by retrospective clonal analysis using ß-galactosidase labeling (Cai et al., 2003; Meilhac et al., 2004; Yuan and Schoenwolf, 2000). This study showed that at E8.5 the second lineage

contributes to both poles of the heart. The left ventricle is the only region which is exclusively colonized by the first lineage, whereas the outflow tract is entirely formed from the second lineage (Cai et al., 2003; Meilhac et al., 2004).

The SHF can be divided in two main subdomains: anterior second heart field (aSHF) and posterior second heart field (pSHF). The anterior second heart field (aSHF) is marked by the expression of Fgf factors *Fgf8* and *Fgf10* (Kelly et al., 2001; Vincent and Buckingham, 2010) and the T-box transcription factor *Tbx1* (Watanabe and Buckingham, 2010; Xu et al., 2004). The aSHF contributes to the RV and the OFT. The posterior second heart field, shown in light green in figure 2.2, gives rise to the venous pole of the heart. This population expresses Islet-1, but is negative for the aSHF markers contributes to the atrial pole of the heart and the atrio-ventricular (AV) canal (Galli et al., 2008; Xu et al., 2004). The addition to the venous pole of the pSHF is dependent on Wnt2 signaling (Cai et al., 2003; Galli et al., 2008; Tian et al., 2010).

Furthermore other cell populations contribuite to the formation of the heart, namely the cardiac neural crest cells which contributes mainly to the arterial pole of the heart (described in 2.1.1) and the proepicardium, which is critical for the development of the epicaridum (described in 2.1.2).

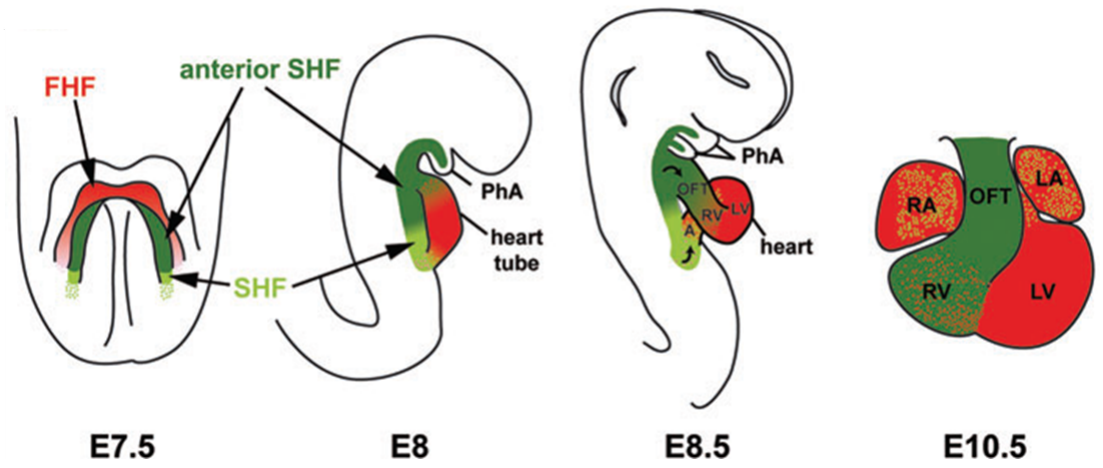

Figure 3.2 Two distinct progenitor populations contribute to the heart: First heart field (FHF) progenitors population is marked in red, second heart field (SHF) progenitors in green. RV, right ventricle; LV, left ventricle; OFT, outflow tract; RA, right atria; LA, left atria; PhA, pharyngeal arches (Adapted from Singh et al., 2010; Watanabe and Buckingham, 2010).

3.1.1. Cardiac neural crest cells

Cardiac neural crest cells (cNCC), shown in yellow in figure 2.1, are of neurectodermal origin and migrate from the dorsal neural tube. cNCC contribute to the smooth muscles of the pharyngeal arch arteries and their derivatives at the arterial pole of the heart (FIG 2.1). These cells migrate through the posterior pharyngeal arches to reach and invade the anterior domain of the SHF (Hutson and Kirby, 2007). cNCC play a major role in remodeling of the anterior part of the heart. In the OFT neural crest cells contribute to the formation of the endocardial cushion (Vincent and Buckingham, 2010). Depletion of neural crest compromises the maturation of the arterial pole and outflow tract septation (Hutson and Kirby, 2007). Furthermore cNCC ablation also results in a reduction in OFT myocardium and consequent arterial pole defects (Waldo et al., 2005). cNCC specific ablation of *Tbx3* affects the development of the OFT and of other sites of the heart (Mesbah et al., 2008). *Pax3* is a key regulator of neural crest. When *Pax3* function is impaired, neural crest migration is reduced causing outflow tract defects, ectopic myocardial differentiation and abnormal distribution of Isl1 positive cells of the SHF (Bradshaw et al., 2009).

3.1.2. Proepicardium

The proepicardium (PEO) is a transitory structure located at the venous pole of the heart (FIG 2.1 displayed in blue). $Isl1^{+}$/$Nkx2\text{-}5^{+}$ cardiac progenitors contribute to the proepicardium, which is marked by the expression of *Wt1* and *Tbx18* (Martínez-Estrada et al., 2010; Moretti et al., 2006; Sun et al., 2007; Vincent and Buckingham, 2010; Zhou et al., 2008a; 2008b). Proepicardial cells undergo epithelial to mesenchymal transition (EMT) and migrate towards the developing heart to form the epicardium proper. Later epicardial-derived cells migrate and contribute to vascular smooth muscle cells, fibroblasts, coronary endothelial cells and cardiomyocytes (Gittenberger-De Groot et al., 2010; Riley and Smart, 2011; Vincent and Buckingham, 2010). *In vitro* experiments, using altered levels of FGF versus BMP signaling, reported myocardial differentiation of PEO-derived cells (Kruithof et al., 2006; Martínez-Estrada et al., 2010; Moretti et al., 2006; Sun et al., 2007; van Wijk et

al., 2009; Zhou et al., 2008a; 2008b). Lineage tracing experiments using a Cre line under the control of *Wt1* (Gittenberger-De Groot et al., 2010; Riley and Smart, 2011; Zhou et al., 2008b) or *Tbx18* (Cai et al., 2008; Kruithof et al., 2006; van Wijk et al., 2009) labeled cardiomyocytes that originated form the PEO in the walls of the cardiac chambers and in the Interventricular septum.

3.1.3. Transcription Factors in the First Heart Field

The term FHF is used to indicate the first wave of mesodermal cells that differentiate to form the linear heart tube and express muscle markers such as MLC3F (Kelly et al., 1997; Saga et al., 1999; 2000; Zhou et al., 2008b) (FIG 2.1 and FIG 2.2).

Since the FHF contributes specifically to the linear heart tube and, subsequently, to the LV, the understanding of the cause of defects seen in the formation of this structure helped to unreveal the contribution of different genes in this context.

Hand1 constitutive knock-out (KO) embryos showed defects in the generation of the LV (Cai et al., 2008; McFadden et al., 2005; Riley et al., 1998), however the death of these embryos for extra-embryonic defects did not allow a proper analysis of the heart phenotype (Firulli et al., 1998; Kelly et al., 1997; Riley et al., 1998; Saga et al., 1999; 2000). Usage of a conditional *Hand1* mutation resulted in a LV hypoplasia (McFadden et al., 2005; Riley et al., 1998).

Tbx5 deficiency led to severe defects in the inflow region of the heart and left ventricle hypoplasia, due to proliferation defects (Bruneau et al., 2001; Firulli et al., 1998; Riley et al., 1998; Takeuchi et al., 2003).

GATA-4 is one of the earliest markers for cardiac precursors with its expression detected from E7 in mouse development which is maintained till adulthood (Brewer and Pizzey, 2006; McFadden et al., 2005). Unfortunately traditional genetic models to study the role of GATA factors, mainly *GATA-4* and *GATA-6*, in mammalian heart development have had liMITED success due to early embryonic lethality of the *GATA-4* null embryos at E7.5-E9.0, indicating their crucial role in heart development (Bruneau et al., 2001; Kuo et al., 1997; Molkentin and Olson, 1997; Takeuchi et al., 2003). In addition these embryos displayed cardia bifida, i.e. the formation of two independent linear heart tubes, due to failure of migration and fusion of the two bilateral progenitor populations (Brewer and Pizzey, 2006; Kuo et al., 1997;

Molkentin and Olson, 1997). Gata4/5- double-deficient embryos exhibit cardiovascular defects including alterations in cardiomyocyte proliferation and cardiac chamber maturation, suggesting a functional redundancy of the GATA factors during embryonic development (Kuo et al., 1997; Molkentin and Olson, 1997; Singh et al., 2010).

3.1.4. Transcription factors in the Second Heart Field

As previously mentioned, the SHF progenitor cells contributes to both poles of the developing heart to form the OFT, the RV and part of the atria (Kuo et al., 1997; Molkentin and Olson, 1997; Vincent and Buckingham, 2010) (FIG 2.1 and FIG 2.2). Several transcription factors and signaling molecules (described in 2.1.7) play important roles in the proper development of SHF derived structures.

Isl1 ablation in mice results in embryonic letality at E9.5-10 due to a severe heart phenotype (Cai et al., 2003). *Isl1*$^{-/-}$ embryos displayed a linear heart tube , consistent of a single ventricular chamber with left ventricular identity (Cai et al., 2003) (for a detailed description of the *Isl1*$^{-/-}$ phenotype see 2.2.2)

At the *sinus venosus* addition of myocardium is driven by the expression of *Tbx18* and the absence of *Nkx2-5* (Christoffels et al., 2006; Galli et al., 2008). These cells expressing *Tbx18* were initially positive for *Nkx2-5* and *Isl1* (Christoffels et al., 2006; Tian et al., 2010).

Tbx1 was shown to regulate the addition of the cells in the pulmonary trunk myocardium in the outlet of the RV (Frank et al., 2002; Maeda et al., 2006). Consistently, this structure is severely reduced in the *Tbx1* mutant hearts (Garg et al., 2001; Jerome and Papaioannou, 2001; Lindsay et al., 2001; Merscher et al., 2001; Théveniau-Ruissy et al., 2008). The expression of *Mef2c* is first detected in the cardiac crescent stage (Edmondson et al., 1994; Maeda et al., 2006; Pollock and Treisman, 1991). Its deletion causes a SHF phenotype with reduced OFT and an undeveloped RV (Lin et al., 1998; Théveniau-Ruissy et al., 2008).

Mef2c was shown to be a target of several important transcription factors involved in heart development, such as Isl1 and GATA4 that activates the AHF enhancer (Dodou et al., 2004; Edmondson et al., 1994; Pollock and Treisman, 1991), and as

well Foxh1 and Nkx2-5 that regulate another regulatory element of the *Mef2c* locus (Both et al., 2004; Lin et al., 1998).

Foxh1 deletion also shows a similar SHF phenotype. The RV and OFT markers are not detected, but a truncated OFT and LV are present. Further, *Tbx5* and *Hand1* expression is maintained and the venous pole seems unaffected (Both et al., 2004; Dodou et al., 2004).

Hand2 deletion also affects the SHF derived structure with mutant embryos showing RV hypoplasia (Both et al., 2004; Srivastava, 1999; Srivastava et al., 1995; 1997). It appears that *Hand1* and *Hand2* factors play a crucial role in ventricular chamber formation, but not in atrial chamber formation. Consistent with this, the double mutant, *Hand1*$^{-/-}$*Hand2*$^{-/-}$ embryos possess a single cardiac chamber that expresses atrial markers (Both et al., 2004; McFadden et al., 2005; Yamagishi et al., 2001).

3.1.5. Pancardiac Transcription factors

Tbx20 is another important T-box transcription factor in heart development. Initially it was thought to be a SHF marker (Srivastava, 1999; Srivastava et al., 1995; 1997; Takeuchi et al., 2005). It is now believed to be a pancardiac marker due to its complex phenotype that affects structures derived from both heart fields (Cai et al., 2005; McFadden et al., 2005; Singh et al., 2005; Stennard and Harvey, 2005; Takeuchi et al., 2005; Yamagishi et al., 2001). In the *Tbx20* mutants *Hand1* expression is absent, indicating defects in the contribution to the LV by the FHF. However hypoplasia of the future RV and lack of the OFT suggest a failure of the contribution from the SHF (Takeuchi et al., 2005).

Nkx2-5 is a transcription factor expressed in both the FHF and SHF (Buckingham et al., 2005; Cai et al., 2005; Singh et al., 2005; Stennard and Harvey, 2005; Takeuchi et al., 2005). Analysis of the *Nkx2-5* null embryos revealed that its deficiency leads to smaller RV and OFT due to decreased proliferation of the SHF progenitors (Prall et al., 2007; Takeuchi et al., 2005) which is a consequence of elevated repression of Bmp2/Smad1 signaling (Buckingham et al., 2005; Prall et al., 2007). Furthermore *Nkx2-5* is also essential for the formation, maturation and maintenance of the conduction system (Jay et al., 2004; Pashmforoush et al., 2004; Prall et al., 2007).

Table 2.2 summarizes the heart phenotypes observed in mouse embryos deficient for the transcription factors mentioned above.

Gene	Phenotype	Reference
Nkx2-5	Single atrial and ventricular compartments; loss of ventricular tissue; smaller RV and OFT; no Hand1 expression	(Lyons, 1996; Prall et al., 2007; Yamagishi et al., 2001)
Hand1	LV disrupted	(Firulli et al., 1998; Jay et al., 2004; Pashmforoush et al., 2004; Riley et al., 1998; Srivastava, 1999)
Tbx5	Sinoatrial defect; hypoplastic LV	(Bruneau et al., 2001; Lyons, 1996; Prall et al., 2007; Takeuchi et al., 2003; Yamagishi et al., 2001)
Tbx1	OFT defects	(Firulli et al., 1998; Garg et al., 2001; Jerome and Papaioannou, 2001; Lindsay et al., 2001; Merscher et al., 2001; Riley et al., 1998; Srivastava, 1999; Xu et al., 2004)
Isl1	Single atrial ventricular compartments with LV identity; no OFT; abnormalities at both poles	(Bruneau et al., 2001; Cai et al., 2003; Takeuchi et al., 2003)
Foxh1	OFT reduced or absent; RV not developed	(Both et al., 2004; Garg et al., 2001; Jerome and Papaioannou, 2001; Lindsay et al., 2001; Merscher et al., 2001; Xu

		et al., 2004)
Mef2c	OFT reduced; RV not developed; *Hand2* downregulated; Inflow tract abnormalities	(Cai et al., 2003; Dodou et al., 2004; Lin et al., 1998)
Tbx20	Chambers do not develop; no Hand1 expression; hypoplastic RV; OFT disrupted	(Both et al., 2004; Cai et al., 2005; Singh et al., 2005; Stennard and Harvey, 2005; Takeuchi et al., 2005)
Hand2	RV abnormalities	(Dodou et al., 2004; Lin et al., 1998; Srivastava et al., 1995; 1997)
GATA-4	Cardiac bifida; common AVC; double outlet RV; hypoplasia of ventricular myocardium	(Cai et al., 2005; Kuo et al., 1997; Molkentin and Olson, 1997; Pu et al., 2004; Singh et al., 2005; Stennard and Harvey, 2005; Takeuchi et al., 2005; Zeisberg et al., 2005)

Table 3.2 Mutant phenotypes of transcription factors involved in myocardial development. AVC, atrioventricular canal; LV, left ventricle; RV, right ventricle; OFT, outflow tract.

3.1.6. Transcription Networks in Second Heart Field

The output of the signaling pathways described in the previous section is mediated by a complex transcriptional network in which the transcription factors *Isl1, Nkx2-5, Mef2c* and *Tbx1* play a central role (Kelly, 2012; Li et al., 2010).

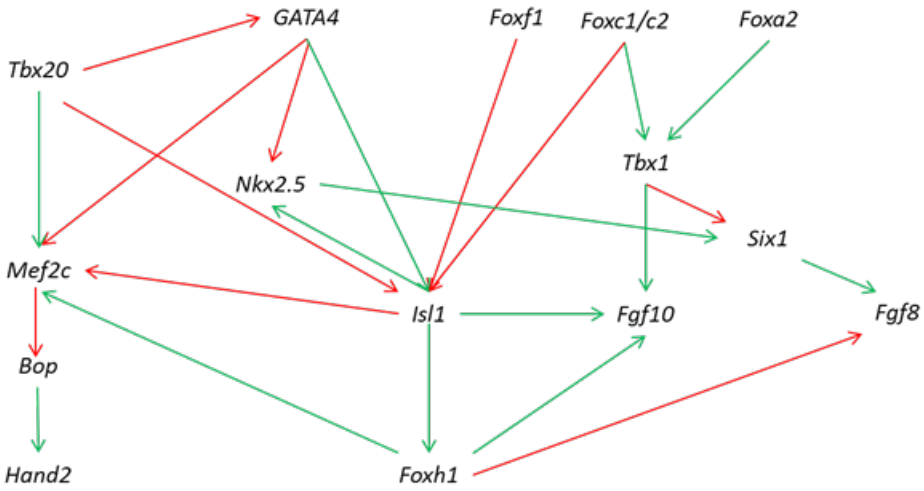

Figure 3.3 Schematic representation of the transcriptional networks in the SHF: Green lines indicate genetic and *in vitro* evidence; red lines indicate *in vivo* evidence. (Modified from (Buckingham et al., 2005; Keegan et al., 2005).

The forkhead family members Foxc1, Foxc2 and Foxa2 transactivate *Tbx1* (Kelly, 2012; Maeda et al., 2006; Seo and Kume, 2006; Yamagishi et al., 2003; Zhang and Baldini, 2010). *Isl1* expression in the SHF was found to be regulated by Foxc1, Foxc2 and Foxf1 through the binding to a downstream enhancer element, which is also bound by GATA4 (Buckingham et al., 2005; Kang et al., 2009; Kappen and Salbaum, 2009). Isl1, together with GATA4, is required for the activation of *Mef2c* expression in the SHF (Dodou et al., 2004; Maeda et al., 2006; Seo and Kume, 2006; Yamagishi et al., 2003; Zhang and Baldini, 2010), which is further regulated by a second specific enhancer bound by NKX2-5 and FOXH1 (Both et al., 2004; Kang et al., 2009; Kappen and Salbaum, 2009). Tbx20 is able to synergistically activate the *Mef2c* AHF-enhancer and the *Nkx2-5* SHF-enhancer, probably via a physical interaction with Isl1 (Dodou et al., 2004; Takeuchi et al., 2005). *Tbx20* and *Nkx2-5* are required for the downregulation of *Isl1* as seen in mutant embryos, where following the loss of one of these transcription factors cardiomyocytes maintain the expression of *Isl1* (Both et al., 2004; Cai et al., 2005; Prall et al., 2007). The homeodomain transcription factor Six1 and its coactivator Eya1 are required for proliferation of the SHF and the survival of adjacent tissues (Guo et al., 2011a; Takeuchi et al., 2005). The Six1/Eya1 complex is downstream of *Tbx1* and *Nkx2-5* but upstream of *Fgf8* (Cai et al., 2005; Guo et al., 2011a; Prall et al., 2007).

3.1.7. Signalling Pathways in the Second Heart Field

The SHF patterning and differentiation is under the control of several signaling pathways affecting cell behavior, specification, proliferation and migration (Dyer and Kirby, 2009; Rochais et al., 2009; Srivastava et al., 1995; 1997; Vincent and Buckingham, 2010) (FIG 2.3).

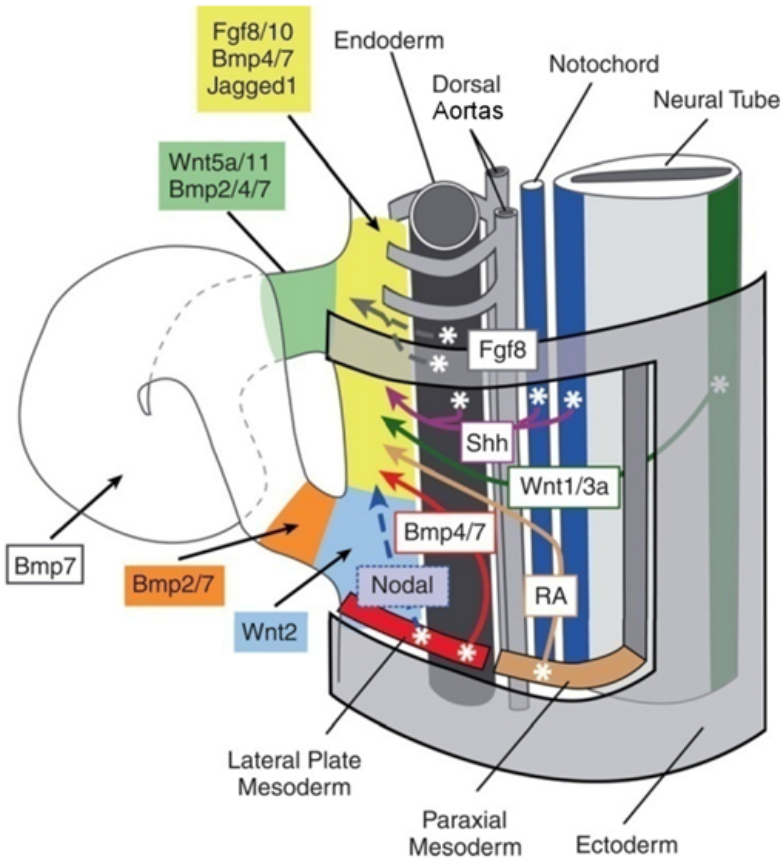

Figure 3.4 Scheme of the different signaling pathway acting on the SHF. Adapted from Kuo et al., 1997; Molkentin and Olson, 1997; Pu et al., 2004; Vincent and Buckingham, 2010; Zeisberg et al., 2005.

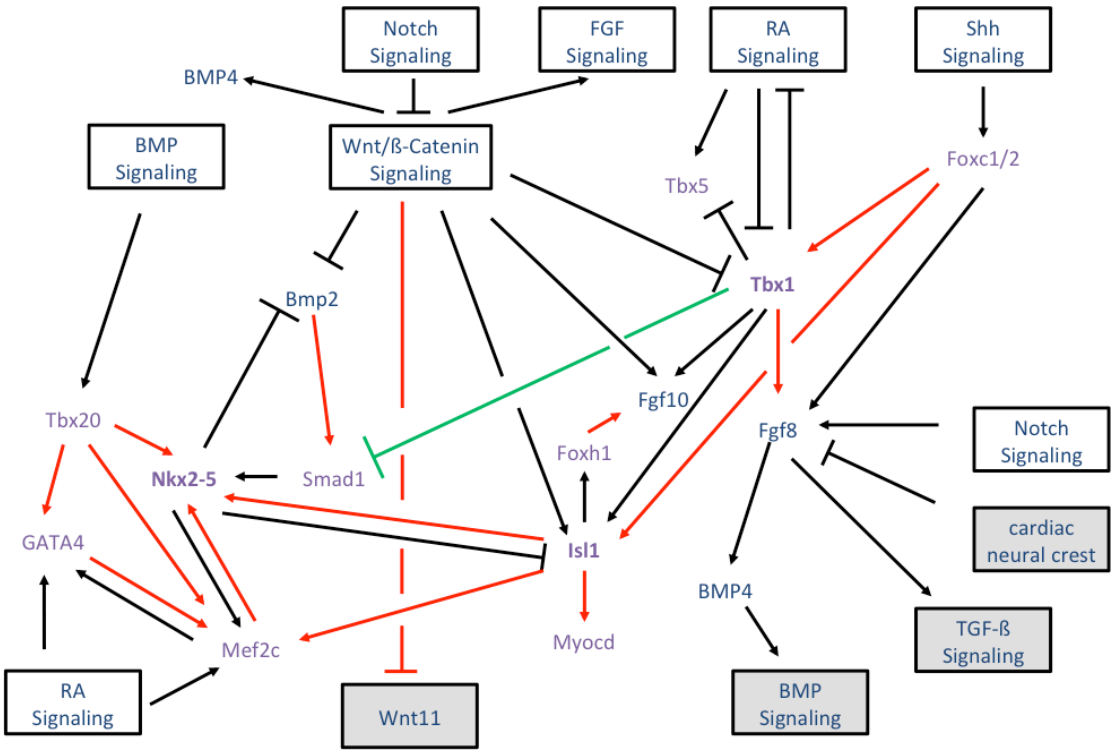

Figure 3.5 Regulatory network in the SHF: Three major nodes are shown: Tbx1, Isl1 and Nkx2-5. Signaling pathways/secreted molecules are shown in blue; transcription factors in purple. Filled grey boxes indicates effects outside of the SHF. Black lines indicate genetic expression data; red lines *in vivo* regulation; green line indicates *in vivo* protein interaction. (Adapted from Vincent and Buckingham, 2010)

3.1.7.1. Canonical Wnt Signaling

Canonical Wnt signaling is important for proliferation and to prevent the differentiation of SHF progenitors cells. Wnt3a and Wnt8, ligands of canonical Wnt signaling, have been shown to inhibit the differentiation of the myocardium (Dyer and Kirby, 2009; Rochais et al., 2009; Schneider and Mercola, 2001; Vincent and Buckingham, 2010). Inhibition of Wnt signaling by Dkk-1 or Crescent is necessary for the correct expression of myocardial specific proteins cTnI and Myh6 (Schneider and Mercola, 2001; Vincent and Buckingham, 2010). Conditional deletion of *CTNNB1* in the cardiac mesoderm led to RV and OFT hypoplasia, possibly due to a reduction of SHF proliferation (Ai et al., 2007; Cohen et al., 2007; Klaus et al., 2007; Kwon et al., 2007; Lin et al., 2007; Qyang et al., 2007; Schneider and Mercola, 2001). CTNNB1 has been shown to be required for the expression of *Isl1* and *Fgf10,* thereby controlling proliferation of this population and preventing the premature differentiation of SHF cells (Cohen et al., 2007; 2008; Lin et al., 2007; Schneider and Mercola, 2001). Moreover LiCl treatment or stabilization of ß-catenin resulted in the

expansion of SHF progenitors (Ai et al., 2007; Cohen et al., 2007; Klaus et al., 2007; Kwon et al., 2007; 2009; Lin et al., 2007; Qyang et al., 2007). Stabilization of ß-catenin also resulted in the maintenance of Isl1+ cells in the OFT, and decrease expression of *Myocardin* (Cohen et al., 2007; 2008; Kwon et al., 2009; Lin et al., 2007).

3.1.7.2. Noncanonical Wnt Signaling

Noncanonical Wnt signaling controls cardiomyocyte differentiation. It plays an important role in SHF development as shown in the *Wnt5a* mutant embryos that exhibit a common ventricular outlet and abnormal neural crest invasion (Kwon et al., 2009; Schleiffarth et al., 2007). The expression of another non canonical Wnt member, *Wnt11*, is regulated in the OFT by canonical Wnt/ß-catenin pathway and Fgf signaling (Kwon et al., 2009; Lin et al., 2007; Park et al., 2006). *Wnt11* mutant embryos have a short OFT, together with septation defects (Schleiffarth et al., 2007; Zhou et al., 2007). *Wnt11,* expressed at high levels in the OFT, is necessary for the correct arterial pole development (Lin et al., 2007; Park et al., 2006; Phillips et al., 2005; 2007).

3.1.7.3. Fgf Signaling

Fgf8 hypomorphic embryos die due to cardiac failure caused by OFT defects (Christoffels et al., 2006; Frank et al., 2002). The phenotype of the aSHF marker *Tbx1* mutant shows some similarity in the cardiac defects to the *Fgf8* hypomorphic allele, but with more severe neural crest defects (Garg et al., 2001; Jerome and Papaioannou, 2001; Lindsay et al., 2001; Merscher et al., 2001; Vincent and Buckingham, 2010). *Fgf8* is the major Fgf ligand involved in the SHF development (Abu-Issa et al., 2002; Frank et al., 2002; Ilagan et al., 2006; Park et al., 2008; Zhou et al., 2007) and plays an important role in the specification of the early cardiac mesoderm (Alsan and Schultheiss, 2002; Phillips et al., 2005; 2007). Early loss of *Fgf8* affects the survival and proliferation of SHF progenitors (Abu-Issa et al., 2002; Frank et al., 2002; Ilagan et al., 2006; Park et al., 2008). Later deletion of *Fgf8* in the pharyngeal mesoderm results in failure of OFT alignment and reduced of expression of *Isl1, Tbx1* and *Wnt11* (Abu-Issa et al., 2002; Alsan and Schultheiss, 2002; Frank et

al., 2002). Fgf signaling in the SHF is positively regulated by *Tbx1*, which is an important center of integration of different signaling pathways since it is itself positively regulated by Shh signaling (Abu-Issa et al., 2002; Frank et al., 2002; Garg et al., 2001; Lin et al., 2006) and negatively regulated by retinoic acid signaling (Abu-Issa et al., 2002; Frank et al., 2002; Roberts et al., 2006; Ryckebusch et al., 2008). *Fgf10*, also expressed in the SHF, does not demonstrate an SHF phenotype (Garg et al., 2001; Lin et al., 2006; Marguerie et al., 2006). However a compound *Fgf8* and *Fgf10* mutant, $MesP1^{Cre/+}Fgf8^{flox/flox}Fgf10^{-/-}$, showed a OFT/RV phenotype (Roberts et al., 2006; Ryckebusch et al., 2008; Watanabe et al., 2010).

Deletion of *Fgfr1* or *Fgfr2*, the two main receptors of *Fgf8* and *Fgf10*, or of an adaptor molecule linking FGF signaling to MAPK in cardiac mesoderm showed an autocrine requirement of FGF signaling in the SHF (Park et al., 2008; Watanabe et al., 2010; Zhang et al., 2008).

In addition to *Fgf8* and *Fgf10*, *Fgf15* plays a role in OFT development (Marguerie et al., 2006; Vincentz et al., 2005).

3.1.7.4. Bmp Signaling

The role of Bmp signaling in promoting cardiac differentiation was first shown in chick embryos (Schultheiss et al., 1997; Vincentz et al., 2005) followed by experiments in mouse embryos (Park et al., 2008; Tirosh-Finkel, 2006; Tirosh-Finkel et al., 2010; Zhang et al., 2008).

Studies in *Drosophila* showed that Dpp, the ortholog of Bmp2, is required to form the progenitor cells of the dorsal vessel, *Drosophila* cardiac organ (Frasch, 1995; Schultheiss et al., 1997; Yin and Frasch, 1998). In early stages Bmp4 plays an important role in the delamination and migration of neural crest cells (Scholl and Kirby, 2009; Tirosh-Finkel, 2006; Tirosh-Finkel et al., 2010). *Bmpr1a* is essential for the induction of the mesoderm, and loss of Bmpr1a is lethal at E9.5 (Frasch, 1995; Mishina et al., 1995; Yin and Frasch, 1998). Inhibition of *Bmp2* blocked the recruitment of SHF progenitors at the arterial pole of the heart (Scholl and Kirby, 2009; Waldo et al., 2001) thus showing a role for Bmp signaling in SHF development. Later on, it was shown that Bmp4 is produced in the SHF and is required, together with Bmp7, for the development of the OFT (Lin, 2004; Liu et al., 2004; McCulley et

al., 2008; Mishina et al., 1995). Consistent with the role of Bmp signaling in the differentiation of the SHF, conditional deletion of the Bmp type 1 receptor, *Bmpr1a,* in *Isl1* expressing cells caused proliferative defects in the RV and OFT morphology, with a decreased expression of *Tbx20* and increased levels of *Isl1* in the OFT (Waldo et al., 2001; Yang et al., 2006). On the same line of evidence, expression of a mutant receptor lacking half of the extracellular domain, $Bmpr2^{\Delta E2}$, displayed defects in the OFT development, and died before birth (Délot et al., 2003; Lin, 2004; Liu et al., 2004; McCulley et al., 2008). Earlier deletion of Bmpr1a in cardiac mesoderm cells, using a *Mesp1* driven Cre line, led to failure to form a differentiating cardiac tube, albeit Isl1+ progenitor cells were present (Klaus et al., 2007; Yang et al., 2006). *Bmp5* and *Bmp7* double-knockout mice are embryonic lethal at E10.5, due to several defects, including defective cardiac cushion formation (Délot et al., 2003; Solloway and Robertson, 1999). Double Knockout of *Bmp6* and *Bmp7* is lethal between E10.5 and E15.5 due to cardiac defects (Kim et al., 2001; Klaus et al., 2007). *Smad5* knockout mice die at E10.5-11.5 due to aberrant left-right asymmetry signaling that causes defects in angiogenesis and cardiac looping (Chang et al., 2000; Solloway and Robertson, 1999; Yang et al., 1999).

3.1.7.5. Sonic Hedgehog Signaling

Shh signaling also plays a role in the development of the SHF. Experiments in chick embryos showed a critical role for Shh signaling in maintaining progenitor cell proliferation (Dyer and Kirby, 2009; Kim et al., 2001). *Shh* null mouse embryos displayed defects in the RV and OFT alignment and septation, that resulted in a common ventricular outlet (Chang et al., 2000; Washington Smoak et al., 2005; Yang et al., 1999). It was further shown that Shh from the endoderm affects *Tbx1* expression at the arterial pole (Dyer and Kirby, 2009; Yamagishi et al., 2003), which has implication for the formation of the pulmonary trunk myocardium (Théveniau-Ruissy et al., 2008; Washington Smoak et al., 2005). Shh produced in the pharingeal endoderm affects the posterior SHF (Lin et al., 2006; Yamagishi et al., 2003). Absence of Shh signaling in this domain causes specific venous pole defects (Goddeeris et al., 2008; Hoffmann et al., 2009; Lin et al., 2006; Théveniau-Ruissy et al., 2008).

3.1.7.6. Notch Signaling

Different components of Notch signaling are present in the SHF. Conditional deletion of *Jagged1*, the principal ligand of Notch signaling in the SHF results in arterial pole defects (High et al., 2009; 2008; Lin et al., 2006; Varadkar et al., 2008). Consistent with this, expression of a dominant negative form of Mastermind-like (MAML), a co-activator of the Notch transcriptional complex, using Isl1- or *Mef2c*- driven Cre lines, led to arterial pole defects (Goddeeris et al., 2008; High et al., 2009; Hoffmann et al., 2009; Lin et al., 2006). Disruption of Notch signaling in the SHF causes down-regulation of Fgf8 in the pharyngeal region (High et al., 2008; 2009; Varadkar et al., 2008) and a decrease in BMP signaling (High et al., 2009; Park et al., 2008), which play crucial roles in SHF development.

3.1.7.7. Retinoic Acid Signaling

Retinoic acid signaling was shown to define the limits of the SHF in the pharyngeal mesoderm (High et al., 2009; Ryckebusch et al., 2008; Sirbu et al., 2008). In mouse embryos lacking *Raldh2* gene the expression of several SHF markers, *Isl1, Tbx1, Fgf10* and *Fgf8, was* expanded in the posterior direction (Park et al., 2008; Ryckebusch et al., 2008; Sirbu et al., 2008). *Raldh2* expression is shifted anteriorly and retinoic acid catabolizing enzymes are downregulated in *Tbx1* mutant embryos (Guris et al., 2006; Ivins et al., 2005; Liao et al., 2008; Roberts et al., 2005; Ryckebusch et al., 2008; Sirbu et al., 2008). In *Raldh2* mutant embryos the heart tube fails to grow (Ryckebusch et al., 2008; Sirbu et al., 2008). Consistently in the retinoic acid receptor mutants the distal outflow tract is missing. This phenotype is associated with a reduction of *Mef2c* expression (Guris et al., 2006; Ivins et al., 2005; Li et al., 2010; Liao et al., 2008; Roberts et al., 2005). Moreover in zebrafish embryo RA signaling controls the size of the cardiac field (Keegan et al., 2005; Ryckebusch et al., 2008).

3.2. Islet-1

Islet-1 (Isl1) is a LIM Homeodomain (LIM-HD) protein isolated for the first time in 1990 for its ability to bind the rat insulin I gene enhancer (Guo et al., 2011a; Karlsson et al., 1990).

3.2.1. Isl1: Gene and Protein structure

The *Isl1* gene in mouse is located on chromosome 13 (116298270 – 116309688, minus strand) and encodes two alternatively spliced variants Isl1-α and Isl1-β, respectively of 349aa and 326aa (Ando et al., 2003; Guo et al., 2011a).

Isl1 protein contains two LIM domains at the N-terminus and a Homeodomain towards its C-terminus (FIG 2.5).

Figure 3.6 Scheme of Isl1α protein showing the different protein domains: LIM1, LIM2, LIM domains; HD, Homeodomain; LBD, LIM binding domain.

The two LIM domains of Isl1 are known to mediate protein-protein interactions. The LIM domains consist of cysteine-histidine rich region, with a consensus sequence $CX_2CX_{16-23}HX_2CX_2CX_2CX_{16-21}CX_2$(C,H,D) coordinating two atoms of zinc (Karlsson et al., 1990; Schmeichel and Beckerle, 1994). Isl1 HD binds to a consensus motif YTAATGR and regulates the expression of insulin, glucagon, somatostatin and *Mef2c* genes (Ando et al., 2003; Dodou et al., 2004; Karlsson et al., 1990; Leonard et al., 1992; Wang and Drucker, 1996). Recent ChIP-seq study in neurons showed that Isl1 can also bind to the consensus motif TAAKKR (Mazzoni et al., 2013; Schmeichel and Beckerle, 1994). After the homeodomain of Isl1 was identified a LIM binding domain (LBD). This domain is structural similar to the $Ldb1_{LID}$, however their aminoacid sequences share low levels of similarity (Bhati et al., 2008; Dodou et al., 2004; Karlsson et al., 1990; Leonard et al., 1992; Wang and Drucker, 1996). $Isl1_{LBD}$ can bind to LIM domain of Lhx proteins (Bhati et al., 2008; Gadd et al., 2011; Mazzoni et al., 2013) or in an intramolecular fashion the LIM domain of Isl1 itself (Bhati et al., 2008;

Gadd et al., 2013). However the $Isl1_{LBD}$-$Isl1_{LIM1}$ interaction is weaker than the interaction between $Ldb1_{LID}$ and $Isl1_{LIM1}$ (Bhati et al., 2008; Gadd et al., 2011; 2013).

3.2.2. Isl1 in development

The first evidence for a role of Isl1 during heart development was obtained with the generation of a constitutive null *Isl1* allele. *Isl1* null embryos died at E9.5-10 with a severely misshaped, unlooped heart, lacking the RV and the OFT (Cai et al., 2003; Gadd et al., 2013). Consistent with the loss of the RV and OFT, expression of *Fgf10* and *Wnt11* was lost in the null embryos and the remaining chamber exhibit a left ventricle phenotype showing expression of FHF markers *Tbx5* and *Hand1* (Cai et al., 2003; Gadd et al., 2013). Analysis of the *Isl1* null embryos showed that *Isl1* is important for proliferation, survival and migration of the progenitor population of the SHF (Cai et al., 2003). In more recent studies in mouse embryos, activation of the highly sensitive FLAP-GATA4 reporter construct using the Isl1-Cre was observed in both FHF and SHF (Ma et al., 2008). These two studies suggest that the role of Isl1 in heart development is not restricted to the SHF, but Isl1 can be considerate as an important pan-cardiac marker.

Isl1 expression, that is only transient in the progenitor cells and lost during differentiation (Cai et al., 2003; Laugwitz et al., 2008; Sun et al., 2007), marks a population of cells that is able to differentiate into all the three major lineages of the cardiovascular system, namely cardiomyocyte, smooth muscle and endothelial cells (Kattman et al., 2006; Moretti et al., 2006; Wu et al., 2006). Using a tamoxifen inducible Isl1-MerCreMer line crossed to R26RlacZ line Sun and colleagues showed that by E9 most Isl1 positive progenitors migrated to the heart and downregulated *Isl1* expression (Sun et al., 2007). Analysis of the same line revealed contribution of Isl1 positive progenitor cells to the pace-maker cells of the sinoatrial and atrioventricular nodes (Sun et al., 2007). Interestingly, a population of Isl1 positive cells can still be found in the postnatal heart of mice, rat and human (Laugwitz et al., 2008; 2005; Sun et al., 2007).

Isl1 function in heart development is maintained through evolution. Homologue of Isl1, *tailup* (*tup*) is found in the fruit fly where it plays a crucial role in heart development (Mann et al., 2009). In lower vertebrates such as in *Xenopus* and

zebrafish *isl1* is expressed in cardiac progenitor population and is required for proper cardiac development (Brade et al., 2007; de Pater et al., 2009; Witzel et al., 2012). Functional ablation of the *isl1* gene in zebrafish does not affect the first wave of differentiation of cardiomyocyte and the linear tube of the zebrafish embryo form normally (de Pater et al., 2009). However the differentiation of cardiomyocytes at the venous pole of the developing heart is affected (de Pater et al., 2009). Consistently down-regulation of a negative regulator of Isl1 transcriptional activity, Ajuba, led to an increase of cardiomyocyte at the venous pole from the second wave of differentiation of the myocardium (Witzel et al., 2012). In zebrafish *isl1* contributes also to the cells at the location where the pace-maker are also found, and the bradycardia shown by the *isl1* mutant embryo may suggest a role for *isl1* in the generation of this structure (de Pater et al., 2009; Tessadori et al., 2012). However, in contrast to mouse embryo, the contribution to the arterial pole is not affected in the *isl1* null embryos (de Pater et al., 2009), suggesting a compensation mechanism from other members of the Islet family in zebrafish.

In Xenopus *isl1* expression is first detected at the end of gastrulation, co-expressed with other cardiac factor (Brade et al., 2007). islMO injections in the developing Xenopus embryos affected normal looping of the linear tube and resulted in smaller malformed hearts (Brade et al., 2007). Expression of critical genes for cardiac development, such as *BMP-4, GATA-4, GATA-6, tbx20* and *nkx2-5,* was downregulated upon loss of function of *isl1* (Brade et al., 2007). Moreover similar to mouse embryo, isl1 expression marks a pluripotent cardio-vascular progenitor population in Xenopus (Brade et al., 2007).

The critical role of Isl1 in heart development must not undermine the importance of Isl1 in the development of other organs in the developing embryo. For example Isl1 was shown to play a critical role in the differentiation of motor neurons (Liang et al., 2011; Pfaff et al., 1996). In the differentiation of the motor neurons Isl1 physically interacts with Ldb1 and Lhx3 and the fine balance of the formed complexes is critical for the cell fate decision of the progenitor cells towards interneuron or motor neuron cell type (Becker et al., 2002). Moreover Isl1 expression is detected in the pancreatic island where promotes proliferation and survival via direct activation of

Cyclin D1 and *c-Myc* (Guo et al., 2011b). *Isl1* deletion using a mesodermal *Bry-Cre* line caused severe bud defects (Narkis et al., 2012). Mutant embryos displayed absence of hind limb bud development and decrease expression of *Fgf10* and *Tbx4* (Narkis et al., 2012). Consistently deletion of Bmpr1a using Isl1-Cre revealed smaller hind limb buds starting by E10 due to decrease proliferation of the Isl1 positive progenitor population (Yang et al., 2006). Moreover Kaku and coworkers showed a key role for Isl1 in the development of the kidney and ureter (Kaku et al., 2013). *Isl1* deletion using a *Hoxb6Cre* line resulted in perinatal lethality with abnormalities in the kidney and ureter development (Kaku et al., 2013). Finally expression of Isl1, together with Ldb1 and Ldb2, was observed in the quiescent cells of the mouse intestinal epithelium (Makarev and Gorivodsky, 2014).

3.2.3. Isl1 involvement in Congenital Heart Diseases

Isl1 role in congenital heart disease is, at the moment, not completely clear. One report in 2010 showed an association of SNPs in the 3'UTR of *ISL1* gene in human to be associated with an higher susceptibility of congenital heart disease in black African/American population (Stevens et al., 2010), however the same polymorphism was not associated to increased risk in the Chinese population (Xue et al., 2012), or in the white population (Cresci et al., 2013). More recently copy number variation of *ISL1* was identified in a patient suffering from Tetralogy of Fallot (TOF) (Bansal et al., 2014). Furthermore *ISL1* haploinsufficiency has been linked to d-transposition of the great arteries (dTGA) in a child with no associated dysmorphic facial features and no cardiac arrhythmias (Osoegawa et al., 2014). In addition five novel transcription variants have associated with hypertrophic (HCM), dilated (DCM), arrhythmogenic right ventricular cardiomyopathy (ARVC), or with Emery–Dreifuss muscular dystrophy (EDMD) (Friedrich et al., 2013). One of these variants is a missense mutation p.Asn252Ser. This mutation was identified in the homozygous state in one DCM patient, and in the heterozygous state in 11 relatives, who did not suffer with DCM but presented other cardiovascular features. p.Asn252Ser variant is a ISL1 gain-of-function variant, which leads to greater activation of downstream targets such as *Mef2c* which are known to be involved in cardiac development, dilation, and hypertrophy (Friedrich et al., 2013).

3.3. Ldb1

Ldb1/NLI/CLIM-2 is a multi-adaptor protein isolated for the first time in three independent studies as a protein able to interact with the LIM domains of all the nuclear LIM containing proteins tested (Agulnick et al., 1996; Bach et al., 1997; Jurata et al., 1996).

3.3.1. Ldb1: Gene and Protein structure

The *Ldb1* gene in mouse is located on chromosome 19 (46107083 - 46119704, minus strand) and consists of 11 exons. Two transcripts producing two proteins of 375aa and 411aa in length, with the size of 42.7 KDa and 46.5 KDa respectively, are produced (Ensembl release 67, May 2012). These two proteins differ in the N-terminal domain (FIG 2.6 and 2.7).

Figure 3.7 Screenshot of the murine Ldb1 transcripts and their conservation degree in mammals.

Ldb1 protein has no DNA binding or enzymatic activities. The interaction with the LIM domain of LIM-Homeodomain (LIM-HD) proteins or LIM-Only (LMO) proteins was mapped to 38aa in the C-terminal domain of Ldb1, called LIM interaction domain (LID), which is able to bind at least one LIM domain (Bach et al., 1997; Jurata et al., 1996). The LID shows no obvious structural motif, but a hydrophobic patch, VMVV, and an acidic patch, DEDE, were identified (Jurata and Gill, 1997). Mutation of one or more of the aminoacids lying in the hydrophobic patch in alanine results in weak to strong perturbation of the binding of LID to LIM domains (Bhati et al., 2008).

```
1    MSVGCACPGCSSKSFKLYSPKEPPNGNAFPPFHPGTMLDRDVGPTPMYPPTYLEPGIGRH   60  P70662   LDB1_MOUSE
1    ----------------------------------MLDRDVGPTPMYPPTYLEPGIGRH   24  P70662-3 LDB1_MOUSE
                                        ************************

61   TPYGNQTDYRIFELNKRLQNWTEECDNLWWDAFTTEFFEDDAMLTITFCLEDGPKRYTIG  120  P70662   LDB1_MOUSE
25   TPYGNQTDYRIFELNKRLQNWTEECDNLWWDAFTTEFFEDDAMLTITFCLEDGPKRYTIG   84  P70662-3 LDB1_MOUSE
     ************************************************************

121  RTLIPRYFRSIFEGGATELYYVLKHPKEAFHSNFVSLDCDQGSMVTQHGKPMFTQVCVEG  180  P70662   LDB1_MOUSE
85   RTLIPRYFRSIFEGGATELYYVLKHPKEAFHSNFVSLDCDQGSMVTQHGKPMFTQVCVEG  144  P70662-3 LDB1_MOUSE
     ************************************************************

181  RLYLEFMFDDMMRIKTWHFSIRQHRELIPRSILAMHAQDPQMLDQLSKNITRCGLSNSTL  240  P70662   LDB1_MOUSE
145  RLYLEFMFDDMMRIKTWHFSIRQHRELIPRSILAMHAQDPQMLDQLSKNITRCGLSNSTL  204  P70662-3 LDB1_MOUSE
     ************************************************************

241  NYLRLCVILEPMQELMSRHKTYSLSPRDCLKTCLFQKWQRMVAPPAEPARQQPSKRRKRK  300  P70662   LDB1_MOUSE
205  NYLRLCVILEPMQELMSRHKTYSLSPRDCLKTCLFQKWQRMVAPPAEPARQQPSKRRKRK  264  P70662-3 LDB1_MOUSE
     ************************************************************

301  MSGGSTMSSGGGNTNNSNSKKKSPASTFALSSQVPDVMVVGEPTLMGGEFGDEDERLITR  360  P70662   LDB1_MOUSE
265  MSGGSTMSSGGGNTNNSNSKKKSPASTFALSSQVPDVMVVGEPTLMGGEFGDEDERLITR  324  P70662-3 LDB1_MOUSE
     ************************************************************

361  LENTQFDAANGIDDEDSFNNSPALGANSPWNSKPPSSQESKSENPTSQASQ  411  P70662   LDB1_MOUSE
325  LENTQFDAANGIDDEDSFNNSPALGANSPWNSKPPSSQESKSENPTSQASQ  375  P70662-3 LDB1_MOUSE
     ************************************************
```

Figure 3.8 Alignment of murine Ldb1 isoforms: Ldb1.1 (top) and Ldb1.3 (bottom).

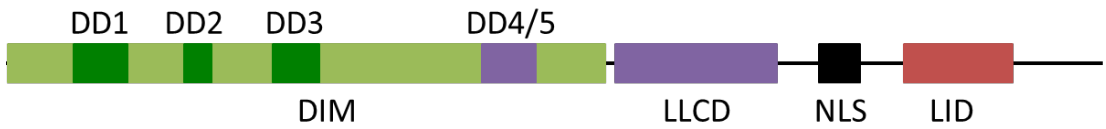

Figure 3.9 Scheme of Ldb1 protein showing the different protein domains. DIM, dimerization domain, DD1-5, subdomain identified in Krivega et al. (Krivega et al., 2014); LLCD, Ldb1/Chip conserved domain; NLS, nuclear localization signal; LID, LIM-interaction domain.

Using two-hybrid assay in yeast Breen and coworkers identified a dimerization domain (DD) comprising the first 200aa of Ldb1 (Breen et al., 1998). More recently using biophysical measurements, such as size exclusions chromatography combined with multi-angle laser light scattering, Matthews lab more accurately defined the DD (Cross et al., 2010). Moreover Cross and colleagues also showed that Ldb1 is able to form trimers more likely than dimers, at least in *in vitro* assays (Cross et al., 2010). Krivega and colleagues recently showed different subdomains within the dimerization domain of Ldb1 (Krivega et al., 2014). Five helices were identified, DD1 to DD5. The first three helix domains DD1 to DD3 are necessary for the dimerization of Ldb1, while DD4/5 is dispensable for dimerization (Krivega et al., 2014). Instead, DD4/5 is required for the interaction and recruitment of FOG1 and NuRD complex, and deletion of these domains leads to decrease histone acetylation and RNA Polymerase II recruitment (Krivega et al., 2014). Another important domain of Ldb1 is the Ldb1/Chip Conserved Domain (LLCD) immediately adjacent to the DD. The LLCD interacts with SSBPs (Chen et al., 2002) and with the E3-ligase RNF12, also

known as RLIM (Güngör et al., 2007). Finally Ldb1 harbors a Nuclear Localization Signal (NLS) in between the LLCD and the LID (Matthews and Visvader, 2003) (FIG 2.8).

3.3.2. *Ldb1 in development*

The important role of Ldb1 in development in association with LIM-containing transcription factors was first demonstrated in *Drosophila*. The balance of the relative amount of Chip (the Drosophila homologous of Ldb1) and Apterous, a LIM-HD transcription factor, is of great importance during wing development (Bach, 2000). Ldb1 role in development was also shown in Danio rerio and Mus musculus.
In zebrafish, *ldb1* transcript can be detected ubiquitously from gastrulation onward (Toyama et al., 1998). To test its function during embryonic development a mRNA encoding a Dominant Negative version of Ldb1 (DN-Ldb1) was injected in the fertilized egg leading to impaired development of the neural system. Injected embryos displayed several defects including absence of the midbrain-hindbrain boundary (MHB), severe inhibition of eye and sensory neurons development (Becker et al., 2002).

```
1    MSVGCACPGCSSKSFKLYSPKEPPNGNAFPPFHPGTMLDRDVGPTPMYPPTYLEPGIGRH   60  P70662   LDB1_MOUSE
1    ------------------------------------MLDRDVGPTPMYPPSYMEPGIGRH   24  O73715   LDB1A_DANRE
                                          **************:*:*******

61   TPYGNQTDYRIFELNKRLQNWTE-ECDNLWWDAFTTEFFEDDAMLTITFCLEDGPKRYTI  119  P70662   LDB1_MOUSE
25   TPYGNQTDYRIFELNKRLQNWTEQDCDNLWWDAFTTEFFEDDAMLTITFCLEDGPKRYTI   84  O73715   LDB1A_DANRE
     ********************** :**********************************

120  GRTLIPRYFRSIFEGGATELYYVLKHPKEAFHSNFVSLDCDQGSMVTQHGKPMFTQVCVE  179  P70662   LDB1_MOUSE
85   GRTLIPRYFRSIFEGGATELFYVLKHPKESFHNNFVSLDCDQCTMVTQNGKPMFTQVCVE  144  O73715   LDB1A_DANRE
     ********************:********:**.********* :****.***********

180  GRLYLEFMFDDMMRIKTWHFSIRQHRELIPRSILAMHAQDPQMLDQLSKNITRCGLSNST  239  P70662   LDB1_MOUSE
145  GRLYLEFMFDDMMRIKTWHFSIRQHREVVPRSILAMHAQDPQMLDQLSKNITRCGLSNST  204  O73715   LDB1A_DANRE
     ***************************:::********************************

240  LNYLRLCVILEPMQELMSRHKTYSLSPRDCLKTCLFQKWQRMVAPPAEPARQQPSKRRKR  299  P70662   LDB1_MOUSE
205  LNYLRLCVILEPMQELMSRHKTYSLSPRDCLKTCLFQKWQRMVAPPAEPARQAPNKRRKR  264  O73715   LDB1A_DANRE
     ************************************************** *.*****

300  KMSGGSTMSSGGGNTNNSNSKKKSPASTFALSSQVPDVMVVGEPTLMGGEFGDEDERLIT  359  P70662   LDB1_MOUSE
265  KMSGGSTMSSGGGNNNNSNSKKKSPASSFALSSQ--DVMVVGEPTLMGGEFGDEDERLIT  322  O73715   LDB1A_DANRE
     **************.************:******  ************************

360  RLENTQFDAANGIDDEDSFNNSPALGANSPWNSKPPSSQESKSENPTSQASQ  411  P70662   LDB1_MOUSE
323  RLENTQFDAANGIDDEDSFNSSPTMGTNSPWNSKAPSSQQGKNDNPSSQSSQ  374  O73715   LDB1A_DANRE
     ********************.**::*:******* ****:.*.:**:**:**
```

Figure 3.10 Alignment of murine Ldb1 and zebrafish Ldb1: aligment of protein sequences of murine (top) and zebrafish (bottom) Ldb1.

In mouse *Ldb1*$^{-/-}$ embryos displayed a clear phenotype at E8.5 and died around E9.5/E10 while heterozygous embryos were indistinguishable from the wild type embryos. Knockout embryos displayed severe anterior-posterior patterning defects,

anterior truncation, absence of blood islands and primitive vessels in the extra embryonic tissue and interestingly absence of heart and foregut formation (Mukhopadhyay et al., 2003).

To better understand the *Ldb1*$^{-/-}$ phenotype, Mukhopadhyay and coworkers performed several *in situ* stainings for some specific neural and mesodermal/cardiac markers. *Six3*, a marker of the forebrain, and *En2*, marker of the MHB, expression was completely absent in *Ldb1*$^{-/-}$ embryos while the expression pattern of other neural markers, i.e. *Krox2*, was abnormal. Molecular analysis of the heart phenotype showed a reduction of *Nkx2-5* expression at E7.75 and an abnormal pattern of one of earliest mesodermal/cardiac maker *Mesp1* at E6.75 suggesting a defect in the generation and/or migration of heart progenitors (Mukhopadhyay et al., 2003). In addition *in situ* analysis of primitive streak and nodal markers showed duplication of both these structures in *Ldb1*$^{-/-}$ embryos (Mukhopadhyay et al., 2003). The deformation of the body axis, disphormic somites and the hemapoietic defects described for the first time in mouse were also observed upon morpholino knock-down of *ldb1* in zebrafish (Meier et al., 2006).

The failure of neurogenesis and erythropoiesis was also observed when embryonic stem (ES) cells lacking *Ldb1* were in vitro differentiated in embryoid bodies (EBs) (Hwang et al., 2008; Mylona et al., 2013). Interestingly the *Ldb1*$^{-/-}$ ESCs were able to differentiate only in smooth muscle-like cells as assessed by sarcomeric α-actinin staining (Hwang et al., 2008). During erythropoiesis *Ldb1* is present in dynamic Ldb1-containing complexes that bind regulatory sequences of key genes in erythropoiesis (Meier et al., 2006; Mylona et al., 2013). Conditional knockout of *Ldb1* in fetal liver using a Tie2Cre led to maturation defects of the erythropoietic lineages showing the requirement of *Ldb1* for definitive erythropoiesis (Li et al., 2011). This *in vivo* result was confirmed *in vitro* showing that *Ldb1*$^{-/-}$ EBs generated hemapoietic colonies at much lower frequency of *Ldb1*$^{+/-}$ or *Ldb1*$^{+/+}$ controls (Li et al., 2011; Mylona et al., 2013). ChIP-seq screening indicated Ldb1-binding sites were in important regulatory domains of critical genes for hemapoietic stem cells self-renewal and differentiation, including *Gata2, Gata1, Raldh2, Sox7, Sox17, Sox18*, *Pbx1, Meis1, Runx1, Myb, Pten*

and *Foxo3*. Further, these genes were downregulated upon deletion of Ldb1 (Li et al., 2011; Mylona et al., 2013).

3.4. Three-dimensional genome organization

During interphase chromosome occupy specific regions of the nuclei called Chromosome Territories (CTs) (FIG 2.10) (Cremer and Cremer, 2010; Cremer et al., 2006; Meaburn and Misteli, 2007). This territorial organization represents a basic feature of nuclear architecture (Cremer et al., 2006). CTs were predicted at the turn of the century by Carl Rabl and Theodor Boveri (Boveri, 1909; Rabl, 1885) The presence of CTs was further confirmed by the Hi-C derived map of the nuclear organization of human lymphoblastoid cell line at 1Mb resolution (Lieberman-Aiden et al., 2009). CTs, estabilished in metaphase, are conserved during cell cycle and results in a symmetrical arrangements of CTs in the two daughter nuclei (Cremer et al., 2006).

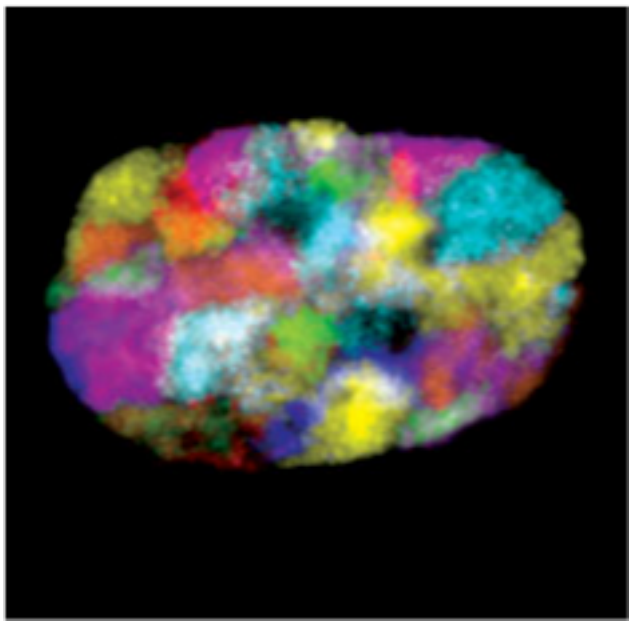

Figure 3.11 Chromosome Territories in human cell nucleus: 24 colors karyotyping of a human cell nucleus. Each chromosome occupies a well defined space in the nucleus, with little overlapping. (Adapted from Speicher and Carter, 2005).

Hi-C studies revealed a further three dimensional organization of the genome inside the nuclei. The genome is organized into Topologically Associated Domains (TADs) that are found in several model organisms, from prokariotes, such as *Caulobacter*

crescentus to yeast, plants and mammals (Dixon et al., 2012; Feng et al., 2014; Jin et al., 2013; Le et al., 2013; O'Sullivan et al., 2004; Rao et al., 2014). The TADs are described as local highly self-interacting megabase-sized regions (Dixon et al., 2012). TADs are flanked by boundary regions that separate topological domains (Dixon et al., 2012). These topological domains are stable in different cell types and higly conserved between different species (Dixon et al., 2012; Shen et al., 2012).

Although rare inter-chromosomal, or even between different TADs, interactions have been mapped using Hi-C approaches these interactions are of critical importance for gene regulation/activation. However, recent improvent of the Hi-C technology started to unveil the presence of interactions between different TADs (Shen et al., 2012). For example following TNF-α stimulation in HUVEC cells three NF-kB-responsive genes (*SAMD4A*, *TNFAIP2*, both located on chromosome 14 but 50Mb apart and *SLC6A5*, located on chromosome 11) engage in chromosomal interactions critical for their transcription (Fanucchi et al., 2013). These long-range, possible interchromosomal, interactions have been previously name “gene kissing” (Kioussis, 2005) or “chromosome kissing” (Cavalli, 2007).

Furthermore three dimensional organization has been proven of critical importance in the regulation of the Hox genes clusters (Noordermeer et al., 2011). In this model the inactive cluster form a single 3D domain organization enriched in H3K27me3. Once transcription starts the Hox cluster assumes a bimodal 3D organization where actively transcribed genes move to a transcriptional permissive, H3K4me3 enriched, chromatin domain (Noordermeer et al., 2011) (FIG 2.11).

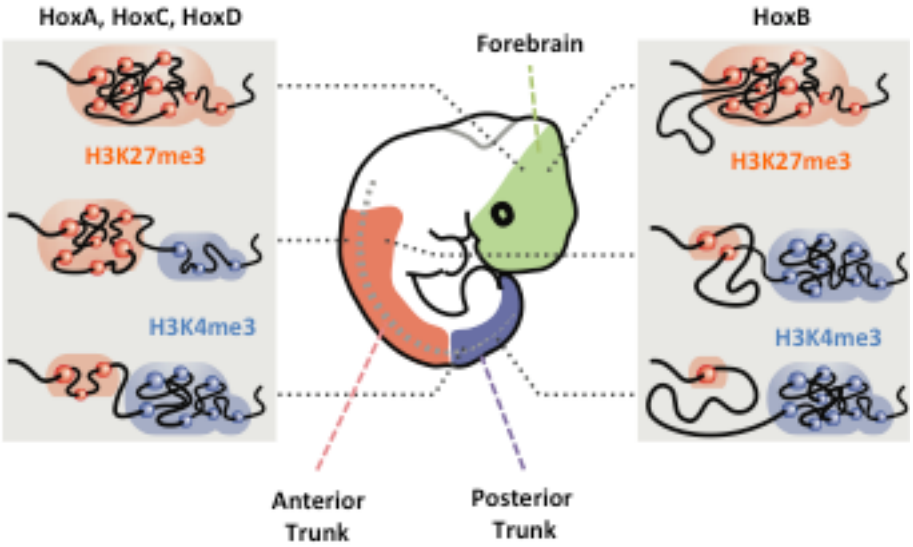

Figure 3.12 Hox genes clusters are organized in three dimensional domains: 3D model of activation of Hox genes in different region of E10,5 mouse embryo. Transcriptionally inactive domains are depicted in red, active domains in blue. Forebrain showed in green, anterior trunk in light-red and posterior trunk in purple-blue. (Noordermeer et al., 2011).

3.5. Long-range enhancer-promoter interactions

Transcriptional regulation of gene expression plays an important role in establishing the diversity of tissues and cell types. It is well established that the tissue specific pattern of expression of genes is achieved through the activity of *cis*-regulatory elements called enhancers and insulators that are able to activate or repress transcription of a given gene in a particular tissue or cell type (Noonan and McCallion, 2010).

In a widely accepted model enhancers recruits transcription factors and form a loop toward the promoter allowing the interaction of the complexes built on these two different regulatory elements (de Wit and de Laat, 2012; Dekker et al., 2002). Activity of the enhancers is dependent on several factors and converge the signal from different environmental stimuli. The ability of the enhancer to be activated only upon specific stimuli and only in a particular subset of tissues or cells makes them difficult to study, as the same enhancer could give different outputs depending on the type of the assay and the cell line used (Noonan and McCallion, 2010).

Enhancers can function over great distances, even reside within or beyond a different transcriptional unit or on a different chromosome (Noordermeer et al., 2008).

To study and identify looping of active enhancers to the specific promoters the Chromosome Conformation Capture assay was developed in the Dekker lab (Dekker et al., 2002). This technology allowed different groups to analyze the spatial organization of several genomic loci spanning few kilobases, as for example the interferon gamma gene domain of 25Kb (Eivazova and Aune, 2004), to loci spanning several hundred kilobases such as the mammalian *ß-globin* locus (Song et al., 2007; Tolhuis et al., 2002).

One of the best-characterized loci that is regulated by chromosomal looping is the *ß-globin* locus. This locus contains five different genes, similarly arranged in human and mouse, embryonic ε, fetal $^{G}\gamma$ and $^{A}\gamma$ and adult б and ß, which are expressed sequentially during development (Kim and Dean, 2012). These genes are under control of the upstream LCR that consist of a series of DNase I hypersensitive sites (HS). The LCR sequentially loops to the promoters and other regions of the different globin genes during development to activate their transcription in the embryo (Kim and Dean, 2012; Palstra et al., 2003). Importantly the chromosome looping between LCR and *ß-globin* promoter is observed only in tissue expressing *ß-globin*, such as the liver at E14.5, but not in the nucleus of cells isolated from brain at E14.5, a tissue negative for *ß-globin*, where the globin locus acquires a linear conformation (Palstra et al., 2003; Tolhuis et al., 2002). The chromatin loops between DNase I hypersensitive sites and the promoter of the globin gene are mediated by the core of active HS, which are enriched for PolII and H3K4Me2 (Fang et al., 2007; Levings et al., 2006). These chromosome loops are mediated by transcription factors specific for erythroid cells, such as GATA-1 and its co-factor FOG-1, that bound the *ß-globin* promoter and LCR (Vakoc et al., 2005) and by the widely expressed factor Ldb1 (Deng et al., 2012; Song et al., 2007). Additionally the interaction between the HS-60/62 and 3'HS1 in mouse and HS-111 and 3'HS1 in human are mediated by CTCF (Palstra et al., 2003; 2008) (FIG 2.10).

The looping paradigm described for the *ß-globin* locus was then generalized to other

genes. The *c-kit* gene expression during development is maintained through the interaction between the enhancer, distant 114Kb, and c-kit promoter mediated by GATA-2. When GATA-1 replaces GATA-2 the enhancer loop is lost in favor to a chromosomal loop between promoter and the gene body resulting in downregulation of *c-kit* (Dean, 2011; Jing et al., 2008).

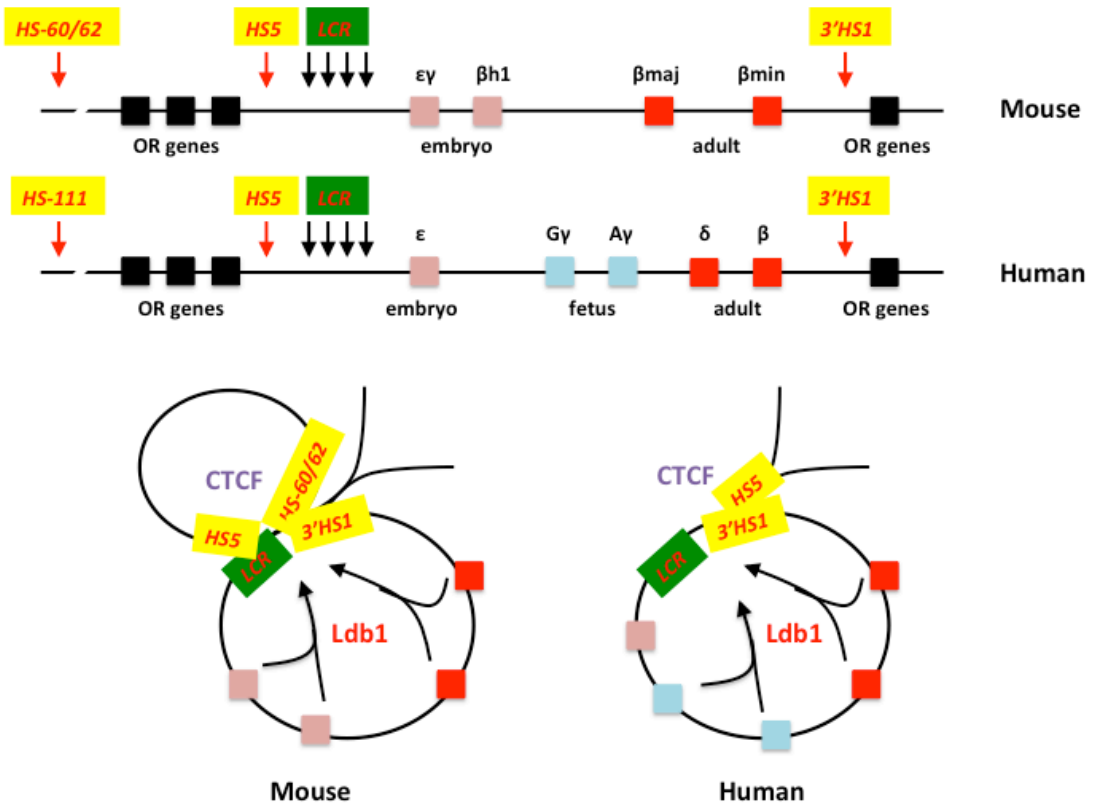

Figure 3.13 Ldb1 and CTCF control long-range interaction in the *ß-globin* locus: The *ß-globin* loci in mouse and human (top panel). DNase I hypersensitive sites are shown in yellow. LCR in green. Olfactory receptors genes are depicted as black boxes. In mouse the εγ and βH1 genes are transcribed in the embryo while the ßmaj and ßmin are transcribed in adult mouse. In human the globin genes are transcribed in three different developmental stages. ε is transcribed in the embryo; Gγ and Aγ in the fetus; δ and β in adult Chromatin loop formation in the *ß-globin* loci (bottom panel). The interactions between HS-60/62, HS5, LCR and 3'HS1 are mediated by CTCF. The developmental regulated chromatin loopings of actively transcribed genes and the HS/LCR are mediated by Ldb1. the globin genes are closely positioned with HS-60/62, HS5, LCR and 3'HS1 in the mouse β-globin locus when they are actively transcribed (Adapted from Kim and Dean, 2012).

4. Aim of the Thesis

Isl1+ cardiovascular progenitors can differentiate in all the lineages of the heart, namely atrial/ventricular cardiomyocytes, endothelial and smooth muscle cells of the vasculature (Kattman et al., 2006; Moretti et al., 2006; Wu et al., 2006), however the molecular mechanisms underlying this process is to date poorly understood.

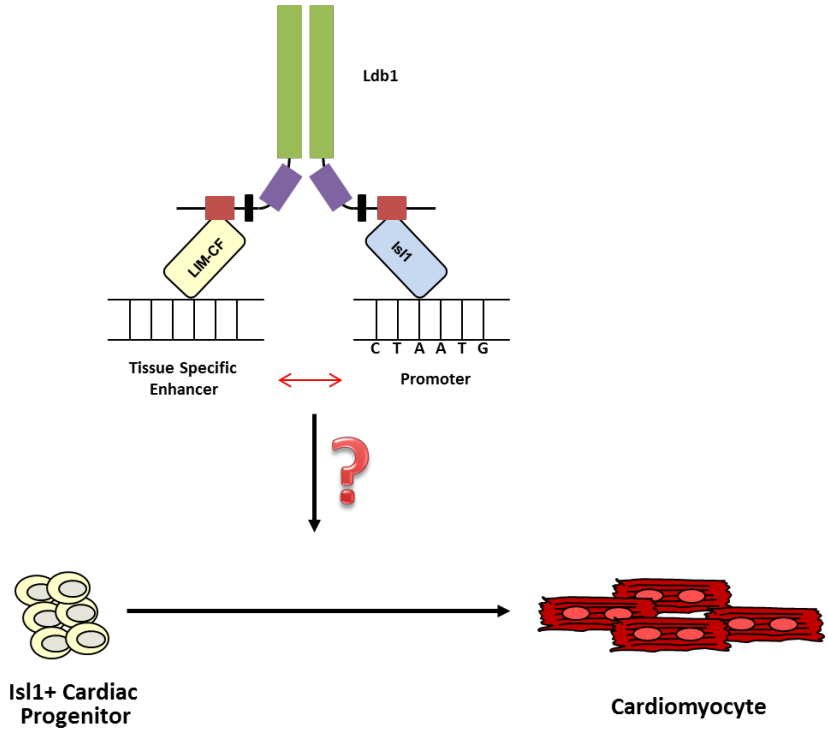

Figure 4.1 Are Ldb1-mediated long range promoter-enhancer interactions important for cardiac development? Thanks to its ability of oligomerize Ldb1 can promote long-range interactions between different LIM- transcription factors containing complexes.

Specifically, during heart development the LIM domain transcription factor Isl1 is required for the proliferation, survival, and migration of SHF cells into the forming heart, as a consequence of which Isl1-deficient mouse embryos lack the right ventricle and the outflow tract, both structures derived from the SHF (Cai et al., 2003). Ldb1 interacts with LIM-containing transcription factors thus serving as a molecular bridge between transcription complexes sitting on promoters and enhancers of important developmental regulated genes during hematopoiesis (Deng et al., 2012; Song et al., 2007; Stadhouders et al., 2012a). However the role of Ldb1 in heart development is completely unknown. On the other hand, Ldb1 deficiency results in early embryonic lethality with a series of developmental defects, including anterior–posterior patterning defects, posterior axis duplication and lack of heart

formation (Mukhopadhyay et al., 2003). Therefore, we reasoned that Isl1 and Ldb1 might work in concert to regulate SHF development by promoting heart specific long-range chromatin interactions leading to cell-type specific transcriptional programs.

5. Results

5.1. Ldb1 Knockout prevents cardiac differentiation

5.1.1. *Ldb1$^{-/-}$ derived embryoid bodies do not beat*

In order to study the role of Ldb1 during cardiogenesis embryonic stem cells *Ldb1$^{+/+}$*, *Ldb1$^{+/-}$* and *Ldb1$^{-/-}$* (Mylona et al., 2013) were differentiated in embryoid bodies and appearance of cluster of cardiomyocytESCs able to autonomously beat (beating foci) was observed.

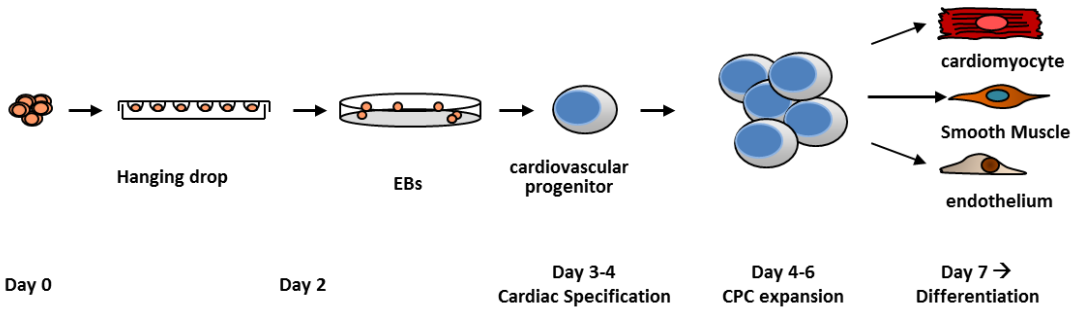

Figure 5.1: Schematic representation of the differentiation process of the embryoid bodies. At day 3-4 of differentiation cardiovascular progenitor cells (CPC) start to specify. Between day 4 and day 6 CPC population expands. Starting from day 7 CPC differentiates into cardiomyocytes, endothelial and smooth muscle cells.

In wild type Ldb1 or heterozygote embryoid bodies first appearance of beating foci was observed at day 6 of development. In contrast Ldb1 KO derived embryoid bodies do not develop any beating foci (FIG 4.2).

Having observed a drastic lack of cardiomyocytes in the Ldb1 KO derived EBs we wanted to understand whether other cardiovascular lineages were affected in Ldb1 KO derived embryoid bodies. Therefore analysis for different lineage markers was performed at day 6 and day 9 of differentiation.

This analysis showed a depletion of endothelial and cardiomyocyte lineages and a shift towards smooth-muscle expressing lineages (FIG 4.3).

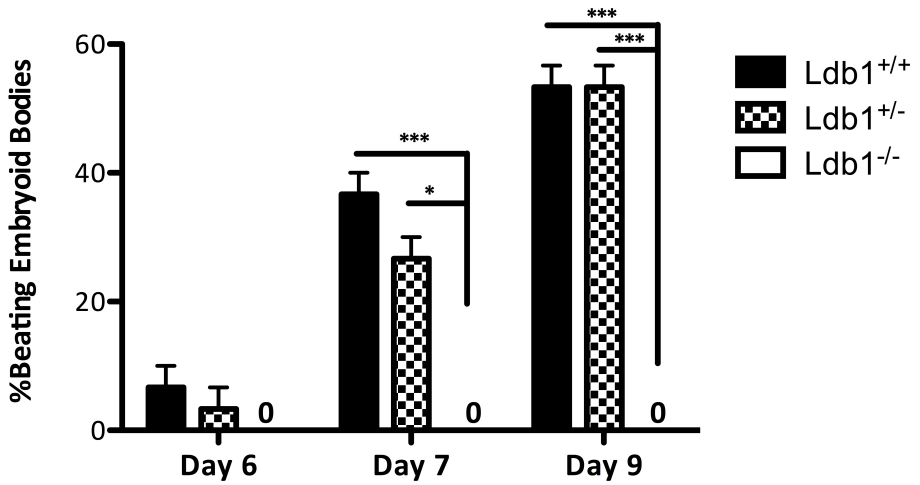

Figure 5.2 Beating analysis: Percentage of beating EBs in control and Ldb1-deficient ES cell lines differentiated.

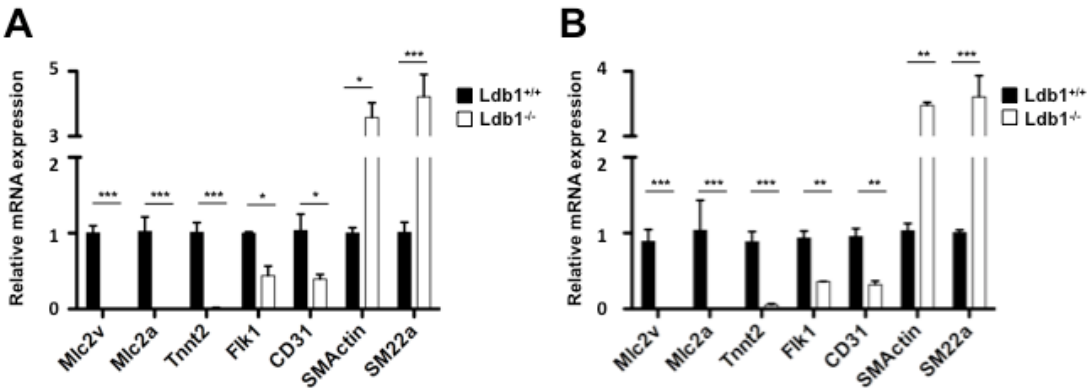

Figure 5.3 Ldb1 depletion blocks cardiomyocyte differentiation: Relative mRNA expression for cardiomyocyte markers (*Mlc2v, Mlc2a, Tnnt2*), and markers for endothelial cells (*Flk1, CD-31*) and smooth muscles (*SM-actin, SM-22α*) in *Ldb1*$^{+/-}$ and *Ldb1*$^{-/-}$ normalized to GAPDH mRNA expression at day 6 **(A)** and day 9 **(B)** of differentiation. (n=3; * p<0,05; ** p<0,01; *** p<0,001)

5.1.2. Mesoderm is formed in Ldb1 KO embryoid bodies

Since cardiovascular progenitor cells are mesoderm derivates (FIG 4.6) we analyzed whether Ldb1-deficiency affects early developmental decisions such as mesodermal induction.

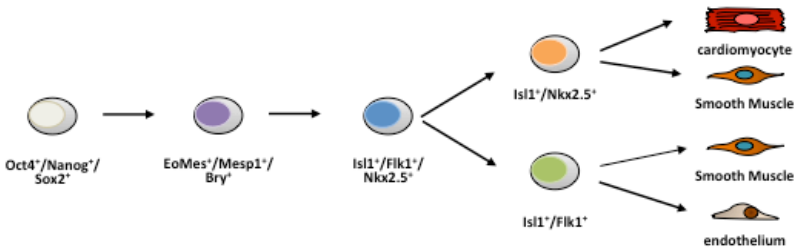

Figure 5.4 Scheme of the differentiation process of mesodermal cells: Multi-potent Isl1/Flk1/Nkx2.5 positive cardiovascular progenitor cells derived from mesodermal EoMes/Mesp1/Bry positive progenitor cells and are able to generate all the cell lineages present in the cardiovascular system (Kattman et al., 2006; Moretti et al., 2007; Wu et al., 2006)

Ldb1$^{-/-}$ derived embryoid bodies were analyzed for the differentiation of mesodermal precursor in order to rule out the possibility that depletion of cardiomyocyte-like cells was due to a depletion of mesodermal lineage. Analysis at different days of differentiation showed a proper expression, albeit one day delayed, of mesodermal markers *Bry, EoMes, Mesp1 and Mesp2* (FIG 4.5) in *Ldb1*$^{-/-}$ EBs compared to control EBs.

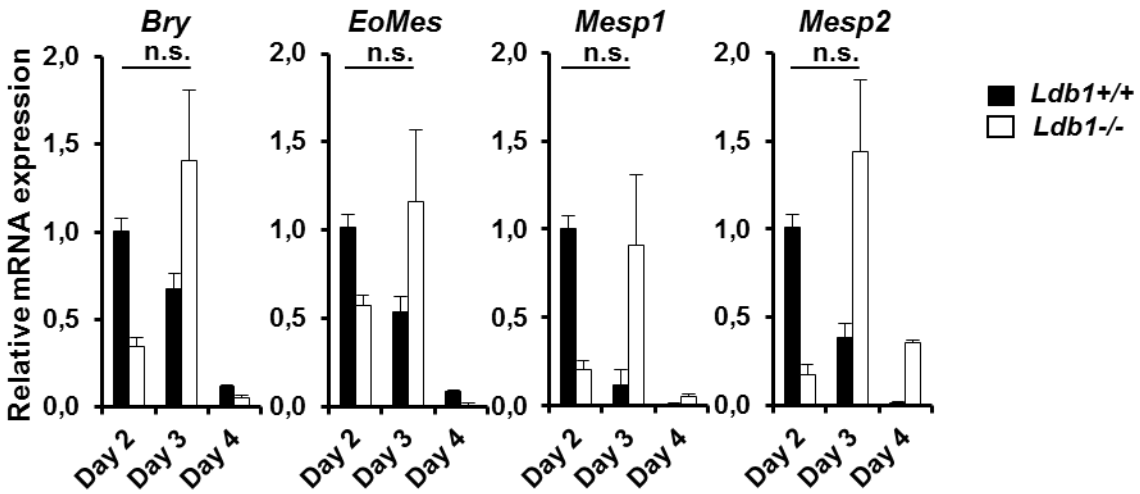

Figure 5.5 Mesodermal formation is not affected in Ldb1 depleted EBs: Relative mRNA expression of mesodermal markers in EBs differentiated from *Ldb1*$^{+/-}$ and *Ldb1*$^{-/-}$ ESCs at different days of EB differentiation (n=3).

5.1.3. Ldb1 knock out affects the expression of Second Heart Field transcription factors

To investigate the cause of depletion in cardiomyocyte and endothelial lineages the expression of cardiovascular progenitor markers was analyzed. Interestingly Ldb1 depleted embryoid bodies showed a significant downregulation of second heart field markers (*Tbx1, Hand2, Fgf10*) and of some pancardiac markers (*Nkx2-5, Mef2c*), while the expression of other pancardiac markers (*Tbx20*) and first heart field markers (*GATA-4, Tbx5, Hand1*) expression was unchanged (FIG 4.6).

On the other hand the expression of *Isl1*, the first marker of the second heart field, was not dramatically reduced (FIG 4.6).

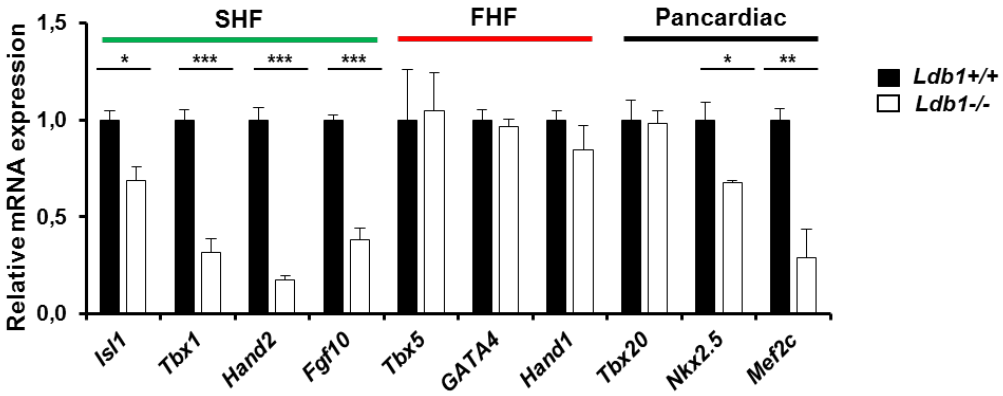

Figure 5.6 SHF markers are downregulated in *Ldb1*$^{-/-}$ EBs: Relative mRNA expression of SHF, FHF and pancardiac progenitor markers normalized to GAPDH mRNA expression at day 4 of EBs differentiation. (n=3; * p<0,05; ** p<0,01; *** p<0,001)

5.2. Specific Deletion of Ldb1 in Second Heart Field is embryonic lethal

To prove the role of Ldb1 in second heart field cardiomyocyte differentiation an Ldb1 conditional allele was generated and the obtained Ldb1$^{+/flox}$ animals were crossed with Isl1-Cre line to obtain a specific deletion in second heart field progenitor cells (FIG 4.7).

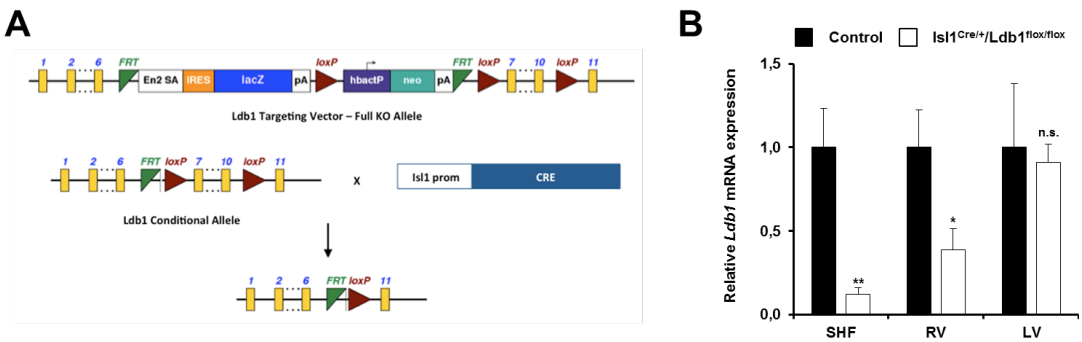

Figure 5.7 Ldb1 depletion in the SHF: Scheme of the Ldb1 flox allele and the resulted floxed allele obtained after crossing with animal bearing the CRE recombinase under control of *Isl1* promoter. **(A)** Relative mRNA of *Ldb1* in microdissect SHF, RV or LV of E9.25 control or $Isl1^{cre/+}Ldb1^{flox/flox}$ embryos. Data are mean ± SEM, n=3 for each genotype. (* p<0,05; ** p<0,01).

Embryos obtained from the crosses revelead that conditional deletion of *Ldb1* in the SHF leads to embryonic lethality at E10.5 (FIG 4.8A). Already at E9.5 $Isl1^{Cre/+}Ldb1^{flox/flox}$ embryos could be recognized by a shortened OFT and a small RV. (FIG 4.8B, FIG 4.9). Careful morphological examination after embedding of the embryos in paraffin and sectioning confirmed the shorter outflow tract and the smaller RV, both structures derived from SHF progenitors (FIG 4.9). Further expression analysis for cardiomyocyte markes *Mlc2a, Mlc2v* and *Tnnt2* showed downregulation in the RV and OFT, but not in the LV and IFT (FIG 4.9C). Alltogether these data support a key role of Ldb1 in SHF development.

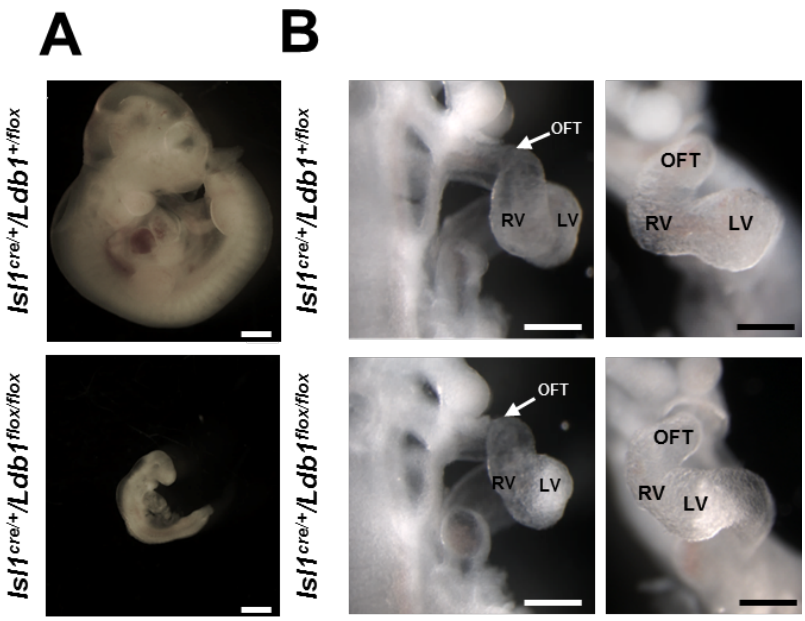

Figure 5.8 Ldb1 deletion in SHF causes growth arrest at E9.5 and cardiac defects: Gross appearance of control ($Isl1^{Cre/+}Ldb1^{+/flox}$) and $Isl1^{Cre/+}Ldb1^{flox/flox}$ embryo at E10.5 showing developmental arrest of the Ldb1-deficient embryos. Scale bars 500 µm. **(A)** Higher magnification of E9.5 embryos showing short OFT and a small RV. Scale bars 200 µm. **(B)**

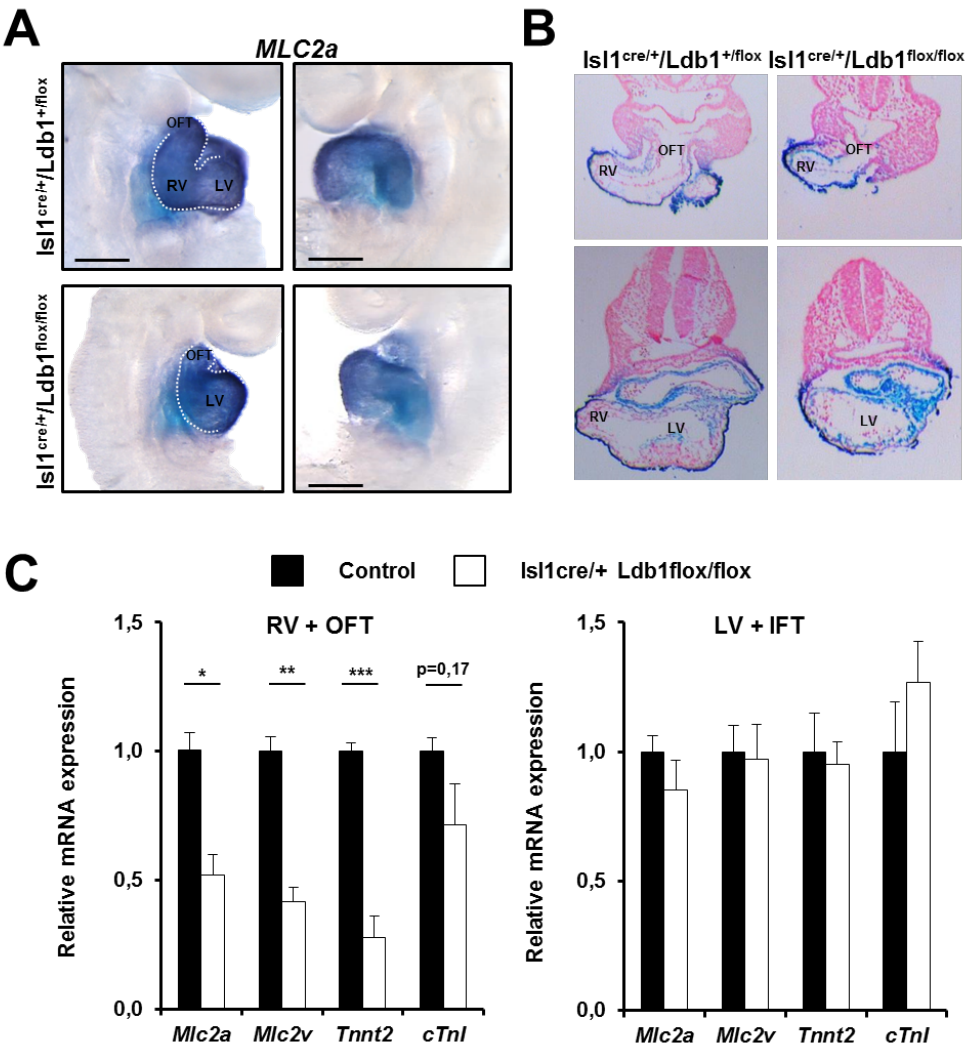

Figure 5.9 Phenotype analysis of *Isl1*$^{Cre/+}$*Ldb1*$^{flox/flox}$ embryos: Right and left views of E9.5 control and *Isl1*$^{Cre/+}$*Ldb1*$^{flox/flox}$ embryos after *in situ* hybridization with MLC2a riboprobe. Scale bars 100 µm. **(A)** Paraffin section analysis of MLC2a *in situ* at E9.5 in control and *Isl1*$^{+/Cre}$*Ldb1*$^{flox/flox}$ embryos. Sections were counterstained with fast red to visualize the embryonic structure. Scale bars 100 µm. OFT, Outflow tract; RV, Right Ventricle; LV, Left Ventricle **(B)** Relative mRNA expression analysis of cardiomyocyte genes in dissected outflow tract and right ventricle or inflow tract and left ventricle of E9.25 wild-type and *Isl1*$^{cre/+}$*Ldb1*$^{flox/flox}$ embryos. Data are mean ± SEMs, n=3 for each genotype **(C)**

5.3. Ldb1 depletion causes Isl1 ablation

To better understand the role and the molecular mechanism underlying Ldb1 function in the formation of SHF progenitor population *Isl1* expression was analyzed at both mRNA and protein level. Interestingly a mild reduction of mRNA expression was observed for *Isl1* (FIG 4.10A), however Isl1+ cells were virtually absent in *Ldb1*$^{-/-}$ EBs (FIG 4.10B). Western blot analysis of nuclear extract of control and *Ldb1*$^{-/-}$ confirmed the low levels of Isl1 in Ldb1 deficient EBs (FIG 4.10C).

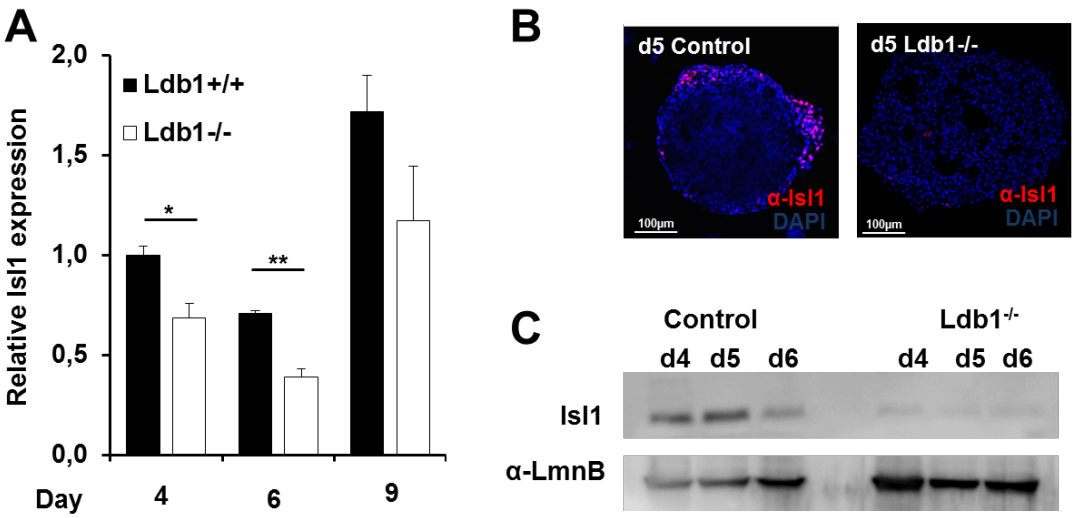

Figure 5.10 Depletion of Ldb1 causes depletion of Isl1 in EBs: Analysis of Isl1 expression in Ldb1 KO embryoid bodies. Relative mRNA level of endogenous *Isl1* transcript at day 4, 6 and 9 of differentiation **(A)**. Embryoid bodies were collected at day 5 and stained with anti-Isl1 antibody **(B)**. Western Blot analysis of nuclear extract of embryoid bodies at day 4, 5 and 6 in *Ldb1*$^{+/-}$ and *Ldb1*$^{-/-}$ derived embryoid bodies, lamin B1 used as loading control **(C)**.

In a similar manner *Isl1* mRNA expression was not changed in *Ldb1*$^{-/-}$ embryos at E8.5 compared to wild type or *Ldb1*$^{+/-}$ littermates control (FIG 4.11A) but it could not be detected at protein level (FIG 4.11B).

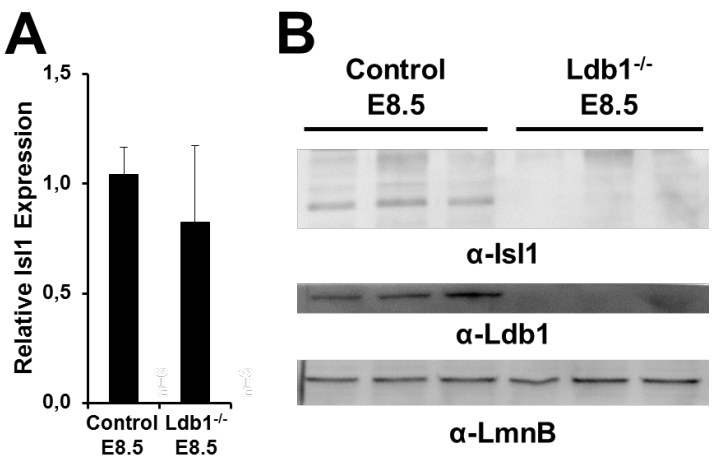

Figure 5.11 Depletion of Ldb1 causes depletion of Isl1 in E8.5 embryos: Relative mRNA expression normalized to GAPDH mRNA of *Isl1* in *Ldb1*$^{-/-}$ and control embryos at E8.5 error bars represent SEMs. **(A)**. Isl1 protein levels in total protein lysate of Control embryos or *Ldb1*$^{-/-}$ embryos at E8.5. LaminB1 is used as loading control **(B)**.

5.4. Isl1 is poli-ubiquitilated and degraded

LIM-HD proteins were shown to be regulated by the proteasome and that binding of Ldb1 to the LIM domains stabilizes their protein levels (Güngör et al., 2007). To

address whether the absence of Isl1 protein could be explained by targeting of Isl1 protein to the proteasomal degradation pathway, HEK293T cells were treated with MG-132, a proteasomal inhibitor, and Isl1 level were analyzed by western blot.

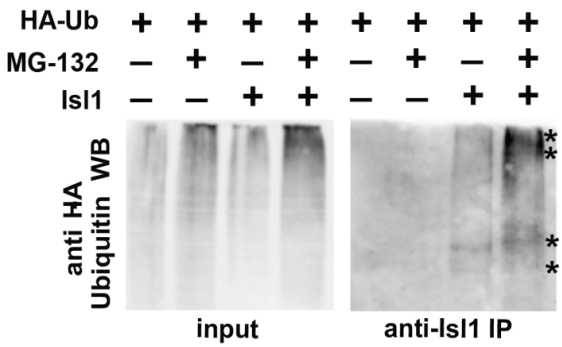

Figure 5.12 Isl1 is poli-ubiquitinated: HEK293T cells were transiently transfected with plasmid expressing a HA-tagged version of ubiquitin and Isl1. Cells were treated with DMSO (control) or 25µM MG-132 for 5 hours and subsequently the protein lysate was precipitated with anti-Isl1 antibody and detected with anti-HA antibody.

Indeed western blot analysis of protein extract of MG-132 treated cells showed the appearance of slower-migrating ubiquitinated forms of Isl1, indicating that Isl1 is targeted to proteasomal degradation (FIG 4.12).

To map which domain is important for the ubiquitination of Isl1, Isl1 full length and deletion constructs were overexpressed in HEK293T and treated as previously with MG-132. Interestingly, the levels of a truncated protein lacking the LIM2 domain did not change upon proteasomal inhibition, while Isl1ΔLIM1 were significantly higher (FIG 4.13).

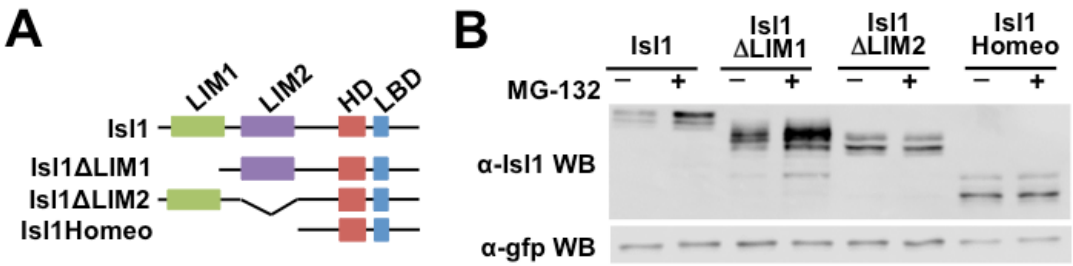

Figure 5.13 The LIM2 domain of Isl1 is critical of Isl ubiquitinilation: Schematic representation of wild type Isl1 and Isl1 deletion constructs, lacking either LIM1 or LIM2 or harboring only the homeodomain **(A)**. HEK293T cells were transiently transfected with Isl1, Isl1ΔLIM1, Isl1ΔLIM2 and Isl1HOMEO, together with GFP (internal control) and treated with DMSO (control) or 25µM MG-132 for 5 hours. Protein levels were detected with anti-Isl1 antibody. GFP was used as internal transfection and loading control **(B)**.

5.5. Ldb1 protects Isl1 at protein level

To investigate whether Ldb1 might protect Isl1 from proteasomal degradation similar to Lhx3 (Güngör et al., 2007), HEK293T cells were transfected with a constant amount of pcDNA3-Isl1 plasmid and increasing amount of plasmid expressing Ldb1 full length (pcDNA3-Flag-HA-Ldb1) or its truncations.

In HEK293T Isl1 protein was efficiently and in a dose dependent manner stabilized by Ldb1. Similarly, a truncated protein lacking the dimerization domain (DD), but containing the LIM-interaction domain (LID), Dominant Negative Ldb1 (DN-Ldb1), stabilized in a dose dependent manner Isl1 protein. These findings corroborate the idea that the stabilization of Isl1 at protein levels depends on its interaction with Ldb1. Consistent with this hypothesis, Ldb1ΔLID, a truncation of Ldb1 that lacks the LID domain, responsible for the interaction of Ldb1 with Isl1, did not have any effect on the levels of Isl1 proteins (FIG 4.14B).

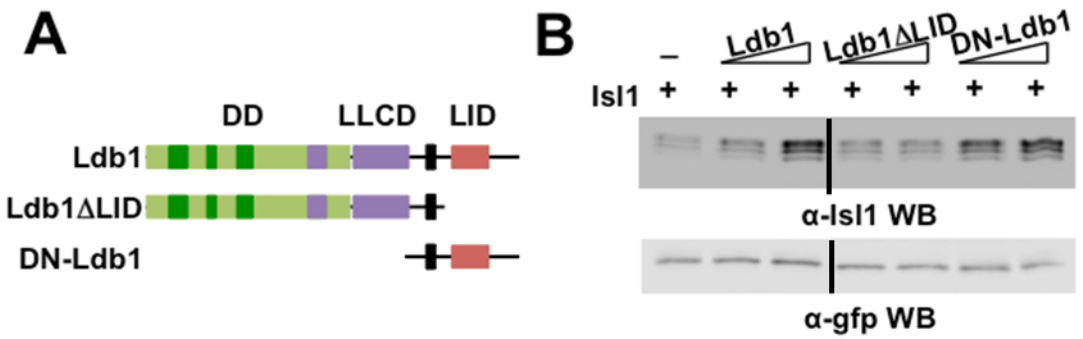

Figure 5.14 Ldb1 stabilizes Isl1: Schematic representation of wild-type Ldb1 and Ldbl1 deletion constructs, lacking either DD and LLCD or LID domain **(A)**. HEK293T cells were transiently transfected with GFP (500ng), constant amount of Isl1 (10µg) alone or with increasing concentration (5 and 9µg) of Ldb1, Ldb1ΔLID and DN-Ldb1. Protein levels were detected with anti-Isl1 antibody. GFP was used as internal transfection and loading control.

To analyze more in detail the mechanism of stabilization of Isl1, Isl1 truncations were overexpressed in presence or absence of DN-Ldb1. DN-Ldb1 led to a significant increase of Isl1 protein levels (FIG 4.15). Interestingly the protein levels of Isl1 truncations lacking either the LIM1 or the LIM2 domain or containing only the homeodomain did not change (FIG 4.15).

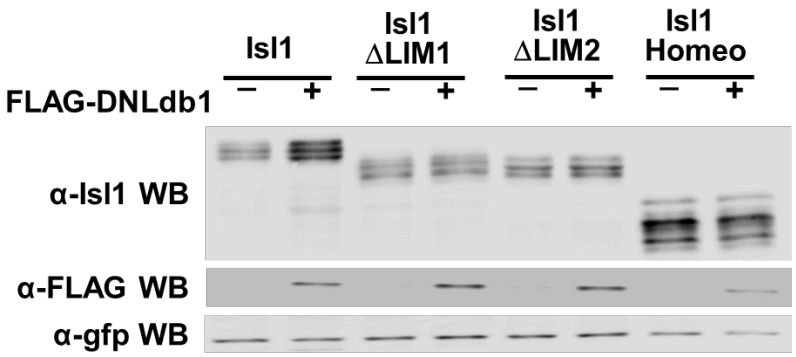

Figure 5.15 Ldb1 interaction stabilizes Isl1: HEK293T cells were transiently transfected with Isl1, Isl1ΔLIM1, Isl1ΔLIM2 and Isl1HOMEO, together with GFP (internal control) in the presence or absence of FLAG-Ldb1. Protein levels were detected with anti-Isl1 and anti-FLAG antibodies. GFP was used as internal transfection and loading control.

5.6. Interaction of Isl1 and Ldb1

In vitro studies mapped the interaction between Isl1 and Ldb1 to the LIM1 domain of Isl1 and the LID domain of Ldb1 (Agulnick et al., 1996; Bach et al., 1997; Jurata and Gill, 1997).

To confirm the interaction in cell system Ldb1 and Isl1, or Isl1 truncations, were transfected in HEK293T. As suggested by the *in vitro* studies previously mentioned the interaction happens via a specific binding of the LIM interaction domain (LID) of Ldb1 and the LIM1 domain of Isl1 (Fig 4.16).

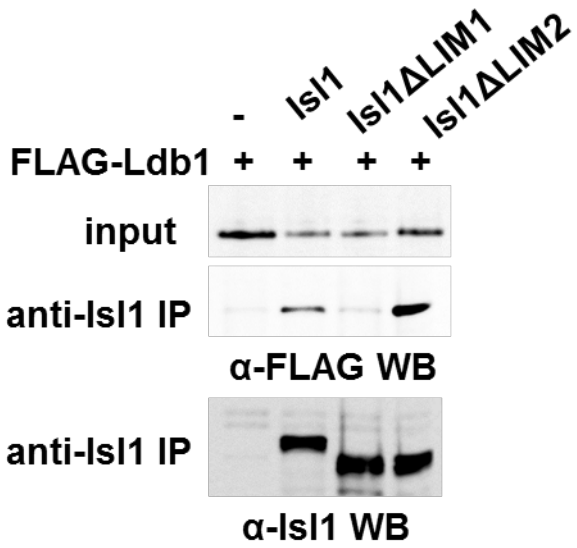

Figure 5.16 LIM1 domain of Isl1 mediates the interaction with Ldb1: FLAG-HA-Ldb1 and Isl1 or Isl1 deletion constructs were transiently expressed in HEK 293T cells and immunoprecipitation with an anti-Isl1 antibody, followed by immunoblot analysis with an anti-FLAG antibody was performed.

5.7. Isl1-Ldb1 interaction stabilize Isl1 at protein levels

Taken together this data suggest that the binding of Ldb1 to LIM1 of Isl1 protects it from ubiquitination and subsequently from proteasomal degradation (FIG 4.17). Moreover, the LIM2 domain of Isl1 is necessary for Isl1 ubiquitination.

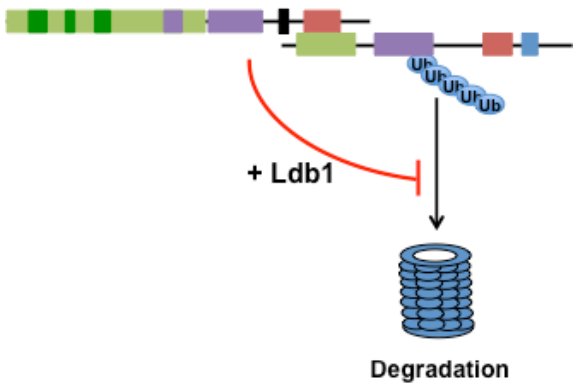

Figure 5.17 Ldb1 binds to Isl1 and protects it from proteasomal degradation. The interaction between the LID domain of Ldb1 and LIM1 domain of Isl1 prevents the ubiquitination of Isl1 through the LIM2 domain stabilizing Isl1 at protein level.

5.8. Ldb1 and Isl1 interact in cardiac progenitors

Ldb1 plays important role as cofactor for LIM-proteins during embryonic development. To test whether the interaction of Isl1 and Ldb1 is important during heart development nuclear lysate from the embryoid bodies differentiated for five days, a stage in which cardiac progenitors are highly enriched, was immunoprecipitated with Ldb1 antibody.

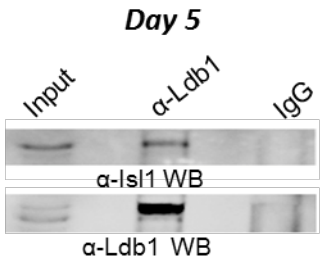

Figure 5.18 Isl1 and Ldb1 physically interacts during cardiogenesis: Nuclear Lysate from day5 EBs was immunoprecipitated with α-Ldb1 and probed with α-Isl1 antibody

Immunoprecipitation with α-Ldb1 antibody could efficiently and specifically co-precipitate Isl1 protein from the lysate (FIG 4.18), strengthening the hypothesis that Isl1 and Ldb1 interact during cardiac development.

When Isl1, Ldb1 and Ldb1/Isl1 were overexpressed in the wild type ESCs an increased number of beating foci in the embryoid bodies could be observed (FIG 4.19). The combination of both factors together resulted in an even higher number of beating foci compared to when Isl1 or Ldb1 alone were expressed (FIG 4.19).

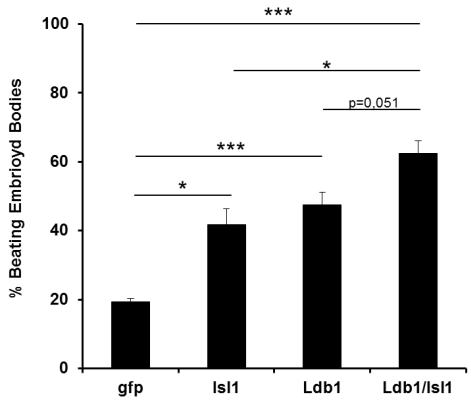

Figure 5.19 Beating analysis of EBs overexpressing Isl1, Ldb1 and their combination: Percentage of beating EBs at day 7 of differentiation derived from ESCs overexpressing either GFP alone (control) or Isl1, Ldb1 or a combination of the factors and GFP.

5.9. Generation of Ldb1, Isl1 or Isl1/Ldb1 stable ES cell lines

In order to investigate more in detail the role of Ldb1 during heart development stable cell line overexpressing Ldb1, Isl1 and in combination were generated.

Lentiviral construct expressing GFP and puromycin were used for fluorescence activated cell sorting (FACS) of the overexpressing cells (FIG 4.20).

GFP-expressing cells isolated by FACS were then subjected to differentiation in EBs.

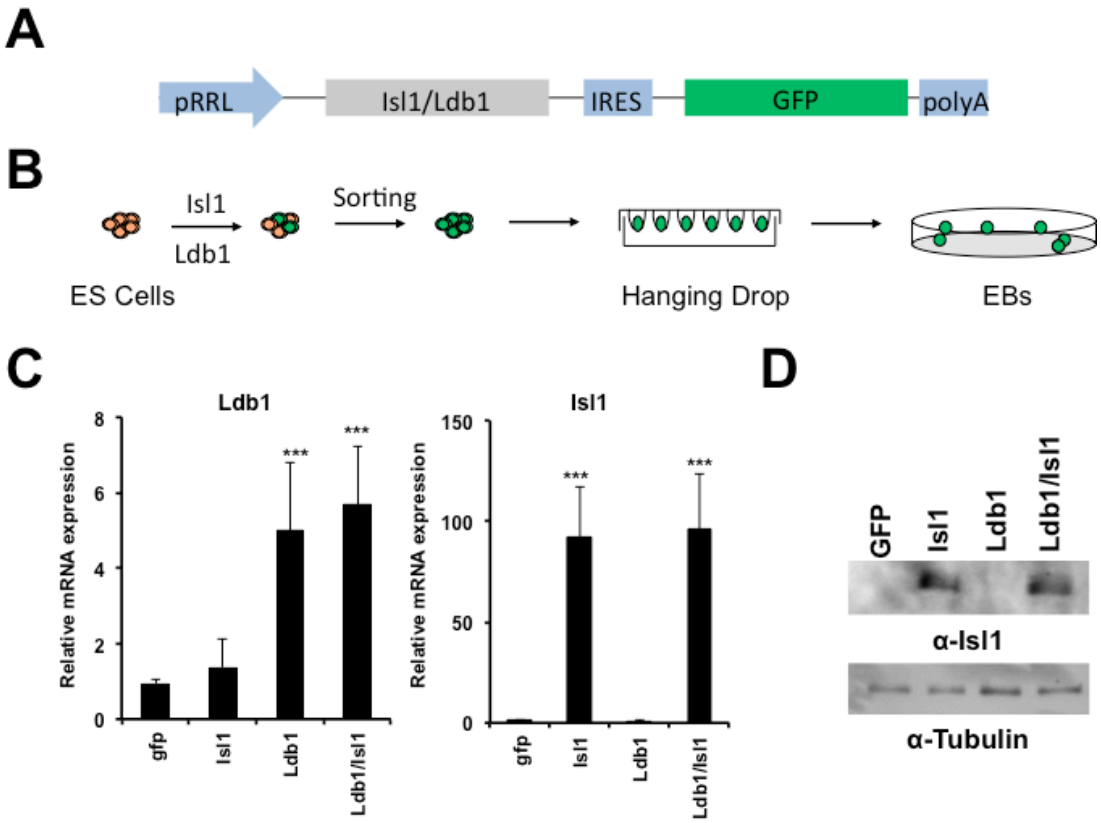

Figure 5.20 Generation of stable ES cell lines: Schematic representation of the plasmid used for overexpression of Isl1 or Ldb1 in ESCs **(A)** Scheme of the experimental approach. **(B)** mRNA expression of Ldb1 and Isl1 in ESCs expressing GFP alone (control) or Isl1, Ldb1 and their combination together with GFP. Data are mean ± SEMs, n=3. **(C)** Total protein extracts of ESCs were probed with anti-Isl1 antibody. Tubulin is used as loading control **(D)**.

5.9.1. Overexpression of Isl1 and Ldb1 affects the differentiation of all cardiovascular lineages

Since Isl1^{+} cardioprogenitor population can give rise to multiple lineages (FIG 4.6 and (Kattman et al., 2006; Moretti et al., 2006; Wu et al., 2006) the expression of markers for cardiomyocytes, endothelial and smooth muscles cell lines was analyzed by qPCR at day 7.

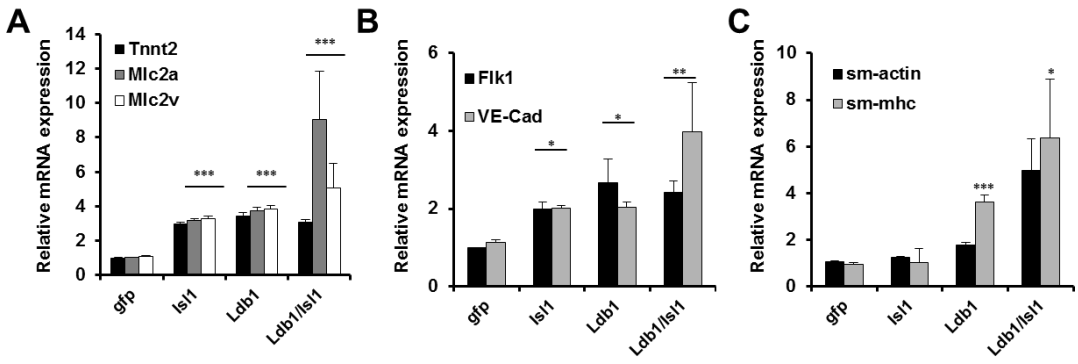

Figure 5.21 Isl1 and Ldb1 increase the differentiation of all cardiovascular lineages: Relative mRNA expression analysis for cardiomyocyte **(A)**, endothelial **(B)** and smooth muscle **(C)** cells markers normalized to GAPDH mRNA at day 7 of differentiation. Error bars represent SEMs derived from three biological replicates.

Consistently with the increase number of beating foci (FIG 4.20) the expression of cardiomyocyte markers (*Tnnt2, Mlc2a and Mlc2v*) was significant increased (FIG 4.21A). Furthermore the expression of endothelial (*Flk1, VE-Cad*) and smooth muscle (*sm-actin, sm-mhc*) was increased (FIG 4.21B and C).

5.9.2. Overexpression of Isl1 or Ldb1 affects the expression of cardiac progenitor markers

To test whether the increased expression of all cardiovascular lineages was due to increased number of cardiovascular progenitor the expression cardioprogenitor markers was analyzed. Cardiac progenitor genes which play key roles in SHF development (*Isl1*, *Mef2c, Hand2, Fgf10*) were significantly up-regulated (FIG 4.22A). On contrast the expression of FHF markers (*GATA-4, Tbx5* and *Hand1*) was not changed at day 4 of EBs differentiation (FIG 4.22B).

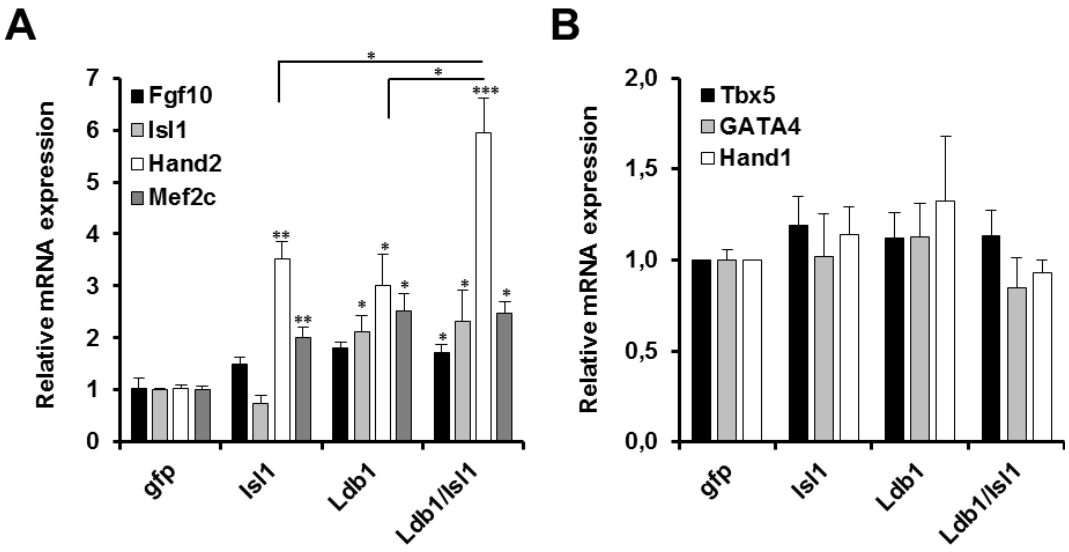

Figure 5.22 Ldb1 expression affects SHF marker genes expression: Relative mRNA expression analysis for SHF progenitor (*Hand2, Mef2c, Fgf10* and *Isl1*) **(A)** and FHF progenitor (*GATA-4*, *Tbx5* and *Hand1*) **(B)** markers normalized to GAPDH mRNA at day 4 of differentiation. Error bars represent SEMs derived from three biological replicates.

5.10. Isl1 and Ldb1 interact genetically

To investigate whether the interaction between Isl1 and Ldb1 is important *in vivo* *Isl1*$^{+/-}$ mice were crossed with *Ldb1*$^{+/-}$. The single heterozygote animal survived till adulthood however only 5% of double heterozygote pups could be recovered at weaning stage, albeit an expected 25% ratio. Further analysis showed that *Isl1*$^{+/-}$ *Ldb1*$^{+/-}$ embryos died immediately after birth (Table 4.1).

Genotype	E9.5	E16.5	Pups	Expected Ratio
Isl1$^{+/+}$ *Ldb1*$^{+/+}$	18 (25,0)	12 (23,5)	26 (34,21)	25
Isl1$^{+/-}$ *Ldb1*$^{+/+}$	18 (25,0)	13 (25,5)	22 (28,95)	25
Isl1$^{+/+}$ *Ldb1*$^{+/-}$	17 (23,6)	12 (23,5)	24 (31,58)	25
Isl1$^{+/-}$ *Ldb1*$^{+/-}$	19 (26,4)	14 (27,5)	4 (5,26)***	25

Table 5.1 *Isl1*$^{+/-}$ *Ldb1*$^{+/-}$ animals die at birth: Analysis of the genotype of born animal from the crosses *Isl1*$^{+/-}$x*Ldb1*$^{+/-}$ shown as number of recovered embryos/pups and percentage. ***p<0,0001 Chi squared test.

5.10.1. Double heterozygous embryos have heart abnormalities

To understand the reason of death of the double heterozygous animals histological analysis of the hearts of the double heterozygous was performed.

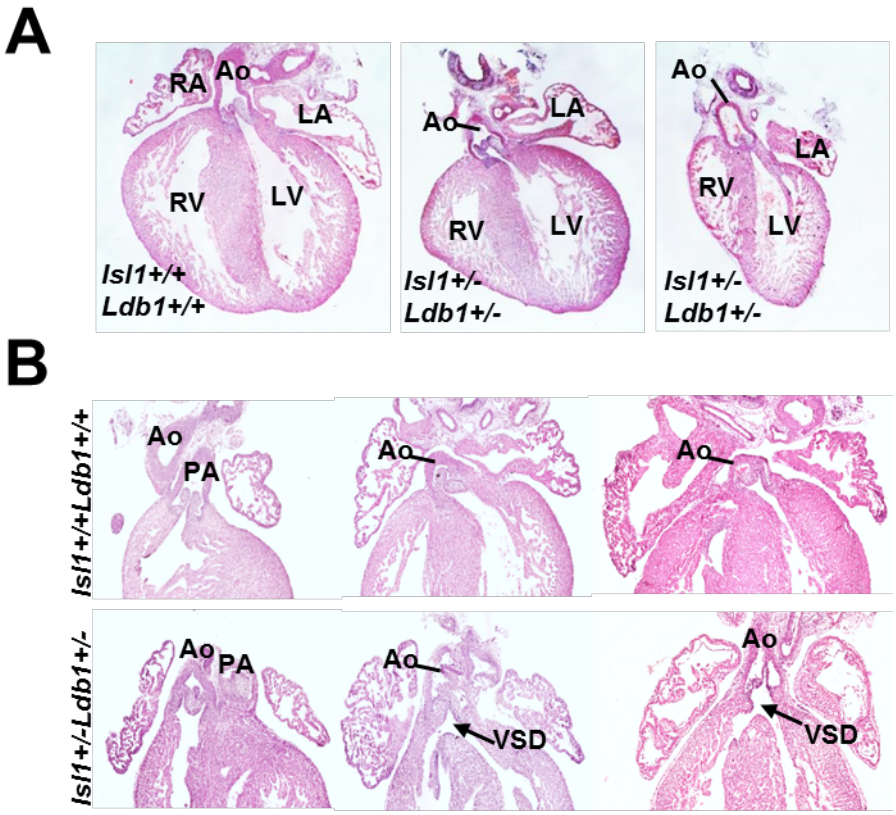

Figure 5.23 *Isl1*$^{+/-}$ *Ldb1*$^{+/-}$ displayed cardiac defects: H&E staining of representative paraffin section of E16.5 **(A)** hearts of wild type, (controls) and double heterozygote *Isl1*$^{+/-}$*Ldb1*$^{+/-}$ embryos. Higher magnification DORV or OA in E18.5 hearts with VSD **(B)**. Abbreviations: Ao, Aorta; LA, left atrium; LV, left ventricle; RA, right atrium; and RV, right ventricle; DORV, double outlet right ventricle; OA, overriding aorta; VSD, ventricular septal defect.

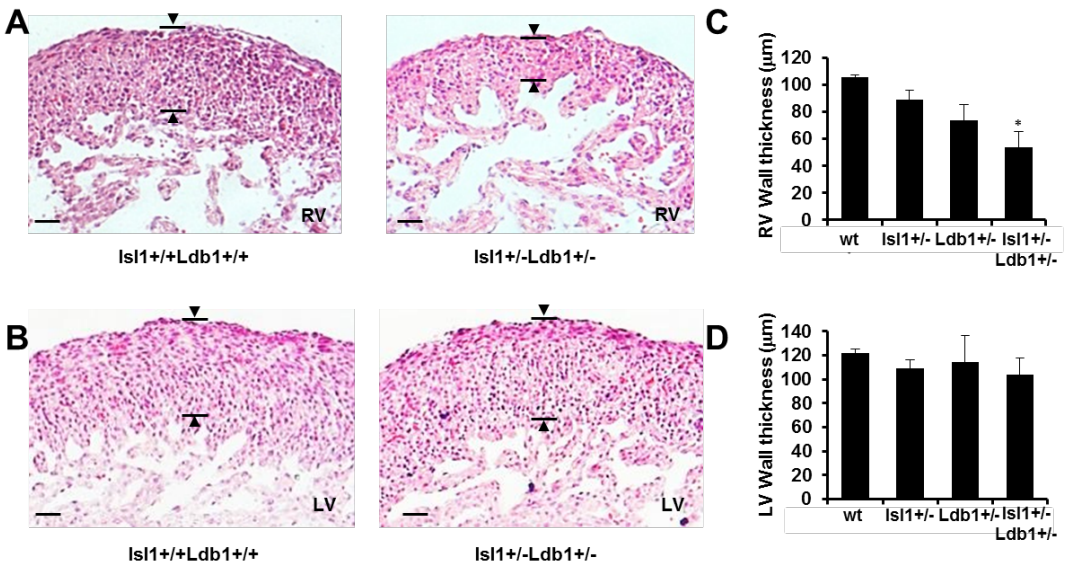

Figure 5.24 *Isl1*$^{+/-}$*Ldb1*$^{+/-}$ embryos displayed thinner RV: H&E staining of representative paraffin section of RV **(A)** and LV **(B)** hearts of wild type, (controls) and double heterozygote *Isl1*$^{+/-}$*Ldb1*$^{+/-}$ embryos. Morphometric analysis of RV **(C)** and LV **(D)** compact myocardial thickness. n=4.

Consistently with the role of Isl1/Ldb1 complex in SHF development the histological analysis of the double heterozygous embryos revealed several defects in heart structures derived from the Isl1+ cardiovascular progenitor population, including ventricular septal defects (VSD) (FIG 4.23A middle panel), malrotation of the OFT vessels (FIG 4.35A right panel; FIG4.23B middle and left panels) and small and thin right ventricle (FIG 4.23 and 4.24).

5.10.2. Decrease number of cardiomyocyte at E14.5

To investigate whether the decrease thickness of the RV is caused by a decrease number of cardiomyocytes a cytofluorimetric analysis was performed.

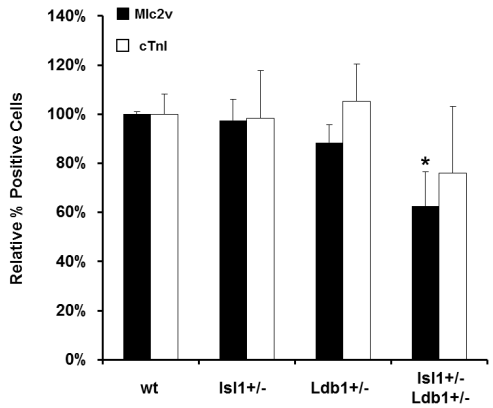

Figure 5.25 Cardiomyocyte number is reduced in *Isl1$^{+/-}$ Ldb1$^{+/-}$* embryos: Relative percentage of cTnI^{pos} (white bars) and Mlc2v^{pos} (black bars) cells in isolated E14.5 ventricles derived from wild type, Isl1$^{+/-}$, Ldb1$^{+/-}$ (controls) and double heterozygote Isl1$^{+/-}$Ldb1$^{+/-}$ embryos analyzed by FACS. Data are mean ± SEMs, n≥4.

Isolated ventricles from E14.5 embryos were dispersed to single cells and stained with α-Mlc2v or α-cTnI antibodies to quantify the number of cardiomyocytes. The analysis showed a significant decrease number of Mlc2v^{pos} cells in the *Isl1$^{+/-}$Ldb1$^{+/-}$* embryos (FIG 4.25).

Taken together these results, namely defects in the right ventricle and in the outflow tract in Isl1/Ldb1 double heterozygous embryos, reinforce our hypothesis of a crucial role for Ldb1 in SHF development.

5.10.3. Expression of cardiomyocyte and SHF markers is decreased at E9.5

To analyze the primary cause of the observed heart defects of the *Isl1*$^{+/-}$*Ldb1*$^{+/-}$ embryos the heart and the SHF from E9.5 embryos were dissected.

qPCR analysis revealed significant downregulation of *Mef2c*, *Hand2*, *Fgf10* in the SHF of Isl1/Ldb1 double heterozygous embryos (FIG 4.26A). In the heart of the double heterozygous embryos specific downregulation of cardiomyocytes markers (*Tnnt2*, *Mef2c*, *Fgf10* and *Mlc2v*) was observed (FIG 4.26B).

These data support a key role of Isl1/ Ldb1 complex in cardiomyocyte differentiation and *Mef2c*, *Hand2* and *Fgf10* expression.

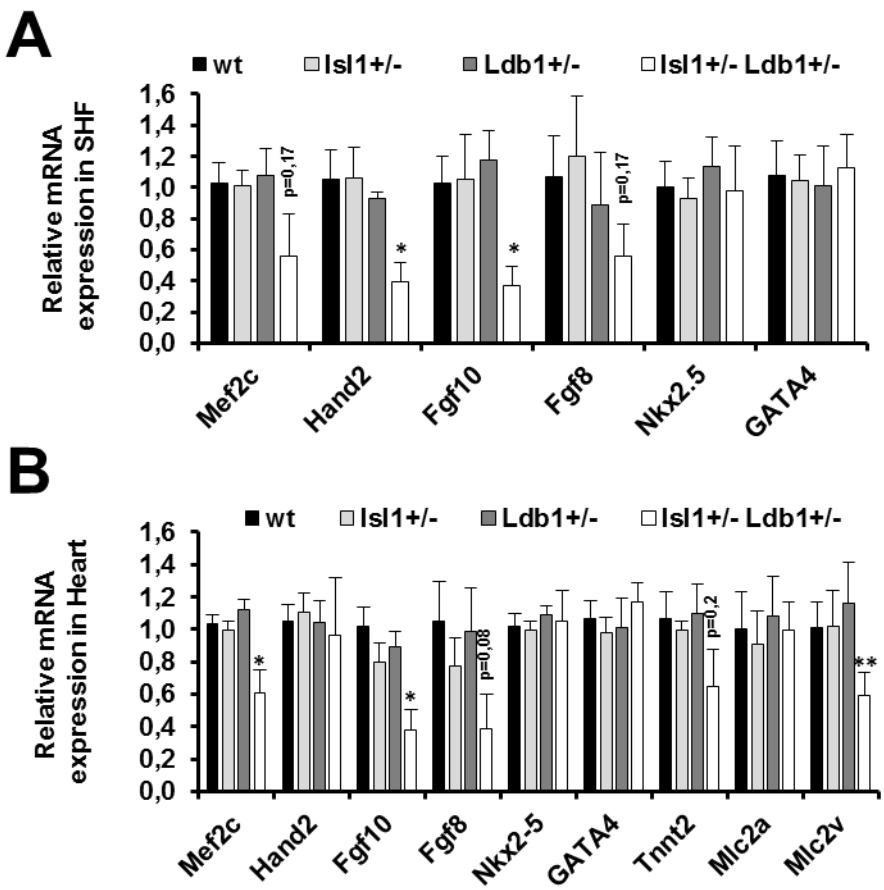

Figure 5.26 Expression of cardiac genes is compromised in haplodeficient embryos : Relative mRNA expression analysis for progenitors markers normalized to GAPDH mRNA from micro dissected SHF region at E9.5 **(A)**. Relative mRNA expression analysis for cardiomyocyte markers normalized to GAPDH mRNA from micro dissected hearts at E9.5 **(B)**. Data are mean ± SEMs, n=4 for each group.

5.11. The dimerization domain of Ldb1 is required for SHF development

To further analyze the functions of Ldb1 and its role in promoting long-range chromosomal interactions during heart development a DN-Ldb1 construct was ectopically express in early stage zebrafish embryos and in Ldb1 KO ESCs (FIG 4.27B and C).

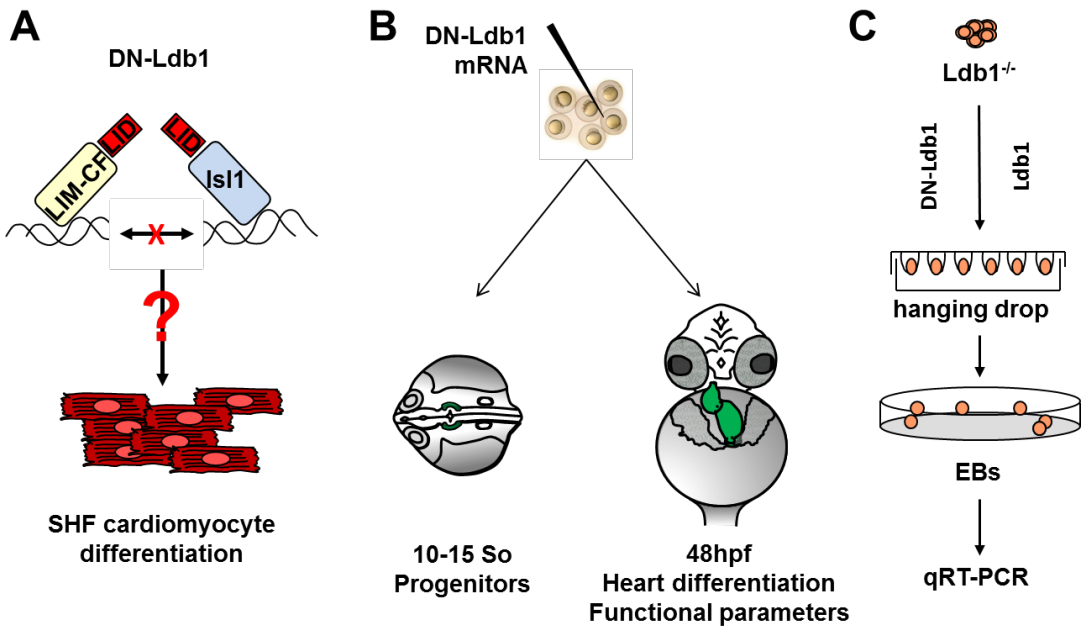

Figure 5.27 Scheme of the experimental approaches to study the role of long-range interactions during cardiac development: Scheme showing the inability of the DN-Ldb1 truncation to promote long-range interactions due to its inability of dimerize **(A)**. Scheme of the experimental approach in zebrafish embryos **(B)** and ESCs **(C)**.

The DN-Ldb1 contains the highly conserved LID domain, which confers the ability to bind with high affinity the LIM domains of LIM containing transcription factors, and can efficiently stabilize Isl1 at protein levels (FIG 4.14 and 4.15), but lacks the dimerization domain, necessary to promote long-range interactions (FIG 4.27A).

5.11.1. Isl1 progenitor population is present in DN-Ldb1 injected embryos

Injection of the in vitro synthesized mRNA encoding for the Flag-HA-DN-Ldb1 led to the expression of the dominant negative construct in an ubiquitous manner in the zebrafish embryo (FIG 4.28). Consistent with previous studies, the overexpression of DN-Ldb1 led to defects in eye and brain development (FIG 4.29) (Becker et al., 2002).

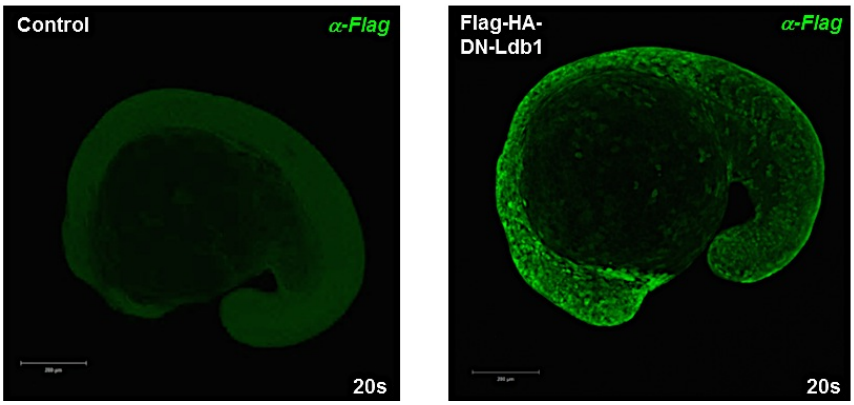

Figure 5.28 DN-Ldb1 is ubiquitously expressed in *D.rerio* embryos: Immunostaining analysis of Flag-HA-DN-Ldb1 in control (left) and injected (right) zebrafish embryos at 20 somites stage.

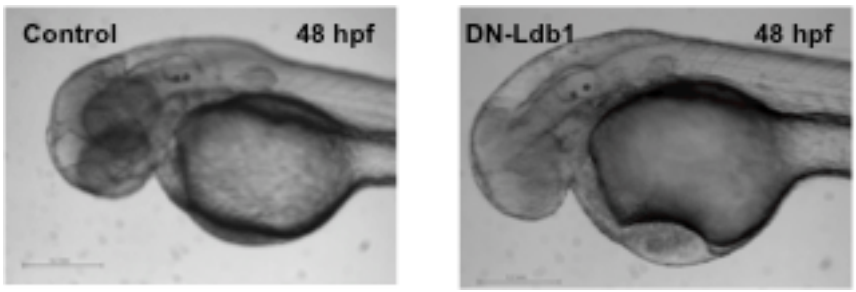

Figure 5.29 DN-Ldb1 overexpression causes brain and eye defects: Control or DN-Ldb1 mRNA injected *Tg(myl7:EGFP-HsHRAS)*^{s833} embryos at 48 hours post fertilization (hpf). Lateral view, anterior to the left.

5.11.2. Loss of function of Ldb1 causes defects of the zebrafish heart

Additionally to the eye and brain phenotype more than 70% of DN-Ldb1 injected fishes developed strong bradycardia and arrhythmia (FIG 4.30).

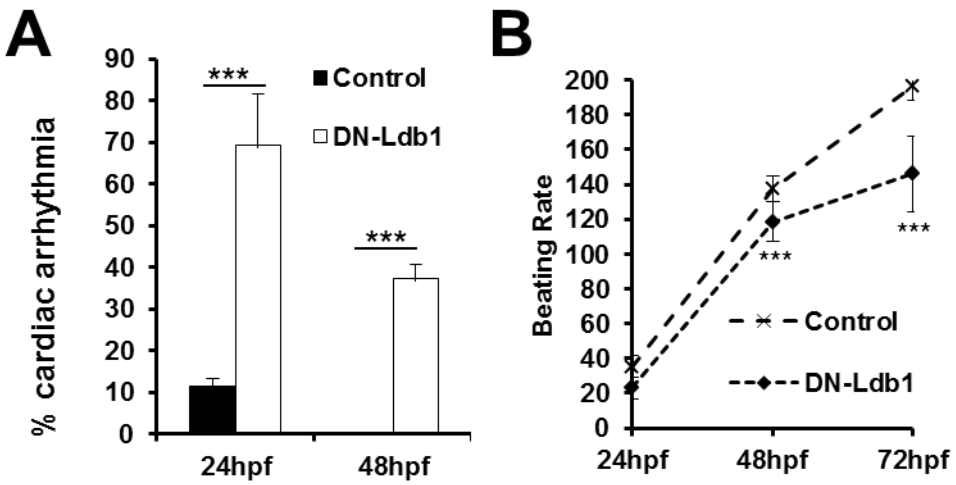

Figure 5.30 DN-Ldb1 overexpression causes bradycardia and arrhythmia: Analysis of beating frequency **(A)** and percentage of embryos with heart arrhythmia **(B)** at different times of embryonic development in control and treated embryos.

At 48hpf, pacemaker cells of the zebrafish heart are located in the inflow tract (de Pater et al. 2009) and *isl1*-deficient embryos showed a similar phenotype as a result of a failure of cardiomyocyte differentiation at the inflow pole (de Pater et al. 2009). To investigate whether injection of the DN-Ldb1 mRNA impaired cardiomyocyte differentiation at the venous pole a zebrafish line that expresses a EGFP-HsHRAS protein (mGFP) under the control of the *myl7* promoter (myl7:EGFP-HsHRAS)^{S883} was used. Confocal analysis of the 48hpf hearts of the zebrafish embryos revealed the absence of Isl1^{pos} cardiomyocytes. Isl1+ cells were found outside of the heart but did not express *myl7* (FIG 4.31A and B), suggesting a critical role of Ldb1 in Isl1 cardiac progenitor cell differentiation. Interestingly, significant shortening of the atria could be observed in DN-Ldb1 injected embryos, in a striking similar fashion to the phenotype observed in Isl1-deficient zebrafish embryos as a result of a failure of cardiomyocyte differentiation at the venous pole (FIG 4.32; (de Pater et al., 2009)).

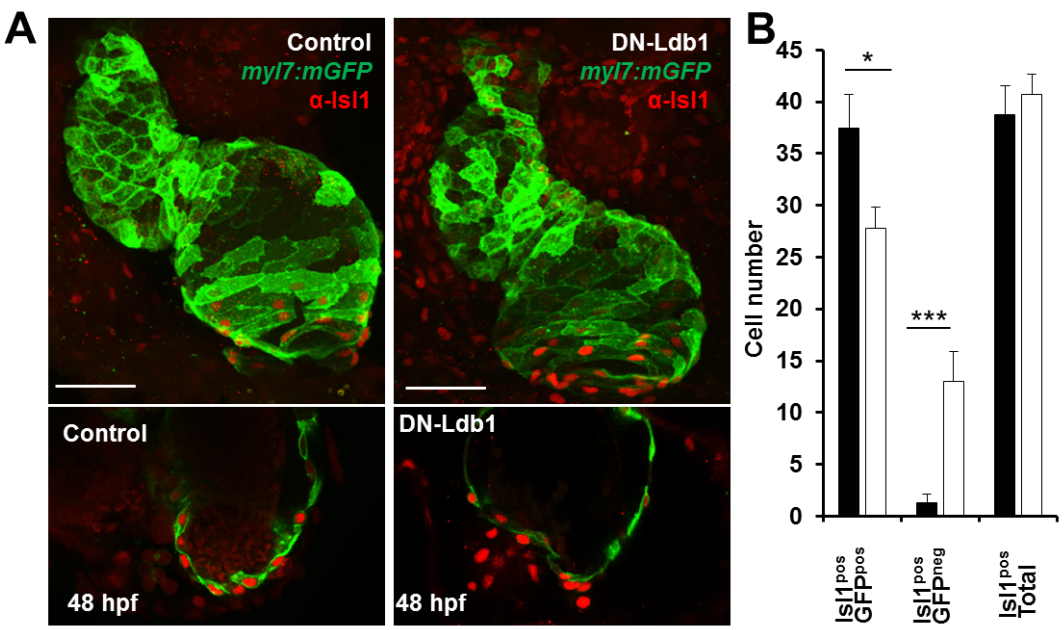

Figure 5.31 Isl1+ cells do not differentiate: Confocal images of control and DN-Ldb1 overexpressing *Tg(myl7:EGFP-HsHRAS)*^{s883} embryos stained with anti-Isl1 antibodies at 48hpf, scale bar 100µm **(A)**. Total number of Isl1^{+} cells and number of Isl1^{+}mGFP^{+} and Isl1^{+}mGFP^{-} cells in the atrium at 48 hpf. Error bars represent SEM (n = 5) **(B)**.

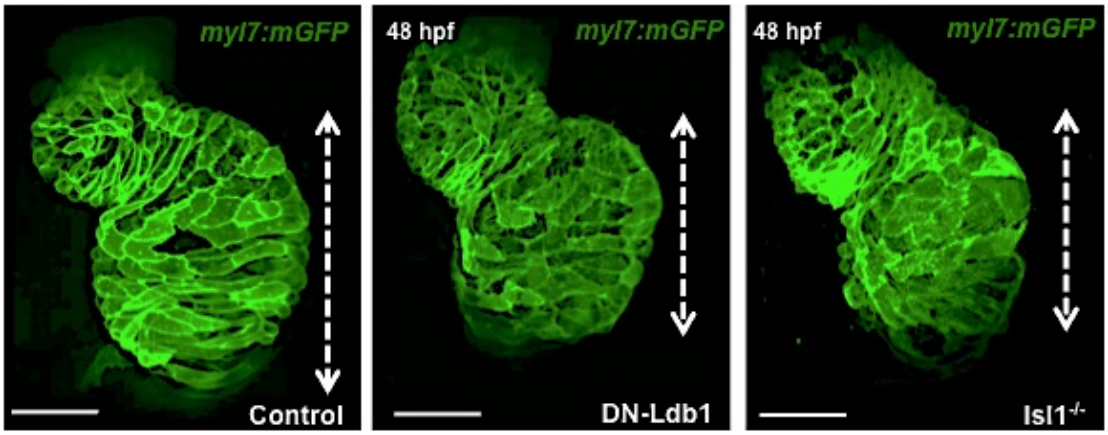

Figure 5.32 DN-Ldb1 injected embryos have shorter atria: Confocal images of control, DN-Ldb1 overexpressing and Isl1 mutant *Tg(myl7:EGFP-HsHRAS)*^{s883} hearts, showing shortening of the atria in DN-Ldb1 overexpressing and Isl1 mutant embryos.

5.11.3. Reduced expression of cardiac markers in DN-Ldb1 injected embryos

To determine the cause of the cardiac defects observed in DN-Ldb1 expressing embryos, *in situ* analysis for important genes involved in heart development at 48 hpf was performed (FIG 4.33).

bmp4 expression was significant lost in the venous pole, although its expression was maintained at the outflow pole and the atrioventricular canal (FIG 4.33). Additionally the expression of another gene important for SHF differentiation in zebrafish, *mef2cb* (Lazic and Scott, 2011) was also downregulated upon DN-Ldb1 expression (FIG 4.33).

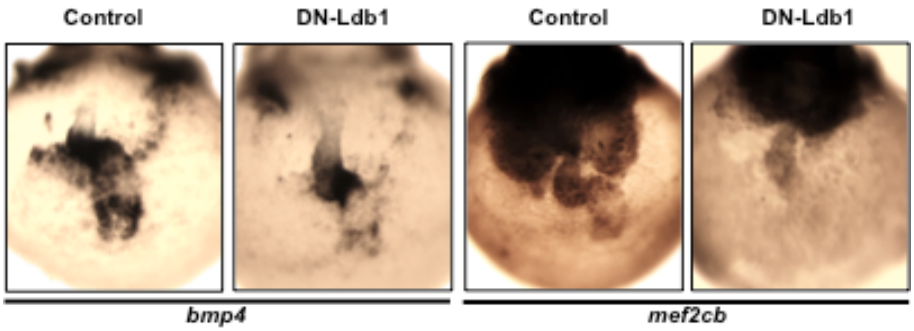

Figure 5.33 Reduced expression of *bmp4* and *mef2cb* in the atria of DN-Ldb1 embryos: In situ analysis in control embryos and DN-Ldb1 overexpressing embryos with probes for *mef2cb* and *bmp4* at 48hpf stage.

Since Isl1 plays a key role in cardiac progenitors during development *isl1* expression analysis by *in situ* hybridization and immunostaining for Isl1 was performed in the DN-Ldb1 injected zebrafish embryos. Immunofluorescence analysis showed that the

bilateral population of Isl1^{pos} cardioprogenitor cells at 10 somites was still present in the injected embryos (FIG 4.34A).

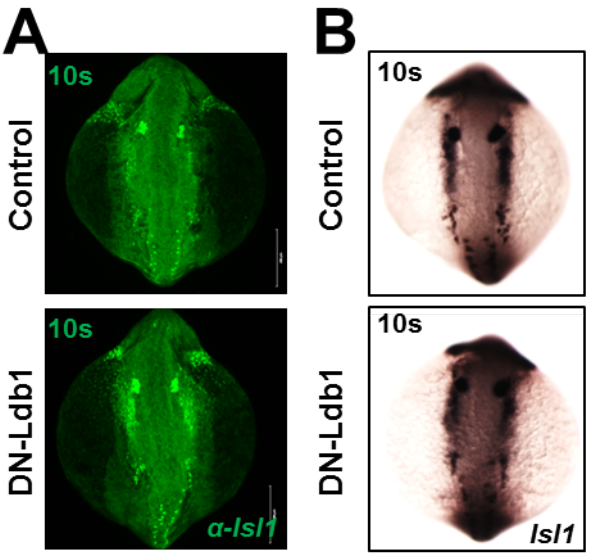

Figure 5.34 Isl1 positive population is not affected by DN-Ldb1 overexpression: Immunostaining analysis of Isl1 levels in control (top) and injected (bottom) zebrafish embryos at 10 somites stages **(A)**. In situ hybridization analysis of control (top) and DN-Ldb1 overexpressing (bottom) embryos at 10 somites stage with an *isl1* probe **(B)**.

Similarly *in situ* analysis did not show difference in *isl1* expression in control or DN-Ldb1 expressing zebrafish embryos (FIG 4.34B), suggesting that Isl1+ progenitor cell numbers were not changed in DN-Ldb1 injected embryos. However, Isl1 staining appeared to be stronger in the injected embryos, consistent with the stabilizing effect of DN-Ldb1 on Isl1 protein levels

In situ hybridization analysis for cardiac progenitor marker genes was performed to address whether the phenotype observed at 48hpf can be due to defects in early steps of heart development.

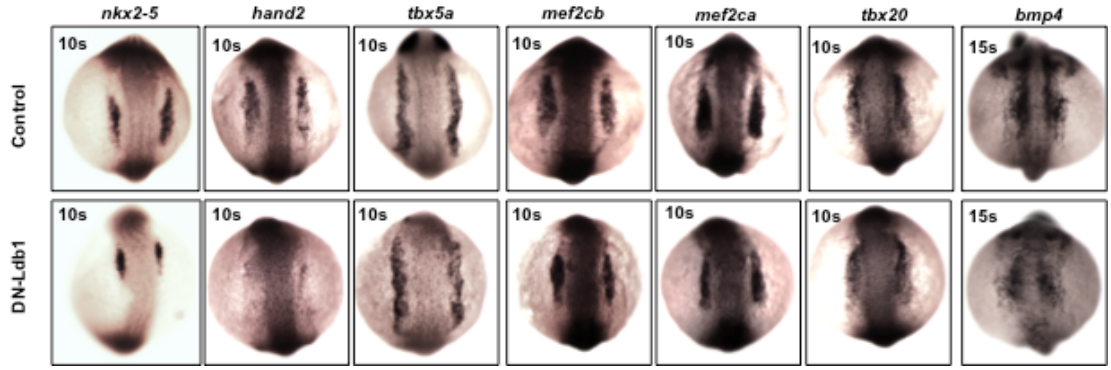

Figure 5.35 SHF marker genes expression is downregulated in DN-Ldb1 embryos: *In situ* hybridization analysis in control embryos (upper panels) and DN-Ldb1 overexpressing embryos (lower panels) with probes for *nkx2-5, hand2, tbx5a, mef2cb, mef2ca, tbx20, bmp4* at 10 or 15 somites stages.

Importantly significant downregulation of cardiac genes *nkx2-5*, *hand2*, *mef2cb* and *bmp4* which plays critical role in the SHF was observed. In contrast, the expression of genes which play key role in FHF development was not significantly affected (FIG 4.35).

Taken together these data suggest that not only the stabilization of Isl1 protein levels but the formation of higher order complexes mediated by the Ldb1 dimerization domain might be important for proper SHF development.

5.11.4. Establishment of stable cells lines in the Ldb1$^{-/-}$ ESCs

To gain further support for the role of the dimerization domain of Ldb1, stable cell lines in the Ldb1-KO ESCs expressing Ldb1, DN-Ldb1 or Isl1, alone or in combination (Ldb1/Isl1 and DN-Ldb1/Isl1) together with GFP were generated. GFP positive ESCs were FACS-sorted (FIG 4.20A and B) and overexpression of the different factors were tested by qPCR and western blot analysis (FIG 4.36A and B).

Consistent with the role of Ldb1 in stabilizing Isl1 protein, Isl1 levels were significant higher, when Ldb1 or DN-Ldb1 were coexpressed (FIG 4.36B), although mRNA levels were similar (FIG 4.36A).

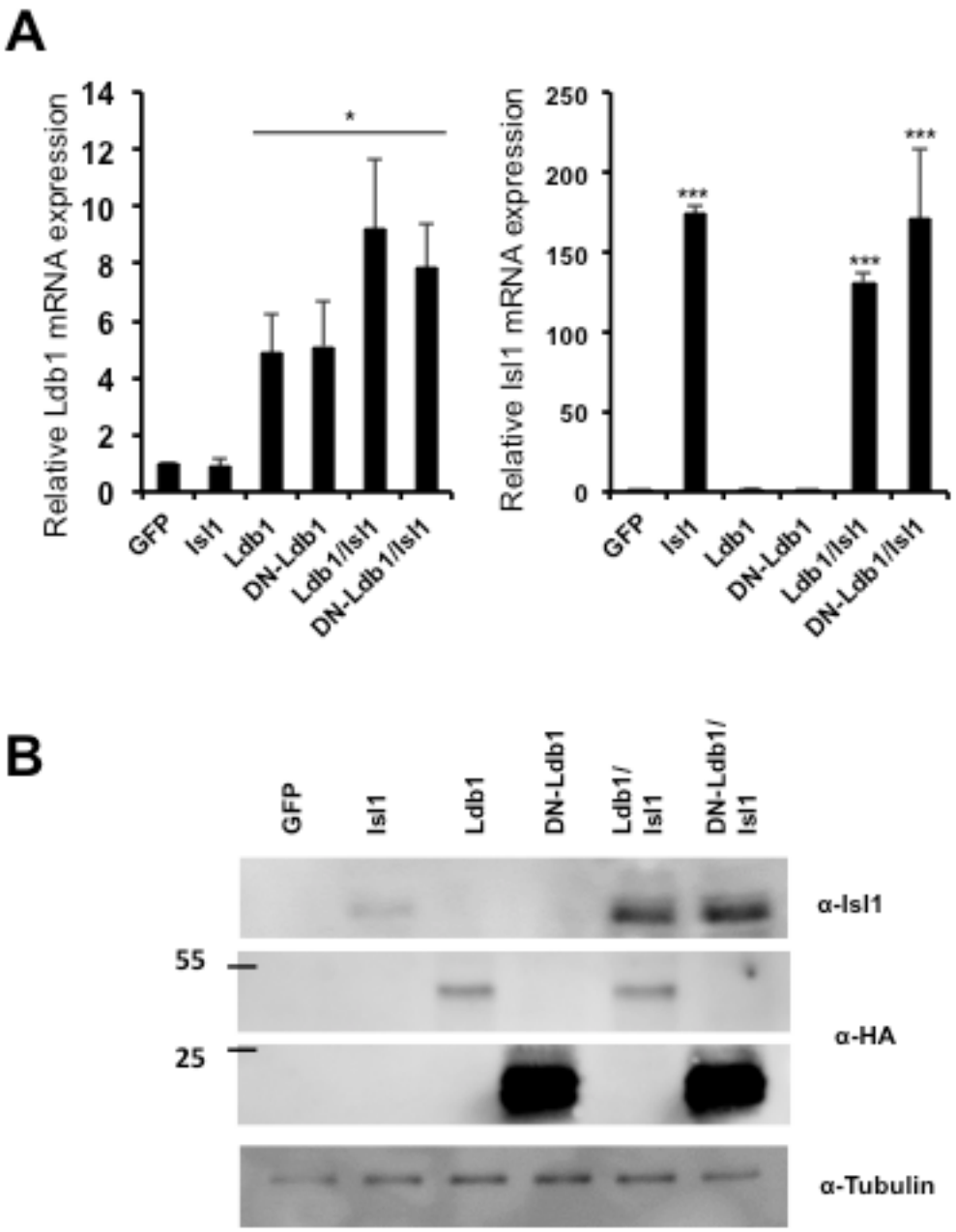

Figure 5.36 Generation of stable ESCs line in *Ldb1*$^{-/-}$ background: mRNA expression of *Ldb1* (left panel) and *Isl1* (right panel) in ESCs expressing GFP alone (control) or Isl1, Ldb1, DN-Ldb1 and their combination together with GFP. Data are mean ± SEMs, n=3. **(A)** Total protein extracts of ESCs was probed with anti-Isl1 or anti-HA antibodies. Tubulin is used as loading control. **(B)**

5.11.5. Overexpression of full length Ldb1 but not DN-Ldb1 rescues the cardiomyocyte differentiation defect of Ldb1$^{-/-}$ *cells*

Importantly, Ldb1 overexpression led to a rescue of cardiac differentiation, as measured by the increased percent of beating EBs and mRNA levels of cardiomyocyte marker genes, *Mlc2a*, *Mlc2v*, *Tnnt2* (FIG 4.39 and 4.40).

The rescue was further potentiated by overexpression of Isl1, confirming a synergistic role of these proteins in cardiomyocyte differentiation. In contrast, overexpression of DN-Ldb1 alone or in combination with Isl1 did not rescue the complete loss of cardiac differentiation of Ldb1-deficient EBs (FIG 4.39 and 4.40).

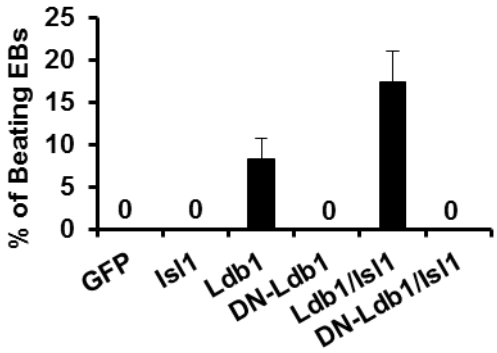

Figure 5.37 Ldb1 overexpression restores cardiac differentiation: Percentage of beating EBs at day 7 of differentiation derived from ESCs overexpressing either GFP alone (control) or Isl1, Ldb1 or a combination of the factors and GFP.

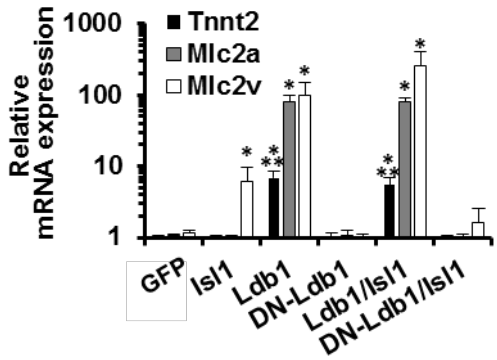

Figure 5.38 Ldb1 overexpression restores cardiac marker genes expression: Relative mRNA expression for cardiomyocyte markers normalized to GAPDH mRNA at day 7 of differentiation. Error bars represent SEMs derived from three biological replicates.

5.11.6. DN-Ldb1 inhibits early mesoderm progenitor

To investigate wheter the inhability of rescue of DN-Ldb1 is due to absence of mesodermal and/or cardiac progenitor cells we analyzed the appeareance of $Flk1^{+}PdgfR\text{-}a^{+}$ early cardiovascular progenitor cells. FACS analysis of these markers revealed that there was no significance difference between control and *Ldb1*$^{-/-}$ derived EBs (FIG4.39A). Furthermore FACS analysis revealed that there was a similar

Flk1+PdgfR-a+ population upon overexpression of Isl1 and Ldb1, showing that the rescue of differentiation is not due to an expansion of early progenitor pool. Interestingly we observed an almost thre fold decrease in this population upon DN-Ldb1 overxpression (FIG 4.39B). This reduction was partially rescued by concomital overexpression of Isl1 (FIG 4.39B), suggesting that the decrease in cardiovascular progenitor cells upon DN- Ldb1 overexpression might be due to interference with the function of LIM only or LIM-HD proteins. Moreover we observed a rescue of Isl1 expression and Isl1+ cells upon overexpression of Ldb1 or DN-Ldb1 (FIG4.40), in agreement with previous results (FIG 4.14). These results suggest that the inhability of DN-Ldb1 to rescue cardiac differentiation is not due to absence of Isl1+ cells, but to their inhability to differentiate.

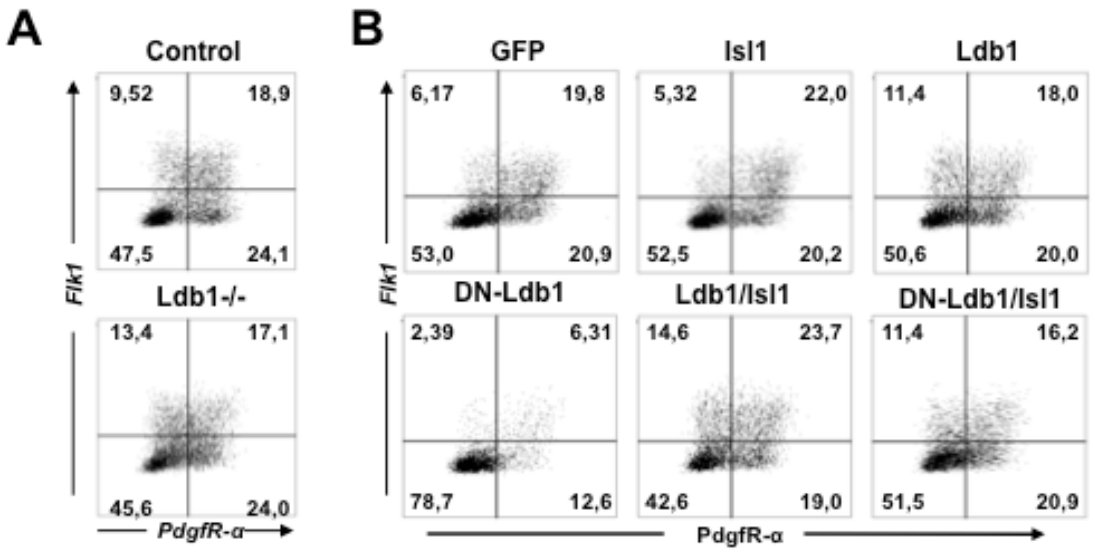

Figure 5.39 FACS analysis of early Flk1^{+}PdgfR-a^{+} cardiovascular progenitors: FACS analysis for Flk1 and PdgfR-a expression in d3.75 EBs derived from control and *Ldb1*$^{-/-}$ ESCs **(A).** FACS analysis for Flk1 and PdgfR-a expression in d3.75 EBs derived from *Ldb1*$^{-/-}$ ESCs expressing GFP alone (control) or Isl1, Ldb1, DN-Ldb1 and their combination together with GFP **(B)**

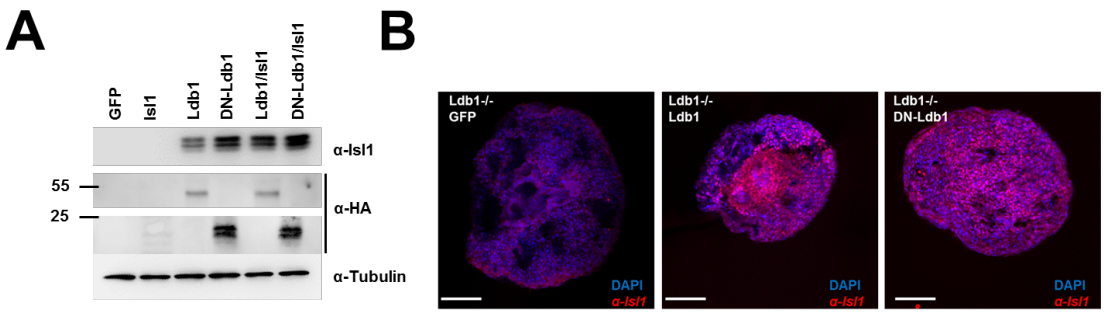

Figure 5.40 Ldb1 and DN-Ldb1 rescue Isl1 protein levels in d5 EBs: Western blot analysis of total protein extract of d5 EBs derived from *Ldb1*$^{-/-}$ ESCs expressing GFP alone (control) or Isl1, Ldb1, DN-Ldb1 and their combination together with GFP. **(A)** Isl1 immunostaining on vibratome sections from d5 EBs differentiated from *Ldb1*$^{-/-}$ ES cells overexpressing either GFP alone (control) or together with Ldb1 and DN-Ldb1. Scale bars, 100 µm. **(B)**

5.11.7. Ldb1 but not DN-Ldb1 restores expression of cardiac progenitor markers

Next the expression of progenitor markers was analyzed. *Mef2c* and *Hand2*, two markers of the second heart field were significantly up-regulated upon overexpression of Ldb1 or of the full Isl1-Ldb1 complex, while expression of the FHF marker GATA4 was unaffected (FIG 4.41).

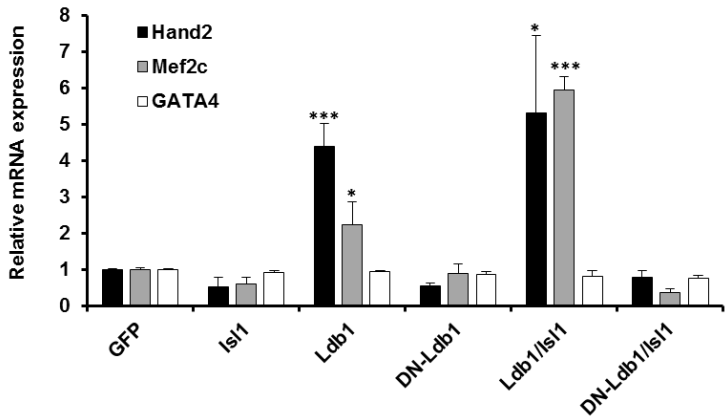

Figure 5.41 SHF marker genes *Mef2c* and *Hand2* are upregulated upon Ldb1 overexpression: Relative mRNA expression analysis for cardiac progenitor markers normalized to GAPDH mRNA at day 4 of differentiation. Mean±SEMs derived from three biological replicates.

5.11.8. Ldb1 but not DN-Ldb1 rescues the expression of endothelial cells markers

Since cardiac progenitor cells can differentiate as well in endothelial and smooth muscle cells analysis expression of markers for these lineages was performed at day 7 of EBs differentiation. The expression of endothelial markes such as *CD-31* and *Flk1* was increase when Ldb1 and Isl1 were coexpressed in the *Ldb1*$^{-/-}$ cells (FIG 4.42), suggesting a role of the Isl1/Ldb1 complex in endothelial cell differentiation.

On the other hand, re-expression of Ldb1, decreases the upregulation of smooth muscle cell markers such as *sm-actin* and *sm-22α* (FIG 4.43).

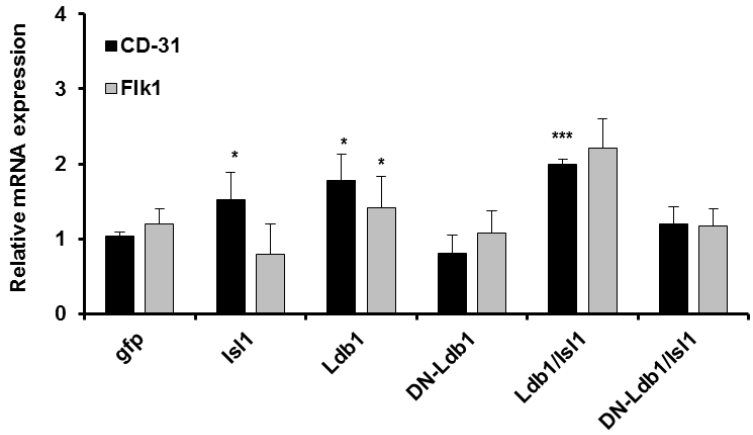

Figure 5.42 Ldb1 restores the expression of endothelial marker genes: Relative mRNA expression analysis for endothelial markers normalized to GAPDH mRNA at day 7 of differentiation. Mean±SEMs derived by three biological replicates.

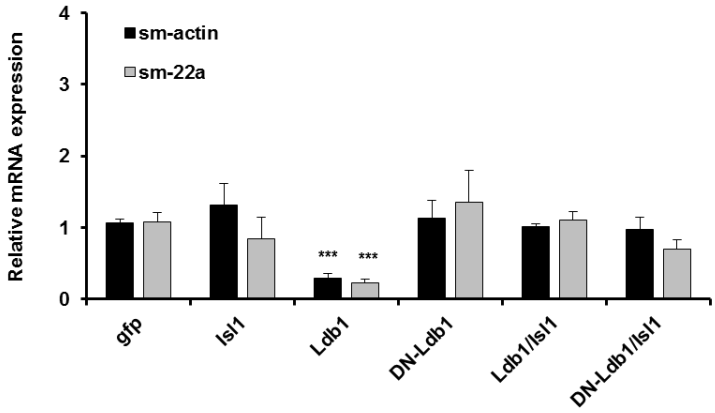

Figure 5.43 Ldb1 expression represses smooth muscle genes: Relative mRNA expression analysis for smooth muscles markers normalized to GAPDH mRNA at day 7 of differentiation. Mean±SEMs derived by three biological replicates.

5.12. Ldb1 and Isl1 form a complex to regulate downstream targets

5.12.1. Isl1 binding sites are found in the Mef2c promoter

Isl1 was shown to regulate *Mef2c* expression through binding of AHF enhancer (Dodou et al., 2004; Witzel et al., 2012). In silico analysis of the *Mef2c* promoter for the presence of Isl1 binding sites (YTAATGR or TAAKKR), GATA-4 (WGATAR) or NKE (TNAAGTG) was performed for the *Mef2c* promoters revealed several Isl1 binding sites, conserved between human and mouse, between the -1,5Kb and the transcriptional starting site of *Mef2c* (FIG 4.44).

Figure 5.44 Alignment of mouse and human *Mef2c* promoter: Isl1 conserved consensus sites are highlighted in yellow, GATA4 in light red and NKE in blue. Restriction sites used for 3C analysis are shown in green. Primers used for ChIP or 3C analysis are shown in grey boxes. *HindIII* restriction sites are shown in green.

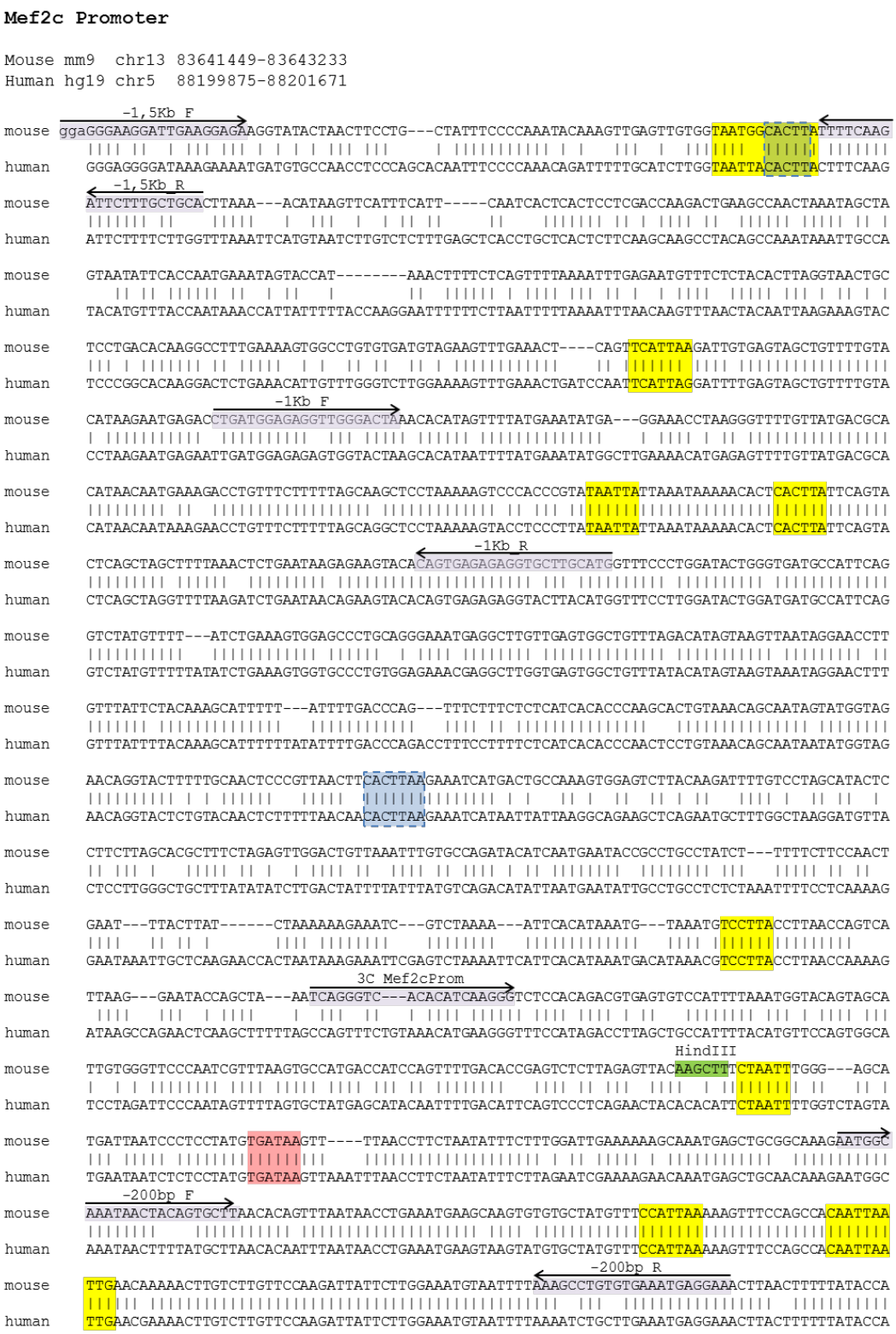

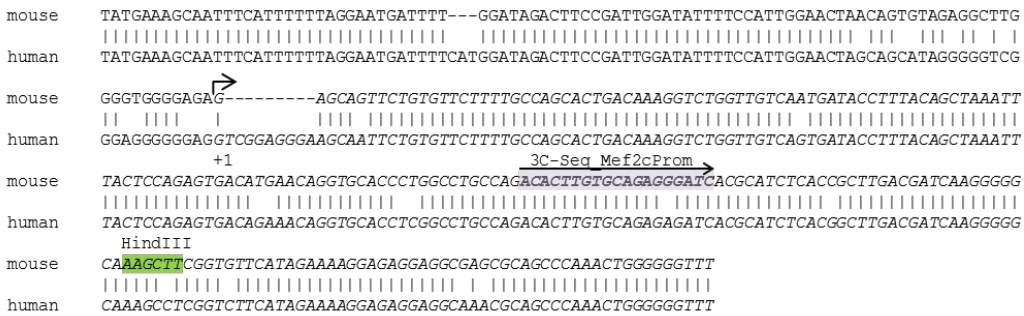

5.12.2. Isl1/Ldb1 transcriptional complex binds to several regulatory regions in the Mef2c locus during development

ChIP-qPCR analysis of the binding of the Isl1/Ldb1 transcriptional complex to the *Mef2c* locus revealed a dynamic binding of the two proteins on the regulatory elements (FIG 4.45). On day 4 of EBs differentiation the Isl1-Ldb1 complex binds to the AHF and to the most proximal promoter (FIG 4.45A), while at day 5 the binding can be detected on all the sites analyzed in the *Mef2c* promoter (FIG 4.45B). Importantly binding to the *Mef2c* locus was also observed *in vivo* when a ChIP was performed using α-Isl1 and α-Ldb1 antibodies from nuclear extract of the cardiogenic region of E8-9 mouse embryos (FIG 4.46). The binding of Ldb1 and Isl1 to the conserved binding sites in the *Mef2c* promoter suggests a role of the Isl1/Ldb1 transcriptional complex in regulating the expression of the *Mef2c* gene.

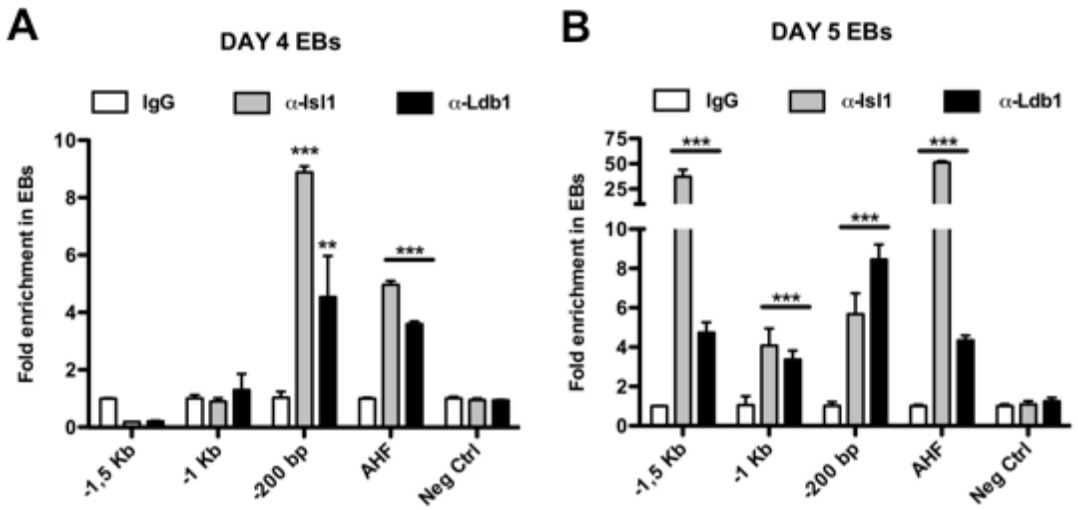

Figure 5.45 Isl1/Ldb1 transcriptional complex bind to *Mef2c* regulatory elements in EBs: ChIP of nuclear extracts from day 4 **(A)** and day 5 EBs **(B)**, using mouse IgG as a control, anti-Isl1 and anti-Ldb1 antibodies. PCRs were performed using primers flanking the conserved Isl1-binding sites in the *Mef2c* regulatory elements analyzed and an intronic region in the actin locus as negative control. Data are mean ± SEMs, n=3.

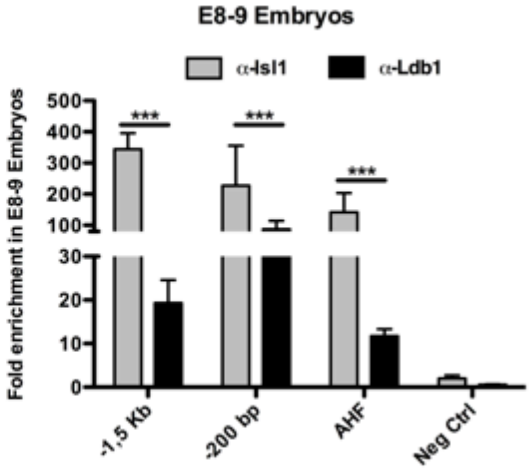

Figure 5.46 Isl1/Ldb1 transcriptional complex bind to *Mef2c* regulatory elements *in vivo*: ChIP of nuclear extracts from E8-9 mouse embryos cardiogenic region using anti-Isl1 and anti-Ldb1 antibodies. PCRs were performed using primers flanking the conserved Isl1-binding sites in the *Mef2c* regulatory elements analyzed. Data are mean ± SEMs, n=3.

5.12.3. Isl1 binding sites are found in the Hand2 regulatory regions

Hand2 expression was significantly altered upon loss and gain of function of Ldb1 in all the model analyzed. *Hand2* plays a key role in second heart field development (Srivastava et al., 1997; Tsuchihashi et al., 2011), and its expression in the heart is specifically driven by cardiac-specific enhancer located between –4.5 kb and –2.7 kb of the *Hand2* transcription start site that was shown to be under control of GATA-4 (OFTRV enhancer) (McFadden et al., 2000).

Therefore we reasoned that *Hand2* could be a direct target for Isl1/Ldb1 transcriptional complex. Consistent with this idea, *in silico* analysis of the OFTRV enhancer and of the proximal promoter of *Hand2* revealed several Isl1 consensus binding sites in conserved between mouse and human in these two important regulatory elements (FIG 4.47 and 4.48).

Hand2 OFTRV

Mouse mm9 chr8 59796493-59797943
Human hg19 chr4 174453397-174454860

Figure 5.47 Alignment of conserved mouse and human *Hand2* OFTRV enhancer: Isl1 consensus sites are shown in yellow and GATA4 in light red. Primers used for ChIP or 3C analysis are shown in grey boxes. *NlaIII* restriction sites are shown in green.

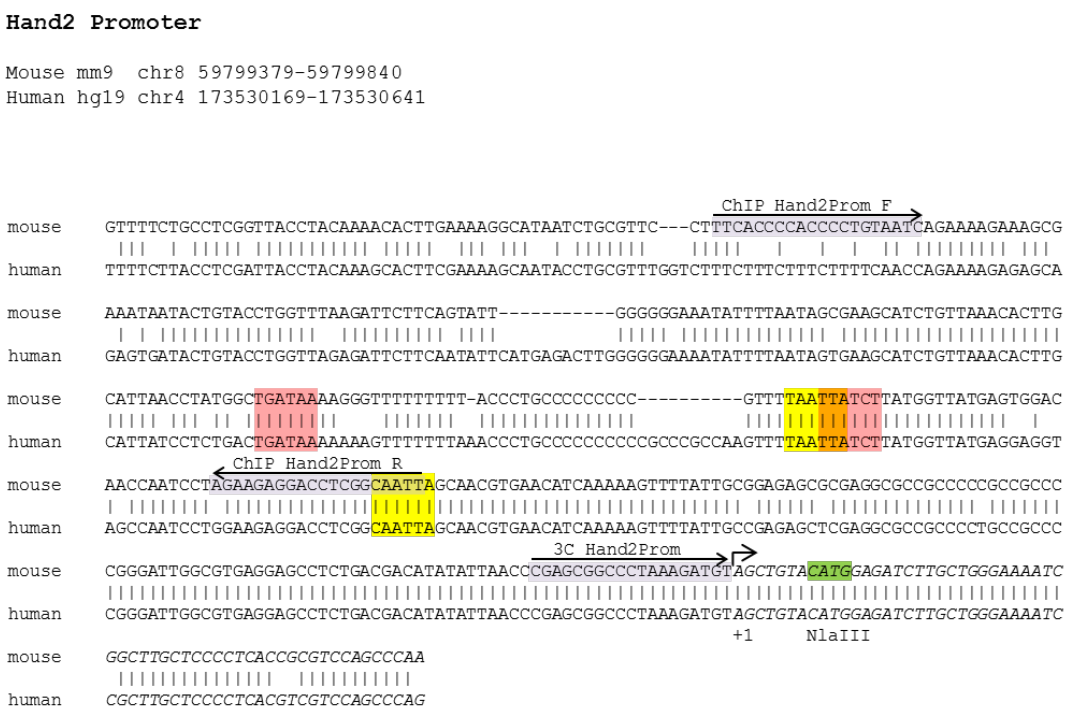

Figure 5.48 Alignment of conserved mouse and human *Hand2* proximal promoter: Isl1 consensus sites are shown in yellow and GATA4 in light red. Primers used for ChIP or 3C analysis are shown in grey boxes. *NlaIII* restriction sites are shown in green.

5.12.4. Isl1/Ldb1 transcriptional complex binds to several regulatory regions in the Hand2 locus during development

The binding of the Isl1/Ldb1 transcriptional complex to the *Hand2* locus was strongly detectable already at day 4 of EBs differentitation and maintained at day 5, reflecting its expression profile in EBs (FIG 4.49).

In a similar manner to the *Mef2c* region, a strong enrichment of Isl1 and Ldb1 was seen at these sites when ChIP experiments were performed using pools of E8-9 embryos (FIG 4.50).

Taken together, the expression data of *Mef2c* and *Hand2* upon gain or loss of function of Ldb1 and the ChIP binding profiles in EBs and *in vivo* in E8-9 embryos suggest that *Mef2c* and *Hand2* are direct target of the Isl1/Ldb1 transcriptional complex.

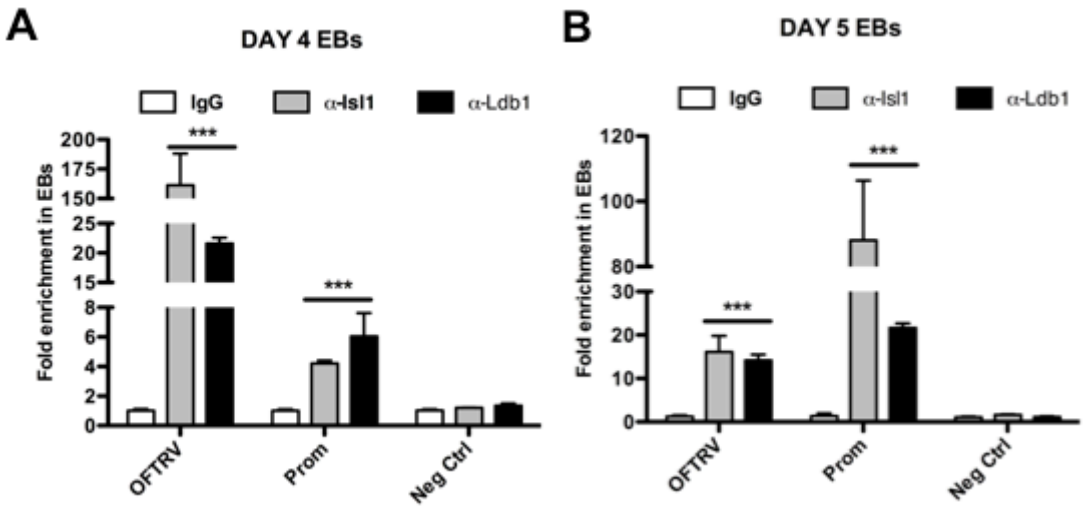

Figure 5.49 Isl1/Ldb1 transcriptional complex bind to *Hand2* regulatory elements in EBs: ChIP of nuclear extracts from day 4 **(A)** and day 5 EBs **(B)**, using mouse IgG as a control, anti-Isl1 and anti-Ldb1 antibodies. PCRs were performed using primers flanking the conserved Isl1-binding sites in the *Hand2* regulatory elements analyzed. Data are mean ± SEMs, n=3.

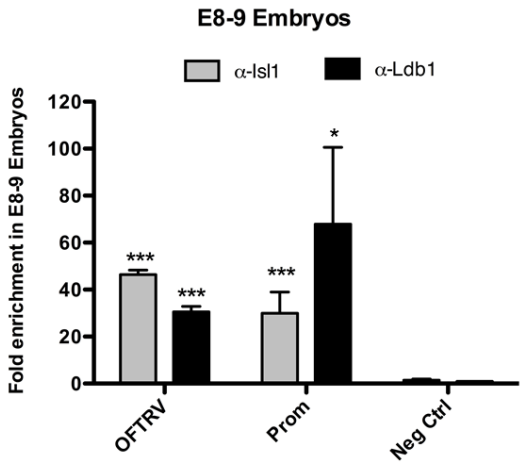

Figure 5.50 Isl1/Ldb1 transcriptional complex bind to *Hand2* regulatory elements *in vivo*: ChIP of nuclear extracts from E8-9 mouse embryos cardiogenic region using anti-Isl1 and anti-Ldb1 antibodies. PCRs were performed using primers flanking the conserved Isl1-binding sites in the *Hand2* regulatory elements analyzed. Data are mean ± SEMs, n=3.

5.13. Ldb1/Isl1 transcriptional complex promotes long range interactions

5.13.1. Ldb1/Isl1 transcriptional complex facilitates long range interactions at the Hand2 Locus

Chromosome Conformation Capture (3C) assay based technologies (de Wit and de Laat, 2012; Dekker et al., 2002) showed that Ldb1 promotes chromosomal looping

events bringing in proximity regulatory elements that are located at great distance in the genome (Deng et al., 2012; Morcillo et al., 1997; Soler et al., 2010; Song et al., 2007).

To analyze if the simultaneous binding of Ldb1 and Isl1 to several regulatory elements at the *Hand2* locus could results in chromosomal looping and promoter-enhancer interaction the 3C-qPCR approach was used (FIG 4.51).

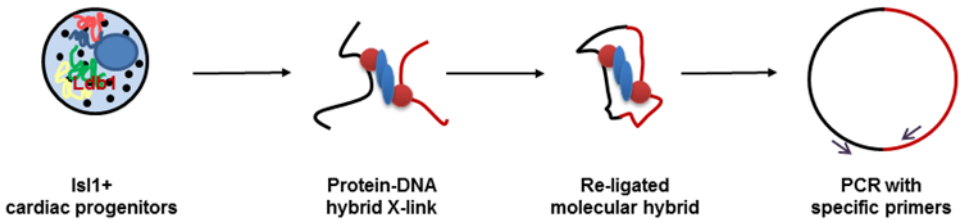

Figure 5.51 Scheme of the experimental procedure: the chromosomal interactions in Isl1-positive progenitor cells are fixed with formaldehyde to create molecular hybrid DNA-Protein in which distant regulatory elements are kept in close proximity by the protein complex. Then the DNA is re-ligated at a low concentration to favor intramolecular ligation of the molecular hybrid and finally the x-link is removed and the new DNA molecule is analyzed.

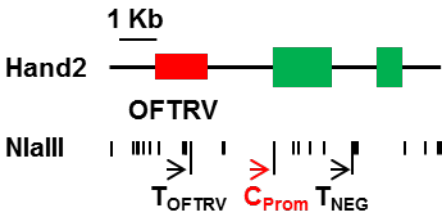

Figure 5.52 Schematic representation of the *Hand2* genomic locus: *Hand2* is located on the chromosome 8 of murine genome, and the position of the restriction sites of *NlaIII*, used in the 3C assay.

Due to the small size of the locus a 4-cutter restriction enzyme, NlaIII (FIG 4.52), was used to generate fragments that were re-ligated at low DNA concentration to generate the 3C library (FIG 4.52B). PCR analysis of the re-ligated fragments showed specific interaction of the promoter with the OFTRV enhancer in the presence of Ldb1 in d5 EBs (FIG 4.53), in contrast no interaction between the promoter and the OFTRV enhancer was observed in Ldb1 deficient EBs. Similarly no looping events were observed in wild type and *Ldb1*$^{-/-}$ embryonic stem cells, which do not express Isl1 protein. Taken together these data suggest that Ldb1/Isl1 regulates the

expression of *Hand2* via chromosomal looping in a similar fashion to the Ldb1/LMO-2/GATA-1 on the *ß-globin* locus.

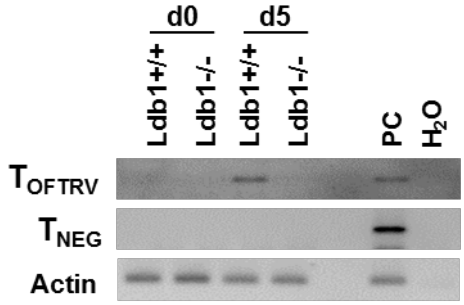

Figure 5.53 Ldb1 mediates *Hand2* promoter-enhancer interaction in d5 EBs: 3C-PCR analysis of d0 and d5 wild type and Ldb1 KO EBs, showing interaction of the *Hand2* promoter and the OFTRV enhancer in d5 wild type EBs. Primer binding in the actin locus are used as loading control for the PCR reaction.

5.13.2. Ldb1, but not DN-Ldb1 rescues the chromosomal looping at the Hand2 locus

Long range interanctions were shown to be of critical importance for the expression of several genes, such as for example the *ß-globin* genes (Deng et al., 2012; 2014; Kim and Dean, 2012; Krivega et al., 2014). Therefore we reasoned that the failure of re-expression of *Hand2* in *Ldb1*$^{-/-}$ EBs expressing Isl1 and/or DN-Ldb1, may be due to the loss of the interaction between the OFTRV enhancer and *Hand2* proximal promoter. To test whether this hypothesis was correct we performed 3C-qPCR analysis of the *Hand2* locus in d5 Ldb1 deficient EBs overexpressing Isl1, Ldb1, DN-Ldb1 and in combinations.

Consistent with this hypothesis the interaction between OFTRV and the *Hand2* promoter could be observed only when Ldb1 full length was overexpressed in the *Ldb1*$^{-/-}$ EBs, but not when Isl1 or DN-Ldb1 were overexpressing. These data strengthen the idea that Ldb1 regulates the interaction between the OFTRV and the *Hand2* promoter in Isl1 positive cardiovascular progenitor cells (FIG 4.54).

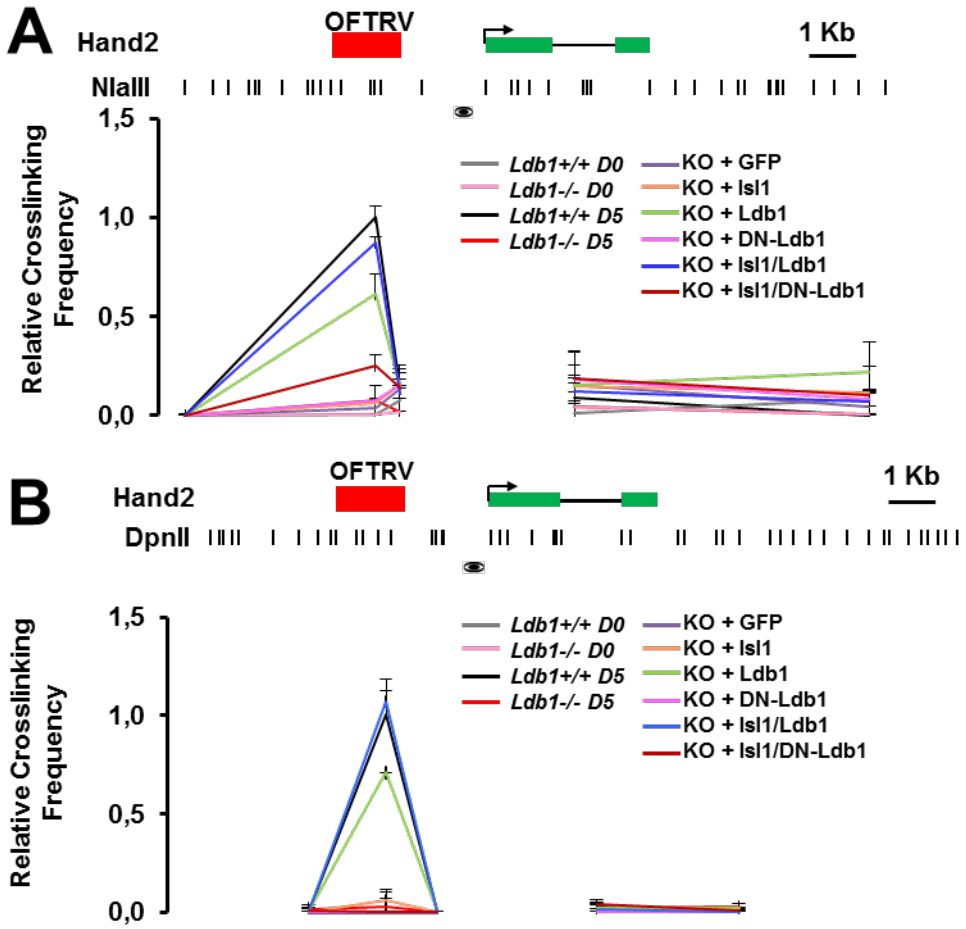

Figure 5.54 DN-Ldb1 can not rescue the interaction between OFT enhancer and promoter: Schematic representation of the *Hand2* genomic locus, the position of the *NlaIII* **(A)** or *DpnII* **(B)** restriction sites, used in the 3C assay. 3C-qPCR relative crosslinking frequency observed in WT, *Ldb1*$^{-/-}$ ESCs and d5 EBs derived from *Ldb1*$^{-/-}$ ESCs overexpressing either GFP alone or together with Isl1, Ldb1, DN-Ldb1 or in different combinations. The *Hand2* promoter was used as viewpoint to the *Hand2* OFTRV enhancer or to negative control regions downstream of the *Hand2* promoter and between the *Hand2* promoter and the OFTRV enhancer. Values were normalized to the *ß-actin* locus and the highest value for the OFTRV enhancer in d5 WT EBs was set as one. Data are mean ± SEMs, n=3.

5.13.3. Ldb1/Isl1 transcriptional complex facilitates long range interactions at the Mef2c Locus

To define the spatial interaction on the *Mef2c* locus 3C followed by paired end sequencing (3C-seq) (Soler et al., 2010; Stadhouders et al., 2013) was performed. Two viewpoints were utilized: the *Mef2c* AHF enhancer, which drives *Mef2c* expression in the AHF, and the *Mef2c* promoter which drives *Mef2c* expression in different cell types (promiscuous promoter).

When the interactions of the promiscuous promoter and the ones obtained by the second heart field specific AHF were compared a striking difference of the looping interactions could be observed within the *Mef2c* locus (FIG 4.55). The AHF enhancer

showed less interactions in the *Mef2c* locus, the strongest of which upstream of the transcriptional starting site, -13Kb to -5,5Kb, and in the region of the last intron, +150Kb, and the 3'UTR, which were virtually lost in *Ldb1*$^{-/-}$ EBs (FIG 4.55). Interestingly when the *Mef2c* Promoter was used as viewpoint multiple interaction in the *Mef2c* locus were observed (FIG 4.55).

In order to confirm the 3C-seq results chromosomal conformation capture assay was performed in wild type EBs at different days (FIG 4.56). This analysis revealed a similar three dimensional conformation of the *Mef2c* locus at d5-6 of EBs differentiation. *In vivo* analysis of the chromosomal conformation of the *Mef2c* locus of chromatin derived from microdissected SHF of E8-9 embryos revealed a similar three dimensional conformation to what identified in wild type d5 EBs (FIG 4.57). Confirming the specificity of these interaction, chromatin isolated from the tail of E8-9 or from the brain of E10.5 embryos, where AHF is not active, did not show any interaction between this important regulatory element and the promoter region or the 3' region of *Mef2c* gene. Interestingly, in a similar manner to what observed in EBs, a dynamic interaction could be observed in the promoter area of the *Mef2c* gene, with a strong interaction between the AHF and the proximal promoter in chromatin isolated from d4 EBs or progenitor cells of the SHF, at the onset of *Mef2c* expression, that was lost in more differentiated cells (FIG 4.56, 4.57).

The *Mef2c* regions interacting with the AHF contain conserved Isl1 binding sites, together with GATA and/or NKE (FIG 4.58; 4.59). ChIP analysis performed at d4 and d5 of wild type EBs development revealed an enrichment for Ldb1 and Isl1 on these regions (FIG 4.60), confirming the idea that Isl1/Ldb1 transcriptional complex is of critical importance in mediating the interactions between the AHF and other regulatory elements of the *Mef2c* gene.

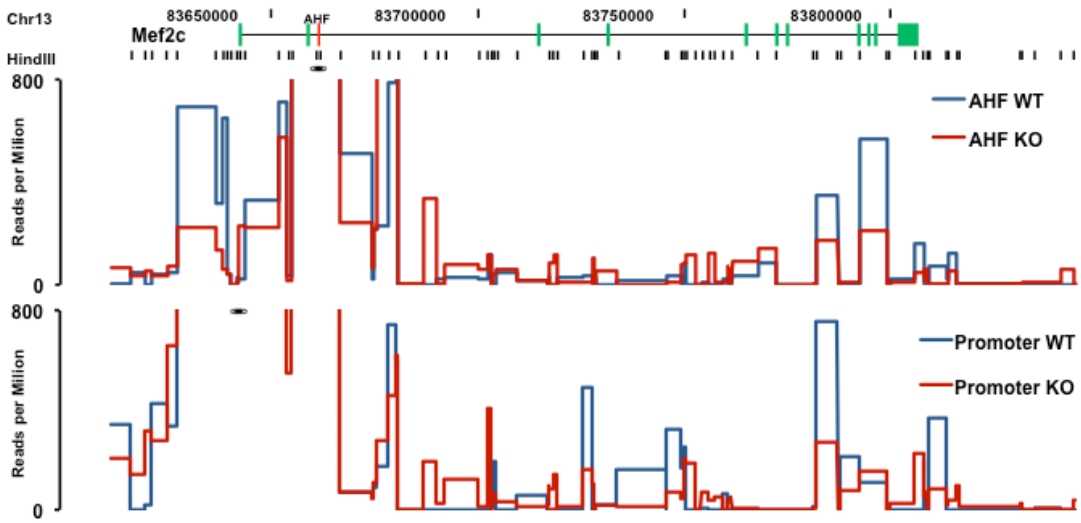

Figure 5.55 3C-seq analysis of the *Mef2c* locus: Schematic representation of the *Mef2c* genomic locus and the position of the restriction sites of *HindIII*, used in the 3C-seq assay (Top panel). 3C-seq analysis of the *Mef2c*-AHF (Middle panel) and *Mef2c*-Promoter (Bottom panel) associated regions in d5 wild type and *Ldb1*$^{-/-}$ EBs. The viewpoint is indicated by an eye symbol.

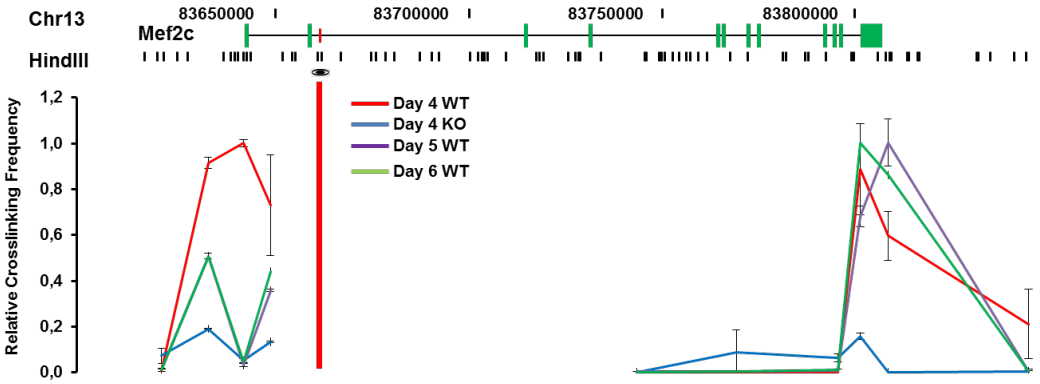

Figure 5.56 Dynamic conformation of the Mef2c locus during EBs differentiation: 3C-qPCR relative crosslinking frequency observed in EBs at different days. Data are mean ± SEMs, n=3. The *HindIII* fragment containing the *Mef2c*-AHF was used as viewpoint (red bar, eye symbol).

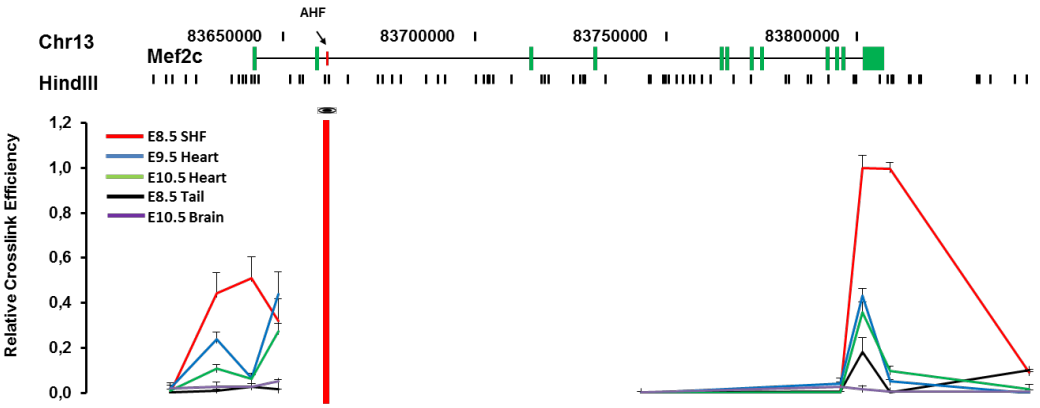

Figure 5.57 Dynamic conformation of the Mef2c locus during embryonic development: 3C-qPCR relative crosslinking frequency observed in microdissected SHF region, brain or tail from pools of embryos at different developmental stages. Data are mean ± SEMs, n=3. The *HindIII* fragment containing the *Mef2c*-AHF was used as viewpoint (red bar, eye symbol).

Mef2c -13Kb

```
Mouse mm9  chr13 83629799-83630029
Human hg19 chr5  88214651-88214411
```

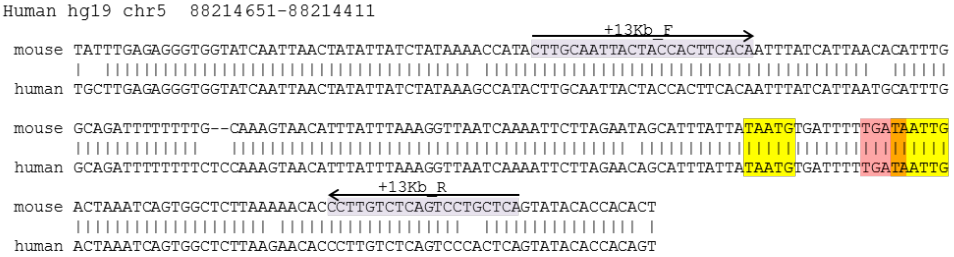

Mef2c -12Kb

```
Mouse mm9  chr13 83631203-83631643
Human hg19 chr5  88213106-88212651
```

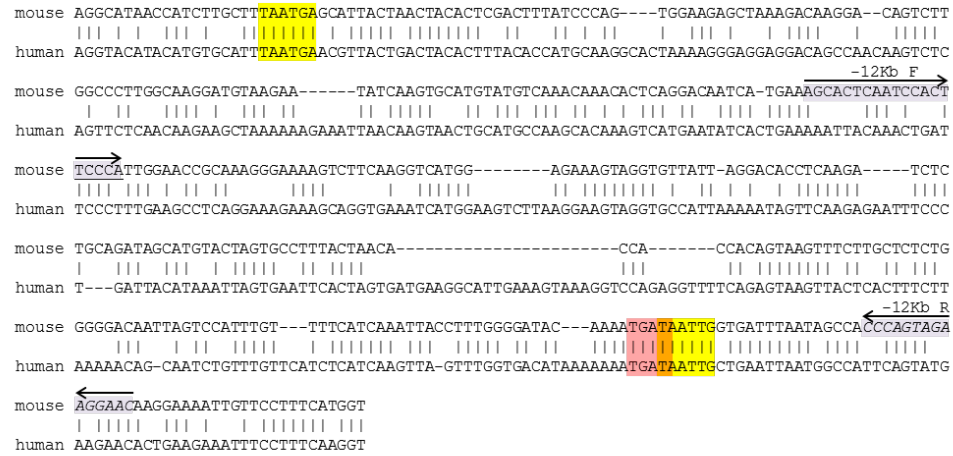

Mef2c +2,7Kb

```
Mouse mm9  chr13 83645570-83645865
Human hg19 chr5  88901607-88901315
```

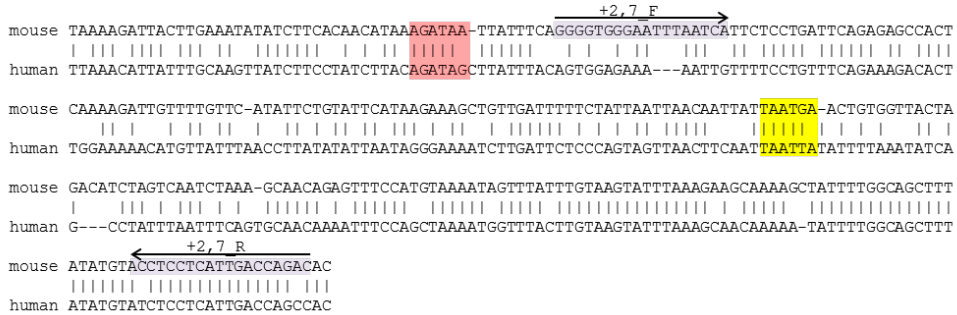

Figure 5.58 Alignment of mouse and human *Mef2c* interacting regions with AHF in the promoter area: Isl1 conserved consensus sites are highlighted in yellow, GATA4 in light red and NKE in blue.

Mef2c +150Kb

Mouse mm9 chr13 83795420-83795807
Human hg19 chr5 88024842-88024459

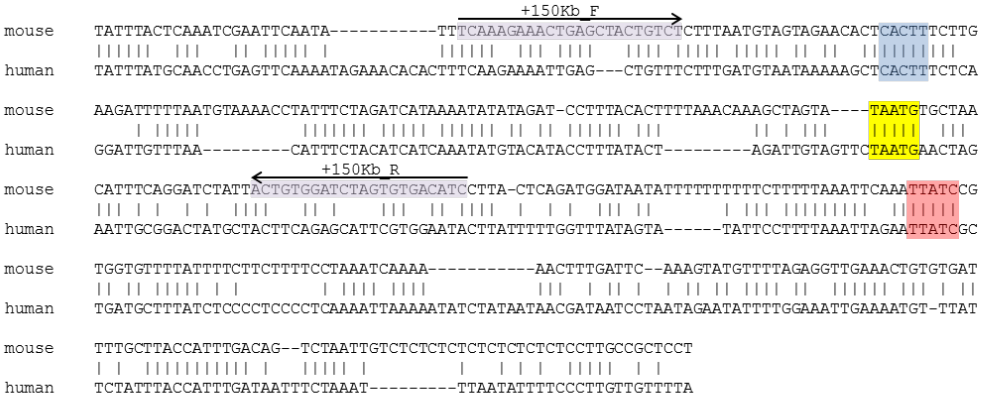

Mef2c 3'UTR

Mouse mm9 chr13 83806345-83807063
Human hg19 chr5 88013663-88014400

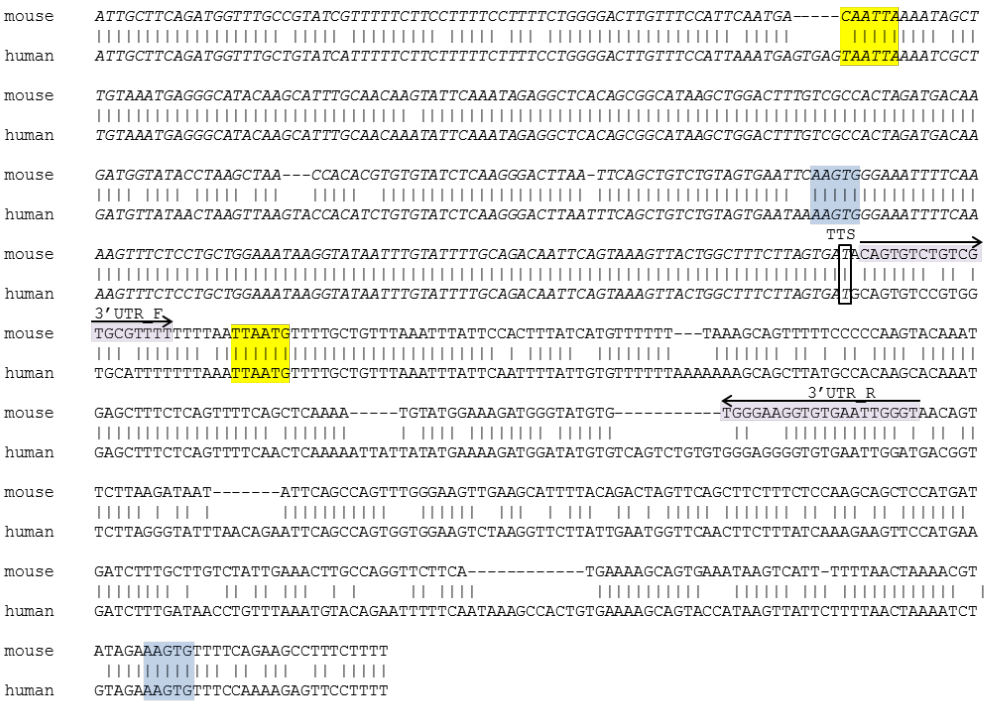

Figure 5.59 Alignment of mouse and human *Mef2c* interacting regions with AHF in the 3' region of *Mef2c* locus: Isl1 conserved consensus sites are highlighted in yellow, GATA4 in light red and NKE in blue. TTS, Trasscriptional Termination Site.

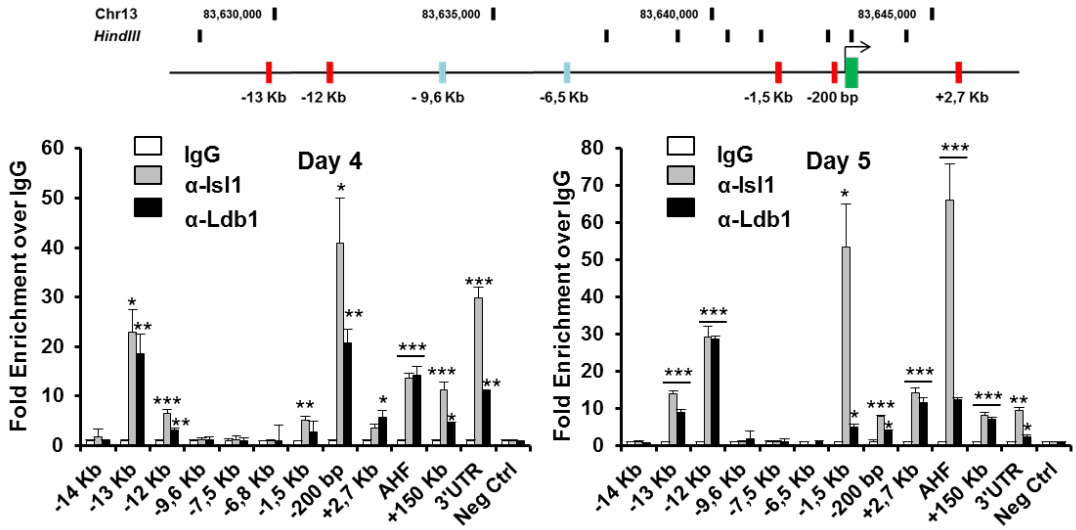

Figure 5.60 Isl1/Ldb1 transcriptional complex binds to 3C-seq identified regions: ChIP of nuclear extracts from d4 (left) or d5 (right) EBs, using mouse IgG as a control, anti-Isl1 and anti-Ldb1 antibodies. PCRs were performed using primers flanking the conserved Isl1-binding sites (red) or not containing Isl1 consensus sites (light blue) in the *Mef2c* locus elements analyzed. Data are mean ± SEMs, n=3

5.13.4. Identification of a novel putative Mef2c enhancer

Given that a single enhance can interact with multiple regulatory elements we investigated wether the sequences interacting with the AHF in the cardiac progenitors may be cardiac specific enhancers. Currently two major features have been used to predict enhancers. The first one relies on the presence of enhancers specific modifications, such as H3K4me1 and H3K27ac, as well as the binding of the histone acetyltransferase P300 and RNAPolII (Buecker and Wysocka, 2012; Bulger and Groudine, 2011; Calo and Wysocka, 2013; Heintzman and Ren, 2009; Heinz and Glass, 2012). ChIP analysis performed at day 4 of EBs differentiation revealed a significant enrichment for these marks, in WT EBs compared to *Ldb1*$^{-/-}$, was observed -13Kb upstream of the TSS (FIG 4.61), the same region bound by the Isl1-Ldb1 transcriptional complex (FIG 4.60), while no significant enrichment was observed in sites not bound by Isl1 and Ldb1.

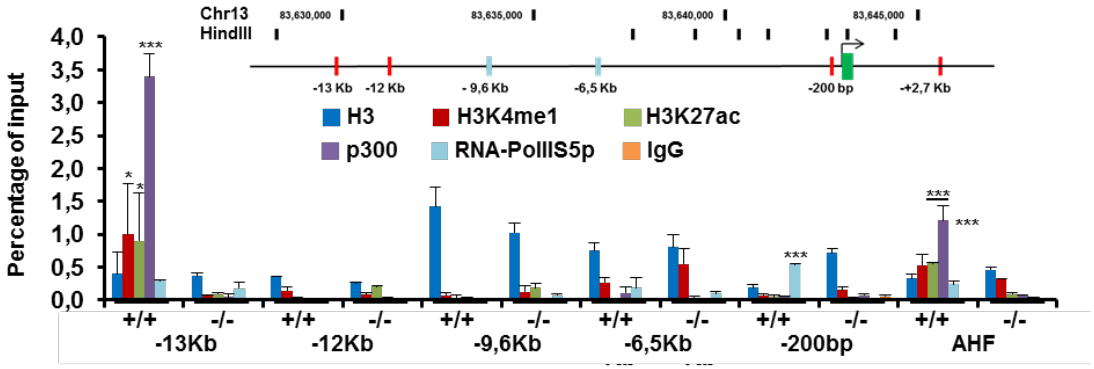

Figure 5.61 Region interacting with the Mef2c-AHF are enriched for enhancer chromatin marks: ChIP of d4 EBs derived from WT and *Ldb1*$^{-/-}$ ESCs using antibodies against H3, H3k4me1, H3K27Ac, p300, RNA-PolIIS5p and IgG as a control. (*p≤0,05, **p≤0,01, ***p≤0,005).

5.13.5. Dynamic interaction to the Mef2c promoter correlates with different Mef2c isoforms expression

Developmental regulated interaction of the LCR to the promoters of the different genes in the *ß-globin* locus has been linked to the expression of embryonic globin genes in erythroid progenitors and adult globin isoforms in definitive erythrocytes (FIG 2.10 and Palstra et al., 2003). Therefore we reasoned that the dynamic interaction of the AHF to the *Mef2c* promoter observed during the course of EBs differentiation and heart development (FIG 4.56, FIG 4.57) may be linked to the expression of alternative *Mef2c* transcripts. In accordance with this idea the longer reference sequence transcript (NM_001170537) was highly expressed in d4 EBs and in dissected SHF, while the annotated transcript with alternative transcriptional start site 1.5 kb downstream of the AHF enhancer (AK077603) was more abundant later during EB differentiation and dissected hearts, implying that the observed dynamic chromatin looping correlates with the expression of alternative transcripts for *Mef2c* (FIG 4.62).

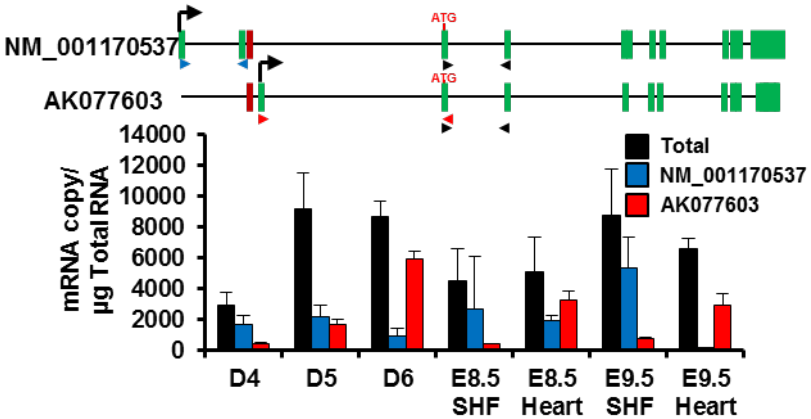

Figure 5.62 *Mef2c* isoform switch during cardiac differentiation: Schematic representation of the *Mef2c* RNA reference sequence (NM_001170537) and an annotated transcript with alternative transcriptional start site 1.5 kb away from the AHF enhancer (top). Absolute quantification of transcripts using the primers indicated in the scheme (bottom).

5.13.6. DN-Ldb1 overexpression prevents chromatin looping formation

Next the requirement for the dimerization domain of Ldb1 to promote the chromatin looping formation in the *Mef2c* locus was analyzed. 3C-qPCR was performed in d5 Ldb1-deficient EBs overexpressing Isl1, Ldb1, DN-Ldb1 alone or in combinations. Indeed chromosomal loop formation was observed in presence Ldb1 or Ldb1/Isl1 but not in Isl1, DN-Ldb1 or DN-Ldb1/Isl1 overepressing *Ldb1*$^{-/-}$ EBs (FIG 4.63). Furthermore no chromosomal loop formation was observed when regions in the *Mef2c* locus that does not contain Isl1 binding site were analyzed.

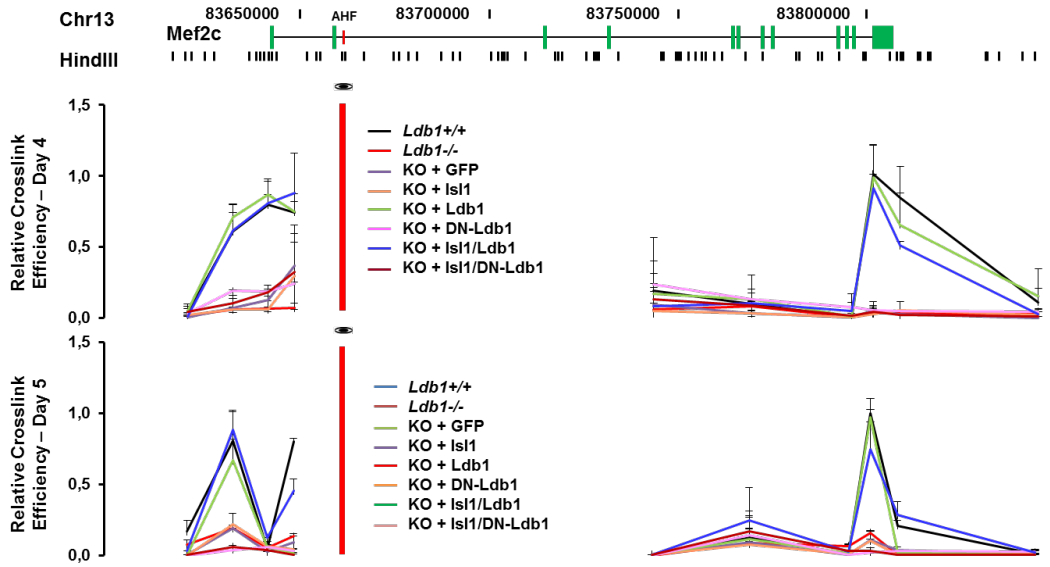

Figure 5.63 Full length Ldb1 restores the 3D conformation of the *Mef2c* locus: 3C-qPCR relative crosslinking frequency observed in d4 (top) or d5 (bottom) EBs derived from WT and *Ldb1*$^{-/-}$ ESCs or *Ldb1*$^{-/-}$ ESCs overexpressing either GFP alone (control) or together with Isl1, Ldb1, DN-Ldb1 in different combinations. Error bars indicate SEM. n=3. The HindIII fragment containing the *Mef2c*-AHF was used as viewpoint (red bar, eye symbol).

5.13.7. DN-Ldb1 binds Mef2c and Hand2 loci similar to Ldb1

In order to rule out the hypothesis that the inability of DN-Ldb1 to promote chromatin loops formation was caused by its failure to bind to the Isl1/Ldb1 binding sites a ChIP analysis using α-HA antibody, that is able to recognize the ectopically expressed HA-Ldb1 and HA-DN-Ldb1, was carried out.

Similar enrichment for HA-Ldb1 or HA-DN-Ldb1 was observed on the regulatory elements tested (FIG 4.64 A and B), suggesting that the inability of DN-Ldb1 to

promote long range interactions is not due to the inhability of the DN-Ldb1 containing complex to bind DNA, but rather on the inability of Ldb1 to dimerize.

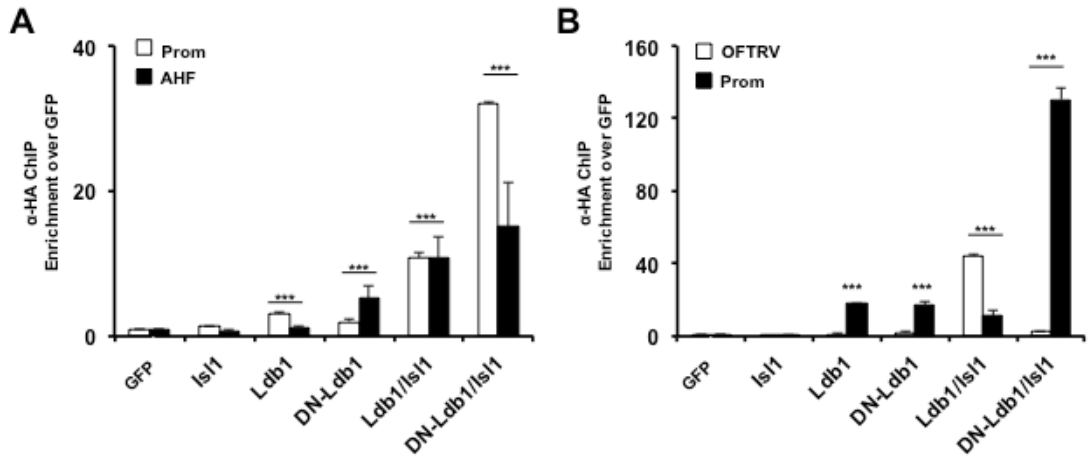

Figure 5.64 DN-Ldb1 is recruited to the regulatory elements of *Mef2c* and *Hand2*: ChIP of nuclear extracts from day 5 EBs using anti-HA antibody. PCRs were performed using primers flanking the conserved Isl1-binding sites in the *Mef2c* **(A)** and *Hand2* **(B)** regulatory elements analyzed. Data are mean ± SEMs, n=3

5.13.8. Mef2c promoter and AHF cooperate during transcription

Luciferase assay using two different construct containing *Mef2c* proximal promoter in combination or not with the AHF was performed in COS-7 cells. If the identified interaction between the *Mef2c* promoter and *Mef2c* AHF enhancer is of biological relevance a synergistic effect on the transcription of the reporter gene should be observed when Isl1 and Ldb1 are coexpressed in presence of the reporter construct harboring both the *Mef2c* promoter and AHF.

Consisting with this hypothesis luciferase assays revealed significantly higher synergistic effect of Isl1 and Ldb1 on a luciferase construct containing the *Mef2c* promoter upstream and the *Mef2c* AHF enhancer downstream of a luciferase gene, in comparison to a reporter construct harboring the *Mef2c* promoter alone. This synergistic effect was abolished when DN-Ldb1 was expressed together with Isl1 (FIG 4.65).

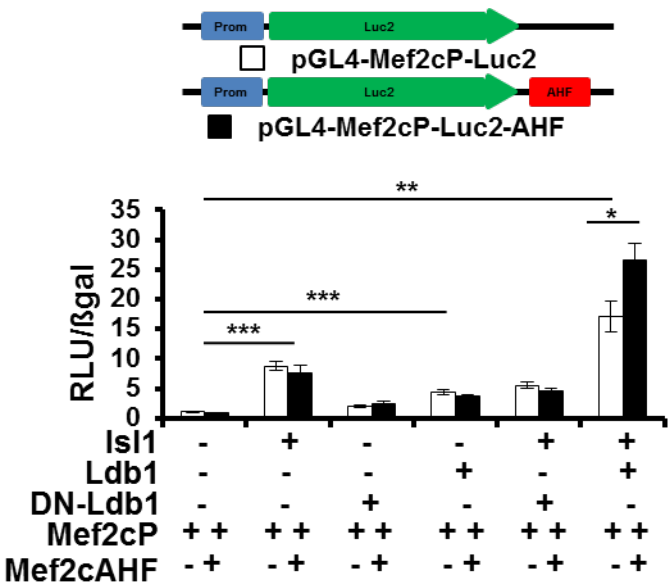

Figure 5.65 Synergistic effect of Isl1 and Ldb1: HEK293T cells were transiently transfected with 100 ng luciferase reporter construct containing the *Mef2c* promoter alone or together the AHF enhancer, alone or together with Isl1 (400 ng), Ldb1 (400 ng),DN-Ldb1 (400 ng), Isl1 and Ldb1 (400 ng both) or Isl1 and DN-Ldb1 (400 ng both). The luciferase levels were normalized for the β-galactosidase activity of a cotransfected RSV-LacZ reporter and presented as fold activation relative to the luciferase levels of the luciferase reporter construct alone. Transfections were performed at least three times in triplicates, and representative experiments with the SEMs are shown. (*p≤0,05, **p≤0,01, ***p≤0,005).

5.14. Ldb1 orchestrate a network for transcriptional regulation and coordination in three-dimensional space during heart development

Analysis of the genes interacting with the *Mef2c*-AHF was performed in order to discover whether Ldb1/Isl1 complex brings genes involved in cardiac/mesodermal development are brought in close proximity to be co-regulated during transcription. Interestingly gene onthology (GO) analysis for the 3C-seq data showed over-representation of genes involved in cardiac muscle development and heart development within the top ten over-represented was found only in the case of WT AHF (FIG 4.66). Only few general cell biological processes were significantly over representated when the same analysis was performed using the interactions of the promoter (FIG 4.67) supporting a role of Ldb1 in organizing a cardiac specific transcriptional program in three dimensional space.

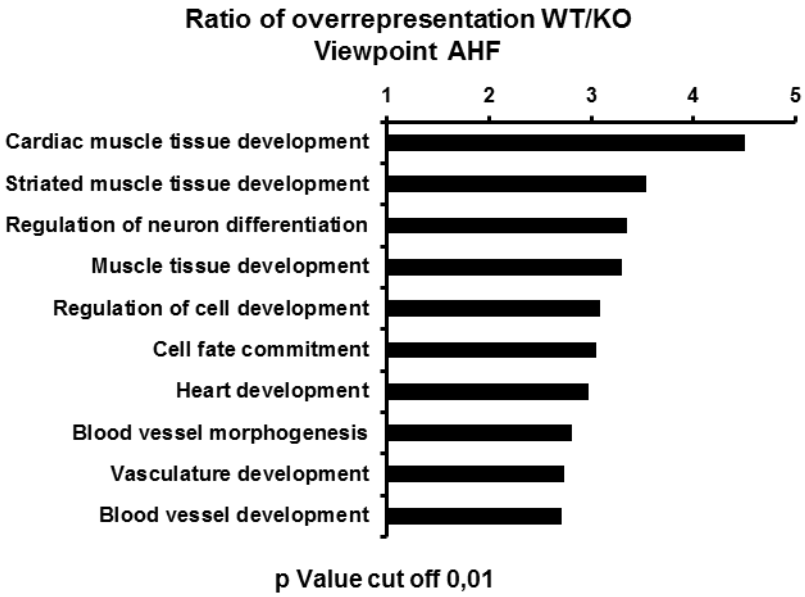

Figure 5.66 Ratio of over representation of GO pathways in WT cells over KO using the *Mef2c*-AHF as viewpoint

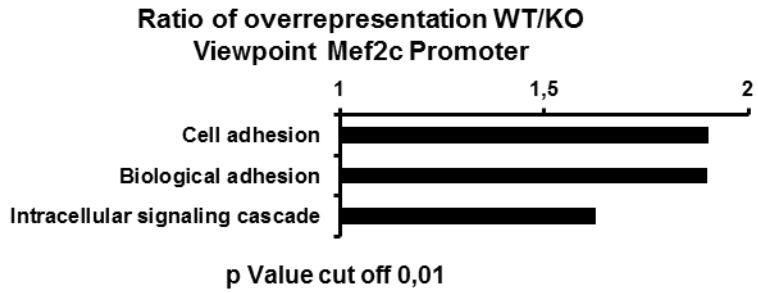

Figure 5.67 Ratio of over representation of GO pathways in WT cells over KO using the *Mef2c*-promoter as viewpoint

Interestingly one of the genes found to interact with *Mef2c* AHF but not to *Mef2c* promoter is Isl1 (FIG 4.68 and Table 4.2). Furthermore interaction with other important transcription factors involved in heart development such as *Myocardin, Irx1, Tbx2* and *Tbx18* were observed. Additional interactions could be detected to important genes involved in signaling pathways (*Fgf10, Bmpr2, Fgfr2, Smad3, Smad2*) and genes involved in cardiomyocyte contraction or potassium channels (*Kcnq1, Kcnj2, Ryr2, Acvr2a*) (Table 4.2, FIG 4.68). Interesting these interaction were specific for AHF in wild type EBs, while were not detected in Ldb1 deficient EBs nor when the *Mef2c* promiscuous promoter was used as viewpoint.

Moreover the AHF enhancer was involved in interactions with a conserved region in the first intron of the Myocardin locus (FIG 4.68). This region, bound by Isl1, is

required for proper *Myocd* expression (Kwon et al., 2009). 3C-qPCR analysis of d5 EBs versus Ldb1 deficient EBs could confirm the interaction identified in the 3C-seq analysis (FIG 4.69A). Moreover, interactions of the AHF to important cardiac genes could be observed *in vivo* using chromatin isolated from microdissected SHF, but not from tails of E8-9 embryos (FIG 4.69B).

Chr	Start	End	RPM	Annotation	Distance to TSS	Nearest PromoterID	Gene Name
chr13	11981622	11981938	206	intron	217432	NM_023868	*Ryr2*
chr13	31858160	31863008	184	Intergenic	-37931	NM_008592	*Foxc1*
chr1	59803431	59814755	160	Intergenic	-12030	NM_007561	*Bmpr2*
chr9	63669998	63671107	151	Intergenic	-64751	NM_016769	*Smad3*
chr13	119681345	119684109	149	Intergenic	179221	NM_008002	*Fgf10*
chr10	36586722	36592524	146	Intergenic	-104727	NM_008229	*Hdac2*
chr2	48581472	48591337	127	Intergenic	-83225	NM_007396	*Acvr2a*
chr7	137429783	137429819	112	Intergenic	-19479	NM_201601	*Fgfr2*
chr13	117092704	117094844	102	intron	6122	NM_021459	*Isl1*
chr2	133314562	133323155	100	Intergenic	-59037	NM_007553	*Bmp2*
chr7	150381521	150383178	95	intron	89190	NM_008434	*Kcnq1*
chr11	85655130	85658708	65	Intergenic	10802	NM_009324	*Tbx2*
chr10	23109550	23111214	46	Intergenic	-39829	NM_010167	*Eya4*
chr9	80066511	80066909	44	intron	53869	NM_001039546	*Myo6*
chr3	128860479	128861244	34	Intergenic	-41935	NM_001286942	*Pitx2*
chr6	17416533	17421131	33	intron	4875	NM_008591	*Met*
chr11	7225059	7227115	31	Intergenic	-112161	NM_008343	*Igfbp3*
chr11	110929486	110937167	28	exon	5848	NM_008425	*Kcnj2*
chr6	15046825	15047873	25	intron	-88157	NM_212435	*Foxp2*
chr13	71948394	71949013	24	Intergenic	152468	NM_010573	*Irx1*
chr13	72006494	72009882	23	Intergenic	92983	NM_010573	*Irx1*
chr11	65079835	65081390	19	intron	2879	NM_145136	*Myocd*
chr14	63886749	63890440	13	Intergenic	-24497	NM_008092	*Gata4*
chr2	24525827	24532218	11	intron	89650	NM_001042528	*Cacna1b*
chr3	142038898	142039133	10	intron	15799	NM_022554	*Pdlim5*
chr9	87552432	87557225	10	Intergenic	71267	NM_023814	*Tbx18*

Table 5.2 Genes involved in cardiac development or cardiomyocyte function interacting with *Mef2c-AHF*: Peak coordinates of sequences interacting with AHF at d5 of EBs differentiation located near genes important for heart development/cardiomyocyte function. RPM, reads per million; TSS, transcriptional start site.

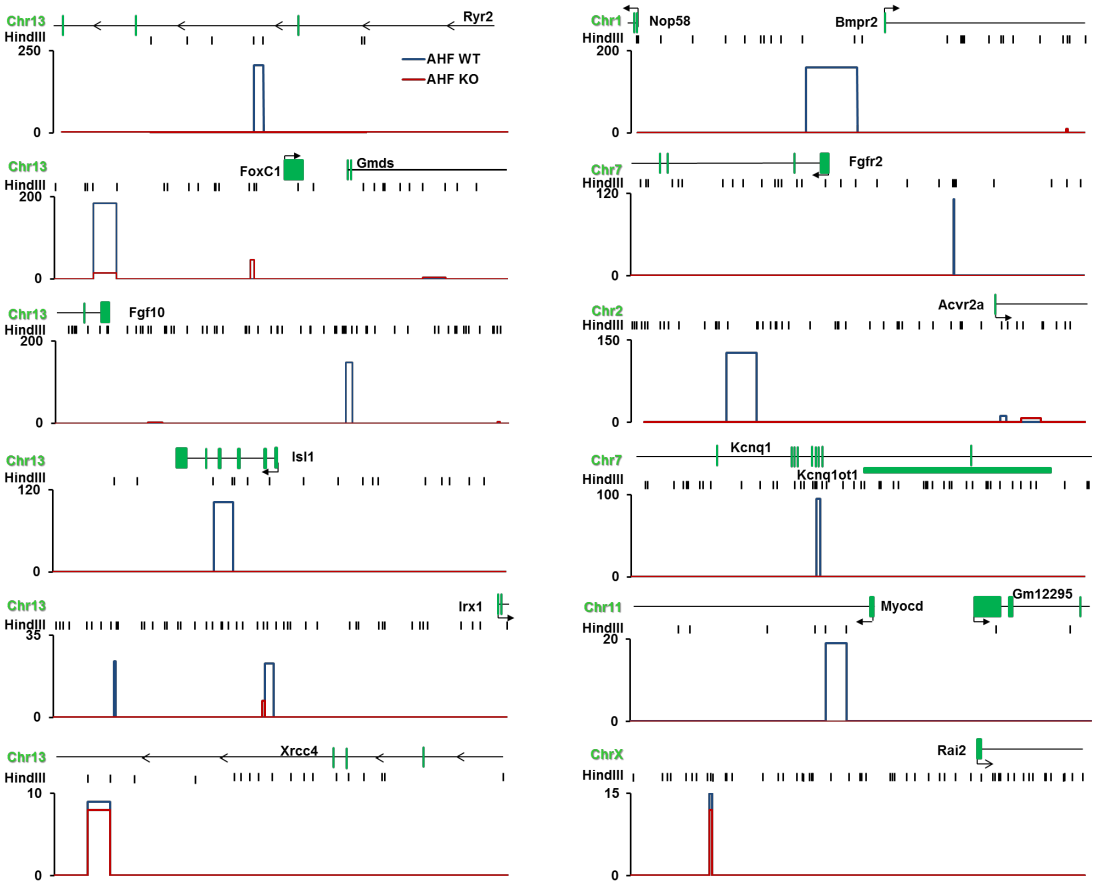

Figure 5.68 Intra- and interchromosomal interactions detected in the 3C-seq approach: Schematic representation of 3C-seq results showing specific interaction of the *Mef2c* AHF to cardiac specific genes on Chromosome 13 (left) or on different Chromosomes (right). The HindIII restriction sites are shown as black bars. Y axes - reads per million. *Xrcc4* (Chr13) and *Rai2* (ChrX), which show equal association to the AHF enhancer in WT and Ldb1-deficient EBs were used as negative controls in the subsequent experiments.

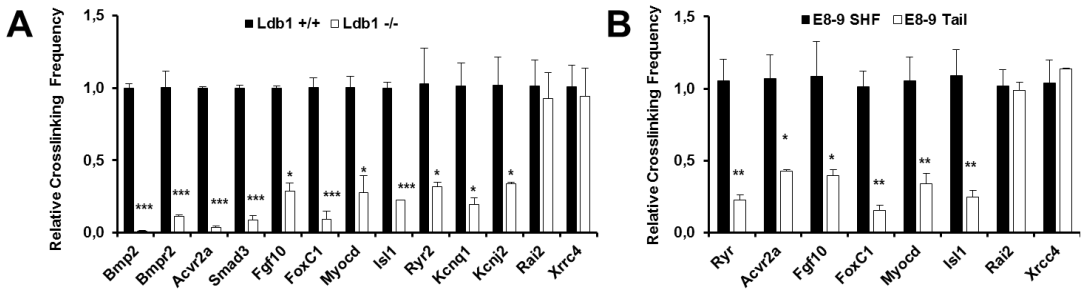

Figure 5.69 Ldb1 mediates tissue specific interaction of cardiac genes with the *Mef2c-AHF* enhancer: 3C-qPCR validation of the interactions observed using the 3C-seq approach in WT or *Ldb1*$^{-/-}$ d5 EBs ***(A)*** or in the microdissected SHF region and tail of E8-9 embryos ***(B)*** using the *Mef2c*-AHF as viewpoint. Error bars indicates SEMs. n=3. (*p≤0,05, **p≤0,01, ***p≤0,005).

5.15. Cardiac transcription binding sites are enriched in AHF-interacting sequences

Regualtory regiions in the genome have been shown to be enriched for binding sites of tissue specific transcription factors (Dogan et al., 2015; Heinz and Glass, 2012). Bionformatics analysis of the regions found in close proximity to the *Mef2c*-AHF enhancers in wild type cells showed a specific enrichment for consensus sites of important cardiac transcription factors, such as Islet-1, GATA-s, Mef2 and Tbx proteins (FIG 4.70).

Figure 5.70 Cardiac transcription factors binding motifs are enriched in the genomic regions interacting with the *Mef2c-AHF*: Motif enriched in the genomic regions found in close proximity to the *Mef2c* AHF in d5 EBs.

Importantly, we observed significant downregulation of selected genes, which show significantly higher association with the AHF enhancer in wild-type versus *Ldb1*$^{-/-}$ EBs, in d4 and d6 Ldb1-deficient EBs (FIG 4.71). In contrast genes, which showed similar association with the AHF enhancer in wild-type and *Ldb1*$^{-/-}$ EBs, were not altered. Furthermore, overexpression of Ldb1 and Isl1, but not the DN-Ldb1, which can not promote long range interactions, strongly promoted the expression of gene associated with the AHF enhancer in wild type EBs (FIG 4.72). Moreover, significant downregulation of these genes was observed in hearts and dissected SHF regions of the compound mutant E9.25 embryos compared to wild type littermates (FIG 4.73). Taken together, these data suggest that Isl1/Ldb1-containing transcription complexes orchestrate a network for transcriptional regulation and coordination in three-dimensional space during heart development in which cardiac specific enhancers are brought in close proximity to achieve proper coregulation.

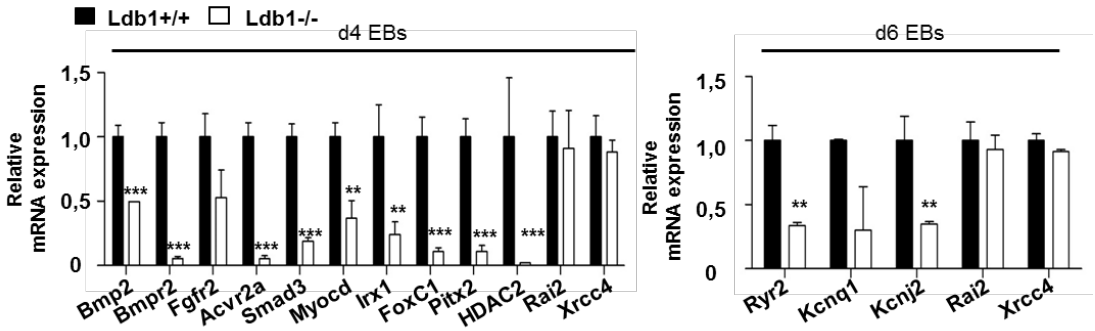

Figure 5.71 Interacting genes expression is sensitive to Ldb1 levels: Relative mRNA expression analysis for selected genes normalized to GAPDH mRNA at different days of differentiation. Error bars represent SEMs derived from three biological replicates.

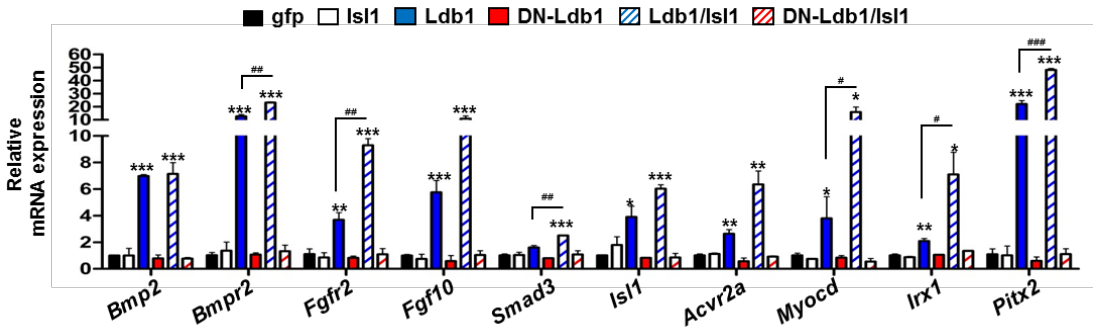

Figure 5.72 Sinergistic effect of Isl1 and Ldb1 on the expression of interacting genes: Relative mRNA expression analysis for selected genes normalized to GAPDH mRNA at day 5 of differentiation. Error bars represent SEMs derived from three biological replicates.

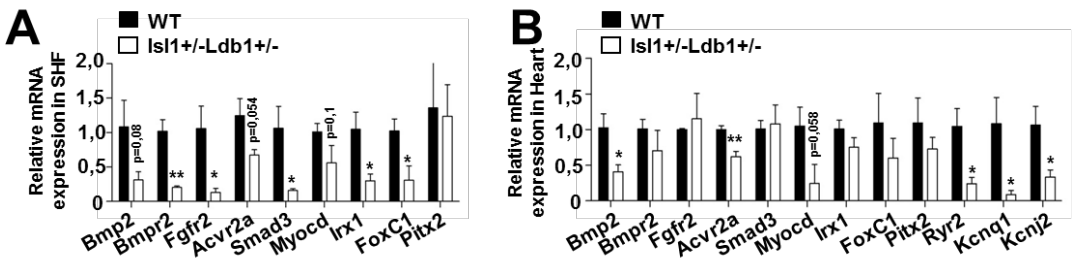

Figure 5.73 Genes identified in the 3C-seq approach are downregulated in *Isl1*$^{+/-}$*Ldb1*$^{+/-}$ embryos: Relative mRNA expression analysis for selected genes normalized to GAPDH mRNA from micro dissected SHF regions at E9.5 **(A)**. Relative mRNA expression analysis for cardiomyocyte markers normalized to GAPDH mRNA from micro dissected hearts at E9.5 **(B)**. Data are mean ± SEMs, n=3 for each group.

5.16. Ldb1 control Second Heart Field differentiation

On a mechanistic level a two-fold importance of Ldb1 in the regulation of the SHF development can be proposed: *(i)* the binding of Ldb1 to Isl1 prevents the ubiquitination and subsequent degration of Isl1 protein, which causes the complete

loss of Isl1+ cardiovascular progenitor cells in Ldb1 deficiency. *(ii)* Ldb1/Isl1 transcriptional complex coordinates the expression of important cardiac genes, by regulating the three-dimensional organization of the DNA. Importantly, Ldb1 deficiency led to dramatically decreased expression of the associated with the AHF enhancer genes and overexpression of Isl1 and Ldb1 alone strongly promoted their expression, supporting a role of Isl1/Ldb1 complex in active chromatin hub formation during cardiogenesis.

Moreover, the dosage-sensitive interdependence between Isl1 and Ldb1, resulting in various cardiac anomalies, further supports a key role of the Isl1/Ldb1 complex in coordinating chromatin looping and heart-specific gene expression.

In conclusion these data suggest a model in which Ldb1/Isl1-containing transcription complexes orchestrate a network for transcriptional regulation and coordination in three-dimensional space during heart development.

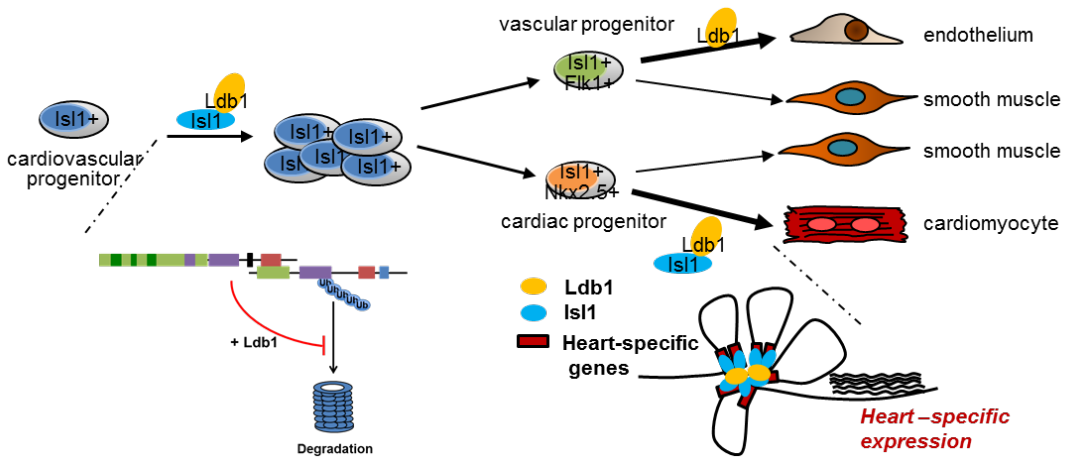

Figure 5.74 Proposed model of the role of Ldb1 during SHF differentiation: On one hand, Ldb1 binds to Isl1 and protects it from proteasomal degradation. On the other hand the Isl1/Ldb1 complex orchestrates a network for transcriptional regulation and coordination in three-dimensional space during heart development.

6. Discussion

The 3D organization of the genome in the nucleus is not random and genome organization plays a fundamental role in regulating gene expression during development. Moreover, this 3D spatial organization of the genome is not static, for example during reprogramming of mouse fibroblast to iPS the genome organization shifts towards a 3D structure similar to the one observed in mouse ESCs (Denholtz et al., 2013). However, the factors involved in mediating the cell type specific enhancer-promoter interactions are not fully known. CTCF and Cohesin, together with the Mediator complex may be involved in constitutive long range interactions, while cell specific transcription factors and their cofactors may be involved in regulating cell- and developmental-specific interactions (Bodnar and Spector, 2013; Denholtz et al., 2013; Kim and Dean, 2012; Phillips-Cremins et al., 2013).

Ldb1 is one example of cofactors mediating cell- and locus-specific long range promoter-enhancer interactions. The role of Ldb1 during development has been proved to be critical in several processes, such as erythropoiesis (Krivega et al., 2014; Song et al., 2010; 2007; Wadman et al., 1997), motor neuron differentiation (Becker et al., 2002) and hind development (Narkis et al., 2012). Interestingly KO of Ldb1 in mouse embryo is embryonic lethal at E9.5 due to severe defects in the development of the neural system and the absence of the heart (Mukhopadhyay et al., 2003), however its role in heart development is completely unknown. Since *Ldb1* is broadly expressed it is inviting to speculate that via the interaction with specific LIM-containing transcription factors Ldb1 mediates long range promoter enhancer interactions. Ldb1 was shown to regulate long-range promoter-enhancer interactions in the *ß-globin* locus during development (Deng et al., 2012; Krivega et al., 2014; Song et al., 2007). Ldb1 function during development has been mediated through its DNA binding partners. Ldb1 binds to all LIM-nuclear transcription factors and has been shown that in different cell types, it can interact to diverse and cell specific LIM transcription factors to regulate the transcriptional program. In erythroid cells, for example, Ldb1 is part of a large transcriptional complex containing LIM proteins, GATA and bHLH factors and epigenetic regulators (Bach et al., 1997; Jurata et al., 1998; Krivega et al., 2014; Meier et al., 2006; Morcillo et al.,

1997; Soler et al., 2010). In these cells, Ldb1-LMO2 complex acts as a molecular adaptor between GATA1 and bHLH factors sitting on different regulatory elements of the *ß-globin* locus and facilitate the juxtaposition of enhancers and promoter (Deng et al., 2012; Krivega et al., 2014; Soler et al., 2010; Song et al., 2007; Wadman et al., 1997).

Noteworthy Ldb1 interacts, during motor neurons development, with Isl1 and Lhx3 to determine the cell fate decision of the progenitor cells (Becker et al., 2002). Isl1 is a LIM-HD transcription required for proliferation, survival and migration of SHF progenitors into the forming heart. Consequently Isl1 deficient embryos display a linear heart tube, where the ventricular chamber display left ventricular identity and lack the RV and the OFT, both structures derived from the SHF (Cai et al., 2003).

It is attractive, therefore, to speculate that during heart development Ldb1 interacts with Isl1 to regulate SHF development, by promoting heart specific long-range chromatin interactions.

6.1. Ldb1 and Isl1 co-operate to promote cardiac differentiation

Consistent with the idea of a role for Ldb1 during cardiogenesis Ldb1 null ESCs were not able to differentiate to cardiomyocytes or endothelial cells, as assessed by beating analysis (FIG 4.2) and expression analysis of cardiomyocyte and endothelial markers at d6 and d9 of differentiation (FIG 4.3). Similar to what was observed in *Ldb1*$^{-/-}$ embryos (Mukhopadhyay et al., 2003) mesoderm formation was not affected in the Ldb1 deficient embryoid bodies (FIG 4.5 and FIG 4.39), however SHF and pancardiac marker genes *Hand2, Tbx1, Mef2c, Fgf10* and *Nkx2-5* expression was severely downregulated in the KO derived EBs compared to the control lines (FIG 4.6). Expression for some of these genes was shown to be lost upon Isl1- or Ldb1-deficiency in embryos (Cai et al., 2003; Mukhopadhyay et al., 2003) suggesting a possible cooperation for both protein in regulating their expression.

Further, conditional Ldb1 deletion in the SHF using the *Isl1-Cre* led to embryonic lethality at E10.5 and caused severe defects in the second heart field derived structure, with a shorter OFT and a smaller RV supporting a crucial role of *Ldb1* for

SHF development (FIG 4.8 and FIG 4.9). *Mef2c* KO embryos displayed a very similar phenotype to what observed in the *Isl1*$^{Cre/+}$*Ldb1*$^{flox/flox}$ embryos, with a undeveloped OFT and absence of the RV (Lin et al., 1997). Moreover *Hand2* deletion in mouse embryos is lethal at E10 due to severe malformation of the heart, absence of RV and defects in the development of the OFT, similar to the phenotpe observed upon deletion of *Ldb1* in the SHF (Srivastava et al., 1997). Furthermore, hypoplasia of both the OFT and RV, was observed in *Fgf8*;*Fgf10* mutants (Watanabe et al., 2010). *Ldb1* deletion in EBs led to downregulation of these important genes (FIG 4.6). It is therefore tempting to speculate that the phenotype observed in our *Isl1*$^{Cre/+}$*Ldb1*$^{flox/flox}$ embryos at E9.0 may partially be caused by loss of expression of *Mef2c, Fgf10* and *Hand2* in the SHF. Consistent with the hypothesis of Ldb1/Isl1 co-operation during cardiogenesis *Ldb1*$^{+/-}$*Isl1*$^{+/-}$ embryos showed genetic interaction (Table 4.1). Level of *Fgf8* and *Fgf10* are critical for the development of the OFT, PAAs and their derivates (Watanabe et al., 2010). *Fgf8/Fgf10* compound mutants present several cardiac defects, such as alignment defects of the aorta and pulmonary trunk (transposition of the great arteries), together with double outlet of the RV (DORV) and ventricular septal defects (VSD), a striking similar sets of defects of the ones observed in *Isl1*$^{+/-}$*Ldb1*$^{+/-}$ embryos at E14.5 and E16.5 (Watanabe et al., 2010) (FIG 4.23 and FIG 4.24). *Fgf10* transcription is regulated by ISL1 in human and mouse embryos (Golzio et al., 2012; Watanabe et al., 2012). Furthermore *Tbx1*$^{-/-}$ embryos also displayed a reduced OFT domain at E10.5, resulting in DORV, VSD and truncus arteriosus communis (TAC) and failure of alignment between the atrioventricular canal and the outflow tract (Théveniau-Ruissy et al., 2008; Vitelli et al., 2002). Interestingly we observed downregulation of these genes in microdissected SHF region or heart of E9.25 *Ldb1*$^{+/-}$*Isl1*$^{+/-}$ embryos (FIG 4.26), or in *Ldb1* deficient EBs at day 4, a stage enriched with cardiac progenitor cells (FIG 4.6). It is tempting to speculate that the defects observed in the *Ldb1*$^{+/-}$*Isl1*$^{+/-}$ embryos are due to the reduction in expression of downstream target genes.

Taken together these data suggest a critical role for the Isl1/ldb1 transcriptional complex to regulate the expression of several SHF genes during heart development.

6.2. Ldb1 regulates Isl1 at protein level

Interestingly Isl1 protein levels were completely absent in case of Ldb1 depletion both in EBs and in embryos (FIG 4.10 and FIG 4.11). Consistently, Güngör and colleagues showed that LIM-HD proteins levels were regulated by proteasomal degradation and that Ldb1 binding prevents their ubiquitination and thereby protects them from degradation (Güngör et al., 2007). Furthermore during erythropoiesis Ldb1 shRNA-knockdown in MEL cells resulted in downregulation of LMO2 at protein level (Song et al., 2007). On the same line of evidence, overexpression of full length or of a Ldb1 form missing the dimerization domain increased endogenous levels of LMO2 (Song et al., 2007). As expected, due to the role of Ldb1 to stabilize LIM-HD transcription factors at protein levels via physical interaction over expression of DN-Ldb1 led to stabilization of full length Isl1 (FIG 4.14). Co-IP studies in HEK293T cells confirmed that the interacton between Isl1 and Ldb1 take place between the LIM1 domain of Isl1 and the LID domain of Ldb1, as was shown previously in *in vitro* and biophysical studies (FIG 4.16 and Bhati et al., 2008; Jurata and Gill, 1997). Confirming that the physical interaction is required for the stabilization of Isl1 at protein level, a truncation of Ldb1 incapable of interacting with Isl1, Ldb1ΔLID, failed to stabilize Isl1 in HEK293T (FIG 4.14). Moreover, DN-Ldb1 failed to stabilize a truncation of Isl1 that can not interact with Ldb1, Isl1ΔLIM1 (FIG 4.15). Finally on a mechanistic level this study could prove a post-transcriptional regulation in which Isl1 is poliubiquitinated via the LIM2 domain (FIG 4.12 and FIG 4.13). Isl1 degradation is blocked by the interaction with Ldb1 or DN-Ldb1 (FIG 4.14 and FIG 4.15) in a similar manner to what was observed for other LIM proteins (Güngör et al., 2007; Song et al., 2007). Interestingly it was shown that stoichiometry between LIM-HD, LIM-only and Ldb1 cofactors in different cells types are of critical importance to determine cell fate (Becker et al., 2002; Song et al., 2009). This post-translational regulation of the LIM transcription factors may contributes to the cell fate decision of the SHF cardiac progenitor population. Although Ldb1 ablation does not affect early cardiovascular commitment, overexpression of DN-Ldb1 led to a significant decrease of $Flk1^{+}PdgfR\text{-}a^{+}$ progenitor cells (FIG 4.39). Together these data show that Ldb1 protects Isl1 in the cardiac progenitor pool of the second heart field

and might have a role in the specification of early cardiac progenitors, process that is perturbed by DN-Ldb1. It can be speculated that Ldb1 will contribute to the formation of cell type-specific transcriptional complexes, similar to what was observed during hematopoiesis (Meier et al., 2006).

6.3. The ability of Ldb1 to promote long range interaction is needed for proper cardiac differentiation

If the interaction and the stabilization effects are sufficient to induce cardiac differentiation, DN-Ldb1 should be able to rescue the *Ldb1*$^{-/-}$ deficiency in the ESCs. On the other hand several reports showed that the looping activity is needed to achieve proper expression of downstream targets (Becker et al., 2002; Krivega et al., 2014). To distinguish between these two hypothesis DN-Ldb1 was ectopically expressed in zebrafish embryos. Expression of this truncated protein was shown to compete with full length Ldb proteins for the binding to nuclear LIM factors and to cause developmental defects (Bach et al., 1999; Becker et al., 2002). DN-Ldb1 expression, although did not alter the Isl1 positive progenitor pool at 10s (FIG 4.34), it caused defects at the venous pole which are strikingly similar to Isl1 mutant fishes (FIG 4.32 and FIG 4.33) (de Pater et al., 2009). In zebrafish the pacemaker activity is located at the venous pole of the heart, a structure derived from Isl1+ progenitor population (de Pater et al., 2009). In a striking parallel to Islet mutant fishes (de Pater et al., 2009; Tessadori et al., 2012), DN-Ldb1 injected embryos displayed bradycardia and arrhythmia (FIG 4.30). Moreover, in contrast to control embryos in DN-Ldb1 expressing embryos Isl1+ cells were found outside of the venous pole demostrantig a key role of Ldb1 in regulating the differentiation of Isl1+ cardiac progenitor cells (FIG 4.31). Furthermore DN-Ldb1 injection led to reduction of expression of *bmp4* (FIG 4.33) at the venous pole of zebrafish heart, similar to what observed in *isl1* mutant fishes (de Pater et al., 2009). Taken together these data suggest that Ldb1 may mediate part of the functions of isl1 during heart development in zebrafish. Moreover these results strengthen our hypothesis that long range interactions mediated by the Isl1-Ldb1 transcriptional complex are of utmost importance for SHF development.

Consistent with this hypothesis, in *Ldb1*$^{-/-}$ ESCs overexpression of DN-Ldb1, alone or in combination with Isl1, failed to rescue the loss of Ldb1 (FIG 4.37 and FIG 4.48). Consistently, in *Ldb1* depleted erythroid cells only the expression of full lengths Ldb1 could restore the differentiation capability, while expression of dimerization deficient truncations of Ldb1 failed to regulate the expression of downstream targets of the Ldb1 complex and to promote differentiation (Krivega et al., 2014; Mylona et al., 2013).

Interestingly expression of DN-Ldb1 did not affect the generation of the Isl1+ progenitor pool in zebrafish embryos nor in Ldb1-depleted EBs (FIG 4.34 and FIG 4.40). On the same line DN-Ldb1, either alone or in combination with Isl1, could not upregulate the expression of progenitors markers *Hand2*, *Mef2c*, *Tbx20* and *Hand1* in EBs derived from *Ldb1*$^{-/-}$ ESCs (FIG 4.41). Taken together these results suggest that long range chromosomal interactions mediated by the Isl1/Ldb1 transcriptional complex are of crucial importance for the differentiation of Isl1+ cardiac progenitor population in both zebrafish and murine models. Moreover we could show that the protection provided to Isl1 by Ldb1, or DN-Ldb1, binding is sufficient to regulate the expansion of the Isl1+ cardiac progenitor pool.

6.4. Isl1/Ldb1 complex facilitates enhancer-promoter interaction in *Mef2c* and *Hand2* loci

Enhancers are short DNA sequences that activate transcription of their target promoters in a distance and orientation independent, tissue specific manner during embryonic development. In eukaryotes, enhancer activation involves the physical interaction between promoter and enhancer through the formation of a chromatin loop mediated by specific transcripition factors complexes (Buecker and Wysocka, 2012; Bulger and Groudine, 2011; Calo and Wysocka, 2013; Kulaeva et al., 2012).

Mef2c expression in the heart is driven by multiple enhancers, one of which confers responsiveness to Isl1 and Gata (Both et al., 2004; Dodou et al., 2004), while the promoter drives its broad expression (Edmondson et al., 1994; Infantino et al., 2013). *Mef2c*-deficient hearts develop OFT abnormalities and the right ventricle fails to form (Lin et al., 1997). Similar to *Mef2c* the expression of *Hand2* in the heart is

under control of a Gata-responsive enhancer (McFadden et al., 2000). Our data revealed the presence of an Isl1-binding site in the *Hand2* controlling enhancer (FIG 4.47). Furthermore *Hand2* and *Mef2c* expression is responsive to the presence of full length Ldb1 both in EBs and *in vivo* model (FIG 4.6, FIG 4.22, FIG 4.26, FIG 4.35 and FIG 4.41) suggesting a role for Ldb1/Isl1 complex in cooperating to regulate their expression. Consistent with this hypothesis ChIP analysis revealed that Isl1 and Ldb1 are bound to the regulatory elements of *Mef2c* and *Hand2* during EBs differentiation at day 4 and day 5, time points when the initial cardiac progenitor cells start to emerge, and in vivo in micro dissected E8-9 cardiogenic region of mouse embryos (FIG 4.45, FIG 4.46, FIG 4.49 and FIG 4.50). Ldb1 containing complexes were shown to regulate dynamic promoter-enhancer interactions in the developmental regulated *ß-globin* locus (Deng et al., 2012; Soler et al., 2010; Song et al., 2010; 2007; Vakoc et al., 2005), as well as in the *Myb* and other loci (Jing et al., 2008; Stadhouders et al., 2012a; 2012b). Consistent with our idea that the Isl1/Ldb1 complex regulates transcription of the downstream target genes by facilitating enhancher-promoter interactions, 3C-seq and 3C-PCR analysis conducted at day 5 of EBs development proved the presence of numerous interaction that were lost in Ldb1-deficient cells. 3C-seq data using the *Mef2c* AHF enhancer (Dodou et al., 2004) and the *Mef2c* promiscuous promoter as viewpoint displayed that at day 5 of EBs development these two regulatory elements are involved in different Ldb1 dependent interactions (FIG 4.55). Recently a 3C based approach was used to investigate the three dimensional conformation of the *Tbx3* and *Tbx5* loci (van Weerd et al., 2014). van Weerd and colleagues, using the 4C-seq analysis, identified two interacting fragments as novel enhancers that drive Tbx3 expression in limb and in the AVC of the developing embryo, but not in the brain (van Weerd et al., 2014). Interestingly, analysis of the fragments interacting with the AHF revealed the presence of several heart-specific transcription binding sites in these sequences (FIG 4.58, FIG 4.59 and FIG 4.70). In a similar manner, we could identified a new putative enhancer region for *Mef2c* expression in cardiac progenitor cells in the region located 13Kb upstream of the TSS (FIG 4.61). This region shows a strong interaction when we utilized the AHF as bait in d5 EBs, as well in different stages of cardiac development (FIG 4.55,

FIG 4.56 and FIG 4.57). The -13Kb putative enhancer is decorated with typical enhacers marks, such as H3K27ac, H3K4me1 and enriched for RNA PolII, contains conserved Isl1 and GATA4 binding sites, and is occupied by Isl1 in cardiac progenitor cells (FIG 4.60 and FIG 4.61; Bulger and Groudine, 2011; Calo and Wysocka, 2013). Moreover similar interactions between a cardiac specific enhancer and the promoter of *Hand2* could be detected in d5 wild type EBs, but was completely lost upon Ldb1 deficiency (FIG 4.53 and FIG 4.54). Strenghtening the idea that these chromatin loopings are of physiological importance *in vivo* analysis using the cardiogenic region of E8-9 embryos, where the *Me2c-AHF* is active (Dodou et al., 2004), identified a similar three dimensional comformation of the *Mef2c* locus. This three dimensional organization was lost in the tail of the embryos, where AHF enhancer is not active (Dodou et al., 2004), in a similar fashion of the previously described *Tbx3* locus where the interaction between the promoter and the two novel enhancers, eA and eB, is lost in the brain, tissue in which eA and eB failed to drive transgenic lacZ or GFP expression (van Weerd et al., 2014).

Of particular interest are also the interactions towards the 3' region of the *Mef2c* gene. Looping of the promoter to the transcription termination sites was observed in several models (Ansari and Hampsey, 2005; Dieci and Sentenac, 2003). These gene loops have been proposed to facilitate efficient recycling of the transcriptional machinery and re-initiation of consecutive rounds of transcription (Ansari and Hampsey, 2005; Dieci and Sentenac, 2003; Palstra, 2009). For example in *Saccharomyces cerevisae* O'Sullivan and colleagues described a looped conformation for two relatively long genes, *SEN1* and *FMP27*, in which the promoter and the terminator regions are in close spatial proximity. This conformation was suggested to facilitate successive reinitation rounds of transcription and/or to function as proofread control sequences before efficient transcription (O'Sullivan et al., 2004). Therefore our data suggest a role for Ldb1, together with Isl1, in organizing the loci of downstream target genes in a transcriptional permissive conformation, and, generating a loop between *Mef2c* promoter and the 3' end of the gene, which might potentially generate a functional reinitation complex for subsequent rounds of *Mef2c* transcription.

Interestingly enrichment at regulatory sequences was observed also for the dimerization deficient DN-Ldb1 (FIG 4.64). However DN-Ldb1, alone or in combination with Isl1, failed to upregulate the expression of *Mef2c* and *Hand2* and subsequently cardiomyocyte markers (*Mlc2a*, *Mlc2v*, *Tnnt2*). Consistently with previous reports (Krivega et al., 2014) and with our hypothesis that Isl1/Ldb1 transcriptional complex regulates transcription by promoting long range interactions, DN-Ldb1 is not able to restore the long-range interaction, identified in wild type EBs, in d5 *Ldb1*$^{-/-}$ EBs, neither in the *Mef2c* locus nor in the *Hand2* locus (FIG 4.54 and FIG 4.63). Similar to ectopically expressed DN-Ldb1, binding of viral expressed OCT4 and NANOG to their downstream target gene promoters in human fibroblast was not sufficient to induced pluripontecy (Zhang et al., 2013). 3C-PCR analysis of the *OCT4* locus demonstrated that *OCT4* promoter interacts to a region located 10Kb. This intrachromosomal looping, necessary for the efficient expression of *OCT4* and the reprogramming of human fibroblast to iPSCs, was lost upon Cohesin loss of function, even with a similar binding of OCT4 (Zhang et al., 2013).

These results, together with the cardiac defects observed in DN-Ldb1 expressing zebrafish embryo suggest the requirement for long range interactions between enhancers and promoters to properly regulate the expression of downstream target genes, similar to what has been reported for the *ß-globin*, *c-Myb, OCT4* and other loci in several model organisms (Jing et al., 2008; Krivega et al., 2014; Soler et al., 2010; Song et al., 2007; Stadhouders et al., 2012a; Zhang et al., 2013).

6.5. A dynamic promoter-enhancer interaction controls *Mef2c* isoform switch during cardiogenesis

Several mRNA isoform of *Mef2c* are annotated in the UCSC genome browser (mm9, (Kent et al., 2002)). Absolute quantification of *Mef2c* expression during cardiogenesis showed a switch of *Mef2c* isoform from the long isoform, transcribed from the annotated promoter, to a shorter isoform with an alternative transcription starting site located 1,5Kb downstream of the AHF (FIG 4.62). This isoform switch is accompanied by a change of chromosomal conformation similar to what observed in the *ß-globin* locus (FIG 4.56 and FIG 4.57) (Palstra et al., 2003). During embryonic

development different globin isoforms are expressed in a precisely timed fashion. This tighly controlled expression is achieved thanks to the specific interactions of the LCR to different globin gene promoters during embryogenesis (FIG 2.13 and (Kim and Dean, 2012)). Ldb1 containg complexes were shown to take place, and control, this process (Kim and Dean, 2012; Soler et al., 2010; Song et al., 2007). Similar dynamic promoter-enhancer interaction was described for the regulation of the expression *c-kit* were replacement of GATA-2 by GATA-1 alters the interchromosomal interaction between enhancer and promoter and results in downregulation of *c-kit* expression (Dean, 2011; Jing et al., 2008).

6.6. The Isl1/Ldb1 transcriptional complex coordinates a three dimensional network during heart development

Highly organized three dimensional configuration of the genome has been observed in different model organism, ranging from prokaryotes, such as *Caulobacter crescentus,* to Arabidopsis thsaliana, yeast and high vertebrates such as mouse and human (Dixon et al., 2012; Feng et al., 2014; Jin et al., 2013; Le et al., 2013; O'Sullivan et al., 2004; Rao et al., 2014). Three dimensional organization of the genome and transcriptional regulation are intimately connected. In *C. crescentus* has been suggested that highly expressed genes are of critical importance for the definition of topological domain boundaries (Le et al., 2013). Moreover the chromatin interaction profile has been succesfuly used to predict co-expression of genes in the mouse brain cortex (Babaei et al., 2015). Recent studies in mouse ESCs and Arabidopsis thaliana have shown that the status of the chromatin plays an important role in the three dimensional organization. The open/active chromatin is more likely to interact with other open genomic regions and Polycomb enriched regions more likely to interact with repressed chromatin (Bonora et al., 2014; Grob et al., 2014). During reprogramming of fibroablasts to iPSCs the genome-wide chromatin interaction landscape is rearranged in a ESCs-like interaction network (Apostolou et al., 2013; de Wit et al., 2013; Denholtz et al., 2013). Genomic regions enriched for clusters of binding sites for the pluripotency transcription factors Oct4, Nanog and Sox2 are found to specifically colocalize in the three dimensional space in

ES and iPS cells, but not in fibroblasts, suggesting that pluripotency-related genes are brought in physical contact for coordinated gene expression (Apostolou et al., 2013; de Wit et al., 2013; Denholtz et al., 2013). General transcription factors, tissue-specific proteins and special "bridging" proteins, such as Cohesin or CTCF, mediate the maintenance of the long-range chromatin interactions between enhancers and promoters (Palstra, 2009; Razin et al., 2013). Similar to what was observed during fibroblast reprogramming our 3C-seq analysis using the AHF as bait identified several specific, Ldb1-mediated interactions with multiple genes that play critical role during cardiac development (FIG 4.68, Table 4.2). These interactions are tissue and cell specific, as they are detected only in cardiac progenitors within the SHF of E8.5 embryos but not in tail. Moreover these interactions are lost upon Ldb1-deficiency (FIG 4.69). GO analysis of the genes located nearby the AHF-interacting regions revealed a striking enrichment for GO-terms connected to heart/embryonic development, in WT d5 EBs in comparison to *Ldb1*$^{-/-}$ EBs (FIG 4.66). This enrichment was lost when the promoter, active in several cell types, was used as bait (FIG 4.67). Importantly expression of these genes was responsive to the levels of Ldb1 and Isl1. Overexpression of Ldb1 strongly activated their transcription, and was further potentiated by overexpression of Isl1 (FIG 4.73). Furthermore the expression of the genes strongly associated with the AHF enhancer was not restored by overexpression of DN-Ldb1 in *Ldb1*$^{-/-}$ cells (FIG 4.72).

Recent studies analyzing enhancer contacts during *Drosophila* development, revealed that a large number of enhancer interactions are unchanged between different tissues and developmental stages and only few show significant changes (Ghavi-Helm et al., 2014). Taken togheter these data revelead one of the first examples of regulation of genome-wide chromatin reorganization mediated by a developmental regulated, cell type specific, transcription complex. The dosage-sensitive interdependence between Isl1 and Ldb1 in the expression of these key factors in cardiogenesis, further supports a key role of the Isl1/Ldb1 complex in coordinating a three dimensional genome organization, upstream of a regulatory network driving cardiac differentiation and heart development.

In conclusion this study highlight a central role for Ldb1 in the regulation of the

second heart field development and differentiation firstly by controlling the abundance of Isl1 at protein level and subsequently by promoting long range promoter-enhancer interactions in concert with Isl1 in order to create active chromatin hub where gene important for heart development can be co-regulated.

7. Future Perspective

This work propose a central role for Ldb1 in the regulation of second heart field development and differentiation.

We show that Ldb1 stabilizes Isl1 and therefore promotes of SHF expansion and differentiation. Finding the E3 ligase responsible for the poli-ubiquitination of Isl1 will help to understand the exact biochemical mechanism of this regulation.

Moreover *ISL1* copy number variations and haploinsufficiency in humans have been recently linked to CHDs (Bansal et al., 2014; Osoegawa et al., 2014). Interestingly the cardiac malformations found in the $Ldb1^{+/-}Isl1^{+/-}$, VSD and OFT defects, partly resemble the ones displayed in humans. It is tempting, therefore, to suggest a possible use of this mouse model to study the role of ISL1 haploinsufficiency in humans.

A possible role for LDB1 in human CHD has not yet been proposed. On the other hand a recent Japanese study found LDB1 to be part of a 3,3 Mb deletion in a patient suffering of CHD and mental retardation (Hayashi et al., 2010). Due to the important role of LDB1 in the development of both cardiac and neural system it is tempting to speculate a role for LDB1 in the etiology of these specific defects. It will be, therefore, of utmost interest to further study the possible role of mutations within the LDB1 gene in humans as cause for CHD and mental retardation.

Furthermore this study is the first to show that the Ldb1/Isl1 complex plays an important role in coordinating the transcription of a large number of cardiac related genes, binding specific regulatory sequences and possibly creating active chromatin hubs. It would be of great interest to confirm this *in vivo* in sorted Isl1 positive cardiac progenitor cells via 3C based methods such as ChIA-PET (Fullwood et al., 2001) or Hi-C (Lieberman-Aiden et al., 2009) that will allow for an unbiased analysis of the higher order chromatin organization in cardiac progenitors. Additionally specific interaction with FISH based analysis should be validated. Moreover analysis of histone marks and recruitment of active RNA Polimerase II on the loci identified by our 3C-seq analysis could further help to characterize the active chromatin hubs formed during heart development.

Finally, since Ldb1 and Isl1 are expressed in multiple tissues during embryogenesis would be of great interest the understanding of what confers the specificity of the chromatin reorganization. Our 3C-seq analysis showed an enrichement for other transcription factors binding sites (GATA-s, Nkx-s, Mef and Tbx-s). It would be helpful in this contest the characterization of the Isl1/Ldb1 complex *in vitro* and/or *in vivo*.

8. Materials and Methods

8.1. Materials

8.1.1. Chemicals

Substance	Source of supply	Reference number
1-Phenyl-2-thiourea (PTU)	Acros	207250250
2-Log DNA ladder (0.1-10.0 kb)	NEB	#N3200L
Acetic anhydride ($(CH_3CO)_2O$)	Sigma	A6404-200ML
Agarose, low melt	Roth	6351.2
Agarose NEEO Ultra	Roth	2267,3
Albumin fraction V (BSA)	Roth	8076.2
Ammonium persulfate (APS) ($(NH_4)_2S_2O_8$)	Sigma	A3678-25G
Ampicillin sodium salt	Sigma	A99518-25G
BM purple AP substrate, precipitating	Roche	11 442 074 001
Bradford reagent, ready-to-use	Fermentas	R1271
Chloroform ($CHCl_3$)	Roth	Y015,1
Chlorophenolred-ß-D-galactopyranoside (CPRG)	Sigma	59767
ddH_2O		
DEAB (4-diethylaminobenzaldehyde)	Sigma-Aldrich	31830
Dimethyl sulfoxide (DMSO) ($(CH_3)_2SO$)	Sigma	D-8779
dNTP (Nucleoside triphosphate) Set 1	Roth	178,1
DTT (Dithiothreitol) ($C_4H_{10}O_2S_2$)	Roth	6908.3
Dry-milk, non fat milk	BIO-RAD	170-6404
EGTA (ethylene glycol tetraacetic acid) ($C_{14}H_{24}N_2O_{10}$)	Roth	3054.2
Ethanol denatured (CH_3CH_2OH)	Roth	K928,3
Ethanol pro analysis (CH_3CH_2OH)	Merck	1,00983,2511
Ethidium bromide solution ($C_{21}H_{20}BrN_3$)	Sigma	E1510-10ML
Ethylenediaminetetraacetic acid (EDTA) ($C_{10}H_{16}N_2O_8$)	Sigma	E5134-250G
FuGENE® HD Transfection Reagent	Roche	4709705/100
Formamide (CH_3NO)	Fluka	47670
Gelatin from bovine skin, Type B	Sigma	G9391-100g
Glutaraldehyde ($CH_2(CH_2CHO)_2$)	Sigma-Aldrich	G5882-10ML
Glycerol ($C_3H_8O_3$)	Roth	3783,1
Glycine (NH_2CH_2COOH)	Sigma	15527
Hexadimethrine bromide (polybrene)	Sigma-Aldrich	#H9268
Isopropanol (C_3H_8O)	Roth	6752,4
Kanamycinsulfate	Roth	T832,1

LB-agar (Lennox)	Roth	X965,2
LB-medium (Lennox)	Roth	X964,2
Levamisole ($C_{11}H_{12}N_2S$)	Fluka	31742
Lithium chloride (LiCl)	Roth	3739.1
Maleic acid ($C_4H_4O_4$)	Roth	K304.1
Methanol (CH_3OH)	Roth	4627,5
MG-132	Calbiochem	474790
Magnesium chloride ($MgCl_2$)	Sigma	M2393-500G
Magnesium sulfate ($MgSO_4$)	Fischer Scientific	M120,37
Magnesium sulfate-heptahydrate ($MgSO_4 \cdot 7H_2O$)	Merck	1.05886.0500
TEMED (Tetramethylethylenediamine) ($(CH_3)_2NCH_2CH_2N(CH_3)_2$)	Roth	2367,1
Nonidet P-40 (NP-40)	Fluka	74385
Paraformaldehyde (PFA) ($OH(CH_2O)_nH$ (n = 8 - 100))	Sigma-Aldrich	15,812-7
Phenol red ($C_{19}H_{14}O_5S$)	Sigma	P0290
Phosphatase inhibitor Cocktail set V	Calbiochem	524632
PIPES (Piperazine-N,N'-bis(2-ethanesulfonic acid)) ($C_8H_{18}N_2O_6S_2$)	Sigma	P1851
PMSF (Phenylmethylsulfonyl fluoride) ($C_7H_7FO_2S$)	Serva	32395
Poly(2-hydroxyethylmethacrylate) PoliHEMA	Sigma	P3932-10G
Potassium chloride (KCl)	Roth	6781.3
Potassium hexacyanidoferrate (II) trihydrate	Sigma	P9387
Potassium hexacyanoferrate (III)	Sigma	P8131-100G
Prestained protein molecular weight marker	Fermentas	#SM0441
Protease inhibitor cocktail set I	Calbiochem	535142
Puromycin	Sigma-Aldrich	#P8833
Rotiphorese® Gel 30 (37.5:1)	Roth	3029.1
Salmon sperm DNA	Upstate	16-157
Sodium dodecyl sulfate (SDS) ($NaC_{12}H_{25}SO_4$)	Sigma	L4390-100G
Sodium phosphate monobasic monohydrate ($NaH_2PO_4 \cdot H_2O$)	Sigma	53522-1KG
Sodium phosphate dibasic dodecahydrate ($Na_2HPO_4 \cdot 12H_2O$)	Sigma-Aldrich	04273
TRIzol® reagent	Ambion	15596-026
Triethanolamine ($C_6H_{15}NO_3$)	Sigma	T1377-500ML
Tricaine methane sulphonate (Tricaine) ($C_{10}H_{15}NO_5S$)	Pharmaq	MS222-100G-V1
TRIS (tris(hydroxymethyl)aminomethane) ($(HOCH_2)_3CNH_2$)	Roth	4855.2
Trisodium citrate dihydrate	Sigma-Aldrich	25116
Triton X-100 ($(C_{14}H_{22}O(C_2H_4O)_n)$)	Sigma	X100-500ML
Tween 20 EP, NF	Sigma	T2700-500ML
Yeast tRNA	Roche	10 109 517 001

X-gal	Roth	2315.2
β-mercaptoethanol (C_2H_6SO)	Sigma	60-24-2

8.1.2. Kits

Kit	Source of supply
2x SYBRGreen	Applied Biosystems
Absolutely RNA® nanoprepkit	Stratagene
GenElute™ gel extraction kit	Sigma
GenElute™ HP plasmid midiprep kit	Sigma
GenElute™ HP plasmid miniprep kit	Sigma
GenElute™ PCR clean-up kit	Sigma
Luciferase assay system	Promega
mMESSAGE mMACHINE® Kit	Ambion
RedTaq® ReadyMix™ PCR Reaction Mix	Sigma

8.1.3. Enzymes

Enzyme	Source of supply
Alkaline phosphatase (FastAP)	Fermentas
FirePol polymerase	Solis BioDyne
Hercules polymerase	Stratagene
Protease, from streptomyces griseus (pronase)	Sigma
Proteinase-K from *Engyodontium album*	Sigma
Restriction enzymes + buffers	NEB
T4-Ligase	NEB
T4-ligase	Fermentas
Trypsin EDTA	GIBCO

8.1.4. Buffers and media

Buffer	Composition
10% Ammonium persulfate	0.44M Ammonium persulfate ($H_8N_2O_8S_2$)
2x SDS PAGE sample buffer	150mM TRIS pH=6.8 (added in solution) 1.2% (v/v) SDS 30% (v/v) glycerol 6.7% (v/v) β-mercaptoethanol 1.8mg bromophenol blue
10x PBS	1.37M NaCl 27mM KCl 0.1M $Na_2HPO_4 \cdot 12H_2O$ 17.6mM KH_2PO_4 (pH titrated to 7.4)
PBST	0.05% (v/v) Tween 20 in 1xPBS

Blotting buffer	20% (v/v) methanol 192mM glycine 25mM TRIS
Buffer A (cytosolic/nuclear fractioning)	10mM HEPES pH=7.9 (added in solution) 10mM KCl 1.5mM $MgCl_2$
Buffer B (cytosolic/nuclear fractioning)	0.45M NaCl 12.5% (w/v) glycerol 15mM HEPES pH=7.9 (added in solution) 5mM KCl 1.5mM MgCl2 0.1mM EDTA
10x agarose gel sample buffer	250mg/100ml (w/v) bromophenol blue 250mg/100ml (w/v) xylene cyanol 50mM TRIS pH=7.6 (added in solution) 60% (v/v) glycerol
Z-buffer	50mM $Na_2HPO_4 \cdot 12H_2O$ 40mM $NaH_2PO_4 \cdot H_2O$ 10mM KCl 1mM $MgSO_4 \cdot 7H_2O$ (pH titrated to 7.0)
E3 zebrafish medium	5mM NaCl 0,17mM KCl 0,33mM $CaCl_2$ 0,33mM $MgSO_4$
E3 + PTU	0,003% phenylthiourea (solved in E3)
10x SDS PAGE running buffer	35mM SDS 250mM TRIS 0.86M glycin
2x RNA-loading dye	100µl Formamide 40µl Formaldehyde 20µl 10xTBE 2µl Ethidium bromide
10x TBE	0.89M TRIS 0.89M H_3BO_3 20mM Na_2EDTA pH=8.0
Co-IP buffer	50mM TRIS-HCl pH=7.5 (added in solution) 15mM EGTA 100mM NaCl 0.1% (v/v) Triton X-100
Stripping solution 1	200mM glycine 500mM NaCl (pH titrated to 2.8)
Stripping solution 2	200mM glycine 500mM NaCl (pH titrated to 2.2)

Stripping solution 3	200mM TRIS-HCl (pH titrated to 7.4)
PTW	0.1% (v/v) Tween 20 in PBS
Hybridization solution	50% (v/v) formamide 25% (v/v) 20x SSC solution pH=4.5 35mM SDS 50mg/l (w/v) heparin 50mg/l (w/v) yeast tRNA
10x MAB	1.5M NaCl 1M maleic acid (pH titrated to 7.5)
MABT	0.1% (v/v) Tween 20 in MAB
Solution I (*in situ*)	50% (v/v) formamide 25% (v/v) 20x SSC solution pH=4.5 35mM SDS
5x blocking buffer (*in situ*)	10% (w/v) blocking reagent powder in MABT
20x SSC	3M NaCl 0.3M trisodium citrate dihydrate (pH titrated to 7.0)
L1 lysis buffer (ChIP)	50 mM Tris pH=8 2mM EDTA pH=8 0.1% (v/v) NP40 10% (v/v) glycerol
L2 nuclear resuspension buffer (ChIP)	50mM Tris pH=8 5mM EDTA pH=8 1% (w/v) SDS
DB-dilution buffer (ChIP)	200mM NaCl 50mM Tris pH=8 5mM EDTA, 50mM 0.5% NP40
NaCl-washing buffer (ChIP)	500mM NaCl 20mM Tris pH= 2mM EDTA NP40 (v/v) 1% 0.1% (w/v) SDS
LiCl-washing buffer (ChIP)	500mM LiCl 20mM Tris pH=8 2mM EDTA 1% (v/v) NP40 0.1% (w/v) SDS
EB-extraction buffer (ChIP)	10mM Tris pH=8 1mM EDTA 2% (w/v) SDS
TE-buffer	10mM Tris pH=8

	1mM EDTA
Lysis Buffer (3C)	10mM Tris pH=8 10mM NaCl 0.2% NP-40 1x Protease Inhibitor
Fixing Solution (whole mount staining)	2% Formaldehyde 0.1M PIPES 1 mM $MgSO_4$ 2mM EGTA
Blocking Solution (whole mount staining)	5% BSA 0.1% Triton X-100 in PBS
Tail Lysis Buffer	100 mM Tris pH=8.5 5mM EDTA 0.2% SDS 200 mM NaCl 100 µg/ml Proteinase K

Culture media/supplements		**Description**
DMEM 1g GlutMax	GIBCO	HEK 293T; COS-7
DMEM 4.5g GlutMax	GIBCO	HEK 293T; COS-7
DMED 4.5g without GlutMax	GIBCO	ESCs
Fetal bovine serum	GIBCO	10% of culture medium; 15% of total ES cell culture medium
100x Pen/Strep	GIBCO	Antibiotics were added to all culture media
100x Pyruvate	GIBCO	
100x Non-essential amino acids (NEAA)	GIBCO	For ES cell culture medium exclusively
100x L-glutamine	GIBCO	For ES cell culture medium exclusively
β-mercaptoethanol	Sigma	8µl/600ml of culture medium; for ES cell culture medium exclusively
Leukemia inhibitory factor (LIF) 1000x (ESGRO)	Millipore	Supplemented to ESCs to keep them undifferentiated; removed for differentiation

8.1.5. Plasmids

pcDNA3-Isl1, pcDNA3-Isl1ΔLIM1, pcDNA3-Isl1ΔLIM2, pcDNA3-Isl1HOMEO are described elsewhere (Witzel et al. 2012).

Ldb1 and Ldb1 truncated proteins were amplified from mouse cDNA and cloned into the *BamHI* site of pcDNA3-Flag-HA vector. The following primers were used for amplification:

Ldb1	Ldb1_F	5’ ggatccatgtcagtgggctgtgcctgtcc 3’
	Ldb1_R	5’ ggatcctcactgggaagcctgtgacgtgg 3’
Ldb1ΔLID	Ldb1_F	5’ ggatccatgtcagtgggctgtgcctgtcc 3’
	Ldb1ΔLID_R	5’ ggatcctcagagagcgaaggtgctggctgggc 3’
DN-Ldb1	DN-Ldb1_F	5’ ggatccatggagcccgcacgacagcagcccag 3’
	Ldb1_R	5’ ggatcctcactgggaagcctgtgacgtgg 3’

The pCS2+Flag-HA-DN-Ldb1 plasmid was generated by subcloning the Flag-HA-DN-Ldb1 *HindIII* - *EcoRV* insert of pcDNA3-Flag-HA-DN-Ldb1 in the blunted *BamHI* site of pCS2+. Orientation of the insert was verified by restriction analysis.

Lentiviral constructs were created by subcloning of the Flag-HA-Ldb1 or the Flag-HA-DN-Ldb1 *HindIII* - *EcoRV* insert from pcDNA3 plasmids into the blunted *BamHI* site of pRRL.sin18-IRES-GFP. Orientation of the insert was verified by restriction analysis.

Mef2c promoter and AHF enhancer were cloned from wild type mouse (C57BL/6) genomic DNA in pJet1.2 (Fermentas) and subsequently subcloned in pGL4-luciferase plasmid (Promega). The following primers were used for amplification:

*Mef2c*promoter_F	5’ gagctctcatactgaaagtgatttgac 3’
*Mef2c*promoter_R	5’ agatcttctccccaccccaagcctct 3’
*Mef2c*AHF_F	5’ ggatcccattaaaatagtactctgca 3’
*Mef2c*AHF_R	5’ gtcgacgggccattaactttcgaatc 3’

List of Plasmids used in the study:

Plasmid	**Source of supply**	**Description**
pCDNA3	Invitrogen (modified)	Mammalian expression vector; a FLAG-HA tag was inserted in frame in front of the start-codon (N-terminal)
pCS2(+)		Eukaryotic expression vector that allows *in vitro* RNA synthesis of sequences cloned into the polylinker
pJET1.2	Fermentas	Unidirectional blunt insertion of PCR product; Insertional inactivation of endonuclease
pRRLSIN.cPPT.PGK-GFP.WPRE	Didier Trono	Mammalian Expression, Lentiviral. http://www.addgene.org/12252/
pCMVΔR.78		Packaging plasmid
pVSV		Packaging plasmid
pLKO.1 -puro	Sigma-Aldrich	Selection marker (puromycin resistance)
pRSV-βgal	MacGregor	Control vector for monitoring transfection

		efficiencies; drive transcription of the bacterial *lac*Z gene
pGL4-luciferase	Promega	Promoter less Firefly Luciferase Vectors optimized for mammalian expression
pCI-neo	Promega	Mammalian expression vector; manly used for equalizing DNA levels during transfections

8.1.6. Primary Antibodies used for Western Blot analysis

Name	Host	Dilution	Company
anti-Isl1 39.4D5	mouse (mc)	1:5 (supernatant)	Developmental Studies Hybridoma Bank
anti-Ldb1	goat (pc)	1:500	Santa Cruz Biotechnology N-18
anti-Ldb1	mouse (mc)	1:1000	Santa Cruz Biotechnology C-9
anti-FLAG-M2	mouse (mc)	1:2500 (in 2,5% Milk)	Sigma F3165
anti-HA	rabbit (pc)	1:500	Santa Cruz Biotechnology Y-11
anti-tubulin	mouse (mc)	1:8000	Sigma T5168
anti-Lamin B	goat (pc)	1:500	Santa Cruz Biotechnology C-20
anti-GFP	rabbit (pc)	1:1000	Abcam ab6556

mc = monoclonal
pc = polyclonal
All antibodies were diluited in PBS, 0,05% Tween20 if not otherwise stated

8.1.7. Secondary Antibodies used for Western Blot analysis

Name	Host	Dilution	Catalog Number
anti-mouse HRP	donkey	1:10000	Jackson ImmunoResearch 715-035-150
anti-rabbit HRP	donkey	1:10000	Jackson ImmunoResearch 111-035-003
anti-goat HRP	donkey	1:10000	Jackson ImmunoResearch 705-035-003

All antibodies were diluited in PBS, 0,05% Tween20 if not otherwise stated

8.1.8. Primary Antibodies used for Immunofluorescence analysis

Name	Host	Dilution	Company
anti-Isl1 39.4D5	mouse (mc)	1:10 (supernatant)	Developmental Studies Hybridoma Bank
anti-FLAG	mouse (mc)	1:250	Sigma F3165

8.1.9. Secondary Antibodies used for Immunofluorescence analysis

Name	Host	Dilution	Company
anti-mouse-Alexa594	donkey	1:500	Invitrogen Molecular Probes
anti-mouse-Alexa488	donkey	1:500	Invitrogen Molecular Probes

8.1.10. Antibodies used for ChIP

Name	Host	µg/10^7 cells	Company
anti-Isl1 39.4D5	mouse (mc)	1	Developmental Studies Hybridoma Bank
anti-Ldb1	goat (pc)	10	Santa Cruz Biotechnology N-18
anti-H3	rabbit (pc)	1	Abcam ab1791
anti-H3K4me1	rabbit (pc)	1	Abcam ab8895
anti-H3K27ac	rabbit (pc)	1	Abcam ab4729
anti-p300	rabbit (pc)	1	Abcam ab10485
anti-RNAPolIIS5p	mouse (mc)	1	Santa Cruz Biotechnology sc-47701
Mouse IgG		1	Santa Cruz Biotechnology sc-2025
Goat IgG		10	Santa Cruz Biotechnology sc-2028
Rabbit IgG		1	Santa Cruz Biotechnology sc-3888

8.1.11. Primary Antibodies used for FACS analysis

Name	Host	µg/10^6cells	Company
anti-myl2	goat (pc)	1	Santa Cruz Biotechnology C-17
anti-cTnI RV-C2	mouse (mc)	1	Developmental Studies Hybridoma Bank

PE-conjugated anti-PDGFRα	rat (pc)	0,5	e-Bioscience 12-1401-81
APC-conjugated anti-Flk1	rat (pc)	0,5	e-Bioscience 17-5821-81
IgG2a K isotype APC-conjugated	rat (pc)	0,5	e-Bioscience 17-4321
IgG2a K isotype PE-conjugated	rat (pc)	0,5	e-Bioscience 12-4321

8.1.12. Secondary Antibodies used for FACS analysis

Name	Host	Dilution	Company
anti-goat-Alexa-594	donkey	1:50	Invitrogen Molecular Probes
anti-mouse-Alexa-488	donkey	1:50	Invitrogen Molecular Probes

8.1.13. Bacterial Strains

TOP10	*F- mcrA Δ(mrr-hsdRMS-mcrBC) φ80lacZΔM15 ΔlacX74 nupG recA1 araD139 Δ(ara-leu)7697 galE15 galK16 rpsL(Str^R) endA1 λ$^-$*
SCS110	*rpsL* (Strr) *thr leu endA thi-1 lacY galK galT ara tonA tsx dam dcm supE44* Δ(*lac-proAB*) [F´ *traD36 proAB lacI*q*ZΔM15*
JM109	*endA1 glnV44 thi-1 relA1 gyrA96 recA1 mcrB$^+$ Δ(lac-proAB) e14- [F' traD36 proAB$^+$ lacI^q lacZΔM15] hsdR17(r$_K^-$m$_K^+$)*

8.1.14. Cell Lines

HEK 293T	Adherent kidney cells from *Homo sapiens* with endothelial morphology. These cells constitutively express the simian virus 40 (SV40) large T antigen (immortalized).
COS-7	Adherent kidney cells from *Cercopithecus aethiops* with fibroblast morphology. These cells constitutively express the simian virus 40 (SV40) large T antigene (immortalized).
E14	Adherent pluripotent embryonic stem cells from *Mus musculus*.
E14-*Ldb1*$^{-/-}$	Adherent pluripotent embryonic stem cells from *Mus musculus*. Both Ldb1 alleles have been targeted with homology recombination (Mylona et al., 2013).
Feeders	Mouse embryonic fibroblasts prepared on E13.5

8.1.15. Zebrafish strains

The following mutant and transgenic lines were used: *Tg(myl7:EGFP-HsHRAS)*^{s883}.

Zebrafish embryos were maintained at 28°C (Advantage-Lab incubator) in E3 medium (5 mM NaCl, 0.17 mM KCl, 0.33 mM CaCl2, 0.33 mM MgSO4). Embryos were treated with 20 µl of pronase (5 mg/ml) (protease, from *Streptomyces griseus*,

Sigma) 5 h post injection. To prevent pigmentation the embryos were treated with PTU (0.003%, Alfa Aesar) before 24 hpf.

8.1.16. Mouse lines

The *Ldb1*$^{tm1a(EUCOMM)Hmgu}$ line was generated by microinjection of *Ldb1*$^{tm1a(EUCOMM)Hmgu}$ ESCs, obtained from the European Conditional Mouse Mutagenesis Program (EUCOMM), into blastocysts.

8.1.17. Primers used for genotyping mouse embryos

Primer Name	Sequence 5'→3'	Allele	Product Size
Isl1_F	ACTATTTGCCACCTAGCCACAGCA	WT	380 bp
Isl1_R	AATTCACACCAAACATGCAAGCTG	CRE	630 bp
Cre_R	CTAGAGCCTGTTTTGCACGTTC		
Ldb1_5'Arm	TACCCCAGGTCAGCAAACCAGCAGG	WT	519 bp
Ldb1_3'Arm	AAACATGAACTCCAGGTACAACCG	cKO	382 bp
LAR3	CAACGGGTTCTTCTGTTAGTCC	Flox	688 bp
flp_F	CATTAAAGAAATTGATTCCTGCTTGG	Flp pos	268 bp
flp_R	CAGTGATCTCCCAGATGCTTTCACC		
Ldb1FlpCreDel_F	GAGGTATATGGTGAACAAGGCG		
Ldb1FlpCreDel_R	AATGAAGGTGACTGTGTATGTG	Ldb1 floxed	338 bp
Ldb1FlpCreDel30_R	GATGGTTATGTGTCTGCCACACAG	Ldb1 floxed	246 bp

8.1.18. Primers used for RT-PCR analysis Mus Musculus

Primer Name	Sequence 5'→3'	Accession Number
qGAPDH_for	AACTTTGGCATTGTGGAAGG	XM_001476707
qGAPDH_rev	GGATGCAGGGATGATGTTCT	
q5'UTRIsl1_for	ACAGCACCAGCATCCTCTCT	NM_021459
q5'UTRIsl1_rev	TCCCATCCCTAACAAAGCAC	
qIsl1_for	GCGACATAGATCAGCCTGCT	NM_021459
qIsl1_rev	GTGTATCTGGGAGCTGCGAG	
qLdb1_for	GGGGGGTGGCAACACCAACAACA	NM_001113408
qLdb1_rev	CCCCCACCACCATCACATCAGGT	
qNkx2.5_for	AAGCAACAGCGGTACCTGTC	NM_008700
qNkx2.5_rev	GCTGTCGCTTGCACTTGTAG	
q*Mef2c*_for	TCCATCAGCCATTTCAACAA	NM_001170537
q*Mef2c*_rev	AGTTACAGAGCCGAGGTGGA	
qTbx1_for	CGACAAGCTGAAACTGACCA	NM_011532
qTbx1_rev	AATCGGGGCTGATATCTGTG	
qTbx20_for	GCAGCAGAGAACACCATCAA	NM_020496

qTbx20_rev	GTGAGCATCCAGACTCGTCA	
qTbx5_for	ATGGTCCGTAACTGGCAAAG	NM_011537
qTbx5_rev	ACAAGTTGTCGCATCCAGTG	
qGATA4_for	TCTCACTATGGGCACAGCAG	NM_008092
qGATA4_rev	GCGATGTCTGAGTGACAGGA	
qHand1_for	GCGGAAAAGGGAGTTGCCTCAGC	NM_008213
qHand1_rev	GCTCCAGCGCCCAGACTTGC	
q*Hand2*_for	CGGAGAGGCGGAGGCCTTCA	NM_010402
q*Hand2*_rev	CAGGGCCCAGACGTGCTGTG	
qMlc2v_for	CTGCCCTAGGACGAGTGAAC	NM_010861
qMlc2v_rev	CCTCTCTGCTTGTGTGGTCA	
qMlc2a_for	CCCATCAACTTCACCGTCTT	NM_022879
qMlc2a_rev	CGTGGGTGATGATGTAGCAG	
qTnnt2_for	ATCCCCGATGGAGAGAGAGT	NM_011619
qTnntt2_rev	CTGTTCTCCTCCTCCTCACG	
qSM-actin_for	CTGACAGAGGCACCACTGAA	NM_007392
qSM-actin_rev	AGAGGCATAGAGGGACAGCA	
qSM-22a_for	AACGACCAAGCCTTCTCTGCC	NM_011526
qSM-22a_rev	TCGCTCCTCCAGCTCCTCGT	
qSM-mhc_for	AGGAAACACCAAGGTCAAGCA	NM_001161775
qSM-mhc_for	AGCCTCGTTTCCTCTCCTGA	
qBry_for	AGGGAGACCCCACCGAACGC	NM_009309
qBry_rev	CCGGGAACATCCTCCTGCCGTT	
qEoMes_for	CAGGGCAGGCGCATGTTTCCT	NM_010136
qEoMes_rev	TCCGCTTTGCCGCAGGTCAC	
qFlk1_for	GGGTTTGGTTTTGGAAGGTT	NM_010612
qFlk1_rev	AGGAGCAAGCTGCATCATTT	
qCD31_for	AACAGAAACCCGTGGAGATG	NM_001032378
qCD31_rev	GGCTTCCACACTAGGCTCAG	
qVE-Cad_for	TGAGGCAATCAACTGTGCTC	NM_009868
qVE-Cad_rev	TTCGTGGAGGAGCTGATCTT	
qIrx1_for	CTTCTCGCAGATGGGCTCTC	NM_010573
qIrx1_rev	TTCGTTGAGCCAGGCTTTCA	
qPitx2_for	GTGGACCCTCTCGGAACTTG	NM_001042504
qPitx2_rev	CTCCATTCCCGGTTATCGGC	
qMyocd_for	GCTGAGACTCACCATGACAC	NM_145136
qMyocd_rev	TGGACCTTTCAGTGGCGGTA	
qFoxC1_for	CAACATCATGACGTCGCTGC	NM_008592
qFoxC1_rev	CTCTGGCCCGGAGAGTAGG	
qBmp2_for	ATCACGAAGAAGCCGTGGAG	NM_007553
qBmp2_rev	CTCGTCACTGGGGACAGAAC	
qBmpr2_for	AGGTGGCCGAACAAATTCCA	NM_007561
qBmpr2_rev	TCTTGTGTTGACTCACCTATCTGT	
qFgfr2_for	CACGACCAAGAAGCCAGACT	NM_010207
qFgfr2_rev	CTCGGCCGAAACTGTTACCT	
qSmad3_for	AAGAAGCTCAAGAAGACGGGG	NM_016769
qSmad3_rev	CAGTGACCTGGGGATGGTAAT	

qAcvr2a_for	TCCTACTCAAGACCCAGGACC	NM_007396
qAcvr2a_rev	TCTGCCAGGACTGTTTGTCC	
qRyr2_for	GACTGAGGAAGGATCAGGGGA	NM_023868
qRyr2_rev	TTGTTGCCGGTCTGAGTTCT	
qKcnq1_for	ACTTCACCGTCTTCCTCATTGT	NM_008434
qKcnq1_rev	AGAGGCGGACCACATATTCTG	
qKcnj2_for	TCTCACTTGCTTCGGCTCAT	NM_008425
qKcnj2_rev	ACTTGTCCTGTTGCTGGTACA	
qFgf10_for	TGCGGAGCTACAATCACCTC	NM_00800
qFgf10_rev	GTTATCTCCAGGACACTGTACG	
qFgf8_for	GCTGAGCTGCCTGCTGTT	NM_010205
qFgf8_rev	GAGAGTGTCAGCTGGGTTCC	
qHDAC2_for	CCCGTCAGCCCTCTTGTC	NM_008229
qHDAC2_rev	TGCCAATATCACCATCATAGTAGT	

8.1.19. Primers used for Mef2c isoforms absolute quantification

Primer Name	**Sequence 5'→3'**
Mef2cTotal_for	ACGAGGATAATGGATGAGCGT
Mef2cTotal _rev	CAGCTTGTTGGTGCTGTTGAA
Mef2cRefSeq_for	GGCAAAGCTTCGGTGTTCAT
Mef2cRefSeq _rev	CTGCTGAGGGCTTTGTTGTC
AK0077603_for	GGTCAGCCTGTCCAAAAGGA
AK0077603_rev	ACAATGGATGTCAGTTGACCCA

8.1.20. Primers used for ChIP analysis Mus Musculus

Primer Name	**Sequence 5'→3'**
Mef2c-1,5Kb_for	CTGATGGAGAGGTTGGGACT
Mef2c-1,5Kb_rev	ATGCAAGCACCTCTCTCACT
Mef2c-1Kb_for	CTGATGGAGAGGTTGGGACT
Mef2c-1Kb_rev	ATGCAAGCACCTCTCTCACT
Mef2c-200bp_for	GAATGGCAAATAACTACAGTGCT
Mef2c-200bp_rev	TCCTCATTTCACACAGGCTT
Mef2c_AHF_for	TCAGTGTCTGCTCCTGCTTC
Mef2c_AHF_rev	TTCCCTCCACACCTTACTGG
Mef2c_-13Kb_for	CTTGCAATTACTACCACTTCACA
Mef2c_-13Kb_rev	CCTTGTCTCAGTCCTGCTCA
Mef2c+2,7Kb_for	GGGGTGGGAATTTAATCA
Mef2c+2,7Kb_rev	GTCTGGTCAATGAGGAGGT
Mef2c_+150Kb_for	TCAAAGAAACTGAGCTACTGTCT
Mef2c_+150Kb_rev	GATGTCACACTAGATCCACAGT
Mef2c_3'UTR_for	CAGTGTCTGTCGTGCGTTTT
Mef2c_3'UTR_rev	ACCCAATTCACACCTTCCCA
Mef2c_-9,6Kb_for	AGTGAAGGAAGAAAAGGTGCA
Mef2c_-9,6Kb_rev	GCTGGCGTTTGTGTTCTCTT
Mef2c_-12Kb_for	ACCCAGAGACACAGGCATAA

Mef2c_-12Kb_rev	TTCCCTTTGCGGTTCCAATG
Mef2c_-14Kb_for	CTCAACTGGTGGTGTTAGC
Mef2c_-14Kb_rev	GCTCAACTGGTGGTGTTAGC
Mef2c_-6,5Kb_for	TGAGGTCCCATTTGTTGATGC
Mef2c_-6,5Kb_rev	TGTCCTCCCACAGTTCTTCA
Mef2c_-7,5Kb_for	TGTGTTCCATTCAGCAGAGG
Mef2c_-7,5Kb_rev	CCCCAAAGAACATGCATGGT
Hand2_promoter_for	TTCACCCCACCCCTGTAATC
Hand2_promoter_rev	AATTGCCGAGGTCCTCTTCT
Hand2_OFTRV_for	CTCAGAGCCAGCCAACTACT
Hand2_OFTRV_rev	TCACTCCTCACTGACAGCAC
Actin_for	GGAGCGGACACTGGCACAGC
Actin_rev	ATGCCCACACCGCGACCCTA
Intergenic_for	AAACCTCAAAGCCCAGGACACA
Intergenic_rev	ACTTGGTCCCGAGTTGATGGAA

8.1.21. Primers used for 3C-seq Analysis

*Mef2c*promoter_F	5' acacttgtgcagagggatc 3'
*Mef2c*promoter_R	5' aagctttctaatttgggagc 3'
*Mef2c*AHF_F	5' ttaatttattactaacattggaggatc 3'
*Mef2c*AHF_R	5' aagcttgtgctctgtgaca 3'

8.1.22. Primers used for 3C-qPCR Analysis

Primer Name	**Sequence 5'→3'**
3C_Mef2cAHF	TTAATTTATTACTAACATTGGAGGATC
3C_Mef2c prom	GGGTCACACATCAAGGGTCT
3C_Mef2c-13Kb	CCTTGCCCAGAATGATCAGC
3C_Mef2c+2,7Kb	CCTTTGGCTCTCTCCTATCCT
3C_Mef2c +150	GCAGAGATTAGCCAGTCTATGC
3C_Mef2c 3'UTR	CCAAGCCGCATATCTACTGC
3C_Mef2c Negative	TGTCTGACTCAGCTGTGGAG
3C_Mef2c Negative2	ACCCAAGAAATTTTGAGAACCAA
3C_Mef2c Negative3	AACTGCAGCTTGTTTCACGT
3C_Mef2C_Negative4	TAGGGGTGGCTTCTGGTTTT
3C_Mef2c Negative5	TGCTTTCCCACATTACTGAAGA
3C_Ryr2	CAAATGTAGTGGTGGGTGCC
3C_FoxC1	CAGCCCAAAGATGTTTCAGGT
3C_Bmpr2	TGGATGAGTGGATGGGTAGA
3C_Bmp2	CACACGCCATCACTTAGCAG
3C_Fgf10	AGTGTTAGGATGCAGGGCTT
3C_Acvr2a	ACTCTGAAGGCTGGGAGTTC
3C_Isl1	GCTTAAAGAGGCAGGCTCC
3C_Smad3	AATATGTCCCAAATGTTTCACAGAA
3C_Myocd	CCACCATGGTCACTCTGTCC
3C_Kcnq1	AGGAACCACTCTCCCAAAGG

3C_Kcnj2	ACCGGTTAGCATGGTTTTAGC
3C_Rai2	GAGAGGCTGGAGGGAAGAAA
3C_Xrcc4	GGGTCCATGATTTGCCAAAGA
3C_Hand2prom	CGAGCGGCCCTAAAGATGTA
3C_Hand2 OFTRV_NlaIII	AAGCTTTAGACCCCTGGATTG
3C_Hand2Negative1_NlaIII	CTTCCCTGTCACATCACCCT
3C_Hand2Negative2_NlaIII	GCATTTCCAGCAAGCATCCT
3C_Hand2Negative3_NlaIII	CTTGTTTGGGGTGAGAAGGG
3C_Hand2Negative4_NlaIII	CACAGGGCAGTTAGGTCTCA
3C_Hand2 OFTRV_DpnII	TGTTGTTGTTGGTGGTGGTG
3C_Hand2Negative1_DpnII	CTAAGGGCTTCTGTTGACACC
3C_Hand2Negative2_DpnII	CCCATAGGCCTTGTTCTGGA
3C_Hand2Negative3_DpnII	CTAAGGTGGCTGGGACTAGG
3C_Hand2Negative4_DpnII	CGTGTGCTGTGTCTTCTCTT
3C_Actin_F	CTTCTGACCTAGAACTCTTGATCCC
3C_Actin_R	CCCTCTACACACACTCAGAATTCATC

8.2. Methods

8.2.1. Cell Culture and Transfection

HEK293T, and COS7 cells were grown in DMEM (Invitrogen) supplemented with 10% FBS (Invitrogen), 2mM L-Glutamine, 100U/ml Penicillin and 100 µg/ml Streptomycin (Invitrogen) at 37°C/5%CO_2. Undifferentiated embryonic stem (ES) cells were maintained on mouse embryonic fibroblast (MEFs) feeder cells in DMEM supplemented with 15% fetal bovine serum (FBS, Invitrogen), 2mM L-Glutamine, 0.1 mM 2-mercaptoethanol (Sigma), 0.1 mM non-essential amino acids (Invitrogen), 1 mM sodium pyruvate (Invitrogen), 4.5 mg/ml D-glucose, and 1,000 U/ml of leukemia inhibitory factor (LIF ESGRO, Millipore). To induce EB formation, dissociated ESCs were cultured in hanging drops of 500 cells per 15 µl of ES cell medium, in the absence of LIF. After 2 days in the hanging drop culture, the resulting EBs were transferred to bacterial culture dishes. For the transfection of HEK293T, cells were seeded at a density of $2x10^6$ cells/10cm dish and transfected with 10-20µg DNA using calcium phosphate precipitation. COS7 were transfected using FuGENE® HD Transfection Reagent (Roche), according to the manufacturer instructions. For stable expression, ESCs were transduced with pRRL.Sin18.PGK-GFP-IRES (control construct) and pRRL.Sin18.PGK-GFP-IRES-Isl1, pRRL.Sin18.PGK-GFP-IRES-Ldb1, pRRL.Sin18.PGK-GFP-IRES-DN-Ldb1 or in combinations. Transduced cells were FACS sorted for GFP

expression and used for EB differentiation. For ubiquitination assay of Isl1, HEK293T were transfected as described above, 40 hours post transfection cells were treated with 25µM MG-132. Treated cells were lysed in co-IP buffer (50mM Tris pH7.5, 100mM NaCl, 15mM EGTA, 0.1%Triton-X100, protease inhibitors SET-I (Sigma), 100µM MG-132).

8.2.2. Luciferase Assay

For Luciferase Assays, $3x10^4$ COS7 cells were seeded in 24 well plates. 48h after transfection, cells were lysed in 100µl lysis buffer (Promega, Luciferase Assay System) and luciferase activity was measured on Mirthras LB 940 (Berthold Technologies) according to the Luciferase Assay System Manual (Promega). β-galactosidase activity was measured incubating 10µl of clarified cell lysed in 200µl of ß-galactosidase substrate (10ml Z-buffer, 100µl 50mM CPRG, 10µl ß-mercaptoethanol) for 1 hour at 37°C in the Mirthras LB 940 (Berthold Technologies). Absorbance was read every minute at 578nm.

8.2.3. Immunoprecipitation

For Co-IPs, transfected cells were lysed in co-IP buffer (50mM Tris pH7.5, 100mM NaCl, 15mM EGTA, 0.1%Triton-X100, protease inhibitors SET-I (Sigma)), sonicated for 10sec and extracts clarified. The lysates were then incubated with the indicated antibodies overnight at 4°C followed by 3 h incubation with Protein-G-Sepharose beads (GE Healthcare). Immunoprecipitates were washed five times in lysis buffer, dissolved in 2xSDS-PAGE sample buffer, and subjected to standard western immunoblot analysis.

8.2.4. Chromatin Immunoprecipitation

Embryoid bodies at day 4 or 5 of differentiation were dissociated with trypsin to obtain single cells suspension and resuspend with complete differentiation medium to obtain a concentration of 10^6 cells/ml. For chromatin immunoprecipitation 0.5 to $1x10^7$ cells from EBs or pool of 30 E8-9 embryos were fixed with 1% Formaldehyde for 10 min. Formaldehyde was quenched with glycine at final concentration of 125 mM and washed three times with PBS. Cells were lysed in L1 lysis buffer (50 mM Tris

pH8, 2 mM EDTA pH8, 0.1% NP-40, 10% glycerol) for 5 min, the nuclei were spun down and resuspended in L2 nuclear resuspension buffer (1% SDS, 5 mM EDTA pH8, 50 mM Tris pH8), followed by sonication to fragment the chromatin. The samples were centrifuged, diluted 1:10 with DB-dilution buffer (0.5% NP40, 200 mM NaCl, 5 mM EDTA, 50 mM Tris pH8) and incubated with primary antibody overnight at 4°C followed by 3 h incubation with Protein-A/G Sepharose beads (GE Healthcare). Immunoprecipitates were washed two times with NaCl-washing buffer (0.1% SDS, NP-40 1%, 2 mM EDTA, 500 mM NaCl, 20 mM Tris pH8), followed by two washes with LiCl-washing buffer (0.1% SDS, 1% NP-40, 2 mM EDTA, 500 mM LiCl, 20mM Tris pH8) and eluted with EB-extraction buffer (TE pH8, 2% SDS). Cross-linking was reverted by overnight incubation at 65°C, DNA was purified and subjected to qPCR analysis.

8.2.5. RNA Isolation, RT-PCR, and Real-Time PCR

RNA was isolated using Trizol (Invitrogen). cDNA was synthesized with the High Capacity cDNA Reverse Transcription Kit (Applied Biosystems) and real-time PCR was performed using the SYBR GREEN PCR master mix (Applied Biosystems) on Applied Biosystems StepOnePlus^{TM} real-time PCR detection system. The cycle numbers were normalized to GAPDH.

8.2.6. Chromosome Conformation Capture Assays- 3C-Seq and 3C-PCR

3C-Seq was performed as described in (Stadhouders, Kolovos et al. 2013). In brief, 1 × 10^7 cells were crosslinked with 2% formaldehyde at room temperature for 10 min, followed by glycine quenching, cell lysis. *HindIII* digestion (for 3C-seq and 3C-PCR of the *Mef2c* locus) or *NlaIII*, or *DpnII* (3C-PCR of the *Hand2* locus), and T4 ligation. For 3C-PCR digestion was performed by addition of 200 U of enzyme for 2 hours, followed by addition of 200 U of enzyme O/N and a final 200 U of enzyme for additional 2 hours (total 600U of enzyme) incubating at 37°C, 900rpm (van de Werken et al., 2012). Digestion efficiency was checked by incubating 5µl of chromatin with 5µl proteinase-K (10 mg/ml) in total volume of 100 µl Tris pH7.5 at 65°C for 1 hour. 20 µl of the mix were loaded on 0.6% agarose gel. As a positive control was used bacterial artificial chromosomes (BAC) containing the entire *Mef2c*

and *Hand2* loci (Invitrogen) digested with *HindII* or *NlaIII* (or *DpnII)* respectively, and relegated to generate random ligation products of *HindII* or *NlaIII* (or *DpnII)* fragments.

8.2.7. DNA extraction from tail pieces

For mice genotyping 5 mm long tail pieces were incubated in 500µl tail lysis buffer at 55°C over night. Next day the tail debris were pelleted for 5 min, 14000 rpm, 4°C and supernatant was transferred into new tubes and mixed with 500µl Isopropanol to precipitate genomic DNA (gDNA). After vigourous shacking the samples were centrifuged for 5 min, 14000 rpm, 4°C and supernatant was removed. Precipitated gDNA was washed with 70% EtOH and centrifuged 5 min, 14000 rpm, 4°C. Again the supernatant was removed and the pellet was air-dried for 10 minutes, RT. Finally, the DNA was resuspend in 100µl ddH_2O.

8.2.8. DNA extraction from embryos

Yolk sacs from E8.5/9.5 embryos or tails from E14.5/16.5 embryos were incubated in 20µl tail lysis buffer for 1 hour at 55°C. Next proteinase K was heat inactivated incubating the sample at 95°C for 10 min. Finally the gDNA solution was diluited in 150µl ddH_2O.

8.2.9. Genotyping

0.5µl of gDNA from tails or embryos was used in the genotyping reaction (total reaction volume 10µl).

For *Isl1* genotyping annealing temperature 64°C, elongation 68°C, 35 cycles.

For *Ldb1* genotyping annealing temperature 56°C, elongation 72°C, 35 cycles.

For flp genotyping annealing temperature 58°C, elongation 72°C, 35 cycles.

For Ldb1 Cre deleted genotyping annealing temperature 60°C, elongation 72°C, 35 cycles.

8.2.10. Whole mount in situ hybridization analysis of mouse embryos

Embryos were fixed overnight in 4% PFA at 4°C, dehydrated in methanol and stored in 100% methanol at -20°C. For *in situ* analysis the embryos were stepwise

rehydrated in PBS, 0.1% Tween20, treated with protease K (10 µg/ml stock) for 10 minutes, re-fixed in 4% PFA, 0.2% Gluteraldheide and incubated overnight at 65°C with the DIG-labelled probe (Mlc2a 0,5µg/µl; Ldb1 1µg/µl). Next day, embryos were washed in 2x30 minutes in Solution I, 2x15 minutes 2xSSC and 2x20 minutes 0.2xSSC at 65°C followed by 1x10 minutes in MABT prior to incubation with 2xBlocking Reagent (Roche) for 2 hours at room temperature and incubated with alkaline phosphatase conjugated anti-DIG antibody (Roche) embryos for 18 h at 4°C. After 6x1 hour washes with MABT+2mM Levamisole embryos were stained with BM-Purple reagent (Roche).

8.2.11. Histological analysis

Embryonic hearts were dissected in ice cold PBS, fixed in 4% PFA O/N at 4°C, dehydrated step wise in Ethanol (30%, 50%, 75%, 80%, 90%, 95%, 100%) and stored at -20°C. For histological analysis, the tissues were incubated in 100% Xylol and embedded in paraffin for further processing. Embedded organs were sectioned using the microtome RM2245 (Leica) and Hematoxilyn-Eosin staining was performed.

8.2.12. Flow Cytometer Analysis

Ventricles were microdissected in ice cold PBS. After three times washes in PBS the ventricles were incubated three times for 10 minutes in predigestion buffer (16 mM BDM (Sigma), 0.4 mg/ml Pankreatin (Sigma), 115 mM NaCl, 8 mM Glucose, 25 mM KCl, 33mM NaH2PO4, 9 mM NaHCO3) at 37°C, followed by two times digestion in digestion buffer (predigestion buffer + Liberase DH (Roche)) for 10 minutes. All supernatant were pooled together and the collected cells were incubated with red blood lysis buffer (140 mM NaCl, 10 mM KHCO3, 1.2 mM EDTA, pH 7.35) for 3 minutes on ice, followed by fixation with 2% PFA at room temperature for 2 minutes. Cells were then stored in 100% methanol at -20°C or immediately analysed with the LSRII Flow Cytometer (BD Bioscience).

For Flk1/PdgfR-a FACS analysis the EBs were dissociated, $1x10^6$ cells were washed with 1 ml PBS and blocked in 100 µl FACS buffer (10% FCS in PBS) for 1 hour at room temperature. After blocking, the cells were stained with 0.5 µg each APC-conjugated anti-Flk1 and PE-conjugated anti-PDGFRα or control rat IgG2a K isotype

APC- or PE-conjugated antibodies. After PBS washes, cells were fixed for 10 minutes at room temperature in 2% PFA. Data were acquired on an LSRII flow cytometer (BD) and analyzed using FlowJo software.

8.2.13. Immunofluorescence of Embryoid Bodies (EBs)

EBs were collected, washed with PBS, embedded in 17% gelatine and fixed O/N at room temperature in 4% PFA. Next day the EBs were sectioned with the vibratome at 70µm section. The obtained sections were fixed in Dong Fixing solution O/N at 4°C, followed by 1 hour blocking (4% BSA + 0.4% Triton x-100) and incubated with primary antibody diluted in blocking solution O/N at 4°C.

8.2.14. GO Analysis

GO analysis was performed using DAVID software (Huang et al., 2009a; 2009b).

8.2.15. mRNA synthesis

pcS2+Flag-HA-DN-Ldb1 vector was linearized with *NotI*. After standard phenol/chloroform purification mRNA was synthesized using the mMessage Sp6 KIT (Ambion) following the manufacturer's instructions.

8.2.16. mRNA injection

mRNA was injected in 1- to 16- cells stage of zebrafish fertilized eggs (drop size 2 nl, mRNA concentration 200 ng/µl for Flag-HA-DN-Ldb1).

8.2.17. Whole mount in situ hybridization analysis of Zebrafish embryos

Embryos were fixed overnight in 4% PFA at 4°C, dehydrated in methanol and stored in 100% methanol at -20°C. For *in situ* analysis the embryos were stepwise rehydrated in PBS, 0.1% Tween20, treated with protease K (10 µg/ml stock) for 1 minute, re-fixed in 4% PFA, 0.2% Gluteraldheide and incubated overnight at 65°C with the DIG-labelled probe (1µg/µl). Next day, embryos were washed in 2x30 minutes in Solution I, 2x15 minutes 2xSSC and 2x20 minutes 0.2xSSC at 65°C followed by 1x10 minutes in MABT prior to incubation with 2xBlocking Reagent (Roche) for 2 hours at room temperature and incubated with alkaline phosphatase

conjugated anti-DIG antibody (Roche) embryos for 18 h at 4°C. After 6x30 minutes washes with MABT+2mM Levamisole embryos were stained with BM-Purple reagent (Roche).

8.2.18. Live imaging of Zebrafish embryos

Live imaging was performed after embedding the embryos in 1% low-melting agarose (Roth) in Tricaine (MP Biomedicals) using a Zeiss LSM 710 confocal microscope (40x objective). Afterwards z-projections of optical sections were performed using ImageJ and cells were counted.

8.2.19. Zebrafish emryos whole mount immufluorescence

Whole-mount staining was performed as described (Dong et al., 2007; Witzel et al., 2012). Confocal images were acquired by a Zeiss LSM 710 system, and the z stacks were projected by Zeiss LSM 710 software.

9. References

Abu-Issa, R., Smyth, G., Smoak, I., Yamamura, K.-I., and Meyers, E.N. (2002). Fgf8 is required for pharyngeal arch and cardiovascular development in the mouse. Development *129*, 4613–4625.

Agulnick, A.D., Taira, M., Breen, J.J., Tanaka, T., Dawid, I.B., and Westphal, H. (1996). Interactions of the LIM-domain-binding factor Ldb1 with LIM homeodomain proteins. Nature *384*, 270–272.

Ai, D., Fu, X., Wang, J., Lu, M.F., Chen, L., Baldini, A., Klein, W.H., and Martin, J.F. (2007). Canonical Wnt signaling functions in second heart field to promote right ventricular growth. Proc Natl Acad Sci USA *104*, 9319–9324.

Alsan, B.H., and Schultheiss, T.M. (2002). Regulation of avian cardiogenesis by Fgf8 signaling. Development *129*, 1935–1943.

Andersen, T.A., Troelsen, K. de L.L., and Larsen, L.A. (2014). Of mice and men: molecular genetics of congenital heart disease. Cell. Mol. Life Sci. *71*, 1327–1352.

Ando, K., Shioda, S., Handa, H., and Kataoka, K. (2003). Isolation and characterization of an alternatively spliced variant of transcription factor Islet-1. J. Mol. Endocrinol. *31*, 419–425.

Ansari, A., and Hampsey, M. (2005). A role for the CPF 3'-end processing machinery in RNAP II-dependent gene looping. Genes & Development *19*, 2969–2978.

Apostolou, E., Ferrari, F., Walsh, R.M., Bar-Nur, O., Stadtfeld, M., Cheloufi, S., Stuart, H.T., Polo, J.M., Ohsumi, T.K., Borowsky, M.L., et al. (2013). Genome-wide chromatin interactions of the Nanog locus in pluripotency, differentiation, and reprogramming. Cell Stem Cell *12*, 699–712.

Babaei, S., Mahfouz, A., Hulsman, M., Lelieveldt, B.P.F., de Ridder, J., and Reinders, M. (2015). Hi-C Chromatin Interaction Networks Predict Co-expression in the Mouse Cortex. PLoS Comput. Biol. *11*, e1004221.

Bach, I. (2000). The LIM domain: regulation by association. Mech Dev *91*, 5–17.

Bach, I., Carrière, C., Ostendorff, H.P., Andersen, B., and Rosenfeld, M.G. (1997). A family of LIM domain-associated cofactors confer transcriptional synergism between LIM and Otx homeodomain proteins. Genes & Development *11*, 1370–1380.

Bach, I., Rodriguez-Esteban, C., Carrière, C., Bhushan, A., Krones, A., Rose, D.W., Glass, C.K., Andersen, B., Izpisúa Belmonte, J.C., and Rosenfeld, M.G. (1999). RLIM inhibits functional activity of LIM homeodomain transcription factors via recruitment of the histone deacetylase complex. Nat Genet *22*, 394–399.

Bansal, V., Dorn, C., Grunert, M., Klaassen, S., Hetzer, R., Berger, F., and Sperling, S.R. (2014). Outlier-based identification of copy number variations using targeted

resequencing in a small cohort of patients with tetralogy of fallot. PLoS ONE *9*, e85375.

Becker, T., Ostendorff, H.P., Bossenz, M., Schlüter, A., Becker, C.G., Peirano, R.I., and Bach, I. (2002). Multiple functions of LIM domain-binding CLIM/NLI/Ldb cofactors during zebrafish development. Mech Dev *117*, 75–85.

Bhati, M., Lee, C., Nancarrow, A.L., Lee, M., Craig, V.J., Bach, I., Guss, J.M., Mackay, J.P., and Matthews, J.M. (2008). Implementing the LIM code: the structural basis for cell type-specific assembly of LIM-homeodomain complexes. Embo J *27*, 2018–2029.

Bodnar, M.S., and Spector, D.L. (2013). Chromatin meets its organizers. Cell *153*, 1187–1189.

Bonora, G., Plath, K., and Denholtz, M. (2014). A mechanistic link between gene regulation and genome architecture in mammalian development. Current Opinion in Genetics & Development *27*, 92–101.

Both, von, I., Silvestri, C., Erdemir, T., Lickert, H., Walls, J.R., Henkelman, R.M., Rossant, J., Harvey, R.P., Attisano, L., and Wrana, J.L. (2004). Foxh1 is essential for development of the anterior heart field. Dev Cell *7*, 331–345.

Boveri, T. (1909). Die Blastomerenkerne von Ascaris megalocephala und die Theorie der Chromosomenindividualität (Arch Zellforsch).

Brade, T., Gessert, S., Kühl, M., and Pandur, P. (2007). The amphibian second heart field: Xenopus islet-1 is required for cardiovascular development. Developmental Biology *311*, 297–310.

Bradshaw, L., Chaudhry, B., Hildreth, V., Webb, S., and Henderson, D.J. (2009). Dual role for neural crest cells during outflow tract septation in the neural crest-deficient mutant Splotch(2H). J. Anat. *214*, 245–257.

Breen, J.J., Agulnick, A.D., Westphal, H., and Dawid, I.B. (1998). Interactions between LIM domains and the LIM domain-binding protein Ldb1. J Biol Chem *273*, 4712–4717.

Brewer, A., and Pizzey, J. (2006). GATA factors in vertebrate heart development and disease. Expert Rev Mol Med *8*, 1–20.

Bruneau, B.G., Nemer, G., Schmitt, J.P., Charron, F., Robitaille, L., Caron, S., Conner, D.A., Gessler, M., Nemer, M., Seidman, C.E., et al. (2001). A murine model of Holt-Oram syndrome defines roles of the T-box transcription factor Tbx5 in cardiogenesis and disease. Cell *106*, 709–721.

Buckingham, M., Meilhac, S., and Zaffran, S. (2005). Building the mammalian heart from two sources of myocardial cells. Nat Rev Genet *6*, 826–835.

Buecker, C., and Wysocka, J. (2012). Enhancers as information integration hubs in development: lessons from genomics. Trends Genet *28*, 276–284.

Bulger, M., and Groudine, M. (2011). Functional and mechanistic diversity of distal transcription enhancers. Cell *144*, 327–339.

Cai, C.-L., Liang, X., Shi, Y., Chu, P.-H., Pfaff, S.L., Chen, J., and Evans, S. (2003). Isl1 identifies a cardiac progenitor population that proliferates prior to differentiation and contributes a majority of cells to the heart. Dev Cell *5*, 877–889.

Cai, C.-L., Martin, J.C., Sun, Y., Cui, L., Wang, L., Ouyang, K., Yang, L., Bu, L., Liang, X., Zhang, X., et al. (2008). A myocardial lineage derives from Tbx18 epicardial cells. Nature *454*, 104–108.

Cai, C.-L., Zhou, W., Yang, L., Bu, L., Qyang, Y., Zhang, X., Li, X., Rosenfeld, M.G., Chen, J., and Evans, S. (2005). T-box genes coordinate regional rates of proliferation and regional specification during cardiogenesis. Development *132*, 2475–2487.

Calo, E., and Wysocka, J. (2013). Modification of enhancer chromatin: what, how, and why? Mol Cell *49*, 825–837.

Cavalli, G. (2007). Chromosome kissing. Current Opinion in Genetics & Development *17*, 443–450.

Chang, H., Zwijsen, A., Vogel, H., Huylebroeck, D., and Matzuk, M.M. (2000). Smad5 is essential for left-right asymmetry in mice. Developmental Biology *219*, 71–78.

Chen, L., Segal, D., Hukriede, N.A., Podtelejnikov, A.V., Bayarsaihan, D., Kennison, J.A., Ogryzko, V.V., Dawid, I.B., and Westphal, H. (2002). Ssdp proteins interact with the LIM-domain-binding protein Ldb1 to regulate development. Proc Natl Acad Sci USA *99*, 14320–14325.

Christoffels, V.M., Mommersteeg, M.T.M., Trowe, M.-O., Prall, O.W.J., de Gier-de Vries, C., Soufan, A.T., Bussen, M., Schuster-Gossler, K., Harvey, R.P., Moorman, A.F.M., et al. (2006). Formation of the venous pole of the heart from an Nkx2-5-negative precursor population requires Tbx18. Circulation Research *98*, 1555–1563.

Cohen, E.D., Tian, Y., and Morrisey, E.E. (2008). Wnt signaling: an essential regulator of cardiovascular differentiation, morphogenesis and progenitor self-renewal. Development *135*, 789–798.

Cohen, E.D., Wang, Z., Lepore, J.J., Lu, M.M., Taketo, M.M., Epstein, D.J., and Morrisey, E.E. (2007). Wnt/beta-catenin signaling promotes expansion of Isl-1-positive cardiac progenitor cells through regulation of FGF signaling. J. Clin. Invest. *117*, 1794–1804.

Cremer, T., and Cremer, M. (2010). Chromosome territories. Cold Spring Harb Perspect Biol *2*, a003889.

Cremer, T., Cremer, M., Dietzel, S., Müller, S., Solovei, I., and Fakan, S. (2006). Chromosome territories--a functional nuclear landscape. Curr. Opin. Cell Biol. *18*, 307–316.

Cresci, M., Vecoli, C., Foffa, I., Pulignani, S., Ait-Ali, L., and Andreassi, M.G. (2013). Lack of association of the 3'-UTR polymorphism (rs1017) in the ISL1 gene and risk of congenital heart disease in the white population. Pediatr Cardiol *34*, 938–941.

Cross, A.J., Jeffries, C.M.J., Trewhella, J., and Matthews, J.M. (2010). LIM domain binding proteins one and two have different oligomeric states. Journal of Molecular Biology 1–37.

de Pater, E., Clijsters, L., Marques, S.R., Lin, Y.-F., Garavito-Aguilar, Z.V., Yelon, D., and Bakkers, J. (2009). Distinct phases of cardiomyocyte differentiation regulate growth of the zebrafish heart. Development *136*, 1633–1641.

de Wit, E., and de Laat, W. (2012). A decade of 3C technologies: insights into nuclear organization. Genes & Development *26*, 11–24.

de Wit, E., Bouwman, B.A.M., Zhu, Y., Klous, P., Splinter, E., Verstegen, M.J.A.M., Krijger, P.H.L., Festuccia, N., Nora, E.P., Welling, M., et al. (2013). The pluripotent genome in three dimensions is shaped around pluripotency factors. Nature *501*, 227–231.

Dean, A. (2011). In the loop: long range chromatin interactions and gene regulation. Briefings in Functional Genomics *10*, 3–10.

Dekker, J., Rippe, K., Dekker, M., and Kleckner, N. (2002). Capturing chromosome conformation. Science *295*, 1306–1311.

Deng, W., Lee, J., Wang, H., Miller, J., Reik, A., Gregory, P.D., Dean, A., and Blobel, G.A. (2012). Controlling long-range genomic interactions at a native locus by targeted tethering of a looping factor. Cell *149*, 1233–1244.

Deng, W., Rupon, J.W., Krivega, I., Breda, L., Motta, I., Jahn, K.S., Reik, A., Gregory, P.D., Rivella, S., Dean, A., et al. (2014). Reactivation of developmentally silenced globin genes by forced chromatin looping. Cell *158*, 849–860.

Denholtz, M., Bonora, G., Chronis, C., Splinter, E., de Laat, W., Ernst, J., Pellegrini, M., and Plath, K. (2013). Long-range chromatin contacts in embryonic stem cells reveal a role for pluripotency factors and polycomb proteins in genome organization. Cell Stem Cell *13*, 602–616.

Délot, E.C., Bahamonde, M.E., Zhao, M., and Lyons, K.M. (2003). BMP signaling is required for septation of the outflow tract of the mammalian heart. Development *130*, 209–220.

Dieci, G., and Sentenac, A. (2003). Detours and shortcuts to transcription reinitiation. Trends Biochem. Sci. *28*, 202–209.

Dixon, J.R., Selvaraj, S., Yue, F., Kim, A., Li, Y., Shen, Y., Hu, M., Liu, J.S., and Ren, B. (2012). Topological domains in mammalian genomes identified by analysis of chromatin interactions. Nature *485*, 376–380.

Dodou, E., Verzi, M.P., Anderson, J.P., Xu, S.-M., and Black, B.L. (2004). Mef2c is a direct transcriptional target of ISL1 and GATA factors in the anterior heart field during mouse embryonic development. Development *131*, 3931–3942.

Dogan, N., Wu, W., Morrissey, C.S., Chen, K.-B., Stonestrom, A., Long, M., Keller, C.A., Cheng, Y., Jain, D., Visel, A., et al. (2015). Occupancy by key transcription factors is a more accurate predictor of enhancer activity than histone modifications or chromatin accessibility. Epigenetics & Chromatin *8*, 16.

Dong, P.D.S., Munson, C.A., Norton, W., Crosnier, C., Pan, X., Gong, Z., Neumann, C.J., and Stainier, D.Y.R. (2007). Fgf10 regulates hepatopancreatic ductal system patterning and differentiation. Nat Genet *39*, 397–402.

Dyer, L.A., and Kirby, M.L. (2009). The role of secondary heart field in cardiac development. Developmental Biology *336*, 137–144.

Edmondson, D.G., Lyons, G.E., Martin, J.F., and Olson, E.N. (1994). Mef2 gene expression marks the cardiac and skeletal muscle lineages during mouse embryogenesis. Development *120*, 1251–1263.

Eivazova, E.R., and Aune, T.M. (2004). Dynamic alterations in the conformation of the Ifng gene region during T helper cell differentiation. Proc Natl Acad Sci USA *101*, 251–256.

Fang, X., Xiang, P., Yin, W., Stamatoyannopoulos, G., and Li, Q. (2007). Cooperativeness of the higher chromatin structure of the beta-globin locus revealed by the deletion mutations of DNase I hypersensitive site 3 of the LCR. Journal of Molecular Biology *365*, 31–37.

Fanucchi, S., Shibayama, Y., Burd, S., Weinberg, M.S., and Mhlanga, M.M. (2013). Chromosomal contact permits transcription between coregulated genes. Cell *155*, 606–620.

Feng, S., Cokus, S.J., Schubert, V., Zhai, J., Pellegrini, M., and Jacobsen, S.E. (2014). Genome-wide Hi-C analyses in wild-type and mutants reveal high-resolution chromatin interactions in Arabidopsis. Mol Cell *55*, 694–707.

Firulli, A.B., McFadden, D.G., Lin, Q., Srivastava, D., and Olson, E.N. (1998). Heart and extra-embryonic mesodermal defects in mouse embryos lacking the bHLH transcription factor Hand1. Nat Genet *18*, 266–270.

Frank, D.U., Fotheringham, L.K., Brewer, J.A., Muglia, L.J., Tristani-Firouzi, M., Capecchi, M.R., and Moon, A.M. (2002). An Fgf8 mouse mutant phenocopies human 22q11 deletion syndrome. Development *129*, 4591–4603.

Frasch, M. (1995). Induction of visceral and cardiac mesoderm by ectodermal Dpp in the early Drosophila embryo. Nature *374*, 464–467.

Friedrich, F.W., Dilanian, G., Khattar, P., Juhr, D., Gueneau, L., Charron, P., Fressart,

V., Vilquin, J.-T., Isnard, R., Gouya, L., et al. (2013). A novel genetic variant in the transcription factor Islet-1 exerts gain of function on myocyte enhancer factor 2C promoter activity. Eur. J. Heart Fail. *15*, 267–276.

Fullwood, M.J., Han, Y., Wei, C.-L., Ruan, X., and Ruan, Y. (2001). Chromatin Interaction Analysis Using Paired-End Tag Sequencing. In Current Protocols in Molecular Biology, (John Wiley & Sons, Inc.).

Gadd, M.S., Bhati, M., Jeffries, C.M., Langley, D.B., Trewhella, J., Guss, J.M., and Matthews, J.M. (2011). Structural basis for partial redundancy in a class of transcription factors, the LIM homeodomain proteins, in neural cell type specification. Journal of Biological Chemistry *286*, 42971–42980.

Gadd, M.S., Jacques, D.A., Nisevic, I., Craig, V.J., Kwan, A.H., Guss, J.M., and Matthews, J.M. (2013). A structural basis for the regulation of the LIM-homeodomain protein islet 1 (Isl1) by intra- and intermolecular interactions. Journal of Biological Chemistry *288*, 21924–21935.

Galli, D., Domínguez, J.N., Zaffran, S., Munk, A., Brown, N.A., and Buckingham, M.E. (2008). Atrial myocardium derives from the posterior region of the second heart field, which acquires left-right identity as Pitx2c is expressed.

Garg, V., Yamagishi, C., Hu, T., Kathiriya, I.S., Yamagishi, H., and Srivastava, D. (2001). Tbx1, a DiGeorge Syndrome Candidate Gene, Is Regulated by Sonic Hedgehog during Pharyngeal Arch Development. Developmental Biology *235*, 62–73.

Gittenberger-De Groot, A.C., Winter, E.M., and Poelmann, R.E. (2010). Epicardium-derived cells (EPDCs) in development, cardiac disease and repair of ischemia. J. Cell. Mol. Med. *14*, 1056–1060.

Goddeeris, M.M., Rho, S., Petiet, A., Davenport, C.L., Johnson, G.A., Meyers, E.N., and Klingensmith, J. (2008). Intracardiac septation requires hedgehog-dependent cellular contributions from outside the heart. Development *135*, 1887–1895.

Golzio, C., Havis, E., Daubas, P., Nuel, G., Babarit, C., Munnich, A., Vekemans, M., Zaffran, S., Lyonnet, S., and Etchevers, H.C. (2012). ISL1 Directly Regulates FGF10 Transcription during Human Cardiac Outflow Formation. PLoS ONE *7*, e30677.

Grob, S., Schmid, M.W., and Grossniklaus, U. (2014). Hi-C analysis in Arabidopsis identifies the KNOT, a structure with similarities to the flamenco locus of Drosophila. Mol Cell *55*, 678–693.

Guo, C., Sun, Y., Zhou, B., Adam, R.M., Li, X., Pu, W.T., Morrow, B.E., Moon, A., and Li, X. (2011a). A Tbx1-Six1/Eya1-Fgf8 genetic pathway controls mammalian cardiovascular and craniofacial morphogenesis. J. Clin. Invest. *121*, 1585–1595.

Guo, T., Wang, W., Zhang, H., Liu, Y., Chen, P., Ma, K., and Zhou, C. (2011b). ISL1 promotes pancreatic islet cell proliferation. PLoS ONE *6*, e22387.

Guris, D.L., Duester, G., Papaioannou, V.E., and Imamoto, A. (2006). Dose-dependent interaction of Tbx1 and Crkl and locally aberrant RA signaling in a model of del22q11 syndrome. Dev Cell *10*, 81–92.

Güngör, C., Taniguchi-Ishigaki, N., Ma, H., Drung, A., Tursun, B., Ostendorff, H.P., Bossenz, M., Becker, C.G., Becker, T., and Bach, I. (2007). Proteasomal selection of multiprotein complexes recruited by LIM homeodomain transcription factors. Proc Natl Acad Sci USA *104*, 15000–15005.

Hayashi, S., Imoto, I., Aizu, Y., Okamoto, N., Mizuno, S., Kurosawa, K., Okamoto, N., Honda, S., Araki, S., Mizutani, S., et al. (2010). Clinical application of array-based comparative genomic hybridization by two-stage screening for 536 patients with mental retardation and multiple congenital anomalies. Journal of Human Genetics *56*, 110–124.

Heintzman, N.D., and Ren, B. (2009). Finding distal regulatory elements in the human genome. Current Opinion in Genetics & Development *19*, 541–549.

Heinz, S., and Glass, C.K. (2012). Roles of lineage-determining transcription factors in establishing open chromatin: lessons from high-throughput studies. Curr. Top. Microbiol. Immunol. *356*, 1–15.

High, F.A., Jain, R., Stoller, J.Z., Antonucci, N.B., Lu, M.M., Loomes, K.M., Kaestner, K.H., Pear, W.S., and Epstein, J.A. (2009). Murine Jagged1/Notch signaling in the second heart field orchestrates Fgf8 expression and tissue-tissue interactions during outflow tract development. J. Clin. Invest. *119*, 1986–1996.

High, F.A., Lu, M.M., Pear, W.S., Loomes, K.M., Kaestner, K.H., and Epstein, J.A. (2008). Endothelial expression of the Notch ligand Jagged1 is required for vascular smooth muscle development. Proc Natl Acad Sci USA *105*, 1955–1959.

Hoffmann, A.D., Peterson, M.A., Friedland-Little, J.M., Anderson, S.A., and Moskowitz, I.P. (2009). sonic hedgehog is required in pulmonary endoderm for atrial septation. Development *136*, 1761–1770.

Huang, D.W., Sherman, B.T., and Lempicki, R.A. (2009a). Bioinformatics enrichment tools: paths toward the comprehensive functional analysis of large gene lists. Nucleic Acids Research *37*, 1–13.

Huang, D.W., Sherman, B.T., and Lempicki, R.A. (2009b). Systematic and integrative analysis of large gene lists using DAVID bioinformatics resources. Nat Protoc *4*, 44–57.

Hutson, M.R., and Kirby, M.L. (2007). Model systems for the study of heart development and disease. Cardiac neural crest and conotruncal malformations. Semin Cell Dev Biol *18*, 101–110.

Hwang, M., Gorivodsky, M., Kim, M., Westphal, H., and Geum, D. (2008). The neuronal differentiation potential of Ldb1-null mutant embryonic stem cells is

dependent on extrinsic influences. Stem Cells *26*, 1490–1495.

Ilagan, R., Abu-Issa, R., Brown, D., Yang, Y.-P., Jiao, K., Schwartz, R.J., Klingensmith, J., and Meyers, E.N. (2006). Fgf8 is required for anterior heart field development. Development *133*, 2435–2445.

Infantino, V., Convertini, P., Menga, A., and Iacobazzi, V. (2013). MEF2C exon α: role in gene activation and differentiation. Gene *531*, 355–362.

Ivins, S., Lammerts van Beuren, K., Roberts, C., James, C., Lindsay, E., Baldini, A., Ataliotis, P., and Scambler, P.J. (2005). Microarray analysis detects differentially expressed genes in the pharyngeal region of mice lacking Tbx1. Developmental Biology *285*, 554–569.

Jay, P.Y., Harris, B.S., Maguire, C.T., Buerger, A., Wakimoto, H., Tanaka, M., Kupershmidt, S., Roden, D.M., Schultheiss, T.M., O'Brien, T.X., et al. (2004). Nkx2-5 mutation causes anatomic hypoplasia of the cardiac conduction system. J. Clin. Invest. *113*, 1130–1137.

Jerome, L.A., and Papaioannou, V.E. (2001). DiGeorge syndrome phenotype in mice mutant for the T-box gene, Tbx1. Nat Genet *27*, 286–291.

Jin, F., Li, Y., Dixon, J.R., Selvaraj, S., Ye, Z., Lee, A.Y., Yen, C.-A., Schmitt, A.D., Espinoza, C.A., and Ren, B. (2013). A high-resolution map of the three-dimensional chromatin interactome in human cells. Nature *503*, 290–294.

Jing, H., Vakoc, C.R., Ying, L., Mandat, S., Wang, H., Zheng, X., and Blobel, G.A. (2008). Exchange of GATA factors mediates transitions in looped chromatin organization at a developmentally regulated gene locus. Mol Cell *29*, 232–242.

Jurata, L.W., and Gill, G.N. (1997). Functional analysis of the nuclear LIM domain interactor NLI. Mol Cell Biol *17*, 5688–5698.

Jurata, L.W., Kenny, D.A., and Gill, G.N. (1996). Nuclear LIM interactor, a rhombotin and LIM homeodomain interacting protein, is expressed early in neuronal development. Proc Natl Acad Sci USA *93*, 11693–11698.

Jurata, L.W., Pfaff, S.L., and Gill, G.N. (1998). The nuclear LIM domain interactor NLI mediates homo- and heterodimerization of LIM domain transcription factors. J Biol Chem *273*, 3152–3157.

Kaku, Y., Ohmori, T., Kudo, K., Fujimura, S., Suzuki, K., Evans, S.M., Kawakami, Y., and Nishinakamura, R. (2013). Islet1 deletion causes kidney agenesis and hydroureter resembling CAKUT. J. Am. Soc. Nephrol. *24*, 1242–1249.

Kang, J., Nathan, E., Xu, S.-M., Tzahor, E., and Black, B.L. (2009). Isl1 is a direct transcriptional target of Forkhead transcription factors in second heart field-derived mesoderm. Developmental Biology *334*, 513–522.

Kappen, C., and Salbaum, J.M. (2009). Identification of regulatory elements in the Isl1 gene locus. Int. J. Dev. Biol. *53*, 935–946.

Karlsson, O., Thor, S., Norberg, T., Ohlsson, H., and Edlund, T. (1990). Insulin gene enhancer binding protein Isl-1 is a member of a novel class of proteins containing both a homeo-and a Cys□His domain. Nature *344*, 879–882.

Kattman, S.J., Huber, T.L., and Keller, G.M. (2006). Multipotent Flk-1+ Cardiovascular Progenitor Cells Give Rise to the Cardiomyocyte, Endothelial, and Vascular Smooth Muscle Lineages. Dev Cell *11*, 723–732.

Keegan, B.R., Feldman, J.L., Begemann, G., Ingham, P.W., and Yelon, D. (2005). Retinoic acid signaling restricts the cardiac progenitor pool. Science *307*, 247–249.

Kelly, R.G., Brown, N.A., and Buckingham, M.E. (2001). The arterial pole of the mouse heart forms from Fgf10-expressing cells in pharyngeal mesoderm. Dev Cell *1*, 435–440.

Kelly, R.G., Zammit, P.S., Schneider, A., Alonso, S., Biben, C., and Buckingham, M.E. (1997). Embryonic and fetal myogenic programs act through separate enhancers at the MLC1F/3F locus. Developmental Biology *187*, 183–199.

Kelly, R.G. (2012). The second heart field. Curr. Top. Dev. Biol. *100*, 33–65.

Kent, W.J., Sugnet, C.W., Furey, T.S., Roskin, K.M., Pringle, T.H., Zahler, A.M., and Haussler, D. (2002). The human genome browser at UCSC. Genome Research *12*, 996–1006.

Kim, A., and Dean, A. (2012). Chromatin loop formation in the β-globin locus and its role in globin gene transcription. Mol Cells *34*, 1–5.

Kim, R.Y., Robertson, E.J., and Solloway, M.J. (2001). Bmp6 and Bmp7 are required for cushion formation and septation in the developing mouse heart. Developmental Biology *235*, 449–466.

Kioussis, D. (2005). Gene regulation: kissing chromosomes. Nature *435*, 579–580.

Kitajima, S., Takagi, A., Inoue, T., and Saga, Y. (2000). MesP1 and MesP2 are essential for the development of cardiac mesoderm. Development *127*, 3215–3226.

Klaus, A., Saga, Y., Taketo, M.M., Tzahor, E., and Birchmeier, W. (2007). Distinct roles of Wnt/beta-catenin and Bmp signaling during early cardiogenesis. Proc Natl Acad Sci USA *104*, 18531–18536.

Krivega, I., Dale, R.K., and Dean, A. (2014). Role of LDB1 in the transition from chromatin looping to transcription activation. Genes & Development *28*, 1278–1290.

Kruithof, B.P.T., van Wijk, B., Somi, S., Kruithof-de Julio, M., Pérez Pomares, J.M., Weesie, F., Wessels, A., Moorman, A.F.M., and van den Hoff, M.J.B. (2006). BMP and

FGF regulate the differentiation of multipotential pericardial mesoderm into the myocardial or epicardial lineage. Developmental Biology *295*, 507–522.

Kulaeva, O.I., Nizovtseva, E.V., Polikanov, Y.S., Ulianov, S.V., and Studitsky, V.M. (2012). Distant activation of transcription: mechanisms of enhancer action. Mol Cell Biol *32*, 4892–4897.

Kuo, C.T., Veselits, M.L., Barton, K.P., Lu, M.M., Clendenin, C., and Leiden, J.M. (1997). The LKLF transcription factor is required for normal tunica media formation and blood vessel stabilization during murine embryogenesis. Genes & Development *11*, 2996–3006.

Kwon, C., Arnold, J., Hsiao, E.C., Taketo, M.M., Conklin, B.R., and Srivastava, D. (2007). Canonical Wnt signaling is a positive regulator of mammalian cardiac progenitors. Proc Natl Acad Sci USA *104*, 10894–10899.

Kwon, C., Qian, L., Cheng, P., Nigam, V., Arnold, J., and Srivastava, D. (2009). A regulatory pathway involving Notch1/β-catenin/Isl1 determines cardiac progenitor cell fate. Nature Publishing Group *11*, 951–957.

la Cruz, de, M.V., Sánchez Gómez, C., Arteaga, M.M., and Argüello, C. (1977). Experimental study of the development of the truncus and the conus in the chick embryo. J. Anat. *123*, 661–686.

Laugwitz, K.-L., Moretti, A., Caron, L., Nakano, A., and Chien, K.R. (2008). Islet1 cardiovascular progenitors: a single source for heart lineages? Development *135*, 193–205.

Laugwitz, K.-L., Moretti, A., Lam, J., Gruber, P., Chen, Y., Woodard, S., Lin, L.-Z., Cai, C.-L., Lu, M.M., Reth, M., et al. (2005). Postnatal isl1+ cardioblasts enter fully differentiated cardiomyocyte lineages. Nature *433*, 647–653.

Lazic, S., and Scott, I.C. (2011). Mef2cb regulates late myocardial cell addition from a second heart field-like population of progenitors in zebrafish. Developmental Biology *354*, 123–133.

Le, T.B.K., Imakaev, M.V., Mirny, L.A., and Laub, M.T. (2013). High-resolution mapping of the spatial organization of a bacterial chromosome. Science *342*, 731–734.

Leonard, J., Serup, P., Gonzalez, G., Edlund, T., and Montminy, M. (1992). The LIM family transcription factor Isl-1 requires cAMP response element binding protein to promote somatostatin expression in pancreatic islet cells. Proc Natl Acad Sci USA *89*, 6247–6251.

Levings, P.P., Zhou, Z., Vieira, K.F., Crusselle-Davis, V.J., and Bungert, J. (2006). Recruitment of transcription complexes to the beta-globin locus control region and transcription of hypersensitive site 3 prior to erythroid differentiation of murine embryonic stem cells. Febs J. *273*, 746–755.

Li, L., Jothi, R., Cui, K., Lee, J.Y., Cohen, T., Gorivodsky, M., Tzchori, I., Zhao, Y., Hayes, S.M., Bresnick, E.H., et al. (2011). Nuclear adaptor Ldb1 regulates a transcriptional program essential for the maintenance of hematopoietic stem cells. Nature Publishing Group *12*, 129–136.

Li, P., Pashmforoush, M., and Sucov, H.M. (2010). Retinoic acid regulates differentiation of the secondary heart field and TGFbeta-mediated outflow tract septation. Dev Cell *18*, 480–485.

Liang, X., Song, M.-R., Xu, Z., Lanuza, G.M., Liu, Y., Zhuang, T., Chen, Y., Pfaff, S.L., Evans, S.M., and Sun, Y. (2011). Isl1 is required for multiple aspects of motor neuron development. Mol. Cell. Neurosci. *47*, 215–222.

Liao, J., Aggarwal, V.S., Nowotschin, S., Bondarev, A., Lipner, S., and Morrow, B.E. (2008). Identification of downstream genetic pathways of Tbx1 in the second heart field. Developmental Biology *316*, 524–537.

Lieberman-Aiden, E., van Berkum, N.L., Williams, L., Imakaev, M., Ragoczy, T., Telling, A., Amit, I., Lajoie, B.R., Sabo, P.J., Dorschner, M.O., et al. (2009). Comprehensive mapping of long-range interactions reveals folding principles of the human genome. Science *326*, 289–293.

Lin, L., Bu, L., Cai, C.-L., Zhang, X., and Evans, S. (2006). Isl1 is upstream of sonic hedgehog in a pathway required for cardiac morphogenesis. Developmental Biology *295*, 756–763.

Lin, L., Cui, L., Zhou, W., Dufort, D., Zhang, X., Cai, C.-L., Bu, L., Yang, L., Martin, J., Kemler, R., et al. (2007). β-Catenin directly regulates Islet1 expression in cardiovascular progenitors and is required for multiple aspects of cardiogenesis.

Lin, Q., Lu, J., Yanagisawa, H., Webb, R., Lyons, G.E., Richardson, J.A., and Olson, E.N. (1998). Requirement of the MADS-box transcription factor MEF2C for vascular development. Development *125*, 4565–4574.

Lin, Q., Schwarz, J., Bucana, C., and Olson, E.N. (1997). Control of mouse cardiac morphogenesis and myogenesis by transcription factor MEF2C. Science *276*, 1404–1407.

Lin, X. (2004). Functions of heparan sulfate proteoglycans in cell signaling during development. Development *131*, 6009–6021.

Lindsay, E.A., Vitelli, F., Su, H., Morishima, M., Huynh, T., Pramparo, T., Jurecic, V., Ogunrinu, G., Sutherland, H.F., Scambler, P.J., et al. (2001). *Tbx1* haploinsufficiency in the DiGeorge syndrome region causes aortic arch defects in mice. Nature *410*, 97–101.

Liu, W., Selever, J., Wang, D., Lu, M.-F., Moses, K.A., Schwartz, R.J., and Martin, J.F. (2004). Bmp4 signaling is required for outflow-tract septation and branchial-arch artery remodeling. Proc Natl Acad Sci USA *101*, 4489–4494.

Lyons, G.E. (1996). Vertebrate heart development. Current Opinion in Genetics & Development *6*, 454–460.

Ma, Q., Zhou, B., and Pu, W.T. (2008). Reassessment of Isl1 and Nkx2-5 cardiac fate maps using a Gata4-based reporter of Cre activity. Developmental Biology *323*, 98–104.

Maeda, J., Yamagishi, H., McAnally, J., Yamagishi, C., and Srivastava, D. (2006). Tbx1 is regulated by forkhead proteins in the secondary heart field. Dev Dyn *235*, 701–710.

Makarev, E., and Gorivodsky, M. (2014). Islet1 and its co-factor Ldb1 are expressed in quiescent cells of mouse intestinal epithelium. PLoS ONE *9*, e95256.

Mann, T., Bodmer, R., and Pandur, P. (2009). The Drosophila homolog of vertebrate Islet1 is a key component in early cardiogenesis. Development *136*, 317–326.

Marguerie, A., Bajolle, F., Zaffran, S., Brown, N.A., Dickson, C., Buckingham, M.E., and Kelly, R.G. (2006). Congenital heart defects in Fgfr2-IIIb and Fgf10 mutant mice. Cardiovascular Research *71*, 50–60.

Martínez-Estrada, O.M., Lettice, L.A., Essafi, A., Guadix, J.A., Slight, J., Velecela, V., Hall, E., Reichmann, J., Devenney, P.S., Hohenstein, P., et al. (2010). Wt1 is required for cardiovascular progenitor cell formation through transcriptional control of Snail and E-cadherin. Nat Genet *42*, 89–93.

Matthews, J.M., and Visvader, J.E. (2003). LIM-domain-binding protein 1: a multifunctional cofactor that interacts with diverse proteins. EMBO Rep. *4*, 1132–1137.

Mazzoni, E.O., Mahony, S., Closser, M., Morrison, C.A., Nedelec, S., Williams, D.J., An, D., Gifford, D.K., and Wichterle, H. (2013). Synergistic binding of transcription factors to cell-specific enhancers programs motor neuron identity. Nat. Neurosci. *16*, 1219–1227.

McCulley, D.J., Kang, J.-O., Martin, J.F., and Black, B.L. (2008). BMP4 is required in the anterior heart field and its derivatives for endocardial cushion remodeling, outflow tract septation, and semilunar valve development. Dev Dyn *237*, 3200–3209.

McFadden, D.G., Charité, J., Richardson, J.A., Srivastava, D., Firulli, A.B., and Olson, E.N. (2000). A GATA-dependent right ventricular enhancer controls dHAND transcription in the developing heart. Development *127*, 5331–5341.

McFadden, D.G., Barbosa, A.C., Richardson, J.A., Schneider, M.D., Srivastava, D., and Olson, E.N. (2005). The Hand1 and Hand2 transcription factors regulate expansion of the embryonic cardiac ventricles in a gene dosage-dependent manner. Development *132*, 189–201.

Meaburn, K.J., and Misteli, T. (2007). Cell biology: chromosome territories. Nature

445, 379–781.

Meier, N., Krpic, S., Rodriguez, P., Strouboulis, J., Monti, M., Krijgsveld, J., Gering, M., Patient, R., Hostert, A., and Grosveld, F. (2006). Novel binding partners of Ldb1 are required for haematopoietic development. Development *133*, 4913–4923.

Meilhac, S.M., Esner, M., Kelly, R.G., Nicolas, J.-F., and Buckingham, M.E. (2004). The clonal origin of myocardial cells in different regions of the embryonic mouse heart. Dev Cell *6*, 685–698.

Merscher, S., Funke, B., Epstein, J.A., Heyer, J., Puech, A., Lu, M.M., Xavier, R.J., Demay, M.B., Russell, R.G., and Factor, S. (2001). TBX1 Is Responsible for Cardiovascular Defects in Velo-Cardio-Facial/DiGeorge Syndrome. Cell *104*, 619–629.

Mesbah, K., Harrelson, Z., and Theveniau-Ruissy, M. (2008). Tbx3 is required for outflow tract development. Circulation.

Mishina, Y., Suzuki, A., Ueno, N., and Behringer, R.R. (1995). Bmpr encodes a type I bone morphogenetic protein receptor that is essential for gastrulation during mouse embryogenesis. Genes & Development *9*, 3027–3037.

Mjaatvedt, C.H., Nakaoka, T., Moreno-Rodriguez, R., Norris, R.A., Kern, M.J., Eisenberg, C.A., Turner, D., and Markwald, R.R. (2001). The Outflow Tract of the Heart Is Recruited from a Novel Heart-Forming Field. Developmental Biology *238*, 97–109.

Molkentin, J.D., and Olson, E.N. (1997). GATA4: a novel transcriptional regulator of cardiac hypertrophy? Circulation *96*, 3833–3835.

Morcillo, P., Rosen, C., Baylies, M.K., and Dorsett, D. (1997). Chip, a widely expressed chromosomal protein required for segmentation and activity of a remote wing margin enhancer in Drosophila. Genes & Development *11*, 2729–2740.

Moretti, A., Lam, J., Evans, S.M., and Laugwitz, K.-L. (2007). Biology of Isl1+ cardiac progenitor cells in development and disease. Cell. Mol. Life Sci. *64*, 674–682.

Moretti, A., Caron, L., Nakano, A., Lam, J.T., Bernshausen, A., Chen, Y., Qyang, Y., Bu, L., Sasaki, M., Martin-Puig, S., et al. (2006). Multipotent embryonic isl1+ progenitor cells lead to cardiac, smooth muscle, and endothelial cell diversification. Cell *127*, 1151–1165.

Mukhopadhyay, M., Teufel, A., Yamashita, T., Agulnick, A.D., Chen, L., Downs, K.M., Schindler, A., Grinberg, A., Huang, S.-P., Dorward, D., et al. (2003). Functional ablation of the mouse Ldb1 gene results in severe patterning defects during gastrulation. Development *130*, 495–505.

Mylona, A., Andrieu-Soler, C., Thongjuea, S., Martella, A., Soler, E., Jorna, R., Hou, J., Kockx, C., van IJcken, W., Lenhard, B., et al. (2013). Genome-wide analysis shows that Ldb1 controls essential hematopoietic genes/pathways in mouse early development

and reveals novel players in hematopoiesis. Blood *121*, 2902–2913.

Narkis, G., Tzchori, I., Cohen, T., Holtz, A., Wier, E., and Westphal, H. (2012). Isl1 and Ldb co-regulators of transcription are essential early determinants of mouse limb development. Dev Dyn *241*, 787–791.

Noonan, J.P., and McCallion, A.S. (2010). Genomics of Long-Range Regulatory Elements. Annu Rev Genom Hum G *11*, 1–24.

Noordermeer, D., Branco, M.R., Splinter, E., Klous, P., van IJcken, W., Swagemakers, S., Koutsourakis, M., van der Spek, P., Pombo, A., and de Laat, W. (2008). Transcription and Chromatin Organization of a Housekeeping Gene Cluster Containing an Integrated β-Globin Locus Control Region. PLoS Genet *4*, e1000016.

Noordermeer, D., Leleu, M., Splinter, E., Rougemont, J., de Laat, W., and Duboule, D. (2011). The dynamic architecture of Hox gene clusters. Science *334*, 222–225.

O'Sullivan, J.M., Tan-Wong, S.M., Morillon, A., Lee, B., Coles, J., Mellor, J., and Proudfoot, N.J. (2004). Gene loops juxtapose promoters and terminators in yeast. Nat Genet *36*, 1014–1018.

Osoegawa, K., Schultz, K., Yun, K., Mohammed, N., Shaw, G.M., and Lammer, E.J. (2014). Haploinsufficiency of insulin gene enhancer protein 1 (ISL1) is associated with d-transposition of the great arteries. Mol Genet Genomic Med *2*, 341–351.

Palstra, R.-J.T.S. (2009). Close encounters of the 3C kind: long-range chromatin interactions and transcriptional regulation. Briefings in Functional Genomics and Proteomics *8*, 297–309.

Palstra, R.-J., de Laat, W., and Grosveld, F. (2008). Beta-globin regulation and long-range interactions. Adv. Genet. *61*, 107–142.

Palstra, R.-J., Tolhuis, B., Splinter, E., Nijmeijer, R., Grosveld, F., and de Laat, W. (2003). The beta-globin nuclear compartment in development and erythroid differentiation. Nat Genet *35*, 190–194.

Park, E.J., Ogden, L.A., Talbot, A., Evans, S., Cai, C.-L., Black, B.L., Frank, D.U., and Moon, A.M. (2006). Required, tissue-specific roles for Fgf8 in outflow tract formation and remodeling. Development *133*, 2419–2433.

Park, E.J., Watanabe, Y., Smyth, G., Miyagawa-Tomita, S., Meyers, E., Klingensmith, J., Camenisch, T., Buckingham, M., and Moon, A.M. (2008). An FGF autocrine loop initiated in second heart field mesoderm regulates morphogenesis at the arterial pole of the heart. Development *135*, 3599–3610.

Pashmforoush, M., Lu, J.T., Chen, H., Amand, T.S., Kondo, R., Pradervand, S., Evans, S.M., Clark, B., Feramisco, J.R., Giles, W., et al. (2004). Nkx2-5 pathways and congenital heart disease; loss of ventricular myocyte lineage specification leads to progressive cardiomyopathy and complete heart block. Cell *117*, 373–386.

Pfaff, S.L., Mendelsohn, M., Stewart, C.L., Edlund, T., and Jessell, T.M. (1996). Requirement for LIM homeobox gene Isl1 in motor neuron generation reveals a motor neuron-dependent step in interneuron differentiation. Cell *84*, 309–320.

Phillips, H.M., Murdoch, J.N., Chaudhry, B., Copp, A.J., and Henderson, D.J. (2005). Vangl2 acts via RhoA signaling to regulate polarized cell movements during development of the proximal outflow tract.

Phillips, H.M., Rhee, H.J., Murdoch, J.N., Hildreth, V., Peat, J.D., Anderson, R.H., Copp, A.J., Chaudhry, B., and Henderson, D.J. (2007). Disruption of planar cell polarity signaling results in congenital heart defects and cardiomyopathy attributable to early cardiomyocyte disorganization. Circulation Research *101*, 137–145.

Phillips-Cremins, J.E., Sauria, M.E.G., Sanyal, A., Gerasimova, T.I., Lajoie, B.R., Bell, J.S.K., Ong, C.-T., Hookway, T.A., Guo, C., Sun, Y., et al. (2013). Architectural protein subclasses shape 3D organization of genomes during lineage commitment. Cell *153*, 1281–1295.

Pollock, R., and Treisman, R. (1991). Human SRF-related proteins: DNA-binding properties and potential regulatory targets. Genes & Development *5*, 2327–2341.

Prall, O.W.J., Menon, M.K., Solloway, M.J., Watanabe, Y., Zaffran, S., Bajolle, F., Biben, C., McBride, J.J., Robertson, B.R., Chaulet, H., et al. (2007). An Nkx2-5/Bmp2/Smad1 Negative Feedback Loop Controls Heart Progenitor Specification and Proliferation. Cell *128*, 947–959.

Pu, W.T., Ishiwata, T., Juraszek, A.L., Ma, Q., and Izumo, S. (2004). GATA4 is a dosage-sensitive regulator of cardiac morphogenesis. Developmental Biology *275*, 235–244.

Qyang, Y., Martin-Puig, S., Chiravuri, M., Chen, S., Xu, H., Bu, L., Jiang, X., Lin, L., Granger, A., Moretti, A., et al. (2007). The renewal and differentiation of Isl1+ cardiovascular progenitors are controlled by a Wnt/beta-catenin pathway. Cell Stem Cell *1*, 165–179.

Rabl, C. (1885). Uber Zelltheilung. Morphol. Jahrb. 10, 214-330 (Morphol. Jahrb).

Rao, S.S.P., Huntley, M.H., Durand, N.C., Stamenova, E.K., Bochkov, I.D., Robinson, J.T., Sanborn, A.L., Machol, I., Omer, A.D., Lander, E.S., et al. (2014). A 3D map of the human genome at kilobase resolution reveals principles of chromatin looping. Cell *159*, 1665–1680.

Razin, S.V., Gavrilov, A.A., Ioudinkova, E.S., and Iarovaia, O.V. (2013). Communication of genome regulatory elements in a folded chromosome. FEBS Lett *587*, 1840–1847.

Riley, P.R., and Smart, N. (2011). Vascularizing the heart. Cardiovascular Research *91*, 260–268.

Riley, P., Anaon-Cartwight, L., and Cross, J.C. (1998). The Hand1 bHLH transcription factor is essential for placentation and cardiac morphogenesis. Nat Genet *18*, 271–

275.

Roberts, C., Ivins, S.M., James, C.T., and Scambler, P.J. (2005). Retinoic acid down-regulates Tbx1 expression in vivo and in vitro. Dev Dyn *232*, 928–938.

Roberts, C., Ivins, S., Cook, A.C., Baldini, A., and Scambler, P.J. (2006). Cyp26 genes a1, b1 and c1 are down-regulated in Tbx1 null mice and inhibition of Cyp26 enzyme function produces a phenocopy of DiGeorge Syndrome in the chick. Human Molecular Genetics *15*, 3394–3410.

Rochais, F., Mesbah, K., and Kelly, R.G. (2009). Signaling Pathways Controlling Second Heart Field Development. Circulation Research *104*, 933–942.

Ryckebusch, L., Wang, Z., Bertrand, N., Lin, S.-C., Chi, X., Schwartz, R., Zaffran, S., and Niederreither, K. (2008). Retinoic acid deficiency alters second heart field formation. Proc Natl Acad Sci USA *105*, 2913–2918.

Saga, Y., Kitajima, S., and Miyagawa-Tomita, S. (2000). Mesp1 expression is the earliest sign of cardiovascular development. Trends in Cardiovascular Medicine *10*, 345–352.

Saga, Y., Miyagawa-Tomita, S., Takagi, A., Kitajima, S., Miyazaki, J.I., and Inoue, T. (1999). MesP1 is expressed in the heart precursor cells and required for the formation of a single heart tube. Development *126*, 3437–3447.

Schleiffarth, J.R., Person, A.D., Martinsen, B.J., Sukovich, D.J., Neumann, A., Baker, C.V.H., Lohr, J.L., Cornfield, D.N., Ekker, S.C., and Petryk, A. (2007). Wnt5a Is Required for Cardiac Outflow Tract Septation in Mice. Pediatr Res *61*, 386–391.

Schmeichel, K.L., and Beckerle, M.C. (1994). The LIM domain is a modular protein-binding interface. Cell.

Schneider, V.A., and Mercola, M. (2001). Wnt antagonism initiates cardiogenesis in Xenopus laevis. Genes & Development *15*, 304–315.

Scholl, A.M., and Kirby, M.L. (2009). Signals controlling neural crest contributions to the heart. Wiley Interdiscip Rev Syst Biol Med *1*, 220–227.

Schultheiss, T.M., Burch, J.B., and Lassar, A.B. (1997). A role for bone morphogenetic proteins in the induction of cardiac myogenesis. Genes & Development *11*, 451–462.

Seo, S., and Kume, T. (2006). Forkhead transcription factors, Foxc1 and Foxc2, are required for the morphogenesis of the cardiac outflow tract. Developmental Biology *296*, 421–436.

Shen, Y., Yue, F., McCleary, D.F., Ye, Z., Edsall, L., Kuan, S., Wagner, U., Dixon, J., Lee, L., Lobanenkov, V.V., et al. (2012). A map of the cis-regulatory sequences in the mouse genome. Nature *488*, 116–120.

Singh, M.K., Li, Y., Li, S., Cobb, R.M., Zhou, D., and Lu, M.M. (2010). Gata4 and Gata5 cooperatively regulate cardiac myocyte proliferation in mice. Journal of Biological ….

Singh, M.K., Christoffels, V.M., Dias, J.M., Trowe, M.-O., Petry, M., Schuster-Gossler, K., Bürger, A., Ericson, J., and Kispert, A. (2005). Tbx20 is essential for cardiac chamber differentiation and repression of Tbx2. Development *132*, 2697–2707.

Sirbu, I.O., Zhao, X., and Duester, G. (2008). Retinoic acid controls heart anteroposterior patterning by down-regulating Isl1 through the Fgf8 pathway. Dev Dyn *237*, 1627–1635.

Soler, E., Andrieu-Soler, C., de Boer, E., Bryne, J.C., Thongjuea, S., Stadhouders, R., Palstra, R.-J., Stevens, M., Kockx, C., van IJcken, W., et al. (2010). The genome-wide dynamics of the binding of Ldb1 complexes during erythroid differentiation. Genes & Development *24*, 277–289.

Solloway, M.J., and Robertson, E.J. (1999). Early embryonic lethality in Bmp5;Bmp7 double mutant mice suggests functional redundancy within the 60A subgroup. Development *126*, 1753–1768.

Song, M.-R., Sun, Y., Bryson, A., Gill, G.N., Evans, S.M., and Pfaff, S.L. (2009). Islet-to-LMO stoichiometries control the function of transcription complexes that specify motor neuron and V2a interneuron identity. Development *136*, 2923–2932.

Song, S.-H., Kim, A., Ragoczy, T., Bender, M.A., Groudine, M., and Dean, A. (2010). Multiple functions of Ldb1 required for -globin activation during erythroid differentiation. Blood *116*, 2356–2364.

Song, S.-H., Hou, C., and Dean, A. (2007). A Positive Role for NLI/Ldb1 in Long-Range β-Globin Locus Control Region Function. Mol Cell *28*, 810–822.

Speicher, M.R., and Carter, N.P. (2005). The new cytogenetics: blurring the boundaries with molecular biology. Nat Rev Genet *6*, 782–792.

Srivastava, D. (1999). HAND proteins: molecular mediators of cardiac development and congenital heart disease. Trends in Cardiovascular Medicine *9*, 11–18.

Srivastava, D., Cserjesi, P., and Olson, E.N. (1995). A subclass of bHLH proteins required for cardiac morphogenesis. Science *270*, 1995–1999.

Srivastava, D., Thomas, T., Lin, Q., Kirby, M.L., Brown, D., and Olson, E.N. (1997). Regulation of cardiac mesodermal and neural crest development by the bHLH transcription factor, dHAND. Nat Genet *16*, 154–160.

Stadhouders, R., Kolovos, P., Brouwer, R., Zuin, J., van den Heuvel, A., Kockx, C., Palstra, R.-J., Wendt, K.S., Grosveld, F., van IJcken, W., et al. (2013). Multiplexed chromosome conformation capture sequencing for rapid genome-scale high-resolution detection of long-range chromatin interactions. Nat Protoc *8*, 509–524.

Stadhouders, R., Thongjuea, S., Andrieu-Soler, C., Palstra, R.-J., Bryne, J.C., van den Heuvel, A., Stevens, M., de Boer, E., Kockx, C., van der Sloot, A., et al. (2012a). Dynamic long-range chromatin interactions control Myb proto-oncogene transcription during erythroid development. Embo J *31*, 986–999.

Stadhouders, R., van den Heuvel, A., Kolovos, P., Jorna, R., Leslie, K., Grosveld, F., and Soler, E. (2012b). Transcription regulation by distal enhancers: who's in the loop? Transcription *3*, 181–186.

Stalsberg, H., and DeHaan, R.L. (1969). The precardiac areas and formation of the tubular heart in the chick embryo. Developmental Biology *19*, 128–159.

Stennard, F.A., and Harvey, R.P. (2005). T-box transcription factors and their roles in regulatory hierarchies in the developing heart. Development *132*, 4897–4910.

Stevens, K.N., Hakonarson, H., Kim, C.E., Doevendans, P.A., Koeleman, B.P.C., Mital, S., Raue, J., Glessner, J.T., Coles, J.G., Moreno, V., et al. (2010). Common Variation in ISL1 Confers Genetic Susceptibility for Human Congenital Heart Disease. PLoS ONE *5*, e10855.

Sun, Y., Liang, X., Najafi, N., Cass, M., Lin, L., Cai, C.-L., Chen, J., and Evans, S.M. (2007). Islet 1 is expressed in distinct cardiovascular lineages, including pacemaker and coronary vascular cells. Developmental Biology *304*, 286–296.

Takeuchi, J.K., Mileikovskaia, M., Koshiba-Takeuchi, K., Heidt, A.B., Mori, A.D., Arruda, E.P., Gertsenstein, M., Georges, R., Davidson, L., Mo, R., et al. (2005). Tbx20 dose-dependently regulates transcription factor networks required for mouse heart and motoneuron development. Development *132*, 2463–2474.

Takeuchi, J.K., Ohgi, M., Koshiba-Takeuchi, K., Shiratori, H., Sakaki, I., Ogura, K., Saijoh, Y., and Ogura, T. (2003). Tbx5 specifies the left/right ventricles and ventricular septum position during cardiogenesis. Development *130*, 5953–5964.

Tessadori, F., van Weerd, J.H., Burkhard, S.B., Verkerk, A.O., de Pater, E., Boukens, B.J., Vink, A., Christoffels, V.M., and Bakkers, J. (2012). Identification and functional characterization of cardiac pacemaker cells in zebrafish. PLoS ONE *7*, e47644.

Théveniau-Ruissy, M., Dandonneau, M., Mesbah, K., Ghez, O., Mattei, M.-G., Miquerol, L., and Kelly, R.G. (2008). The del22q11.2 candidate gene Tbx1 controls regional outflow tract identity and coronary artery patterning. Circulation Research *103*, 142–148.

Tian, Y., Yuan, L., Goss, A.M., Wang, T., Yang, J., Lepore, J.J., Zhou, D., Schwartz, R.J., Patel, V., Cohen, E.D., et al. (2010). Characterization and in vivo pharmacological rescue of a Wnt2-Gata6 pathway required for cardiac inflow tract development. Dev Cell *18*, 275–287.

Tirosh-Finkel, L. (2006). Mesoderm progenitor cells of common origin contribute to the head musculature and the cardiac outflow tract. Development *133*, 1943–1953.

Tirosh-Finkel, L., Zeisel, A., Brodt-Ivenshitz, M., Shamai, A., Yao, Z., Seger, R., Domany, E., and Tzahor, E. (2010). BMP-mediated inhibition of FGF signaling promotes cardiomyocyte differentiation of anterior heart field progenitors. Development *137*, 2989–3000.

Tolhuis, B., Palstra, R.-J., Splinter, E., Grosveld, F., and de Laat, W. (2002). Looping and interaction between hypersensitive sites in the active beta-globin locus. Mol Cell *10*, 1453–1465.

Toyama, R., Kobayashi, M., Tomita, T., and Dawid, I.B. (1998). Expression of LIM-domain binding protein (ldb) genes during zebrafish embryogenesis. Mech Dev *71*, 197–200.

Tsuchihashi, T., Maeda, J., Shin, C.H., Ivey, K.N., Black, B.L., Olson, E.N., Yamagishi, H., and Srivastava, D. (2011). Hand2 function in second heart field progenitors is essential for cardiogenesis. Developmental Biology *351*, 62–69.

Vakoc, C.R., Letting, D.L., Gheldof, N., Sawado, T., Bender, M.A., Groudine, M., Weiss, M.J., Dekker, J., and Blobel, G.A. (2005). Proximity among distant regulatory elements at the beta-globin locus requires GATA-1 and FOG-1. Mol Cell *17*, 453–462.

van de Werken, H.J.G., de Vree, P.J.P., Splinter, E., Holwerda, S.J.B., Klous, P., de Wit, E., and de Laat, W. (2012). 4C technology: protocols and data analysis. Meth. Enzymol. *513*, 89–112.

van Weerd, J.H., Badi, I., van den Boogaard, M., Stefanovic, S., van de Werken, H.J.G., Gomez-Velazquez, M., Badía-Careaga, C., Manzanares, M., de Laat, W., Barnett, P., et al. (2014). A large permissive regulatory domain exclusively controls Tbx3 expression in the cardiac conduction system. Circulation Research *115*, 432–441.

van Wijk, B., van den Berg, G., Abu-Issa, R., Barnett, P., van der Velden, S., Schmidt, M., Ruijter, J.M., Kirby, M.L., Moorman, A.F.M., and van den Hoff, M.J.B. (2009). Epicardium and myocardium separate from a common precursor pool by crosstalk between bone morphogenetic protein- and fibroblast growth factor-signaling pathways. Circulation Research *105*, 431–441.

Varadkar, P., Kraman, M., Despres, D., Ma, G., Lozier, J., and McCright, B. (2008). Notch2 is required for the proliferation of cardiac neural crest-derived smooth muscle cells. Dev Dyn *237*, 1144–1152.

Vincent, S.D., and Buckingham, M.E. (2010). How to make a heart: the origin and regulation of cardiac progenitor cells. Curr. Top. Dev. Biol. *90*, 1–41.

Vincentz, J.W., McWhirter, J.R., Murre, C., Baldini, A., and Furuta, Y. (2005). Fgf15 is required for proper morphogenesis of the mouse cardiac outflow tract. Genesis *41*, 192–201.

Virágh, S., and Challice, C.E. (1973). Origin and differentiation of cardiac muscle cells in the mouse. Journal of Ultrastructure Research *42*, 1–24.

Vitelli, F., Morishima, M., Taddei, I., Lindsay, E.A., and Baldini, A. (2002). Tbx1 mutation causes multiple cardiovascular defects and disrupts neural crest and cranial nerve migratory pathways. Human Molecular Genetics *11*, 915–922.

Wadman, I.A., Osada, H., Grütz, G.G., Agulnick, A.D., Westphal, H., Forster, A., and Rabbitts, T.H. (1997). The LIM-only protein Lmo2 is a bridging molecule assembling an erythroid, DNA-binding complex which includes the TAL1, E47, GATA-1 and Ldb1/NLI proteins. Embo J *16*, 3145–3157.

Waldo, K.L., Kumiski, D.H., Wallis, K.T., Stadt, H.A., Hutson, M.R., Platt, D.H., and Kirby, M.L. (2001). Conotruncal myocardium arises from a secondary heart field. Development *128*, 3179–3188.

Waldo, K.L., Hutson, M.R., Stadt, H.A., Zdanowicz, M., Zdanowicz, J., and Kirby, M.L. (2005). Cardiac neural crest is necessary for normal addition of the myocardium to the arterial pole from the secondary heart field. Developmental Biology *281*, 66–77.

Wang, M., and Drucker, D.J. (1996). Activation of amylin gene transcription by LIM domain homeobox gene isl-1. Molecular Endocrinology *10*, 243–251.

Washington Smoak, I., Byrd, N.A., Abu-Issa, R., Goddeeris, M.M., Anderson, R., Morris, J., Yamamura, K., Klingensmith, J., and Meyers, E.N. (2005). Sonic hedgehog is required for cardiac outflow tract and neural crest cell development. Developmental Biology *283*, 357–372.

Watanabe, Y., and Buckingham, M. (2010). The formation of the embryonic mouse heart: heart fields and myocardial cell lineages. Annals of the New York Academy of Sciences *1188*, 15–24.

Watanabe, Y., Miyagawa-Tomita, S., Vincent, S.D., Kelly, R.G., Moon, A.M., and Buckingham, M.E. (2010). Role of mesodermal FGF8 and FGF10 overlaps in the development of the arterial pole of the heart and pharyngeal arch arteries. Circulation Research *106*, 495–503.

Watanabe, Y., Zaffran, S., Kuroiwa, A., Higuchi, H., Ogura, T., Harvey, R.P., Kelly, R.G., and Buckingham, M. (2012). Fibroblast growth factor 10 gene regulation in the second heart field by Tbx1, Nkx2-5, and Islet1 reveals a genetic switch for down-regulation in the myocardium. Proc Natl Acad Sci USA *109*, 18273–18280.

Witzel, H.R., Jungblut, B., Choe, C.P., Crump, J.G., Braun, T., and Dobreva, G. (2012). The LIM protein Ajuba restricts the second heart field progenitor pool by regulating Isl1 activity. Dev Cell *23*, 58–70.

Wu, S.M., Fujiwara, Y., Cibulsky, S.M., Clapham, D.E., Lien, C.-L., Schultheiss, T.M., and Orkin, S.H. (2006). Developmental origin of a bipotential myocardial and smooth muscle cell precursor in the mammalian heart. Cell *127*, 1137–1150.

Xu, H., Morishima, M., Wylie, J.N., Schwartz, R.J., Bruneau, B.G., Lindsay, E.A., and Baldini, A. (2004). Tbx1 has a dual role in the morphogenesis of the cardiac outflow

tract. Development *131*, 3217–3227.

Xue, L., Wang, X., Xu, J., Xu, X., Liu, X., Hu, Z., Shen, H., and Chen, Y. (2012). ISL1 common variant rs1017 is not associated with susceptibility to congenital heart disease in a Chinese population. Genet Test Mol Biomarkers *16*, 679–683.

Yamagishi, H., Maeda, J., Hu, T., McAnally, J., Conway, S.J., Kume, T., Meyers, E.N., Yamagishi, C., and Srivastava, D. (2003). Tbx1 is regulated by tissue-specific forkhead proteins through a common Sonic hedgehog-responsive enhancer. Genes & Development *17*, 269–281.

Yamagishi, H., Yamagishi, C., Nakagawa, O., Harvey, R.P., Olson, E.N., and Srivastava, D. (2001). The Combinatorial Activities of Nkx2.5 and dHAND Are Essential for Cardiac Ventricle Formation. Developmental Biology *239*, 190–203.

Yang, L., Cai, C.-L., Lin, L., Qyang, Y., Chung, C., Monteiro, R.M., Mummery, C.L., Fishman, G.I., Cogen, A., and Evans, S. (2006). Isl1Cre reveals a common Bmp pathway in heart and limb development. Development *133*, 1575–1585.

Yang, X., Castilla, L.H., Xu, X., Li, C., Gotay, J., Weinstein, M., Liu, P.P., and Deng, C.X. (1999). Angiogenesis defects and mesenchymal apoptosis in mice lacking SMAD5. Development *126*, 1571–1580.

Yin, Z., and Frasch, M. (1998). Regulation and function of tinman during dorsal mesoderm induction and heart specification in Drosophila. Dev. Genet. *22*, 187–200.

Yuan, S., and Schoenwolf, G.C. (2000). Islet-1 marks the early heart rudiments and is asymmetrically expressed during early rotation of the foregut in the chick embryo. Anat. Rec. *260*, 204–207.

Zeisberg, E.M., Ma, Q., Juraszek, A.L., Moses, K., Schwartz, R.J., Izumo, S., and Pu, W.T. (2005). Morphogenesis of the right ventricle requires myocardial expression of Gata4. J. Clin. Invest. *115*, 1522–1531.

Zhang, H., Jiao, W., Sun, L., Fan, J., Chen, M., Wang, H., Xu, X., Shen, A., Li, T., Niu, B., et al. (2013). Intrachromosomal looping is required for activation of endogenous pluripotency genes during reprogramming. Cell Stem Cell *13*, 30–35.

Zhang, J., Lin, Y., Zhang, Y., Lan, Y., Lin, C., Moon, A.M., Schwartz, R.J., Martin, J.F., and Wang, F. (2008). Frs2alpha-deficiency in cardiac progenitors disrupts a subset of FGF signals required for outflow tract morphogenesis. Development *135*, 3611–3622.

Zhang, Z., and Baldini, A. (2010). Manipulation of endogenous regulatory elements and transgenic analyses of the Tbx1 gene. Mamm Genome *21*, 556–564.

Zhou, B., Gise, von, A., Ma, Q., Rivera-Feliciano, J., and Pu, W.T. (2008a). Nkx2-5- and Isl1-expressing cardiac progenitors contribute to proepicardium. Biochemical and Biophysical Research Communications *375*, 450–453.

Zhou, B., Ma, Q., Rajagopal, S., Wu, S.M., Domian, I., Rivera-Feliciano, J., Jiang, D., Gise, von, A., Ikeda, S., Chien, K.R., et al. (2008b). Epicardial progenitors contribute to the cardiomyocyte lineage in the developing heart. Nature *454*, 109–113.

Zhou, W., Lin, L., Majumdar, A., Li, X., Zhang, X., Liu, W., Etheridge, L., Shi, Y., Martin, J., Van de Ven, W., et al. (2007). Modulation of morphogenesis by noncanonical Wnt signaling requires ATF/CREB family-mediated transcriptional activation of TGFbeta2. Nat Genet *39*, 1225–1234.

10. Appendix

10.1. Affirmation

I hereby declare that I have written this work independently, with no different sources or aides from what indicated.

Frankfurt am Main, Luca Caputo

10.2. Ethical Statement

I hereby declare that all animal experiments were done in accordance with the regulations issued by the Committee for Animal Rights Protection of the State of Hessen (Regierungspraesidium Darmstadt).

Frankfurt am Main, Luca Caputo

10.3. Publications

The Isl1/Ldb1 Complex Orchestrates Genome-wide Chromatin Organization to Instruct Differentiation of Multipotent Cardiac Progenitors *Cell Stem Cell* (2015), L Caputo, H-R Witzel, P Kolovos, S Cheedipudi, M Looso, A Mylona, W-F van Ijcken, K-L Laugwitz, S Evans, T Braun, F Grosveld, G Dobreva

The Histone Acetyltransferase PCAF Associates with Actin and hnRNP U for RNA Polymerase II Transcription, *MCB*, (2008) A Obrdlik, A Kukalev, E Louvet, AK Östlund Farrants, L Caputo, P Percipalle

Isl1 Regulates Dowstream Regulatory Networks that Orchestrates Cardiac Morphogenesis and Differentiation, (prepared for submission to *Nature Genetics*). S Cheedipudi, **L Caputo**, J Cordero, H-R Witzel, N Tyagi, S Günther, C Kuenne, G Barreto, T Braun, G Dobreva

Ret Inhibition Reduces Metastasis of Highly Aggressive Lamin B1-Deficient Malignant Pulmonary Tumors, Manuscript in preparation, J Yia, **L Caputo**, J Vong, A Mehta, S Günther, BK Garvalov, L Fink, T Acker, W Seeger, G Barreto, R Savai, G Dobreva

10.4. Conferences and Retreats

Retreats
2009

- ECCPS retreat 2009 (Poster)
- 1st MBML/IMPRS joint annual retreat 2009 (Talk)

2010

- ECCPS retreat 2010 (Poster)
- 2nd MBML/IMPRS joint annual retreat 2010 (Talk)

2011

- TRR81-MGK retreat 2011 (Talk)
- 3rd IMPRS retreat 2011 (Poster)

2012

- TRR81-MGK retreat 2012 (Talk)

2013

- MPI-HLR retreat 2013 (Talk)

2014

- MPI-HLR retreat 2014 (Talk)

International conferences

2011

- ECCPS symposium - June 16th to 18th 2011- Bad Nauheim - Poster
- 1st Chromatin Changes in Differentiation and Malignancies - September 12nd to 14th 2011 - Gießen - Poster
- EMBO Molecular Medicine Conference: Molecular Insights for Innovative Therapies - December 1st to 3rd December 2011 - Heidelberg – Poster

2012

- Epigenetics and Chromatin – September 11th to 15th 2012 – Cold Spring Harbour – Poster

2014

Joint Symposium ECCPS / PVRI 2014 - January, 27th – 31st, 2014 - Bad Nauheim, Germany – **Best Abstract selected for oral presentation**

Transcription and Chromatin – August 23rd to 26th 2014 – Heidelberg – Poster

2015

- 3rd Chromatin Changes in Differentiation and Malignancies - September 14th to 16th 2015 - Marburg - Poster

10.5. Awards

Menzione Onorevole/Honorable mention "Certamen della Chimica" December 2001

Scholarship from "Cavalieri del Lavoro – Ravenna" Cavalieri del Lavoro – Ravenna 2001 Scholarship from "Cavalieri del Lavoro – Ravenna" for emeritus student in chemistry course at I.T.I.S. of Ravenna

Certificate of Merit Ministry of Education, University and Research July 2002 Certificate of merit issued by Ministry of Education, University and Research for mark 100/100 in state exam 2001/02

10.6. Curriculum Vitae

Personal Information

Name: Luca Caputo
Date and place of birth: 10.04.1983 in Trieste (Italien)
Marital Status: Married
Address for correspondence: Max-Planck-Institut für Herz- und Lungenforschung
W.G. Kerckhoff-Institut
Parkstraße 1
D-61231 Bad Nauheim
Telephone: +49 (0) 6032 705225
E-mail: luca.caputo@mpi-bm.mpg.de

School Education

1989-1994 Primary School
1989-1991 "N. Sauro" Trieste (Primary School)
1991-1994 "F. Mordani" Ravenna (Primary School)
1994-1997 Scuola Media "G. Novello" Ravenna
1997-2002 I.T.I.S. "N. Baldini" Ravenna (High School)
July 2002 **High School Diploma,** Chemistry specialization, final mark 100/100 with encomium

University Education

2002-2005 B.Sc**.** in Biotechnology Università di Bologna
May-July 2005 Training period at Department of Cell and Molecular Biology, **Karolinska Institute** – Stockholm, supervisor Dr. Percipalle
September 2005 Degre **B.Sc.** in Biotechnology Mark 103/110
2005-2008 M.Sc. in Pharmaceaticaul Biotechnologies Università di Bologna
April-December 2007 Training period at Department of Cell and Molecular Biology, **Karolinska Institute** – Stockholm, supervisor Dr. Percipalle
November 2007 Course on "Chromatin and RNA Processing" at Stockholm University, course organizer Ann-Kristin Östlund Farrants and Neus Visa, Guest speakers Jane Mellor and Christian Muchardt.
28th March 2008 Degre **M.Sc.** in Biotechnology Mark 110/110 cum Laude

Teaching experience

Supervising Diploma thesis of Mr. Patrick Coyle from April 2009 to February 2010
Training of juniors students

Management experience

Organisation of the 5th TRR81 -MGK- PhD Minisymposium 14th February 2013. "Transcriptional and Epigenetic regulation of Development and Malignance"

Languages

Italian Native Speaker
English Excellent
German Basic Level

10.7. PhD Portfolio – MGK

PhD Portfolio - MGK

Summary of PhD training

Name of PhD student: Luca Caputo

Affiliation:
Max Planck Institute for Heart and Lung Research
Parkstraße 1
D-61231Bad Nauheim
tel: 06032-705-225
fax:
e-mail: Luca.Caputo@mpi-bn.mpg.de

Start of PhD work: October 2008

Topic of PhD thesis work:
The Isl1/Ldb1 complex orchestrates heart-specific chromatin organization and transcriptional regulation

Thesis committee:
1. Gergana Dobreva (Supervisor)
2. Prof. Rolf Marschalek
3. Prof. Thomas Braun

Meetings of the thesis committee:
- 28 July 2009
- 10 August 2010
- 06 October 2011
- 14 June 2012
- 01 October 2012
- 12 December 2013

PhD training

General courses

- German Language Course Level 1 (November 2010 till April 2011)
- Presentations Skills (22-23 November 2010)

Specific courses

- Models, tools and pitfalls in applied stem cell research (12 November 2010, 2 hours)
- shRNA Technology (10 December 2010, 2 hours)
- Mass-Spec Proteomics (21 January 2011, 2 hours)
- Transgenic Animals (03 February 2011, 2 hours)
- How to address epigenetic regulations (04 February 2011, 2 hours)
- ES and iPS cell culture (11 March 2011, 2 hours)

Seminars and workshops

Presentations:

Journal Club:

- Nkx2.5 transactivates the ETS-related protein 71 gene and specifies an endothelial/endocardial fate in developing embryo (Bad Nauheim, MPI for Heart and Lung Research, 21 April 2009, 1 hour seminar 1 day preparation)
- Ubiquitination-dependent cofactor exchange on LIM homeodomain transcription factors (Bad Nauheim, MPI for Heart and Lung Research, 07 July 2009, 1 hour seminar 1 day preparation)
- Directed transdifferentiation of mouse mesoderm to heart tissue by defined factors (Bad Nauheim, MPI for Heart and Lung Research, 22 June 2010, 1 hour seminar 1 day preparation)
- Chromatin regulation by Brg1 underlies heart muscle development and disease (Bad Nauheim, MPI for Heart and Lung Research, 30 August 2011, 1 hour seminar 1 day preparation)
- PRC2 directly methylates GATA4 and repress its transcriptional activity (Bad Nauheim, MPI for Heart and Lung Research, 22 May 2012, 1 hour seminar 1 day preparation)
- Genome-wide analysis shows that Ldb1 controls essential hemapoietic genes/pathways in mouse early development and reveals novel players in hemapoiesis (Bad Nauheim, MPI for Heart and Lung Research, 28 May 2013, 1 hour seminar 1 day preparation)

Chromatin Methods Club:

- Detection and Analysis of postmodified proteins (Marburg, IMT, 12 July 2011, 2 hours preparation, 10 minutes talk)
- Protein Ligation Assay (Marburg, IMT, 12 March 2013, 2 hours preparation, 10 minutes talk)

Transregio 81 Seminar:
- The Role of Isl1-Ldb1 Transcriptional Complex in Heart Development (Gießen, IFZ, 06 October 2011, 45 minutes talk, 1 day preparation)
- The Role of Isl1-Ldb1 Transcriptional Complex in Heart Development (Gießen, IFZ, 14 June 2012, 45 minutes talk, 1 day preparation)
- The Role of Isl1-Ldb1 Transcriptional Complex in Heart Development (Gießen, IFZ, 12 December 2013, 45 minutes talk, 1 day preparation)

Others seminars:
- The Role of Isl1-Ldb1 Transcriptional Complex in Heart Development - Institute Colloquium, MPI Bad Nauheim, 01 Nov 2012 (45 minutes talk, 1 day preparation)
- The Role of Isl1-Ldb1 Transcriptional Complex in Heart Development - IMPRS Evaluation, MPI Bad Nauheim, 27 Nov 2012(15 minutes talk, 1 day preparation)
- The Role of Isl1-Ldb1 Transcriptional Complex in Heart Development - MPI Retreat, Schloss Ringberg am Tegernsee, September 2013 (15 minutes talk, 1 day preparation)
- The Role of Isl1-Ldb1 Transcriptional Complex in Heart Development - LOEWE Workshop, Uniklinikum Frankfurt am Main, 20 Jun 2014 (15 minutes talk, 1 day preparation)

Retreats:
- ECCPS retreat 2009 (Poster)
- 1st MBML/IMPRS joint annual retreat 2009 (Talk)
- ECCPS retreat 2010 (Poster)
- 2nd MBML/IMPRS joint annual retreat 2010 (Talk)
- TRR81-MGK retreat 2011 (Talk)
- 3rd IMPRS retreat 2011 (Poster)
- TRR81-MGK retreat 2012 (Talk)
- MPI-HLR retreat 2013 (Talk)

(Inter)national conferences
- ECCPS symposium - June 16th to 18th 2011- Bad Nauheim - Poster
- Chromatin Changes in Differentiation and Malignancies - September 12th to 14th 2011 - Gießen - Poster
- EMBO Molecular Medicine Conference: Molecular Insights for Innovative Therapies - December 1st to 3rd December 2011 - Heidelberg – Poster
- Epigenetics and Chromatin – September 11th to 15th 2012 – Cold Spring Harbour – Poster
- Transcription and Chromatin – August 23rd to 26th 2014 – Heidelberg - Poster

Organisation of student workshops/minisymposia on specific topics
14th February 2013: 5th TRR-81- PhD MiniSympomsium *"Transcriptional and Epigenetic regulation of Development and Malignance"* held in MPI Bad Nauheim.

Others
- Supervising Diploma thesis of Mr. Patrick Coyle from April 2009 to February 2010.

- October 2008 October 2011: successfully completed the “International Max Planck Research School for Heart and Lung Research” program.